ENANTIOSELECTIVE TOTAL SYNTHESIS OF TETRAHYDROISOQUINOLINE ALKALOIDS AND ANTHRAX LETHAL FACTOR INHIBITORS

AHMED L. ZEIN

Enantioselective Total Synthesis of Tetrahydroisoquinoline Alkaloids and Anthrax Lethal Factor Inhibitors

By

© **Ahmed L. Zein**

A thesis submitted to the School of Graduate Studies

in partial fulfillment of the requirements for the degree of

Doctor of Philosophy

Department of Chemistry

Memorial University

2011

St. John's Newfoundland and Labrador

To my family,

Mostafa and Anas

Abstract

Tetrahydroisoquinolines ('THIQ') which contain a B ring that is reduced at the C1–C2 and C3–C4 positions are known to be key biosynthetic precursors to many naturally occurring alkaloids. The enantioselective synthesis of each of the enantiomers of *N*-norlaudanidine, a minor *Papaver somniferum* opium benzyltetrahydoisoquinoline alkaloid has been achieved using a (*S*)- or (*R*)-α-methylbenzylamine chiral auxiliary-mediated strategy. The use of this chiral auxiliary has proven to be convenient and effective in a Bischler-Napieralski cyclization-reduction to enantioselectively form each of the enantiomers of *N*-norlaudanidine as confirmed by X-ray crystallography. Structures of each of these secondary amines are reported as well as the tetrahydroprotoberberine alkaloids (-)-(*S*)-tetrahydropalmatrubine and (-)-(*S*)-corytenchine. The thesis will also report on our findings to date toward the total synthesis of (1*R*,1'*S*)-temuconine using this strategy. Temuconine was isolated from *Aristolochia elegans* by Shamma and coworkers who stated it to be the enantiomer of a compound previously obtained by others, from Chilean *Berberis valdiviana*. (-)-Temuconine has been reported to have potent antiplasmodial activities, but its structure is different to that reported earlier by Shamma.

A second set of synthetic targets reported herein are potential anthrax lethal factor inhibitors. Anthrax is an acute infectious disease that normally affects animals and is caused by the *Bacillus anthracis* bacterium. Some tetrahydroisoquinoline unit-containing compounds, which were racemic, were recently found by Wong to be anthrax lethal

factor inhibitors. This finding prompted us to investigate the enantioselective synthesis of these compounds using our chiral auxiliary-mediated strategy.

Acknowledgments

It's my great pleasure to thank the following people for their contributions to the work contained in this thesis. It is my privilege to acknowledge that without their efforts and assistance on my behalf, this work would never have been completed. To my supervisor Prof. Paris Georghiou go my profoundest thanks. Paris without your knowledge, desire, drive, encouragement and enthusiasm this degree would never have been completed. My thanks for the papers, discussions, ideas, and all the little things; things I could not have done without. To my supervisory committee members Prof. Bob Davis and Prof. Ray Poirier, thank you for providing me with comments, suggestions during my doctoral program and for your critical evaluation of these documents. Thanks are also due to Prof. Graham Bodwell, Prof. Sunil Pansare, and Prof. Yuming Zhao for helpful discussions and encouragements.

I would like to thank my family, Dad, Mum, my brother and sisters, my aunt and her husband for all their love, support and encouragement. My wife Walaa, perhaps only you know the amount you have contributed and sacrificed to see this project to completion. Your love and support, belief, encouragement, and steadfast attitude stagger me beyond words and have kept me going, through the good and bad times, until the end. This is yours as much as mine.

My deep thanks to Dr. Louise Dawe for an X-ray crystal structure determination. Louise, your efforts are exemplary and much to be admired. Also, I would like to thank

Ms. Linda Winsor, for training and support with mass spectroscopy and Dr. Celine Schneider and Ms. Julie Collins for training and support with NMR spectroscopy.

To the following people go my thanks for their support and help during my program. Ms. Viola Martin, Ms. Mary Flinn, Ms. Roslaind Collins, Ms. Janet Horlick, Ms. Sarah Keating for the administrative support and Mr. Dave Murphy for his computer-related support throughout my program. I am thankful for the storeroom support provided by Mr. Steve Ballard, Ms. Bonita Smith, and Mr. John Power.

To the members of the Georghiou group, both past and present, it has been a great joy to me to work together over the past 4 years. The people I have worked with comprise the fondest memories of my studies, and have helped make the research and learning enjoyable.

And last, but not least, my appreciation is also extended to the Egyptian government for a scholarship and the Egyptian culture bureau staff in Montreal for their assistance.

Table of Contents

Page

CHAPTER 1
Introduction

CHAPTER 2

Enantioselective Syntheses of Selected Benzyltetrahydroisoquinolines:Syntheses of (*S*)- and (*R*)-*N*-Norlaudanidine: Trace Opium Constituents

Enantioselective Syntheses of Tetrahydroprotoberberines: (-)-(*S*)-Tetrahydropalmatrubine and (-)-(*S*)-Corytenchine

CHAPTER 3

Enantioselective Total Synthesis of (1*R*, 1′*S*)-Temuconine, a Bisbenzyltetrahydroisoquinoline Alkaloid

Chapter 4

Synthesis of Anthrax Lethal Factor Inhibitors Containing Tetrahydroisoquinoline Units

List of Tables

List of Figures

Chapter 1 **Page**

Chapter 2

Chapter 3

Chapter 4

List of Abbreviations

Å	angstrom
Aq	aqueous
APCI-MS	atmospheric pressure chemical ionization mass spectrometry
BBIQ	bisbenzyltetrahydroisoquinoline
BIQ	benzyltetrahydroisoquinoline
Bn	benzyl
BNC	Bischler-Napieralski cyclization
bs	broad singlet (in NMR)
bd	broad doublet (in NMR)
CA	chiral auxiliary
δ	chemical shift in ppm downfield from tetramethylsilane
DMF	*N,N*-dimethylformamide
DMSO	dimethyl sulfoxide
Et	ethyl
h	hour
Hz	hertz
J	coupling constant (Hz)
m	multiplet (in NMR)
M^+	molecular ion
Me	methyl
mol equiv	molar equivalent

mp	melting point
MAPKK	Mitogen-activated protein kinase kinase
MS	mass spectrometry
MW	microwave
NMP	*N*-methyl-2-pyrrolidone
NBS	*N*-bromosuccinimide
NMR	nuclear magnetic resonance
p	para
Ph	phenyl
PLC	preparative layer chromatography
ppm	parts per million
PSC	Pictet-Spengler cyclization
q	quartet (in NMR)
rt	room temperature
s	singlet (in NMR)
t	triplet (in NMR)
tert	tertiary
THF	tetrahydrofuran
TLC	thin-layer chromatography
TMHD	2,2,6,6-tetramethylheptane-3,5-dione
TMS	tetramethylsilane (in NMR)

List of Appendix

Chapter 1

Isoquinoline Alkaloids: An Overview

Part of this Chapter has been accepted to published as an invited review in

Studies in Natural Product Chemistry: Bioactive Natural Products **2011**; (in print).

Chapter 1

Asymmetric Synthesis of Isoquinoline Alkaloids: An Overview

1.1 Definition and Classification of Alkaloids.

1.1.1 Alkaloids.

The name "alkaloids" was introduced in 1819 by the German chemist Carl F.W. Meissner,[1,2a] to describe plant-derived substances that react like alkalis. He wrote:

> "To me it seems wholly appropriate to refer to those plant substances currently known not by the name alkalis, but alkaloids, since in some of their properties they differ from alkalis considerably, and would thus find their place before the plant acids in the field of plant chemistry."

The word alkaloids is thus derived from the two words "alkali" (which, in turn, comes from the Arabic "*al qualja*", which means "ashes of plants") and "*ειδοσ*", the Greek word meaning "similarity" to give the meaning to alkaloids as being substances with alkali-like character. However, the term alkaloid was widely used after Jacobsen published a review article in 1880 in the chemical dictionary of Albert Ladenburg.[2a]

Many other definitions have been proposed to describe the term alkaloids but none of them really appears satisfactory. In 2002, Hesse[2a] collected many of these definitions of alkaloids in his book "Alkaloids: Nature's Curse or Blessing", and he summarized them in the following definition, which is very appropriate:

"Alkaloids are nitrogen-containing organic substances of natural origin with a greater or lesser degree of basic character."

1.1.2 Classification of alkaloids.

Alkaloids can be found in many sources. These range from plants such as potatoes and tomatoes to animals such as shellfish. They also can be found in fungi such as mushrooms. Alkaloids can be extracted from their respective sources by treatment with acids such as hydrochloric acid or sulfuric acid, although organic acids such as maleic acid and citric acid are sometimes also used.

Due to the great structural diversity of alkaloids compared to other classes of natural compounds, it was difficult to classify them into specific groups. First, it was believed that classification could be done by their common natural sources,[3] *e.g.* a particular type of plant. However, it was difficult to categorize them into specific groups since there was a lack of knowledge about the chemical structures of alkaloids in general.

Recently, classifications are based on the similarity of the carbon skeleton (*i.e.*, structural relationship), biogenesis, biological origin, and spectroscopic/spectrometric properties. According to those standards used for alkaloid classification, as Hesse has described in his book,[2b] alkaloids are often divided into the following six major groups and each group could be classified into other sub-groups:

1.1.2.1 Heterocyclic alkaloids.

These are true (typical) alkaloids that are derived from amino acids and have a nitrogen atom in a heterocyclic ring, and these compounds should meet the following criteria:

(I) Nitrogen is a part of the heterocyclic ring.

(II) The compound originates from an amino acid.

(III) The compound shows significant physiological activity.

They are again subdivided into the following groups:

- Pyrrolidine alkaloids *e.g.* nicotine.
- Indole alkaloids *e.g.* strychnine, reserpine, ergotamine.
- Piperidine alkaloids *e.g.* coniine.
- Tropanes and related bases *e.g.* atropine, cocaine.
- Histamine, imidazole, and guanidine alkaloids *e.g.* alchornine.
- Isoquinoline alkaloids *e.g.* papaverine, narcine, berberine.
- Quinoline alkaloids *e.g.* quinine, quinidine.
- Quinazoline alkaloids *e.g.* glycosmicine.
- Benzoxazines and benzoxazoles *e.g.* 3-hydroxyoxindole.
- Pyrrolizidine alkaloids *e.g.* (-)-retronecanol.
- Indolizidine alkaloids *e.g.* crepidamine.
- Quinolizidine alkaloids *e.g.* (-)-lupinine.
- Pyrazine alkaloids *e.g.* 2-methoxy-3-methylpyrazine.
- Purine bases *e.g.* adenine, caffeine.

- Pteridines alkaloids *e.g.* pteridine, leucopterin.

1.1.2.2 Alkaloids with N-atoms in the exocyclic position including aliphatic amines.

This class of alkaloids is subdivided into six categories:

- Erythrophleum alkaloids *e.g.* cassaine.
- Phenylalkylamine alkaloids *e.g.* (-)-ephedrine.
- Benzylamine alkaloids *e.g.* capsaicine.
- Colchicine alkaloids *e.g.* colchicine.
- Khat alkaloids *e.g.* merucathine.
- Muscarines alkaloids *e.g.* (+)-muscarine.

1.1.2.3 Putrescine, spermidine, and spermine alkaloids.

Some examples of this class are paucine, inandenine-12-one, and (+)-lunarine.

1.1.2.4 Peptide alkaloids.

An example of this class is ergot peptide alkaloid.

1.1.2.5 Terpene and steroid alkaloids.

This class of alkaloids includes:

- Diterpenes alkaloids *e.g.* (-)-veatchine, (-)-atisine.
- Daphniphyllum alkaloids *e.g.* (+)-daphniphylline.
- Taxus alkaloids *e.g.* taxusin, baccatin.
- Steroid alkaloids *e.g.* funtumine, terminaline.

1.1.2.6 Dimeric alkaloids.

These are also known as *bis-alkaloids*, and an example of this class is (+)-salutadimerine.

It was noted that some alkaloids do not have the carbon skeleton characteristics of their group. For example, galantamine (**1**) and homoaporphines do not contain the isoquinoline fragment, however they are considered as isoquinoline alkaloids.

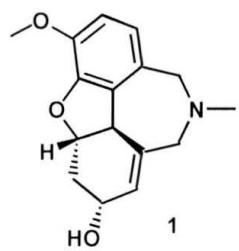

1

Figure 1.1. Structure of galantamine **(1).**

1.1.3 Biological activities of alkaloids.

Alkaloids are antibacterial, antifungal, antiviral, can offer protection against UV-irradiation, are insecticides and are also herbicides, and these properties may extend to toxicity towards animals.[4,5,6]

Plant protection is a well known function of alkaloids.[7,8] For example, the aporphine alkaloid liriodenine (**2**) protects tulip trees from parasitic mushrooms. Therefore, the presence of alkaloids in plants may prevent insects and animals from eating them. On the other hand, some animals can adapt to the alkaloids and use them for their own metabolism.

Another example of alkaloids that work as plant protectors against insect attacks is (-)-senecionine **(3)**, which is a highly effective defence for the plants that produce it.[8,9]

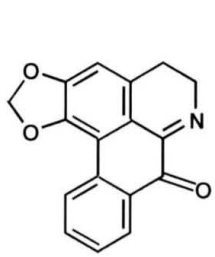

Liriodenine (2)

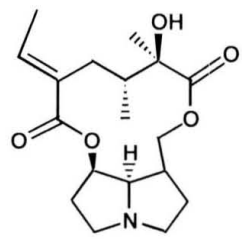

(-)-Senecionine (3)

Figure 1.2. Structures of liriodenine (**2**) and senecionine (**3**).

The use of alkaloids in medicine is very common and they are usually used in the form of salts. Table 1.1 lists some selected alkaloids and their actions.[2c]

Table 1.1. Some selected alkaloids and their actions.

Alkaloid	**Action**
Sparteine	Treatment of arrhythmia
Atropine	Parasympatholytics
Codeine	Cough medicine
Cocaine	Anesthetic
Morphine	Analgesic
Reserpine	Antihypertensive
Tubocurarine	Muscle relaxant

1.2 Isoquinoline Alkaloids.

Isoquinoline alkaloids are a large family of naturally occurring alkaloids having a broad variety of biological activities. More than *ca.* 1,200 isoquinolines are known today.[2a] Among the important biological activities that many of these compounds exhibit are anti-inflammatory, anti-microbial, anti-leukemic and anti-tumor properties.[10] This class of alkaloids notably includes morphine and codeine, which are widely used in medicine.

Isoquinoline alkaloids are synthetically derived from a 3,4-dihydroxytyramine (dopamine) linked to an aldehyde or ketone and typically found in many plant families such as *Papaveraceae*, *Berberidaceae* and *Ranunculaceae*.[11] Compound **4** is known as quinoline and when the nitrogen is in position 2 in the B-ring as in compound **5**, the compound is known as isoquinoline. Compound **6** is known as 1,2,3,4-tetrahydroisoquinoline. Introduction of benzyl group in position 1 in the B-ring produces the benzyltetrahydroisoquinoline motif as shown in **7** (Fig. 1.3).

4 5 6 7

Figure 1.3. Derivation of the terms of THIQ and BTHIQ.

1.2.1 Classification of isoquinolines.

On the basis of structural criteria, isoquinoline alkaloids are divided into various groups. They are again subdivided into sub-groups that contain a relatively few members and others that have a great many. The structures of some of these compounds are shown in Figure 1.4.[2d]

- Simple isoquinoline alkaloids *e.g.* (+)-salsoline, hydrohydrastinine (**8**), lophcerine.
- Naphthylisoquinoline alkaloids *e.g.* (-)-ancistrocladine, *N*-methyltriphyophylline (**9**).
- Benzylisoquinoline alkaloids *e.g.* papaverine (**10**), (+)-laudanosine.
- Phenytetrahydroisoquinoline alkaloids *e.g.* (+)-cryptostylline I (**11**).
- Phthalideisoquinoline alkaloids *e.g.* (+)-(1*S*, 1′*S*)-α-hydrastine, (*Z*)-*N*- methylhydrastine.
- Rhoeadine and papaverrubine alkaloids *e.g.* (+)-rhoeadine (**12**), (+)-papaverrubine A.
- Ipecacuanha alkaloids *e.g.* (-)-emetine (**13**).
- Cryptaustoline alkaloids *e.g.* (-)-cryptaustoline.
- Aporphine and homoaporphine alkaloids *e.g.* (+)-glaucine, (-)-multifloramine.
- Proaporphine and homoproaporphine alkaloids *e.g.* (+)-pronuciferine.
- Cularine alkaloids *e.g.* (+)-cularine, yagonine.
- Protoberberine alkaloids *e.g.* (-)-canadine, (-)-ophiocarpine.
- Protopine alkaloids *e.g.* protopine, corycavidine.
- Benzophenanthridine alkaloids *e.g.* corynolamine, oxynitidine.
- Spirobenzylisoquinoline alkaloids *e.g.* (-)-fumaricine, (+)-ochtensine
- Pavine and isopavine alkaloids *e.g.* (-)-argemonine, (-)-amurensine.
- Morphine alkaloids *e.g.* (-)-morphine, (-)-sinomenine.

- Amaryllidaceae alkaloids *e.g.* (-)-lycorine, (+)-amberlline.
- Erythrina alkaloids *e.g.* (+)-erysodine, (+)-β-erythroidine.

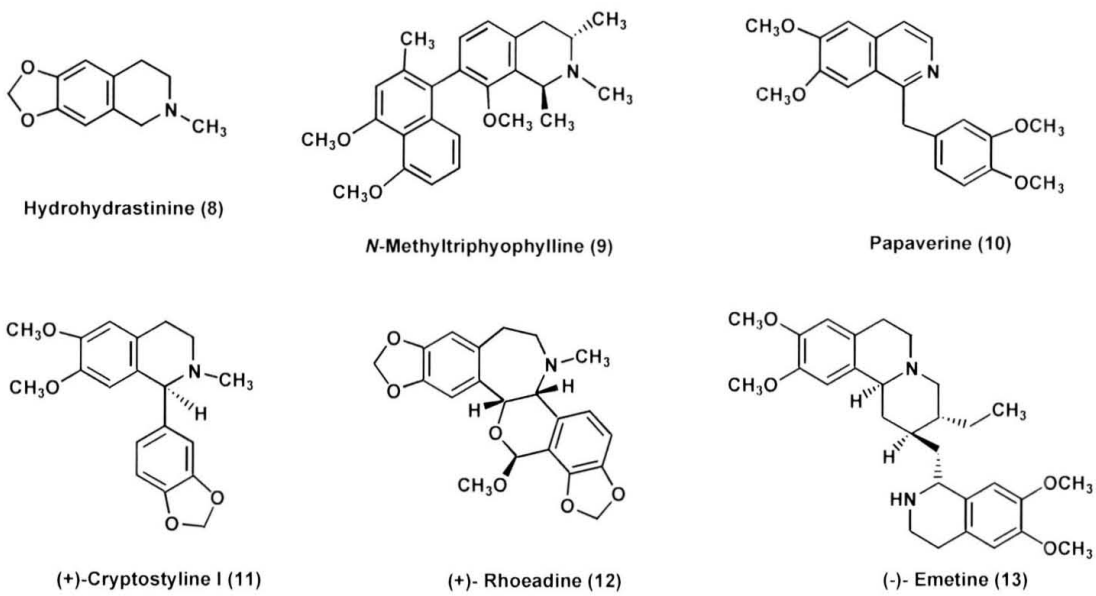

Figure 1.4. Some selected examples of isoquinoline alkaloids.

Figure 1.5 shows a statistical breakdown in terms of the location of oxygenated substituents on the ring skeleton of the most important subclasses, referred to as Types I-IX.[2c]

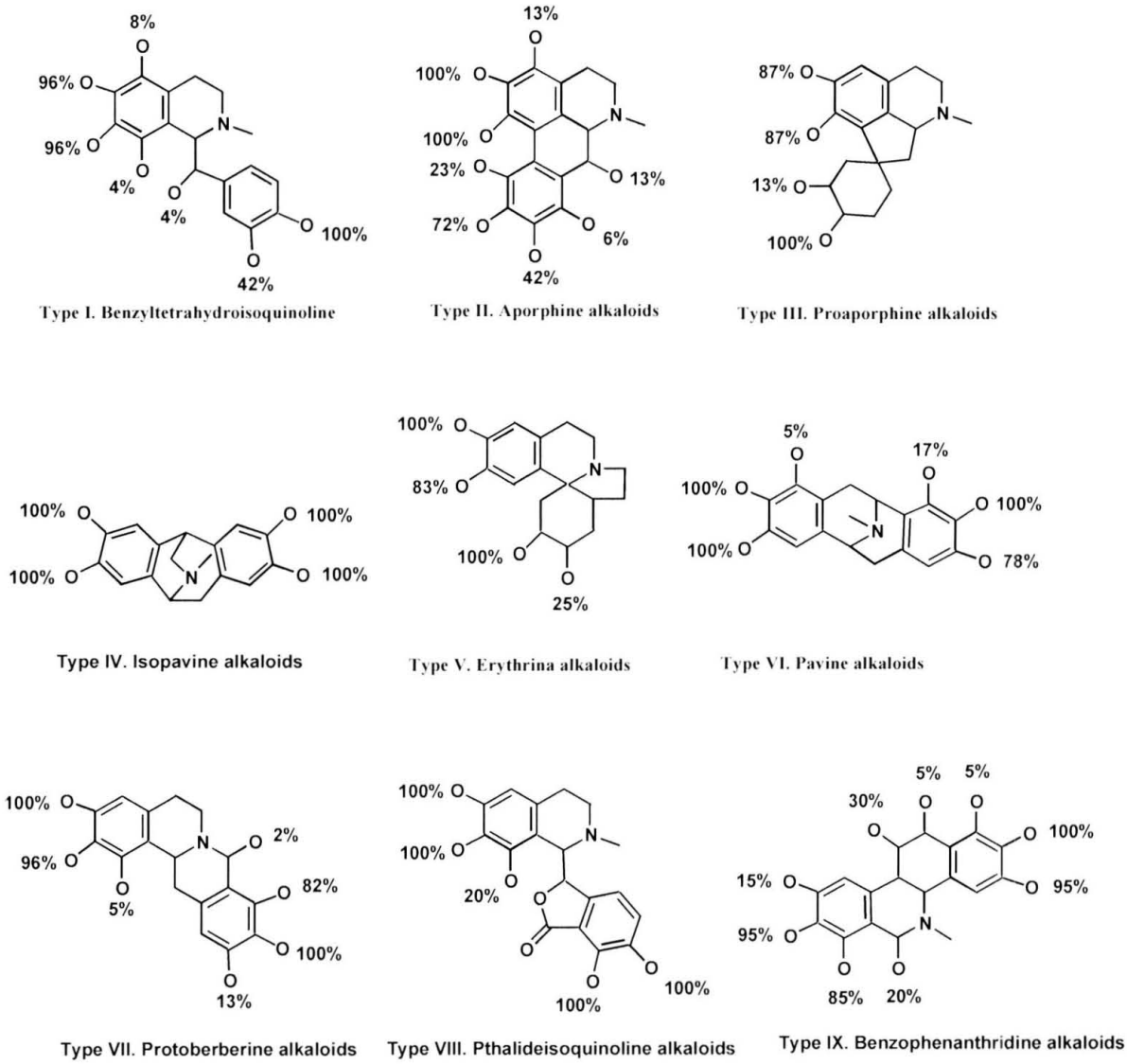

Figure 1.5. Statistical breakdown in the terms of the location of oxygenated substituents on the ring skeleton of some important subclasses.[2e]

These nine isoquinoline subclasses each contain an isoquinoline unit and the number of skeleton C-atoms could either be 16 or 17. Many of these structures in Figure 1.5 show that the number and relative orientations of the O-substituted ring C-atoms is

very important and most of these compounds have two of the four C-atoms that are bonded to oxygen in *vicinal* relationships. In most cases, however, one of the C-atoms in each pair carries a 2-aminoethyl residue in a *para*-position (Type IX however is an exception), for which the most common arrangement is given by the general formula (**14**) (Figure 1.6).[2e]

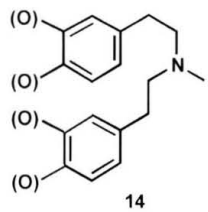

14

Figure 1.6. The general formula for the most common arrangement of the oxygen functionalities.

Due to this observation, a hypothesis is possible regarding the transformation involved to explain the biogenetic interconversions in plants of the individual skeleton types. For example, the transformation of 1-benzyl-1,2,3,4-tetrahydroisoquinoline alkaloids (Type 1) into protoberberine (Type VII) can be achieved from an immonium ion by a Mannich reaction via the intermediate **15** (Figure 1.7).[2e]

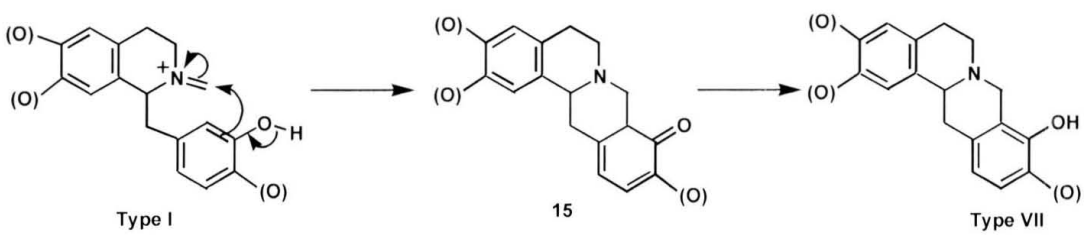

Figure 1.7. Transformation of (Type I) to (Type VII).

However, cyclization of 1-benzyl-1,2,3,4-tetrahydroisoquinoline (Type I) alkaloids also produces the pavine (Type VI) and isopavine (Type IV) alkaloids. Dehydrogenation at both C-2 and C-3 in the skeleton of Type I followed by ring closure form the pavine (Type VI) alkaloids. On the other hand, for the transformation of Type I into isopavine (Type IV) alkaloids, the Type I should have an oxygen functionality at C-4. Thus, only alkaloids of Type I with O-substitution at C-6, C-7, C-3′, and C-4′ are converted into those of the isopavine type (Figure 1.8).[2c]

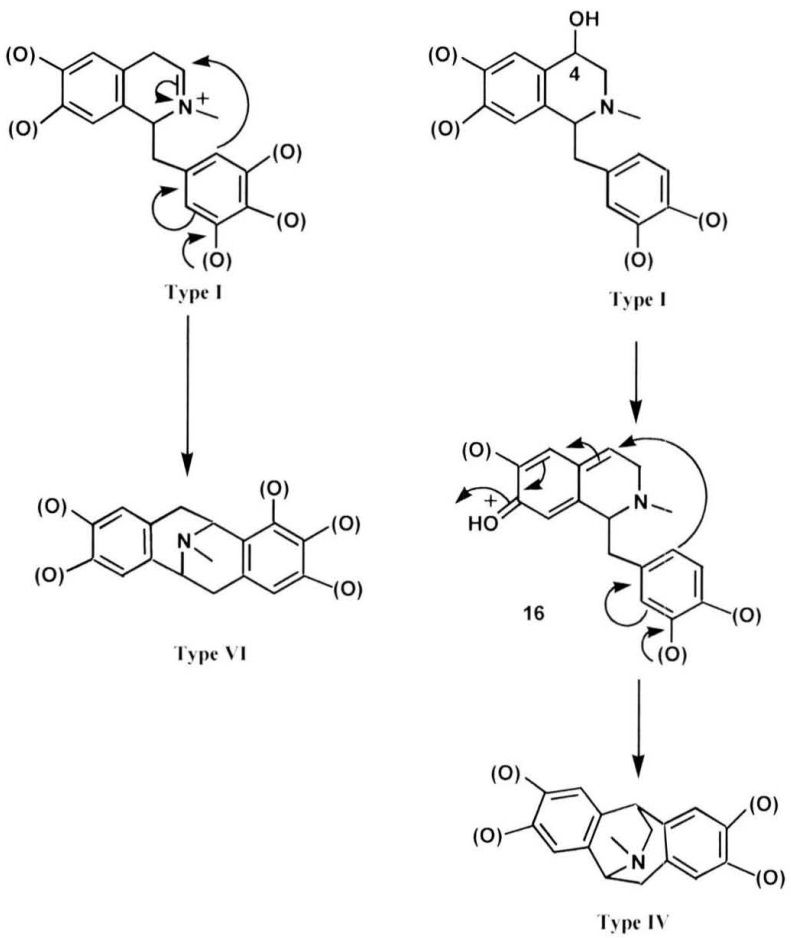

Figure 1.8. Transformations of Type I into Type VI and Type IV alkaloids.

The synthesis of particular alkaloids in a number of different plants therefore does not have to proceed in the same manner in all cases and many different transformations can happen to produce a variety of alkaloids. The clearly close relationship between individual subgroups of 1-benzyl-1,2,3,4-tetrahydroisoquinoline (Type I) alkaloids has acted to spur the identification of the reactions which can allow the chemical correlation between certain alkaloid groups.

1.2.2 Therapeutic potential of nucleic acid-binding isoquinoline alkaloids.

In general, plant products play a very important role in human therapy and healing. Alkaloids, and in particular isoquinoline alkaloids, are the largest group of plant chemicals which are extensively distributed in nature and that exhibit a variety of pharmacological activities. Isoquinoline alkaloids are of importance in contemporary biomedical research and drug discovery, and a number of these compounds have attractive biological activities that are exerted through specific and noncovalent interactions with DNA.[12]

DNA interaction of a small molecule can be classified into two major categories.[13] The first is known as *irreversible covalent interactions*, and the other is known as *reversible noncovalent interactions*. Covalent interactions include base modifications, alkylation, cross-linking of strands, and strand breakage. However, noncovalent interactions can be further classified in terms of intercalation, groove binding, and outside binding.[14]

Intercalation involves the insertion of a planar molecule of a ligand between DNA base pairs parallel to the base pair, which induces conformational changes in DNA by decreasing the DNA helical twist and lengthening of the DNA. This is the main feature distinguishing intercalation from other modes of binding, such as groove binding, and outside binding, as shown in Figure 1.9 (left) and (right) respectively.[13]

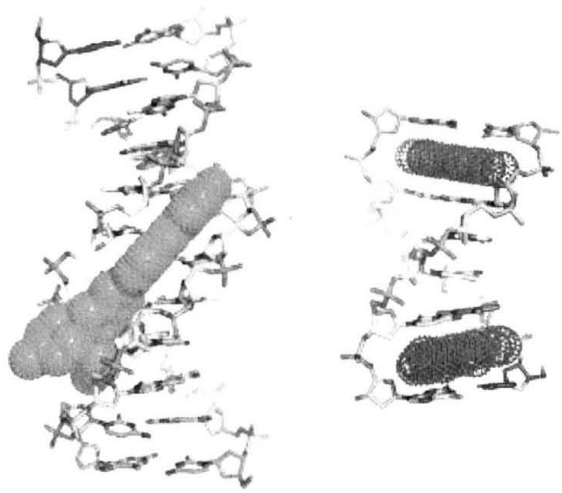

Figure 1.9. Different modes of DNA binding by small molecules (Figure adapted from Reference 13).

A large number of DNA-binding natural and synthetic isoquinoline alkaloids have been studied. The most important of these compounds are berberine derivatives (**17a-c**). The presence of a cationic substituent, or an electrophilic functional group on the ring of these berberine derivatives have highlighted the potential of these alkaloids as promising lead compounds for the development of effective DNA-binders. This is due to the cationic quaternary nitrogen center, in these compounds which is essential for an initial attraction and attachment to the anionic DNA.[15,16]

The binding affinities of berberine towards duplex DNA have been explored using several analytical techniques including absorption, fluorescence and NMR spectroscopy, and electrospray ionization mass (ESI-MS) spectrometry.[17] Since these binding affinities were found to be only moderate, and in the range of 1.0-2.0 x 10^4 M^{-1}, appropriate structural modifications are required in order for such molecules to serve as novel DNA-binding agents with enhanced binding affinities.[18] Figure 1.10 shows how berberine binds to Topo-I DNA.[12]

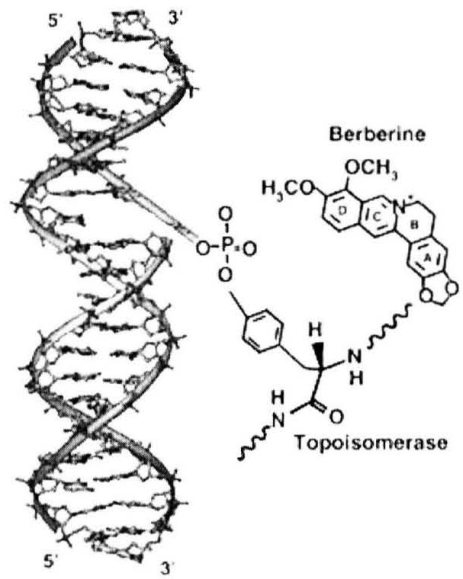

Figure 1.10. berberine binds to Topo-I DNA.[12]

Berberrubine (**18a**), which has a hydroxyl group in the C-9 position, has been found to be a more potent inducer of Topo-II-DNA cleavable complexes than berberine (**17a**) itself which contains a methoxy group at the same position. It is presumed that berberrubine's hydroxyl group allows for easier intercalation formation than is possible with berberine (**17a**).[12,19, 20, 21]

Pilch *et al.*[22] using computer modeling studies on protoberberine–DNA complexes, proved that only rings C and D intercalate into the host DNA helix, while rings A and B protrude out of the helix interior into the minor groove.

In order to develop more effective berberine alkaloid-based DNA binding, berberine dimers (**19a–f**) (Scheme 1.1) were synthesized by the linkage of berberrubine (**18a**) with alkyl chains of varying lengths.[18]

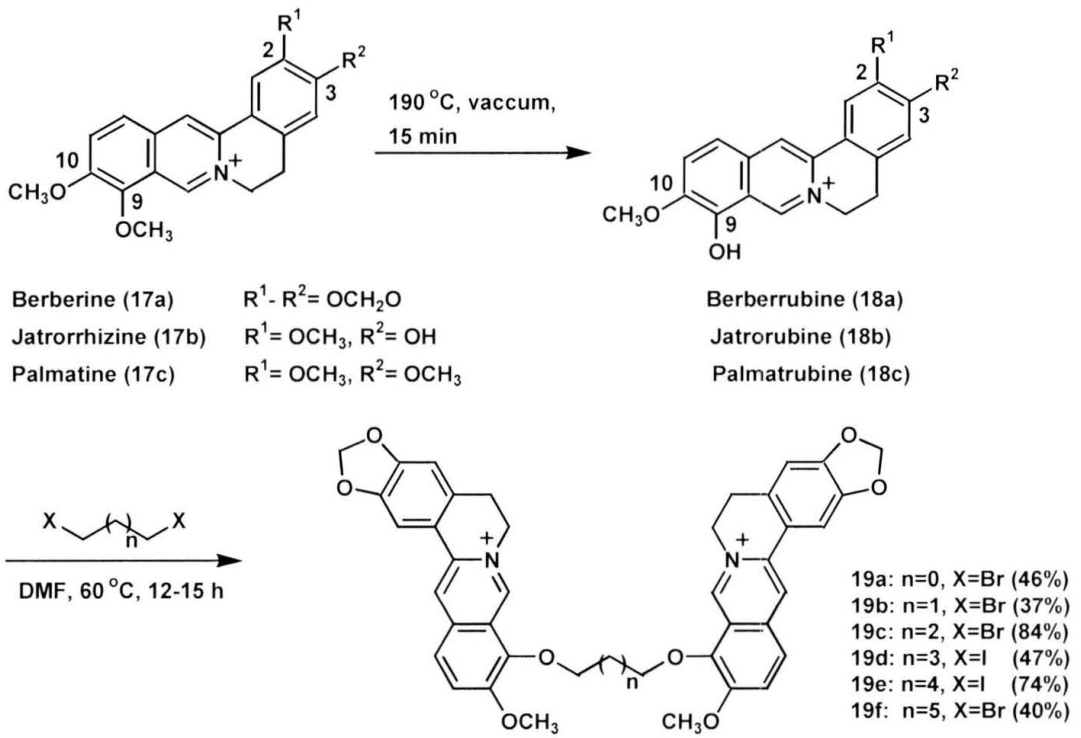

Scheme 1.1. Synthetic route to berberine dimers **(19a-f)**.

The DNA-binding affinity of benzophenanthridine alkaloids such as nitidine, chelerythrine, and chelidonine were also studied, but the overall data indicate that sanguinarine is the more potent DNA intercalator.[12] The alkaloid-DNA interactions, and more recently, alkaloid-RNA interactions studies, are in progress and further understanding of these aspects will enable the development of newer isoquinoline-based molecules.

1.3 Asymmetric Synthesis of Isoquinoline Alkaloids.

The asymmetric synthesis of isoquinoline alkaloids usually relies on one of three different strategies: (i) formation of the C-1, C-8a bond of the isoquinoline core using stereochemical modification using one of the usual, typical methods, either the Bischler-Napieralski[23] or the Pictet-Spengler[24] cyclizations; (ii) alkylation at position C-1 of the isoquinoline via nucleophilic or electrophilic activation;[25] and (iii) formation of the C-4,C-4a bond by a Pomeranz-Fritsch reaction.[26]

1.3.1 Asymmetric Bischler-Napieralski cyclization-reduction syntheses.

The Bischler-Napieralski reaction (Scheme 1.2) is notably one of the most-widely used reactions in the synthesis of 3,4-tetrahydroisoquinolines from β-ethylamides of electron-rich arenes, using condensation reagents such as P_2O_5, $POCl_3$ or $ZnCl_2$. The number and the position of the electron-donating groups on the aryl ring of the β-arylethylamides influence the regioselectivity of the reaction.[27] The choice, however, of

the reducing agent in the next step to produce the tetrahydroisoquinoline ring is crucial since the reduction generates a new stereogenic center at C-1. [28]

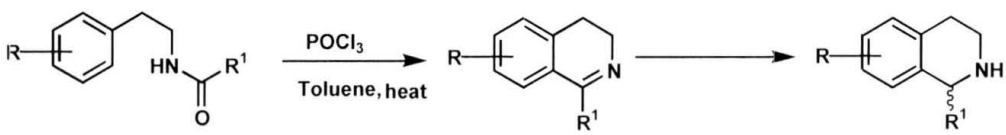

Scheme 1.2. General formula for the Bischler-Napieralski cyclization-reduction reaction.

Two types of mechanism for the Bischler–Napieralski reaction have been reported.[28,29] In 1980, Nagubandi and Fodor proposed a mechanism (Mechanism I) for the Bischler-Napieralski reaction which involves a dichlorophosphoryl imine-ester intermediate **23** formed after the Lewis acid initially coordinates with the carbonyl oxygen of the amide **20**. Electrophilic attack by the aromatic ring and elimination occurs with imine formation after cyclization. The resultant imine **25** is then reduced by a reducing agent to the corresponding tetrahydoisoquinoline (Scheme 1.3).

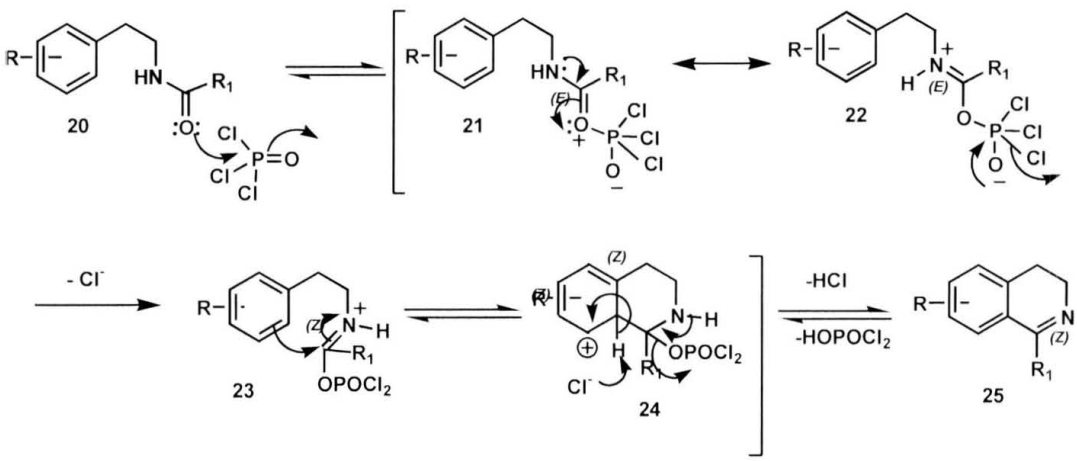

Scheme 1.3. Mechanism I for the Bischler-Napieralski reaction.

Mechanism II involves formation at room temperature of stable imidoyl salts that form nitrilium salts **27** upon mild heating. The nitrilium ion intermediate is produced by elimination of the carbonyl oxygen in the starting amide. Electrophilic attack by the aromatic ring and subsequent re-aromatization results in the formation of the imine (Scheme 1.4).

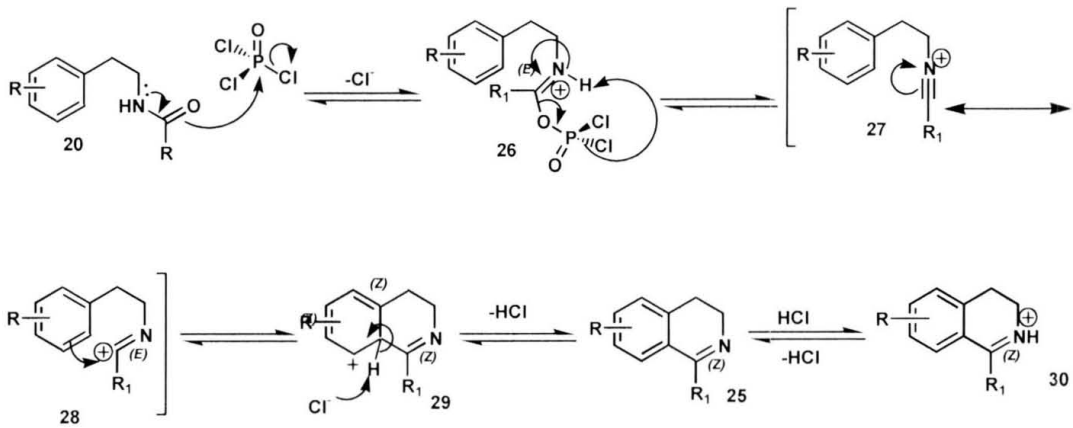

Scheme 1.4. Mechanism II for the Bischler-Napieralski reaction.

Regardless of its mechanism of formation, the resultant imine **25** can be reduced using different methods, such as by hydride reduction, or by catalytic hydrogenation. In some cases a chiral auxiliary can be attached to the imine nitrogen, resulting in subsequent enantioselective reduction with a high enantiomeric excess.

1.3.1.1 Using asymmetric catalytic hydrogen-transfer hydrogenation.

Hydrogen-transfer reactions are reduction reactions of multiple bonds using a hydrogen donor in the presence of a catalyst. In most cases, the hydrogen donors are alcohols, including chiral ones, and formic acid. In asymmetric hydrogen-transfer reactions chiral phosphines are the most popular ligands used in the asymmetric catalysts. Recently, for enantioselective hydrogen-transfer reactions, the most commonly used have chiral auxiliaries containing nitrogen, and not phosphorus, as the donor atom.[30]

Asymmetric transfer hydrogenation catalyzed by suitably designed chiral Ru(II) complexes, as developed by Noyori *et al.* [31] has been shown to be an excellent method for the enantioselective reduction of cyclic imines with formic acid/triethylamine. Since its development, Noyori's method has become the method of choice for the enantioselective hydrogen-transfer reduction of cyclic imines. Asymmetric transfer hydrogenations have been used to produce important chiral enantio-enriched compounds and many different tetrahydroisoquinolines have been prepared in high yields with *ee* values ranging from 90 to 97% using Noyori's catalyst and formic acid/triethylamine as the hydrogen source. Some recent examples are illustrative of this methodology.

(-)-(*S*)-Stepholidine (**36**), is a tetrahydroprotoberberine, a class of naturally-occurring tetracyclic alkaloids that also contain an isoquinoline core, and is one of the protoberberine alkaloids extracted from *Stephania intermedia*. (-)-(*S*)-Stepholidine display a unique pharmacological activity toward dopamine receptors and also plays a major role in the treatment of drug abuse.[32] Yang's synthesis[33] of **36** proceeded via the

chiral tetrahydroisoquinoline **35** which, in turn, was synthesized as outlined in Scheme 1.5.

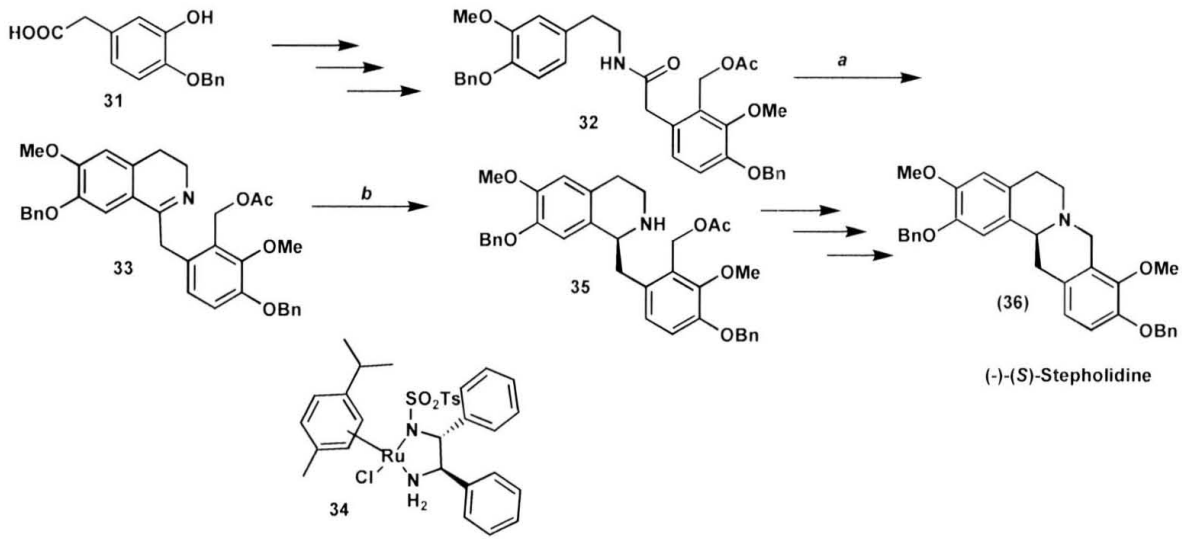

a: $POCl_3$, CH_3CN; *b*: **34**, HCO_2H, TEA, DMF, 84% for 2 steps.

Scheme 1.5. Synthesis of (-)-stepholidine.

Yang used a Noyori asymmetric hydrogen-transfer reaction catalyzed by the chiral Ru(II) complex **34** to reduce the imine **33** to **35** using formic acid/triethylamine. Imine **33** was prepared from the corresponding amide **32**, which was synthesized from the phenylacetic acid **31**, via a Bischler-Napieralski cyclization reaction. The Bischler-Napieralski reaction was the key step used to produce **33** in excellent yield using $POCl_3$ in CH_3CN. Since this imine was found to be unstable at room temperature, it was reduced directly when freshly prepared, without further purification.

Opatz and coworkers[34] synthesized the tetrahydroisoquinolines (–)-(*S*)-norlaudanosine (**37**), (+)-(*R*)-*O*,*O*-dimethylcoclaurine (**38**), and (+)-(*R*)-salsolidine (**39**) (Figure 1.11) as outlined in Scheme 1.6. The syntheses were accomplished via the intermediate α-aminonitrile **42**. Functionalization of **40** with formic acid and a subsequent classic $POCl_3$-mediated Bischler-Napieralski reaction produced the imine **41** which, with potassium cyanide, afforded the α-aminonitrile **42**. Alkylation of **42**, spontaneous elimination of HCN, and then asymmetric hydrogen-transfer reduction using the Noyori catalyst (**45**) with formic acid/triethylamine afforded the respective target compounds. The configuration of the catalyst controlled the configuration of the newly-formed C-1 stereogenic center: With the (*S*,*S*)-enantiomer of the catalyst, the (*R*)-configured *O*,*O*-dimethylcoclaurine (**38**) and salsolidine (**39**) were obtained with 96% and 91% *ee*, respectively. However, using the (*R*,*R*)-enantiomer of the catalyst, the (*S*)-enantiomer of norlaudanosine (**37**) was obtained in 93% *ee* (Figure 1.11).

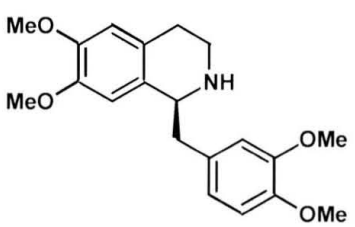

37:(-)-Norlaudanosine
78% from **42** using (*R*, *R*)-45, 93% *ee*

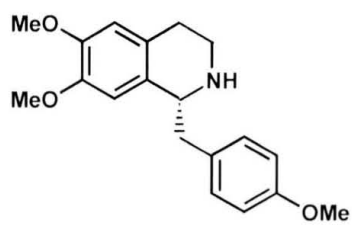

38: (+)-*O*,*O*-Dimethylcoclaurine
55% from **42**, 96% *ee*

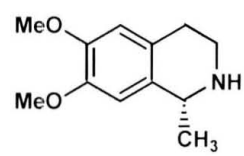

39:(+)-Salsolidine
51% from **42**, 91% *ee*

Figure 1.11. Tetrahydroisoquinolines synthesized by Opatz *et al.*[34]

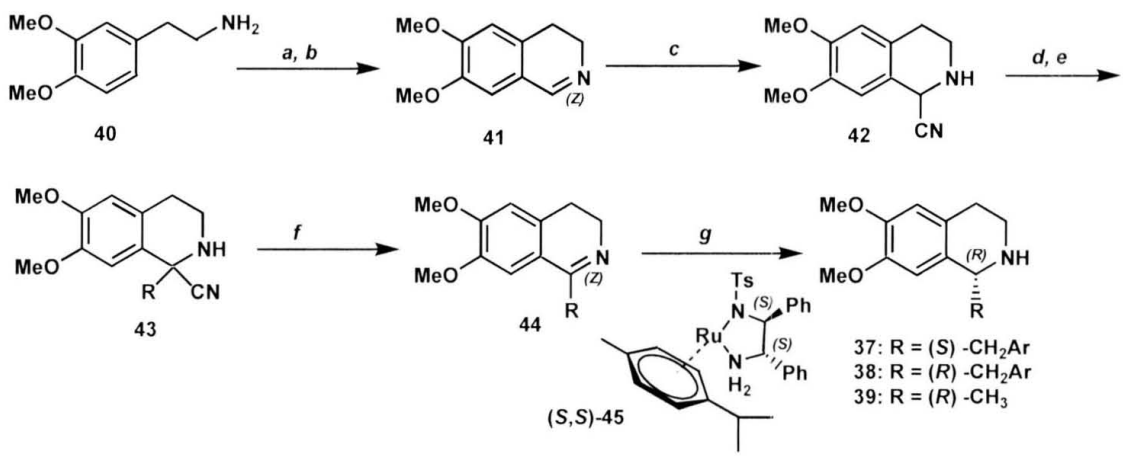

a: HCO_2H, heat; ***b***: $POCl_3$, heat; ***c***: KCN, HCl, 60%; ***d***: KHMDS, THF, -78 °C; ***e***: RX, THF, -78 °C; ***f:*** spontaneous -HCN; ***g***: **45**, HCO_2H, Et_3N.

Scheme 1.6. Some tetrahydroisoquinolines synthesized by Opatz *et al.*[34]

1.3.1.2 Using chiral-auxiliary-modified amines.

Chiral benzyltetrahydroisoquinoline alkaloids can be also be asymmetrically synthesized via Bischler-Napieralski cyclization followed by stereoselective hydride reduction of the 3,4-dihydroisoquinolinium salts derived from the amine functionalized with a chiral auxiliary. Many different chiral auxiliaries have been used in such reactions and the conditions and solvents used are very crucial in the reduction step to produce the C-1 stereogenic center.

The Georghiou group[35] found (*S*)-α-methylbenzylamine (see discussion in Chapter 2) to be a very efficient chiral auxiliary in the Bischlar-Napieralski reaction step in the multistep synthesis of (-)-tejedine (**52**), a seco-bisbenzylisoquinoline alkaloid

(Scheme 1.7). The amide **50**, was prepared from the chiral amine **47** (starting from the commercially available vanillin (**46**) in 13 synthetic steps) and the acid **49** (which was synthesized from 4-hydroxybenzaldehyde (**48**) in 11 steps). Bischler–Napieralski cyclization-$NaBH_4$ reduction of the amide **50** afforded the desired regioisomer of tetrahydroisoquinoline **51** in 40% yield and with 99% *ee*. The synthesis of (-)-tejedine (**52**) was completed after an additional series of transformations (in total, *ca.* 35 steps).

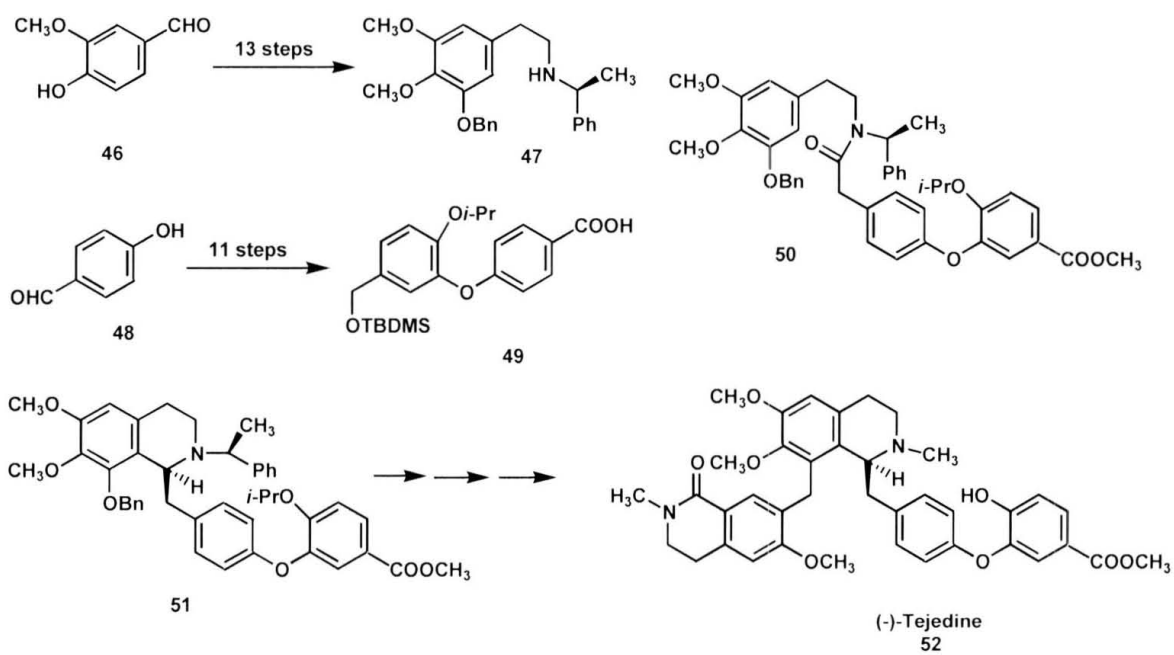

Scheme 1.7. The total synthesis of (-)-tejedine (**52**).

Lipshutz *et al.*[36] synthesized the nonracemic korupensamines B (**57**) via a troposelective intermolecular Suzuki-Miyaura biaryl coupling for construction of the fully fashioned naphthylisoquinoline framework that invokes π-stacking as a possible source of the stereocontrol (Scheme 1.8).

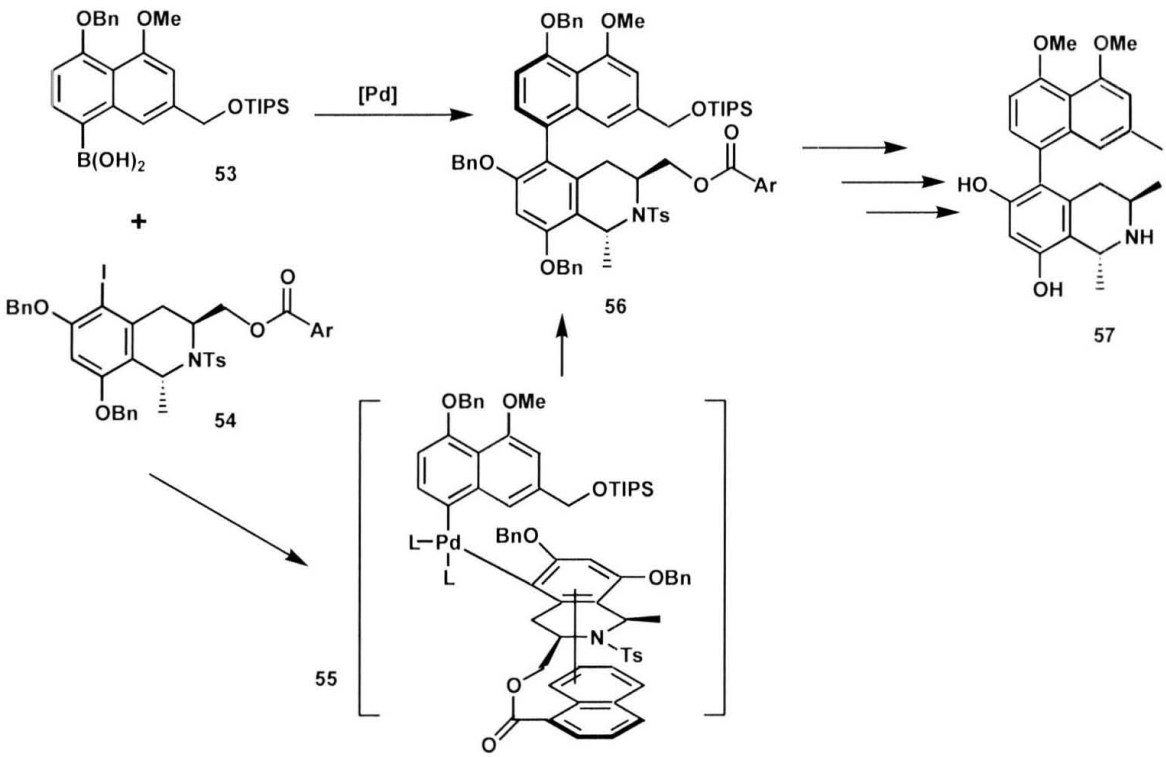

Scheme 1.8. The total synthesis of korupensamine B (**57**).

The tetrahydroisoquinoline **60**, which has stereogenic centers at C-1 and C-3, was prepared as the major diastereomer in a Bischler-Napieralski cyclization step using $POCl_3$ in combination with 2-methylpyrazine, to afford the corresponding imine in 73% yield. The crucial intermediate, formamide **59**, in turn, was prepared from the chiral primary amine obtained from the commercially available 1-bromo-3,5-difluorobenzene (**58**) via several steps. The imine was then treated with MeMgCl in Et_2O at low temperature to produce korupensamine B (**57**) in 85% isolated yield with excellent *trans* diastereoselectivity (>20:1 dr) (Scheme 1.9).

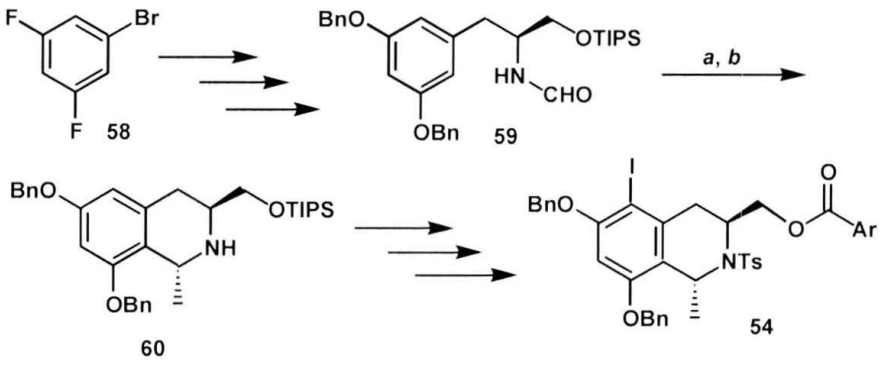

a: $POCl_3$, 2-methylpyrazine,CH_2Cl_2, 0 ^{0}C to rt, 73%; ***b***: MeMgCl.Et_2O, -78 ^{o}C to rt, 85% (trans:cis > 20:1).

Scheme 1.9. Synthesis of the tetrahydroisoquinoline **54.**

1.3.2 Asymmetric Pomerantz-Fritsch and related reactions.

Acid-catalyzed cyclization of a benzalaminoacetal results in the formation of the isoquinoline nucleus. This reaction was first reported by Pomeranz and Fritsch[37] and with some of the modifications described below, has been used in the synthesis of a variety of isoquinoline and other isoquinoline-ring based compounds. The basic reaction is carried out in two stages. In the first step, condensation of an aromatic aldehyde and an aminoacetal leads to the formation of a benzalaminoacetal (a Schiff base). In the second step, an acid-catalyzed ring closure leads to the isoquinoline (Scheme 1.10).

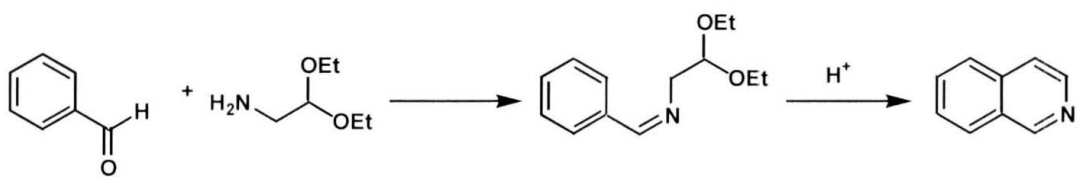

Scheme 1.10. General formula for the Pomeranz and Fritsch reaction.

An alternative route is the Schlittler-Müller modification,[38] which involves the condensation of a benzylamine with glyoxal semiacetal (Scheme 1.11).

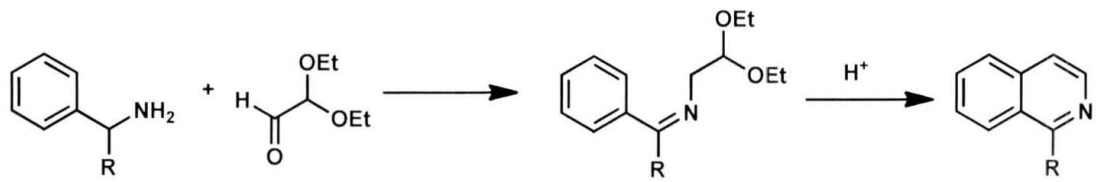

Scheme 1.11. General formula for the Schlittler-Müller modification reaction.

The Bobbitt modification of the Pomeranz-Fritsch methodology involves the reductive cyclization of an *N*-benzylaminoacetaldehyde to afford the 1,2,3,4-tetrahydroisoquinoline core.[39]

Chrzanowska *et al.*[40] synthesized (*S*)-(-)- and (*R*)-(+)-*O*-methylbharatamines (**65**) in high enantiomeric purity using the Pomeranz-Fritsch-Bobbitt methodology (Scheme 1.12). In this synthetic approach, a new stereogenic centre was created by addition of the Pomeranz-Fritsch imine **61** to the benzylic carbanion generated from enantiopure *o*-toluamide. Treatment of (*S*)-(-)-*O*-toluamide **62**, or its (*R*)-(+)-enantiomer with *n*-butyllithium, followed by addition of the prochiral imine **61** at -72 °C leads to the formation of compound **63**. Further transformation, involving LAH-reduction of **63** to give compound **64**, followed by cyclization-hydrogenolysis, resulted in the formation of (*S*)-(-)-methylbharatamine (**65**) in 88% *ee*, or its corresponding enantiomer in 73% *ee*.

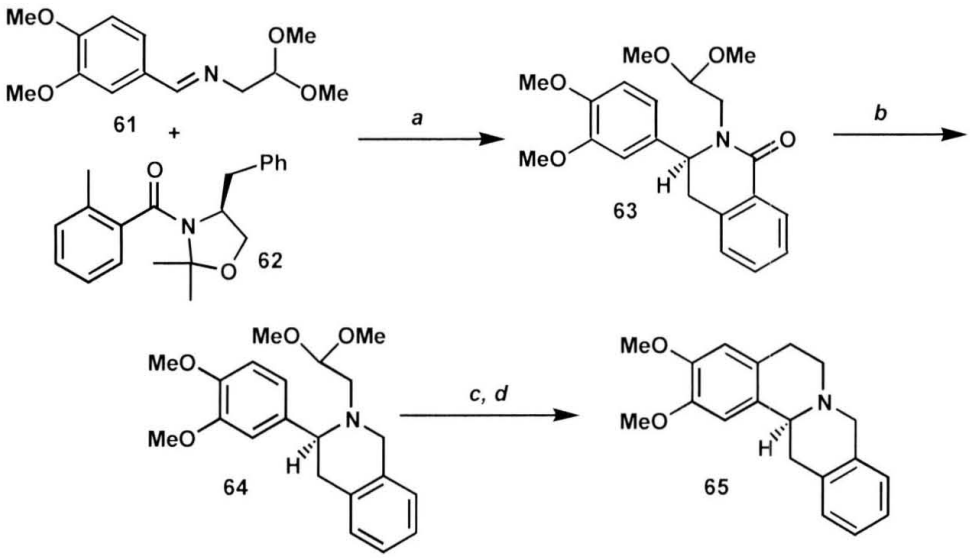

a: *n*-BuLi, THF, -78 °C; ***b***: $LiAlH_4$, THF; ***c***: 5.0 M HCl_{aq}; ***d***: $NaBH_4$/TFA.

Scheme 1.12. Synthesis of (*S*)-(-)-methylbharatamine (**65**).

1.3.3 Asymmetric Pictet-Spengler syntheses.

The Pictet-Spengler reaction which was discovered in 1911 by Amé Pictet and Theodor Spengler[41] has remained an important reaction in alkaloid and pharmaceuticals synthesis. The reaction is an important acid-catalyzed transformation for the synthesis of tetrahydroisoquinolines from carbonyl compounds and β-arylethylamines (Scheme 1.13). The reactions are usually carried out in an aprotic solvent in the presence of an acid catalyst and afford high yields when the number of electron–donating groups on the phenylethylamine aromatic ring is increased.

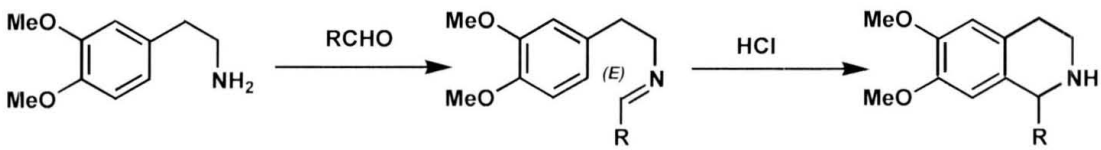

Scheme 1.13. General scheme for the Pictet-Spengler reaction.

The regioselectivity for isoquinoline synthesis in a Pictet–Spengler cyclization depends on the electron-donating group in the aromatic ring of phenylethylamine, and that the less sterically-hindered *ortho* position is the predominant cyclization site. Some other catalysts and dehydrating agents such as trifluoromethanesulfonic acid, acetic acid, and trifluoroacetic acid can also be used to increase the yield and regioselectivity. No relationship, however, has been established between this reaction's pH and yield, or its regioselectivity.[42] When an aldehyde other than formaldehyde is used, a new chiral center at C-1 is generated. The chirality of this new centre can be controlled by using a chiral auxiliary introduced to either the β-arylethylamine or the aldehyde component, thereby effecting involving a diastereoselective synthesis.

1.3.3.1 Using chiral amines.

The use of a chiral amine or carbonyl component in an intermolecular Pictet-Spengler condensation is a valuable strategy for obtaining chiral iminium intermediates and achieving the chirality to the newly-generated C-1 stereocenter.

Using a chiral cyclohexyl-based auxiliary on **66**[43] in the synthesis of (*R*)-(-)-laudanosine (**68**) is an example of using a chirally-modified amine to achieve the chirality in C-1 position (Scheme 1.14).

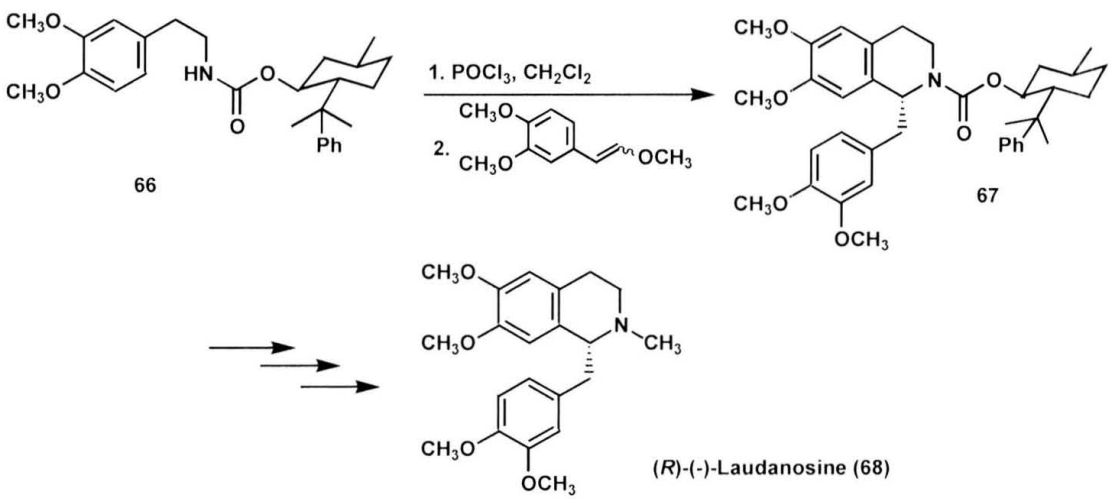

Scheme 1.14 Synthesis of (*R*)-(-)-laudanosine (**68**).

1.3.3.2 Using chiral aldehydes or chiral catalysts.

Many natural and biologically important alkaloids have been synthesized using optically active carbonyl components in a Pictet-Spengler reaction as one of the key steps. These include the use of sulfur chirality, cyclohexyl derivatives such as menthol, and bicyclics such as camphor, and amino acid-derived aldehydes.[44]

Czarnocki *et al.*[45] used the chiral aldehyde **70** to control the formation of the chiral center at C-1 and to achieve the total synthesis of (*S*)-(+)-laudanosine **72** in 80% yield and 78.9% *ee* (Scheme 1.15).

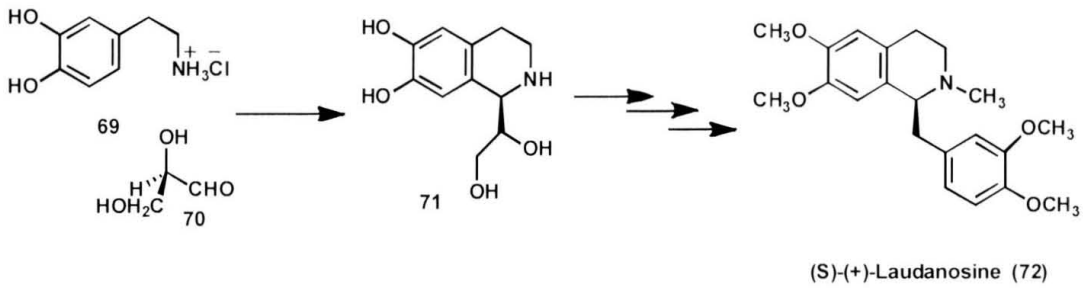

Scheme 1.15. Use of a chiral aldehyde to form the desired stereocenter at C-1.

1.4 Conclusion

The isoquinoline alkaloids are a large group of naturally occurring compounds that have demonstrated significant biological activities. Some of these may eventually find their way into the arsenal of therapeutic agents that are increasing importance. In many cases the classical methodologies, with minor modifications, have been successfully employed to afford highly enantioselective products. In the following chapters, the enantioselective syntheses are described of selected isoquinoline alkaloids. In particular, the syntheses of benzyltetrahydroisoquinolines (*S*)- and (*R*)-*N*-norlaudanidine and tetrahydroprotoberberine alkaloids, (*S*)-tetrahydropalmatrubine and (*S*)-corytenchine are reported. The syntheses were achieved using the chiral auxiliaries (*S*)- or (*R*)–α-methylbenzylamine in Bischler-Napieralski cyclization-reduction strategies (Chapter 2). In Chapter 3 the enantioselective synthesis of (1*R*,1′*S*)-temuconine, a bisbenzyltetrahydroisoquinoline alkaloid is described. In Chapter 4 a second set of targets using the same chiral auxiliary-mediated strategy to produce potential anthrax lethal factor inhibitors is described.

References

(1) Meissner, W. *J. Chem. Phys.* **1819**, *25*, 379-384.

(2) (a) Hess, M. *Alkaloids: Nature's Curse or Blessing?:* Wiley-VCH: New York, **2002**; pp. 1-5. (b) *Ibid*, pp. 11-113. (c) *Ibid*, pp. 303-312. (d) *Ibid*, pp. 36-54. (e) *Ibid*, pp. 259-282.

(3) Daly, J. W.; Brown, G. B.; Mensah-Dwumah, M.; Myers, C. W. *Toxicon* **1978**, *16*, 163-188.

(4) Clark, A. M.; Hufford, D. C. In *The Alkaloids: Antifungal Alkaloids;* Cordell, G., Ed.; Academic Press: **1992**; Vol. 42, pp. 117-150.

(5) Wink, M. In *The Alkaloids*; Cordell, G., Ed.; Academic Press: **1993**; Vol. 43, pp. 1-118.

(6) Daly, J. W.; Garraffo, H. M; Spande, T. F. *The Alkaloids*: *Amphibian Alkaloids*; Cordell, G., Ed., Academic Press: **1993**; Vol. 43, pp. 185-288.

(7) Roberts, M. F.; Wink, M. *Alkaloids-Biochemistry: Ecological Functions and Medical Applications*; Plenum Press: New York, **1998**; pp. 1-486.

(8) Wink, M. *Theor. Appl. Genet.* **1988**, *75*, 225-233.

(9) Wink, M. *The role of quinolizidine alkaloids in plant insect interaction*: *Insect plant interactions;* Bernays E. A., Ed.; **1992**, Vol. IV, 133-169.

(10) (a) Martin, M. L.; Diaz, M. T.; Montero, M. J.; Prieto, P.; Roman, L. S.; Cortes, D. *Planta Med.* **1993**, *59*, 63–67. (b) Kashiwada, Y.; Aoshima, A.; Ikeshiro, Y.; Chen, Y. P.; Furukawa, H.; Itoigawa, M.; Fujioka, T.; Mihashi, K.; Cosentino, L. M.; Morris-Natschke, S. L.; Lee, K. H. *Bioorg. Med. Chem.* **2005**, *13*, 443–448.

(11) Barton, D. H.; Kirby, G. W.; Steglich, W.; Thomas, G. M.; Battersby, A. R.; Dobson, T. A.; Ramuz, H. *J. Chem. Soc.* **1965**, 2423–2438.

(12) Bhadra, K.; Kumar, G. S. *Med. Res. Rev.* **2010**, DOI 10.102/med.

(13) Palchaudhuri, R.; Hergenrother, P. J. *Curr. Opin. Biotech.* **2007**, *18*, 497-503.

(14) Lerman, L. S. *J. Mol. Biol.* **1961**, *3*, 18-30.

(15) Snyder, R. D. *Mutat. Res.* **2007**, *623*, 72-82.

(16) Snyder, R. D.; McNulty, J.; Zairov, G.; Ewing, D. E.; Hendry, L. B. *Mutat. Res.* **2005**, *578*, 88-99.

(17) (a) Krey, A. K.; Halm, F. E. *Science* **1969**, *166*, 755–757. (b) Saran, A.; Srivastava, S.; Coutinho, E.; Maiti, M. *Indian J. Biochem. Biophys.* **1995**, *32*, 74–77. (c) Li, W.Y.; Lu, H.; Xu, C. X.; Zhang, J. B.; Lu, Z. H. *Spectrosc. Lett.* **1998**, *31*, 1287–1298. (d) Li, W. Y.; Lu, Z. H. *Microchem. J.* **1998**, *60*, 84–88. (e) Gong, G. Q.; Zong, Z. X.; Song, Y. M. *Spectrochim. Acta Part A* **1999**, *55*, 1903–1907. (f) Mazzini, S.; Bellucci, M. C.; Mondelli, R. *Bioorg. Med. Chem.* **2003**, *11*, 505–514. (g) Kumar, G. S.; Das, S.; Bhadra, K.; Maiti, K. *Bioorg. Med. Chem.* **2003**, *11*, 4861–4870.

(18) Chen, W. H.; Pang, J. Y.; Qin, Y.; Peng, Q.; Cai, Z.; Jiang, Z. H. *Bioorg. Med. Chem. Lett.* **2005**, *15*, 2689–2692.

(19) Kim, S. A.; Kwon, Y.; Kim, J. H.; Muller, M. T.; Chung, I. K. *Biochemistry* **1998**, *37*, 16316–16324.

(20) Park, H. S.; Kim, E. H.; Sung, Y. H.; Kang, M. R.; Chung, I. K. *Bull. Kor. Chem. Soc.* **2004,** *25*, 539–544.

(21) Kobayashi, Y.; Yamashita, Y.; Fujii, N.; Takaboshi, K.; Kawakami, T.; Kawamura, M.; Mizukami, T.; Nakano, H. *Planta Med.* **1995**, 61, 414–418.

(22) Li, T. K.; Bathory, E.; LaVoie, E. J.; Srinivasan, A. R.; Olson, W. K.; Sauers, R. R.; Liu, L. F.; Pilch, D. S. *Biochemistry* **2000**, *39*, 7107–7116.

(23) For a review, see: (a) Whaley, W. M.; Govindachari, T. R. *Org. React.* **1951**, *6*, 74–150. (b) Jadhav, V. B.; Nayak, S. K.; Row, T. N. G.; Kulkarni, M. V. *Eur. J. Med. Chem.* **2010**, *45*, 3575–3580. (c) Bringmann, G.; Gulder, T.; Hertlein, B.; Hemberger, Y.; Meyer, F. *J. Am. Chem. Soc.* **2010**, *132*, 1151–1158.

(24) For reviews, see: (a) Cox, E. D.; Cook, J. M. *Chem. Rev.* **1995**, *95*, 1797–1842. (b) Whaley, W. M.; Govindachari, T. R. *Org. React.* **1951**, 6, 151–190. For recent examples, see: (c) Znabet, A.; Zonneveld, J.; Janssen, E.; De Kanter, F. J.; Helliwell, M.; Turner, N. J.; Ruijter, E.; Orru, R. V. *Chem. Commun.* **2010**, *46*, 7706–7708. (d) Barbero, M.; Bazzi, S.; Cadamuro, S.; Dughera, S. *Tetrahedron Lett.* **2010**, *51*, 6356–6359. (e) Magnus, N. A.; Ley, C. P.; Pollock, P. M.; Wepsiec, J. P. *Org. Lett.* **2010**, *12*, 3700–3703.

(25) (a) Coppola, G. M. *J. Heterocycl. Chem.* **1991**, *28*, 1769–1772. (b) Azzena, U.; Pisano, L.; Pittalis, M. *Heterocycles* **2004**, *63*, 401–409. (c) Tokitoh, N.; Okazaki,

R. *Bull. Chem. Soc. Jpn.* **1988**, *61*, 735–740. (d) Louafi, F.; Hurvois, J. P.; Chibani, A.; Roisnel, T. *J. Org. Chem.* **2010**, *75*, 5721–5724. (e) Liermann, J. C.; Opatz, T. *J. Org. Chem.* **2008**, *73*, 4526–4531.

(26) Bobbitt, J. M.; Steinfeld, S.; Weisgraber, K. H.; Dutta, S. *J. Org. Chem.* **1969**, *34*, 2478–2479.

(27) Nagubandi, S.; Fodor, G. *Heterocycles* **1981**, *15*, 165-177.

(28) Fodor, G.; Gal, J.; Phillips, B. *Angew. Chem., Int. Ed. Engl.* **1972**, *11*, 919-920.

(29) Nagubandi, S.; Fodor, G. *Tetrahedron* **1980**, *36*, 1279-1300.

(30) Zassinovich, G.; Mestroni, G. *Chem. Rev.* **1992**, *92*, 1051-1069.

(31) Uematsu, N.; Fujii, A.; Hashiguchi, S.; Ikariya, T.; Noyori, R. *J. Am. Chem. Soc.* **1996**, *118*, 4916–4917.

(32) Memetzidis, G.; Stambach, J. F.; Jung, L.; Schott, C.; Heitz, C.; Stoclet, J. C. *Eur. J. Med. Chem.* **1991**, *26*, 605–611.

(33) Cheng, J.; Yang, Y. *J. Org. Chem.* **2009**, *74*, 9225–9228.

(34) Werner, F.; Blank, N.; Opatz, T. *Eur. J. Org. Chem.* **2007**, 3911–3915.

(35) Wang, Y.; Georghiou, P. E. *Org. Lett.* **2002**, *4*, 2675-2678.

(36) Huang, S.; Petersen, T.; Lipshutz, B. *J. Am. Chem. Soc.* **2010**, *132*, 14021-14023.

(37) (a) Pomeranz, C. *Monatsh. Chem.* **1893**, *14*, 116-119. (b) Fritsch, P. *Ber.* **1893**, *26*, 419-422.

(38) Schlittler, E.; Müller, J. *Helv. Chim. Acta* **1948**, *31*, 1119-1132.

(39) (a) Bobbitt, J. M.; Kiely. J. M.; Khanna, K. L.; Ebermann, R. *J. Org. Chem.* **1965**, *30*, 2247-2250. (b) Bobbitt, J. M.; Steinfeld, A. S.; Weisgraber, K. H.; Dutta, S. *J. Org. Chem.* **1969**, *34*, 2478-2479.

(40) Chrzanowska, M.; Dreas, A.; Rozwadowska, M. D. *Tetrahedron asymm.* **2005**, *16*, 2954- 2958.

(41) Pictet, A.; Spengler, T. *Ber.* **1911**, *44*, 2030-2036.

(42) Quevedo, R.; Baquero, E.; Rodriguez, M. *Tetrahedron Lett.* **2010**, *51*, 1774-1778.

(43) Comins, D. L.; Thakker, P. M.; Baevsky, M. F.; Badawi, M. M. *Tetrahedron* **1997**, *53*, 16327-16340.

(44) Taylor, M. S.; Jacobsen, E. N. *J. Am. Chem. Soc.* **2004**, *126*, 10558-10559.

(45) Czarnocki, Z.; Maclean, D. B.; Szarek, W. A. *Can. J. Chem.* **1986**, *64*, 2205-2011.

Chapter 2

Enantioselective Syntheses of Selected Benzyltetrahydroisoquinolines: Syntheses of (*S*)- and (*R*)-*N*-Norlaudanidine: Trace Opium Constituents
&
Enantioselective Syntheses of Tetrahydroprotoberberines: (-)-(*S*)-Tetrahydropalmatrubine and (-)-(*S*)-Corytenchine

Part of the work described in this chapter has been published in

Tetrahedron Lett. **2010**, *51*, 177-180.

&

J. Nat. Prod. **2010**, *73*, 1427-1430.

Chapter 2

Enantioselective Syntheses of Selected Benzyltetrahydroisoquinolines: Syntheses of (*S*)- and (*R*)-*N*-Norlaudanidine: Trace Opium Constituents

2.1 Introduction.

Benzyltetrahydroisoquinolines ('BTHIQ') which contain a B ring that is reduced at the C-1, C-2 and C-3, C-4 positions are known to be key biosynthetic precursors to many naturally-occurring alkaloids. These include morphine and codeine which are found in, or are derived from, the opium poppy *Papaver somniferum*.[1,2,3,4,5] The global problem of narcotics abuse, especially involving heroin (**1**) and illegal opium poppy cultivation and processing, has prompted renewed research into the analytical chemistry of heroin[5,6] which also includes the detection and analysis of the minor BTHIQ constituents. Some of these constituents of interest (Figure 2.1) include (*S*)-(+)-laudanosine (**2**), (±)-reticuline (**3**), (*S*)-(+)-codamine (**4**) and (±)-laudanine (**5**). Reticuline and laudanine, which is also known as "racemic laudanidine", are known to occur in both enantiomeric forms in opium.[7]

The recent report by Toske *et al.*[5] which described the GC-MS analysis of neutral heroin impurities derived from BTHIQs **1-5**, piqued our interest in the application of our synthetic methodology towards the enantioselective syntheses of each of the (*S*)- and (*R*)-enantiomers of *N*-norlaudanidine (**6a**) and (**6b**), respectively, and to unambiguously assign the chirality of these compounds with X-ray crystallographic proof. This work,

which was published by us in 2010,[8] forms the basis of the following section of this thesis.

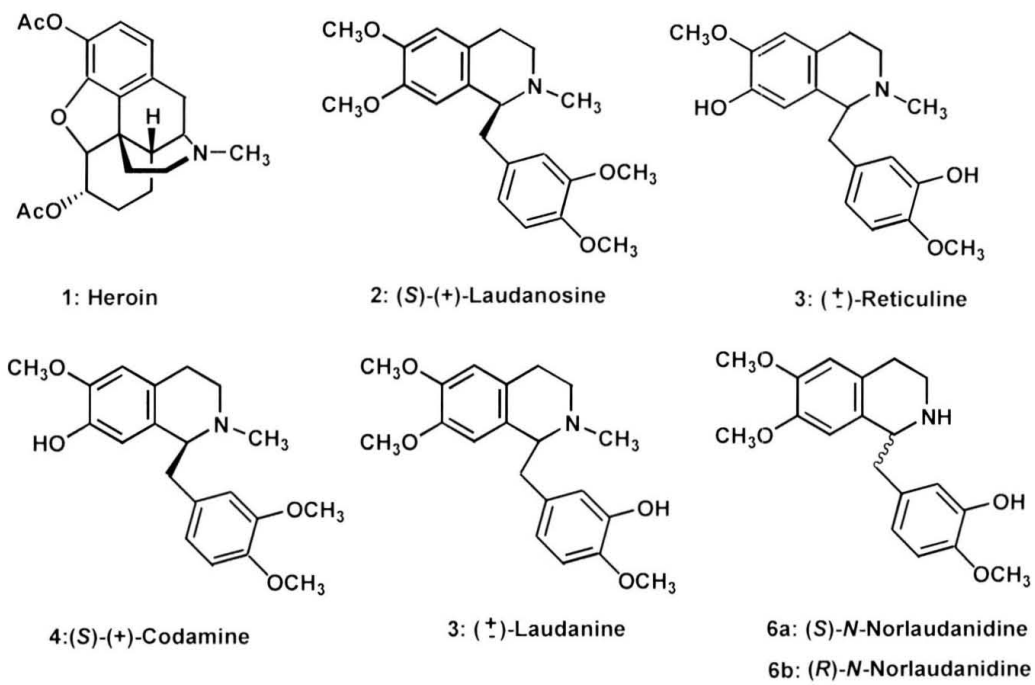

Figure 2.1. Structures of heroin (**1**) and some BTHIQ alkaloids.

(-)-*N*-Norlaudanine is a component part of the pathway for the biosynthesis of the benzylisoquinoline alkaloids in *Papaver somniferum*.[7] It has been found to be incorporated into palaudine (**7**) another minor benzylisoquinoline constituent found in opium (Figure 2.2).[9] The fact that radiolabelled *N*-norlaudanine, whose absolute configuration was not defined by Brochmann-Hannssen and co-workers,[7] was incorporated into palaudine (**7**) was evidence that complete methylation was not necessary for dehydrogenation to take place in *Papaver somniferum*.

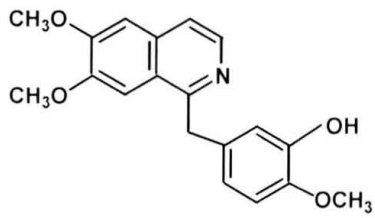

Figure 2.2. Structure of Palaudine (**7**).

The 1960's and 70's witnessed a great deal of interest and advances in the chemistry and biogenetic aspects of the BTHIQ alkaloids, due primarily to their significant and important medicinal and pharmacological activities. The groups of Battersby[10] and Brochmann-Hannssen[7] published a series of papers on the biosynthetic pathways of benzylisoquinolines and BTHIQs, in particular with reference to the opium alkaloids.

Many of the structural elucidations of BTHIQs in the past were conducted with painstaking degradation studies and correlations with reference compounds whose absolute configurations were unambiguously defined.[11] In some instances, X-ray crystallographic determinations have been obtained on key BTHIQs. In most cases however, in which the total syntheses of target BTHIQs have been reported, the syntheses have yielded only racemic mixtures, even though the chirality of a large number of naturally-occurring BTHIQs is due to the presence of only a single stereogenic centre at the C-1 position of the tetrahydroisoquinoline unit.

Enantioselective syntheses of BTHIQ and bisbenzyltetrahydroisoquinoline ("BBIQ") alkaloids via the Bischler-Napieralski cyclization reaction in particular, have recently been reviewed by Chrzanowska and Rozwadowska,[12,13] and by us.[14] In efforts directed toward the syntheses of some selected BBIQs by the Georghiou group, the chiral auxiliary (*S*)-α-methylbenzylamine was used for the enantioselective synthesis of (-)-tejedine (**8**), a *seco*-bisbenzyltetrahydroisoquinoline, via a Bischler-Napieralski cyclization-reduction sequence.[15]

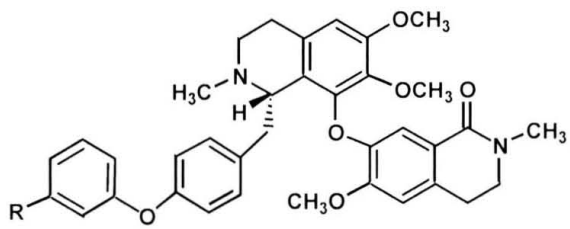

8: Tejedine R = CO_2CH_3
9: Baluchistanamine R = CHO

Figure 2.3. Structure of Tejedine (**8**).

The enantioselective synthesis of each of the enantiomers of *N*-norlaudanidine **6a** and **6b**, the minor *Papaver somniferum* opium benzyltetrahydoisoquinoline alkaloids, using the same chiral auxiliary-mediated Bischler-Napieralski cyclization-sodium borohydride reduction strategy are described in this chapter.

2.1.1 Results and discussion.

The Bischler-Napieralski cyclization followed by hydride reduction of the 3,4-dihydroisoquinolinium salts derived from the precursor amine which is functionalized with a chiral auxiliary has been used for the stereoselective synthesis of chiral benzyltetrahydroisoquinoline alkaloids. Many different chiral auxiliaries have been used in such reactions, and the number and the position of the electron-donating groups on the aryl ring of the β-arylethylamides influence the regioselectivity of the reaction.[16] The choice, however, of the reducing agent in the next step to produce the tetrahydroisoquinoline ring is crucial since it generates the stereogenic center at C-1.[17]

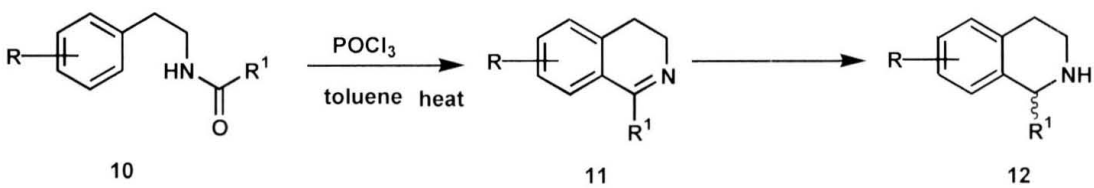

10 11 12

Scheme 2.1. The Bischler-Napieralski cyclization reaction.

Outlined in Scheme 2.2 is an initial retrosynthetic analysis for the enantioselective synthesis of each of these *N*-norlaudanidine enantiomers. The first retrosynthetic disconnection gives the amide **13a,b** and the second dissects the amide **13a,b** into the key intermediates: the carboxylic acid **15** and the chiral amine **17a,b** having either (*S*)- or (*R*)-α-methylbenzylamine as the chiral auxiliary. These two intermediates are required for the Schotten-Baumann reaction to afford the amide (**13a,b**).

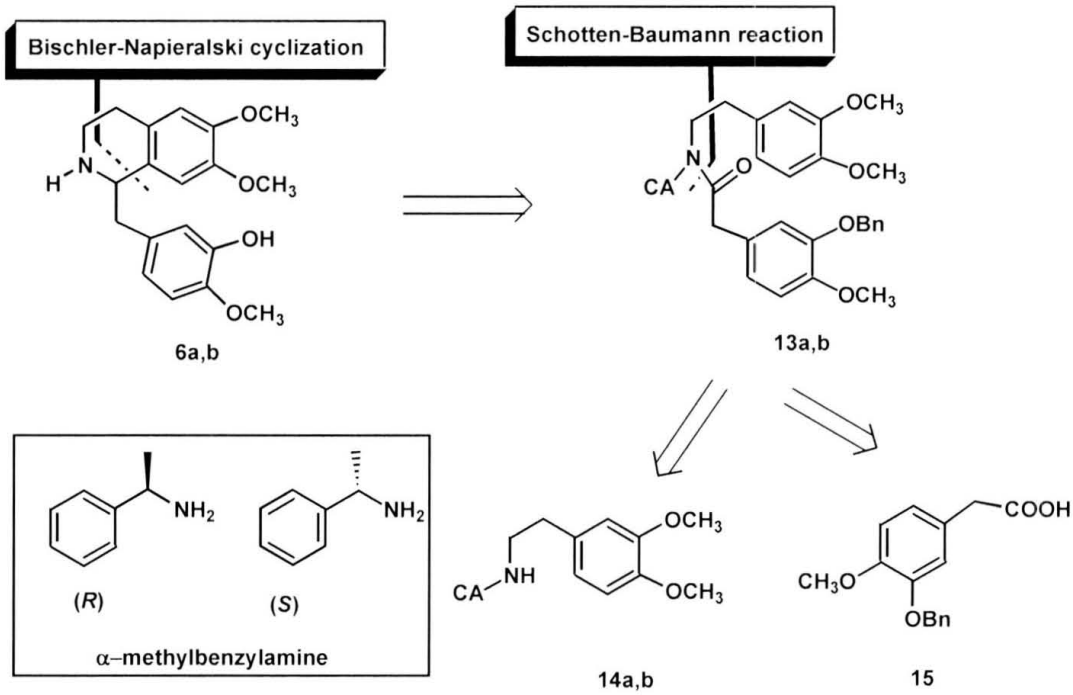

Scheme 2.2. Retrosynthetic analysis for *N*-Norlaudanine **6a,b**.

2.1.1.1 Synthesis of the Key Intermediate 15.

The benzyl component was synthesized via the intermediate **15**, which was obtained in 78% overall yield[18] over 5 steps starting from commercially-available 3-hydroxy-4-methoxybenzaldehyde (**16**) which has substituent groups that are suitable for further functionalization. Selective protection and deprotection of those functional groups are necessary in this synthesis, and the needed protecting groups should be easily removed at a later stage. The benzyl group was chosen as the protecting group since it can be easily removed in the final step of the total synthesis and is also stable during the synthesis in both acid and basic conditions.

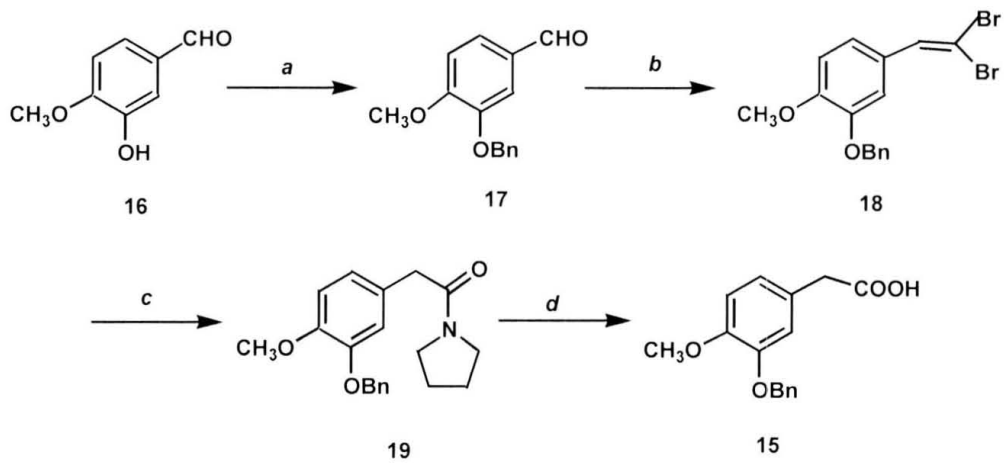

a: BnBr, DMSO, 98%; ***b:*** CBr_4, PPh_3, CH_2Cl_2, 93%; ***c:*** pyrrolidine, H_2O, rt, 91%; ***d:*** 1.0 M $HCl_{(aq)}$/dioxane, rt, 94%.

Scheme 2.3. Synthesis of the arylacetic acid **15**.

Protection of the phenolic group as the benzyl ether **17** was achieved in 98% yield and was followed by homologation of the carbonyl group using the Kim and coworkers method.[19] The required dibromoalkene **18** was prepared efficiently by the Wittig-type dibromo-olefination of the corresponding aryl aldehyde **17**. The reaction with pyrrolidine gave a high yield of the product, amide **19**. Hydrolysis of the amide afforded an excellent yield of the corresponding acid **15** under mild conditions.

2.1.1.2 Synthesis of the Chiral Auxiliary-Protected Amines 14a,b.

With the only difference being the choice of the chiral auxiliary, the protected amines **14a** or **14b** could be obtained in 70% overall yield in 6 steps from vanillin (Scheme 2.4).

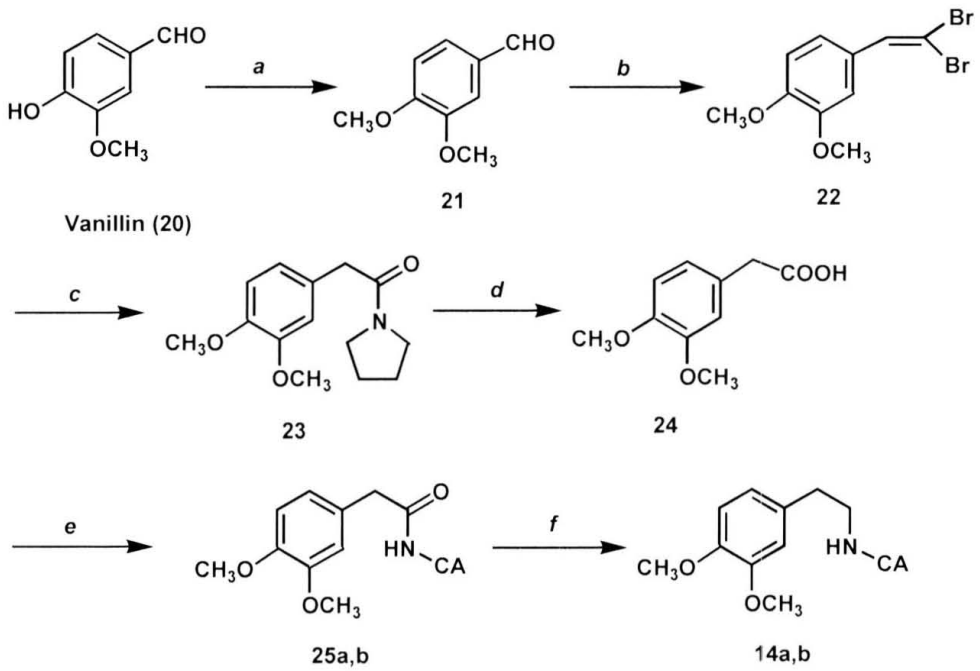

a: $(CH_3)_2SO_4$, K_2CO_3, acetone, 95%; ***b:*** CBr_4, PPh_3, CH_2Cl_2, 92%; ***c:*** pyrrolidine, H_2O, rt, 91%; ***d:*** 1.0 M HCl(aq)/dioxane; ***e:***1. $(COCl)_2$, benzene, 96%; 2. CA = (*S*)- or (*R*)-α-methylbenzylamine, 5% NaOH(aq), CH_2Cl_2, 92%; ***f:*** B_2H_6, THF, $BF_3 \bullet Et_2O$, 86%.

Scheme 2.4. Synthesis of the chiral auxiliary-protected amines **14a,b**.

Commercially-available vanillin (**20**) could be converted into the corresponding 3,4-dimethoxybenzaldhyde (**21**) in 95% yield using dimethyl sulfate and potassium carbonate in acetone. The same method for homologation was achieved using Kim's method to produce the dibromoalkene **22** in 92% yield, which was followed by amide formation using pyrrolidine as a solvent. The amide **23** could be easily hydrolyzed into the corresponding phenylacetic acid (**24**) under mild conditions using 1.0 M $HCl_{(aq)}$/dioxane. Reaction of the phenylacyl chloride, formed *in situ* from phenylacetic acid (**24**), with (*S*)-(+)-α-methylbenzylamine under Schotten-Baumann conditions

resulted in the formation of the chiral auxiliary-containing amide **25a** (92%). The enantiomer **25b**, was obtained in the same manner using (*R*)-α-methylbenzylamine as the chiral auxiliary. Reduction of **25a** or **25b** to the corresponding secondary chiral auxiliary-containing amines **14a** or **14b** was accomplished in 86% yield via BF_3•etherate-mediated reactions with B_2H_6 in THF.

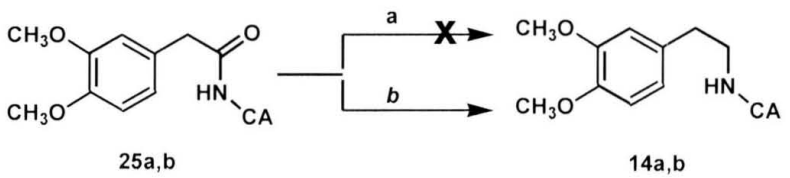

25a,b **14a,b**

a: $LiAlH_4$, THF, 0%; ***b***: B_2H_6, THF, BF_3• Et_2O, 86%.

Scheme 2.5. Reduction of the chiral auxiliary-protected amides **25a,b**.

Although the use of $LiAlH_4$ in THF has been reported to be a suitable reagent for the reduction of the amide group, using this reagent to reduce **25a** (or **25b**) did not succeed. Instead, the use of borane tetrahydrofuran complex (BH_3•THF) with a catalytic amount of boron trifluoride etherate (BF_3•THF) afforded the desired products **14a** or **14b**, respectively in 86% yields (Scheme 2.5).

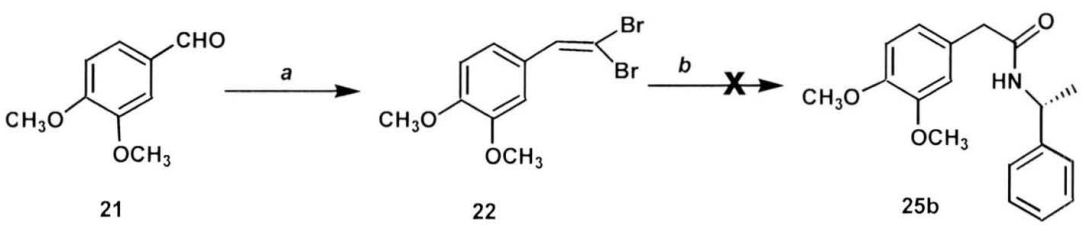

21 **22** **25b**

a: CBr_4, PPh_3, CH_2Cl_2, 92%; ***b:*** (*R*)-α-methylbenzylamine, H_2O, rt.

Scheme 2.6. Formation of the chiral auxiliary-containing amide **25b**.

Although an aqueous solution of pyrrolidine produced the corresponding amide **23** in good yield, in order to shorten the synthesis, a trial experiment was conducted using (*R*)-α-methylbenzylamine, a primary amine, as the solvent. However, the expected amide **25b** product was only obtained in poor yield (Scheme 2.6) with many products seen by the TLC analysis.

2.1.1.3 *Completion of the Total Syntheses.*

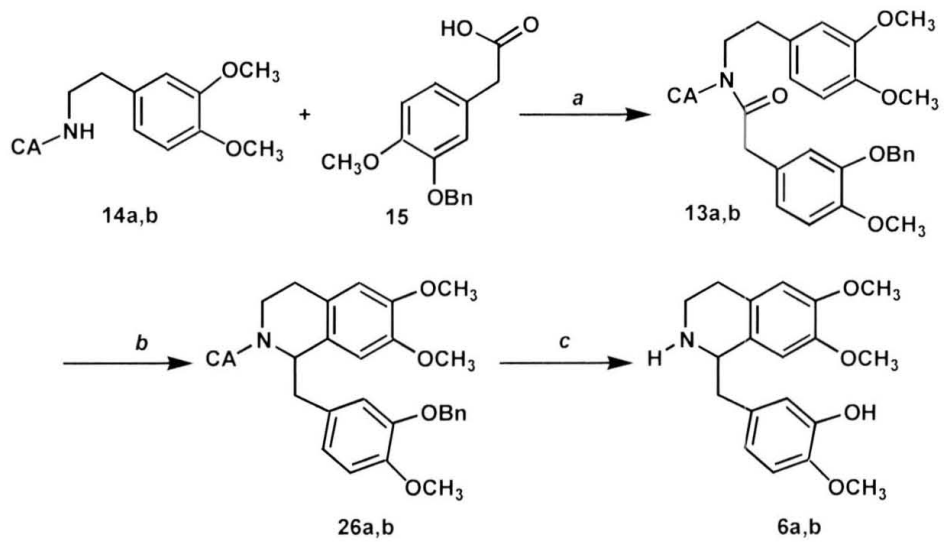

a: 1. **15**, $(COCl)_2$, benzene; 2. **14a,b,** 5% NaOH(aq), CH_2Cl_2, 72%; ***b:*** 1. $POCl_3$, benzene; 2. $NaBH_4$, MeOH, 75%, (95% *de*); ***c:*** H_2, 10% Pd/C, EtOH, EtOAc, 10% HCl(aq): **6a** or **6b** ~72%.

Scheme 2.7. Completion of the total synthesis of (*S*)- and (*R*)-*N*-norlaudanidine.

Schotten-Baumann amidation between **14a** (or **14b**) and **15** formed the amides **13a** (or **13b**) in 72% yields. Bischler-Napieralski cyclization-$NaBH_4$ reduction of **13a** or **13b** afforded **26a** and **26b** respectively, with ~95% *de*, as determined from integrations of

the signals at δ = 5.82 ppm (major) and 5.89 ppm in the respective ^{1}H-NMR spectra of the major and minor diastereomers in the crude reaction products (Figure 2.4).

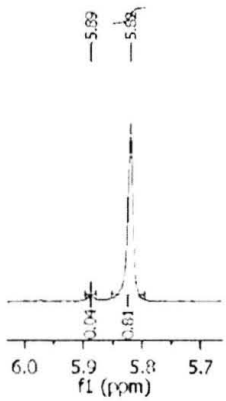

Figure 2.4. ^{1}H-NMR spectrum of the crude product for compound **27a**.

The Georghiou group has previously shown that (*S*)-α-methylbenzylamine could be effectively used as a chiral auxiliary in the Bischler-Napieralski cyclization-reduction sequence in the enantioselective synthesis of (-)-tejedine (**8**) in a high enantiomeric excess.[15] The use of this chiral auxiliary was first reported by Kametani *et al.*[20] However, the optical purity for his products ranged only between 39-44%, presumably because simpler functionalized amides were used in their case (Scheme 2.8).

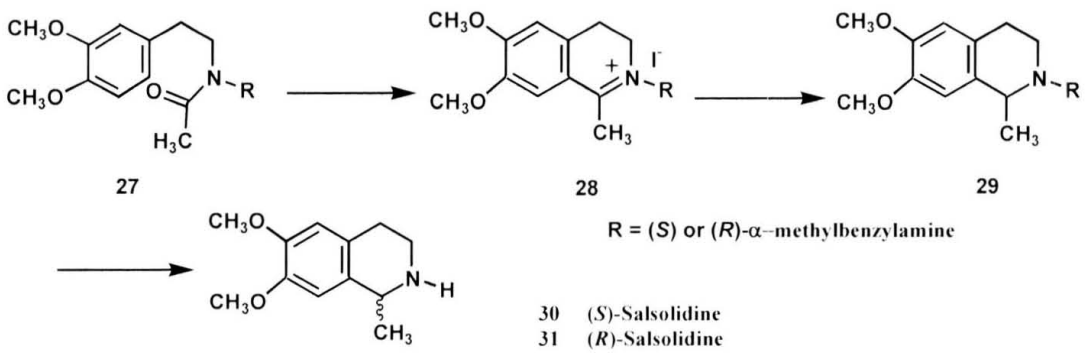

Scheme 2.8. Synthesis of salsolidine using (*S*)- or (*R*)-α-methylbenzylamine.[20]

The presence of the chiral auxiliary most likely causes the reduction to occur from the less-hindered *Si*-face, to produce the desired sterogenic center. This would be as a result of the steric hindrance offered to the *Re*-face by the phenyl ring of the chiral auxiliary and the phenyl group of the benzyl group attached to the C-1 position (Figure 2.5). It is possible that edge-to-π stacking between the phenyl group of the chiral auxiliary and the benzyl part, and also the π stacking interaction between the *O*-benzyl group and the aromatic ring of the dihydroisoquinoline moiety, as shown in Figure 2.5, could be a reasonable source of the stereocontrol for the stereogenic center at C-1.

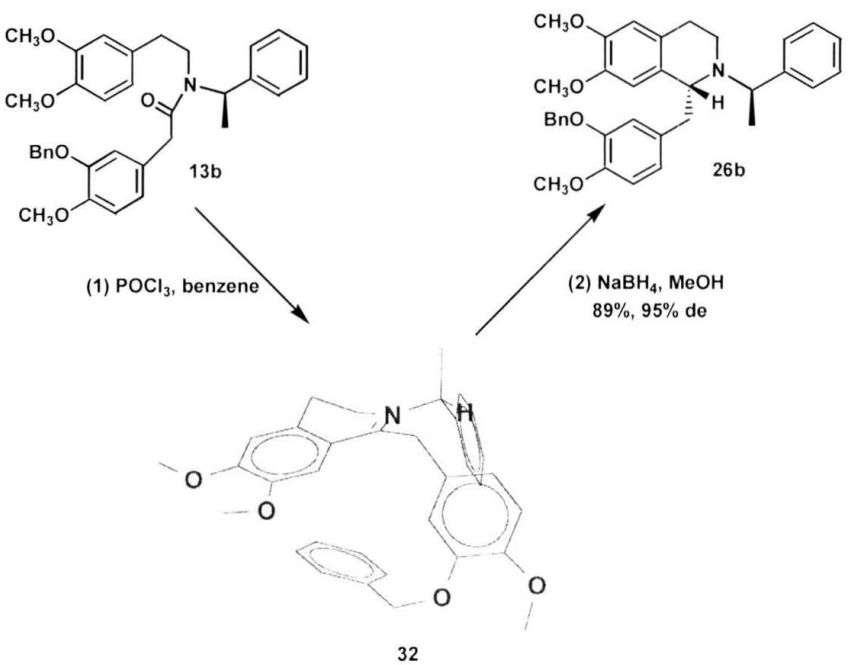

Figure 2.5. Effect of the chiral auxiliary in the direction of the reduction.

The regioselectivity in a Bischler-Napieralski cyclization depends on the position of the electron-donating group in the aromatic ring of the phenylethylamine, and the least sterically-hindered *para* position to that group is the predominant cyclization site. The cyclization to the site *para* to one of the methoxy groups in **14a** or **14b** was clearly preferred to that of the alternative site, due to the steric hinderance offered by the methoxy group.

Catalytic hydrogenolysis of **26a** and **26b** produced the secondary amine with concomitant removal of the benzyl protecting groups, to afford **6a** and **6b**, respectively, in 70% yields. Crystallization afforded **6a** and **6b,** both in optically pure forms with $[\alpha]_D$ values of $+9^o$ and -9^o, respectively.

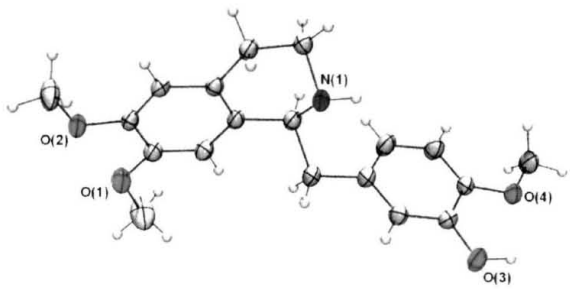

Figure 2.6. 50% Probability ellipsoid ORTEP X-ray structure of **6a**. Solvent benzene molecule omitted for clarity.

In contrast to reports [21] that unprotected secondary amines in similar compounds are unstable, both enantiomers were crystallized from benzene, single-crystal X-ray structures were obtained, and their optical rotations were determined. Figure 2.6 shows the X-ray structure of **6a** which, like compounds **2** and **4**, is both *S* and dextrorotatory.

The X-ray structure revealed that a molecule of benzene is present in the crystal lattice. The single-crystal X-ray of **6b** (Figure 2.7) had similar X-ray data and as expected, it also contained a molecule of benzene in the crystal lattice.

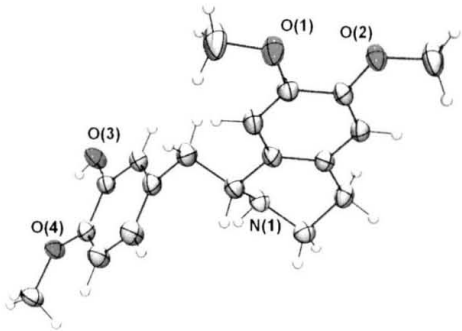

Figure 2.7 50% probability ellipsoid ORTEP X-ray structure of **6b**. Solvent benzene molecule omitted for clarity.

(*S*)-*N*-Norlaudanidine could be effectively used as intermediate in the syntheses of tetrahydroprotoberberines (-)-(*S*)-tetrahydropalmatrubine and (-)-(*S*)-corytenchine, a class of naturally-occurring tetracyclic alkaloids which also contain an isoquinoline core, using an asymmetric Pictet-Spengler cyclization reaction. The strategy is described in the second part of this chapter.

Enantioselective Syntheses of Tetrahydroprotoberberines: (-)-(*S*)-Tetrahydropalmatrubine and (-)-(*S*)-Corytenchine

2.2 Introduction.

BTHIQs are also biosynthetic precursors to the tetrahydroprotoberberine (THPB) alkaloids,[22] a class of naturally-occurring tetracyclic alkaloids which also contain an isoquinoline core,[23] and are a subclass of the protoberberine alkaloids.[24] These compounds are found in at least eight plant families and possess a variety of biological activities including, for example, anti-inflammatory, antimicrobial, antifungal and antitumor properties.[25] The most common of these THPB derivatives, such as (*S*)-tetrahydropalmatrubine (**33**), have oxygen functionalities at the C-2, C-3 and C-9, C-10 positions on the A and D aromatic rings, respectively.[22] Less common is the class of "*pseudo*-THPBs", such as (*S*)-corytenchnine (**34**) and (*S*)-xylopinine (**35**), for which oxygen functionalities are on the C-2, C-3 and C-10, C-11 positions (Figure 2.8).

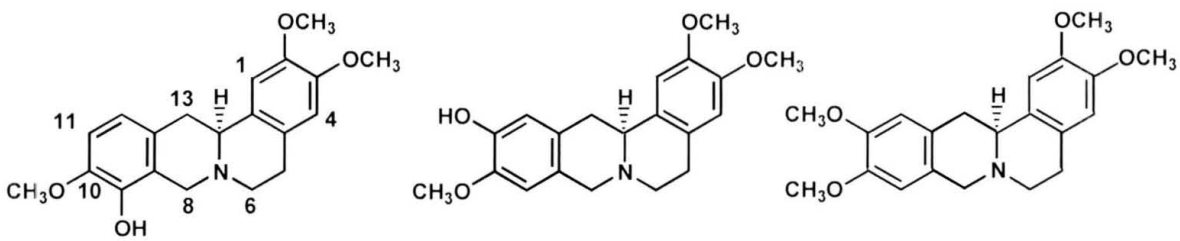

33: (*S*)-Tetrahydropalmatrubine 34: (*S*)-Corytenchine 35: (*S*)-Xylopinine

Figure 2.8. Structures of THPB alkaloids.

(*S*)-*N*-Norlaudanidine (**6a**) and its (*R*)-enantiomer (**6b**), have also been shown by Iwasa *et al.*[22] to be bioconverted into stereoisomeric mixtures of both **33** and **34**. Interestingly, these authors concluded that the *R* isomer of **33** and the *S* isomer of **34** are the major enantiomers formed in their metabolic studies using cell cultures of *Macleaya* and *Corydalis* species, suggesting "stereospecific bioconversion".[22] In this study, however a racemic mixture of (*S*)- and (*R*)-*N*-norlaudanidine, which was isolated from a mixture produced by an acid-mediated reaction of racemic tetrahydropapaverine (**36**), was employed. Among the different strategies that have been used for the construction of a THPB core, the classical Pictet-Spengler reaction,[26] one of the most important acid-catalyzed transformations for the synthesis of tetrahydroisoquinolines from carbonyl compounds and β-arylethylamines, has been the most widely used. As noted before, the reactions are usually carried out in an aprotic solvent in the presence of an acid catalyst and afford high yields when the ring is substituted by two or more electron-donating groups.

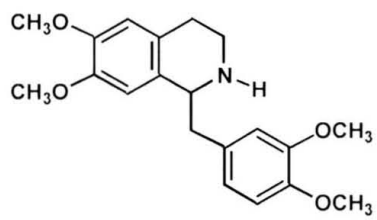

Figure 2.9. Structure of (±) tetrahydropapaverine (**36**).

Many biologically important alkaloids have been synthesized using optically active carbonyl components in a Pictet-Spengler reaction as one of the key steps. These

include the use of cyclohexyl derivatives such as menthol, and bicyclics such as camphor, and amino acid-derived aldehydes.[27]

The use of a chiral amine or carbonyl component in an intermolecular Pictet-Spengler condensation is a valuable strategy for obtaining chiral iminium intermediates and achieving the chirality to the newly-generated C-1 stereocenter. Although several racemic syntheses of THPBs have been reported, there are only a few asymmetric syntheses which have been reported. Asymmetric syntheses have been reported of the (*S*)-(-)-xylopinine (**35**) using different approaches,[28] and also of (*S*)-tetrahydropalmatine (**37**).[29]

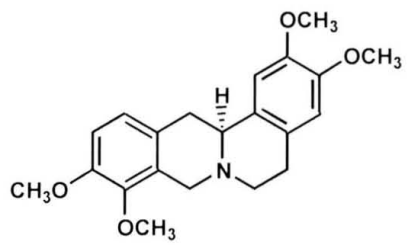

37: (*S*)-Tetrahydropalmatine

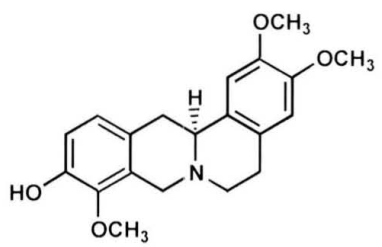

38: (*S*)-Stepholidine

Figure 2.10. Structures of (*S*)-tetrahydropalmatine (**37**) and (*S*)-stepholidine (**38**).

These two compounds, however, are both tetramethoxylated *i.e.* 2,3,10,11- and 2,3,9,10-tetramethoxyTHPBs, respectively. Very recently, Cheng and Yang[30] reported a > 99% *ee* enantioselective synthesis of (*S*)-stepholidine (**38**), a compound which has attracted a great deal of attention since it was reported to display a unique pharmacological profile toward dopamine receptors. This alkaloid has a 2,11-dihydroxy-

3,10-dimethoxy substitution pattern on the A and D rings and was synthesized via an asymmetric Bischler-Napieralski cyclization/reduction approach.

2.2.1 Results and discussion.

Based upon our recent synthetic studies,[8] we targeted the 2,3,10-trimethoxy-9-hydroxy-functionalized THPB, *i.e.*, (*S*)-tetrahydropalmatrubine (**33**) and the 2,3,10-trimethoxy-11-hydroxy-functionalized THPB, *i.e.*, (*S*)-corytenchnine (**34**), using the Pictet-Spengler cyclization reaction,[31]as shown in Scheme 2.9.

Conversion of **6a** into (*S*)-corytenchnine (**34**) was then effected by reaction with formaldehyde (37% formalin) in acetonitrile at 0 °C, followed by addition of $NaBH_3CN$ and then by acetic acid. The reaction afforded almost quantitative formation of **34**, for which the NMR spectroscopic properties are generally in agreement with those reported by da Silva[32] and Martinez-Vazquez[33] who, respectively, isolated **34** from *Xylopia langsdorffiana* (Annonaceae), and from the roots of *Annona cherimolia* Mill. (Annonaceae).

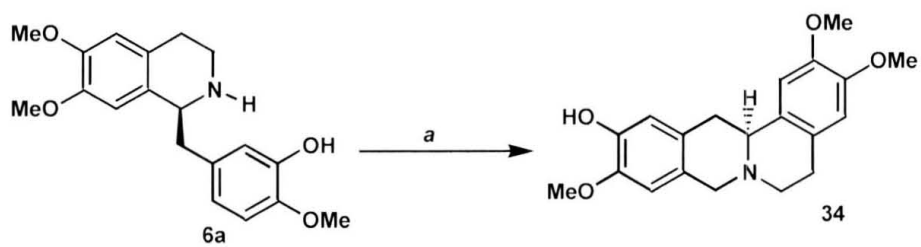

a: 1. HCHO, CH_3CN, 0 °C; 2. $NaBH_3CN$; CH_3CO_2H, 95%.

Scheme 2.9. Synthesis of (*S*)-corytenchnine (**34**).

Since the product obtained in the present study had other physical properties similar to those reported above, but with slight differences in several of the NMR assignments, unequivocal evidence from X-ray crystallography was sought. The X-ray structure shown in Figure 2.11 confirmed the structure as (*S*)-corytechnine (**34**), based upon the absolute structure of the precursor **6a** for which the X-ray structure was previously established.

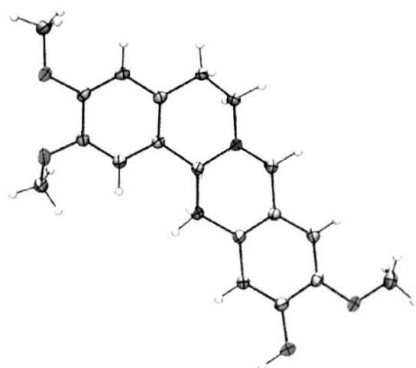

Figure 2.11. X-ray structure of **34** with 50% probability ellipses.

Earlier, Kametani *et al.* reported the isolation of **34** from *Corydalis ochotensis* (Turcz)[34] but had previously synthesized a "dibenzo[*a,g*]quinolizine", which they called "*O*-demethyl-tetrahydroxylopine", having the same substitution pattern as **34**, presumably as a racemate, by a similar procedure from racemic **6a** using formalin in ethanol "without acid".[35] In that paper, the authors reported that they were unable to obtain a compound having the same substitution pattern as tetrahydropalmatrubine (**33**).

When Kametani's methodology was employed as described,[36] a mixture was obtained which by its ^{1}H NMR data showed approximately 70% of **34** and 30% of the

regioisomeric product, for which the spectroscopic properties and X-ray structure (Figure 2.12, as the hydrochloride salt) showed it to be (*S*)-tetrahydropalmatrubine (**33**) (Scheme 2.10).

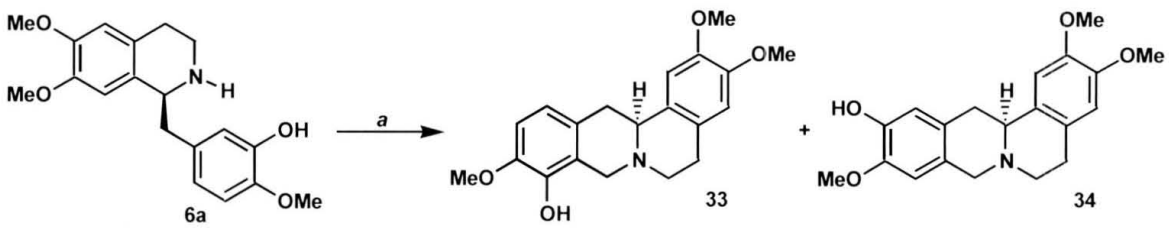

a: 1. HCHO, MeOH, rt; 2. $NaBH_4$, ~30% **33** & 70% **34**.

Scheme 2.10. Synthesis of (*S*)-tetrahydropalmatrubine (**33**).

The X-ray structure shown in Figure 2.12 confirmed the structure as (*S*)-tetrahydropalmatrubine (**33**) as the hydrochloride salt, based upon the absolute structure of the precursor **6a** for which the X-ray structure was previously established.[8]

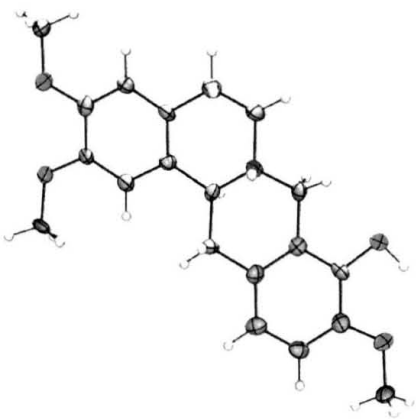

Figure 2.12. X-ray structure of **33** with 50% probability ellipses. Solvent water molecules and chloride ion omitted for clarity.

Compound **33** has also been named as "schefferine" in several publications in the literature and in some cases this is confusing. In 1972 Gellert and Rudzats[36] isolated two THPBs from *Schefferomitra subaequalis*, of which one was named "schefferine" and which has the same structure represented as **33**. However, Brochmann-Hanssen[37] later re-assigned this structure as being the regioisomeric compound having the substitution pattern on the D ring transposed, with the hydroxy group at C-10 and the methoxy group at C-9, and indicated that it was the same as "kikemanine". "Kikemanine" was so-named by Kametani[38] who isolated it from *Corydalis pallida* in 1970, and which was also equivalent to "corydalmine", previously isolated by Imaseki and Taguchi[39] from another *Corydalis* species (named as "engosan"); and also by Cava[40] in 1968 from *Stephania glabra*. Corydalmine was synthesized by Bradsher[41] in 1965. In 1977, Kametani's group also reported the synthesis of schefferine via a photochemical route[42] and stated it to be "identical with an authentic sample", although the compound they were referencing it to was ambiguous with respect to the ring D substitution pattern. In 2000 Bianchi and Kaufman[43] published two papers in which they reported the synthesis via a tosyliminium ion–based route, of "(±)-schefferine", to which was assigned the substitution pattern of **33**. However their NMR data were not consistent with the proposed structure and are at odds with those determined herein for (*S*)-tetrahydropalmatrubine (**33**), and by Iwasa *et al.*[22] The ^{13}C-NMR spectra were also reported by Kametani *et al.*[44] for a series of dibenzo[*a,g*]quinolizidines, which included a structure identical with **33**.

2.3 Conclusions.

The synthesis of both enantiomers of the opium alkaloids, (*S*)- and (*R*)-*N*-norlaudanidine **6a** and **6b**, respectively, were synthesized in high enantioselectivity using the chiral auxiliaries (*S*)- or (*R*)–α-methylbenzylamine in Bischler-Napieralski cyclization-reduction reactions. These free secondary amines could be isolated in high yields and for the first time afforded successful X-ray crystallographic structures and optical rotations. The use of (*R*)- and (*S*)-α-methylbenzylamine as a chiral auxiliary has proven to be convenient and effective in a Bischler-Napieralski cyclization-reduction reaction to enantioselectively form (*R*)-*N*-norlaudanidine.

In particular, (*S*)-*N*-norlaudanidine is targeted as a key intermediate for an enantioselective total synthesis of tetrahydroprotoberberine alkaloids (*S*)-tetrahydropalmatrubine and (*S*)-corytenchine.

Enantioselective total syntheses and X-ray structures of both (*S*)-tetrahydropalmatrubine (**33**) and (*S*)-corytenchine (**34**) are reported for the first time. They were both derived from (*S*)-*N*-norlaudanidine, a benzyltetrahydroisoquinoline that was synthesized with high (>95% *ee*) enantioselectivity using a chiral auxiliary-assisted Bischler-Napieralski cyclization/reduction approach.

Experimental

General

All reactions requiring anhydrous conditions were performed under a positive pressure of nitrogen using oven-dried glassware (120 ^{o}C) that was cooled under nitrogen. ^{1}H and ^{13}C NMR spectra were recorded on a Bruker 500 MHz and 300 MHz NMR spectrometers and were referenced to the solvent ($CDCl_3$) and TMS, unless otherwise specified. Overlap may have prevented the reporting of all resonances. LC-MS and HRMS were conducted using a GCT Premier Micromass spectrometer. X-Ray structures were measured with a Rigaku Saturn CCD area detector equipped with a SHINE optic using Mo Kα radiation. Silicycle Ultrapure silica gel (0-20 μm) G and F-254 was used for the preparative-layer TLC, and Silicycle Silia-P Ultrapure Flash silica gel (40-63 μm) was used for flash column chromatography. TLC was conducted on Polygram SIL G/UV_{254} pre-coated plastic sheets. All solvents and reagents used were either of the highest commercial grades available or were distilled. THF and benzene were distilled from sodium benzophenone ketyl, and CH_2Cl_2 was distilled from calcium hydride. Methanol was dried over Mg and I_2. Optical rotations were recorded on a JASCO DIP-370 polarimeter. All melting points are uncorrected.

The numerical listing of the compounds following is based upon the Schemes described in this Chapter. Compounds **15**, **17** and **21** have been reported previously by others. Their spectral data which are presented herein are provided merely for convenient referencing only and no claim by the author is implied that they are new compounds.

Experimental

3-Benzyloxy-4-methoxybenzaldehyde (17).

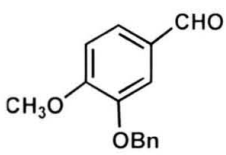

To a suspension of anhydrous potassium carbonate (22.3 g, 161 mmol) in DMSO (70 mL) was added 3-hydroxy-4-methoxybenzaldehyde (**16**) (9.81 g, 64.5 mmol) and benzyl bromide (9.21 mL, 77.5 mmol). After being stirred for 4 h, water was added and the mixture was extracted with EtOAc (50 mL x 3). The combined organic extracts were washed with brine (15 mL x 3), dried over anhydrous $MgSO_4$, filtered, and the solvent was evaporated to afford **17** (15.3 g, 98%) as a colorless solid, mp 62-63 °C; ^{1}H NMR ($CDCl_3$, 300 MHz): δ 9.81 (s, 1H, CHO), 7.48-7.47 (m, 4H), 7.39 (t, J = 6.9 Hz, 2H), 7.32 (d, J = 6.9 Hz, 1H), 7.00 (dd, J = 6.9 and 1.7 Hz, 1H), 5.19 (s, 2H), 3.96 (s, 3H); ^{13}C NMR ($CDCl_3$, 75.46 MHz): δ 190.8, 155.0, 148.7, 136.3, 130.0, 128.6, 128.1, 127.4, 126.8, 111.4, 110.8, 70.8, 56.2; GCMS (*m/z*): 242 (M^+, 22), 91 (100), 65 (20).

1,1-Dibromo-2-(3-benzyloxy-4-methoxyphenyl)ethene (18).

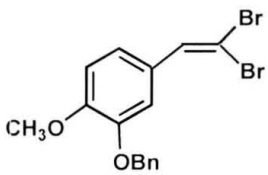

To an ice-cold stirred solution of **17** (15.2 g, 62.6 mmol) and CBr_4 (31.2 g, 93.9 mmol) in dry CH_2Cl_2 (80 mL) was added PPh_3 (49.3 g, 187 mmol) in CH_2Cl_2 (70 mL) over 15 min using a dropping funnel. After the reaction was completed, the reaction mixture was concentrated under reduced pressure and then $CHCl_3$ (20 mL) was added to the residue. The mixture was filtered to remove triphenylphosphine oxide, which was washed with $CHCl_3$ (20 mL).

The combined filtrates were concentrated under reduced pressure, and the crude product was purified by column chromatography (10% EtOAc/hexane) to give the dibromoalkene **18** (23.2 g, 93%); ^{1}H NMR ($CDCl_3$, 500 MHz): δ 7.43 (d, J = 7.2 Hz, 2H), 7.36 (t, J = 7.5 Hz, 2H), 7.33 (s, 1H), 7.29 (t, J = 7.3 Hz, 1H), 7.21 (d, J = 2.2 Hz, 1H), 7.05 (dd, J = 8.4, 2.2 Hz, 1H), 6.86 (d, J = 8.4 Hz, 1H) , 5.17 (s, 2H), 3.97 (s, 3H); ^{13}C NMR ($CDCl_3$, 125.77 MHz): δ 150.3, 148.0, 137.2, 136.6, 128.2, 128.2, 128.2, 127.6, 122.9, 114.2, 111.6, 87.7, 71.4, 56.3; APCI-MS (*m/z*): 397.9 (M^+, 5), 319.0 (20), 238.0 (100).

Pyrrolidyl 2-(3-benzyloxy-4-methoxyphenyl)acetamide (19).

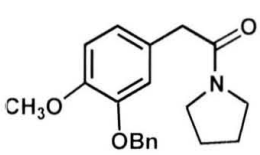

To a solution of pyrrolidine (5 mL) and water (5 mL) was added **18** (0.214 g, 0.536 mmol) at room temperature. After stirring overnight, the resulting mixture was concentrated under reduced pressure to remove excess amine. An aqueous 10% HCl (20 mL) solution was added to the residue, and the resulting mixture was extracted with $CHCl_3$ (10 mL). The combined organic layers were washed with an aqueous saturated $NaHCO_3$ solution (10 mL) and then water (10 mL), dried over anhydrous $MgSO_4$, filtered, and concentrated under reduced pressure. The crude product was purified by column chromatography (50% EtOAc/ hexane) to give the amide **19** (0.159 g, 91%) as a colorless oil; ^{1}H NMR ($CDCl_3$, 300 MHz): δ 7.45-7.28 (m, 5H), 6.85-6.81 (m, 3H), 5.14 (s, 2H), 3.86 (s, 3H), 3.53 (s, 2H), 3.43 (t, J = 13.2 Hz, 2H), 3.28 (t, J = 13.2 Hz, 2H), 1.86-1.76 (m, 4H); ^{13}C NMR ($CDCl_3$, 75.46 MHz): δ 169.6, 148.5, 148.0, 137.1, 128.4, 127.7, 127.3, 121.6, 114.8, 111.9, 70.8, 56.0, 46.7, 45.8, 41.8, 26.1, 24.2; APCI-MS (*m/z*): 326.3 (M+1, 100).

2-(3-(Benzyloxy)-4-methoxyphenyl)acetic acid (15).

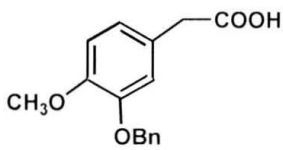

To a solution of aqueous 1.0 M HCl (3 mL) and 1,4-dioxane (5 mL) was added amide **19** (0.161 g, 0.496 mmol). The reaction mixture was heated under reflux for 72 h. The resulting mixture was extracted with chloroform (10 mL), and the combined organic layers were dried over $MgSO_4$ and concentrated under reduced pressure. The crude product was purified by column chromatography (40% EtOAc/ hexane) to give the acid, **15** (0.127 g, 94%) as a yellow solid, mp 101-102 °C; ^{1}H NMR ($CDCl_3$, 500 MHz): δ 7.43 (d, J = 7.3 Hz, 2H), 7.35 (t, J = 7.3 Hz, 2H), 7.28 (t, J = 7.3 Hz, 1H), 6.85-6.84 (m, 3H), 5.12 (s, 2H), 3.86 (s, 3H), 3.53(s, 2H); ^{13}C NMR ($CDCl_3$, 125.77 MHz): δ 177.1, 149.0, 148.2, 136.9, 128.5, 127.8, 127.4, 125.6, 122.2, 115.3, 111.9, 71.0, 56.0, 40.4; GCMS (*m/z*): 272 (M^+, 22), 91 (100).

3,4-Dimethoxybenzaldehyde (21).

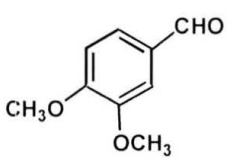

To vanillin (**20**) (15.2 g, 100 mmol) in acetone (70 mL) were added potassium carbonate (34.5 g, 249 mmol) and dimethyl sulfate (9.48 mL, 100 mmol). The mixture was stirred at room temperature for 3 h, and then diluted by the addition of water (30 mL). The mixture was extracted with EtOAc (20 mL x 3). The combined organic extracts were washed with water (15 mL x 3), dried over anhydrous $MgSO_4$, filtered, and the solvent was evaporated to afforded **21** (16.3 g, 98%) as a colorless solid, mp 40-41 °C; ^{1}H NMR ($CDCl_3$, 300 MHz): δ 9.86 (s, 1H), 7.46 (dd, J = 8.1, 1.8 Hz, 1H), 7.42 (d, J = 1.8, 1H), 6.99 (d, J = 8.1 Hz, 1H), 3.97 (s, 3H),

3.95 (s, 3H); ^{13}C NMR ($CDCl_3$, 75.46 MHz): δ 190.9, 154.5, 149.6, 130.1, 126.8, 110.3, 108.9, 56.2, 56.0; GCMS (*m/z*): 166 (M^+, 100), 151 (25), 95 (40), 77 (30).

1,1-Dibromo-2-(3,4-dimethoxyphenyl)ethene (22).

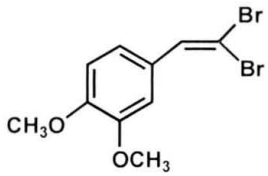

To an ice-cold stirred solution of **21** (13.2 g, 79.5 mmol) and CBr_4 (39.6 g, 119 mmol) in dry CH_2Cl_2 (80 mL) was added PPh_3 (62.6 g, 239 mmol) in CH_2Cl_2 (70 mL) using a dropping funnel for 20 min. After the reaction was completed, the reaction mixture was concentrated under reduced pressure and then $CHCl_3$ (50 mL) was added to the residue. The mixture was filtered to remove triphenylphosphine oxide, which was washed with $CHCl_3$ (50 mL). The combined filtrates were concentrated under reduced pressure, and the crude product was purified by column chromatography (10% EtOAc/hexane) to give dibromoalkene **22** (23.6 g, 92%); ^{1}H NMR ($CDCl_3$, 500 MHz): δ 7.41 (s, 1H), 7.19 (d, J = 1.9 Hz, 1H), 7.10 (dd, J = 8.3, 1.9 Hz, 1H), 6.85 (d, J = 8.3 Hz, 1H), 3.90 (s, 3H), 3.89 (s, 3H); ^{13}C NMR ($CDCl_3$, 125.77 MHz): δ 149.7, 149.0, 136.8, 128.3, 122.3, 111.5, 111.2, 87.7, 56.3, 56.2; GCMS (*m/z*): 323.0 (M+1, 20), 243.9 (100), 167 (80), 139.1 (85).

Pyrrolidyl 2-(3,4-dimethoxyphenyl)acetamide (23).

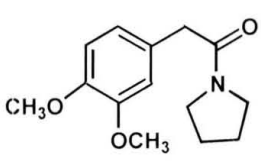

To a solution of pyrrolidine (5 mL) and water (5 mL) was added **22** (0.162 g, 0.504 mmol) at room temperature. After stirring for 24 h, the resulting mixture was concentrated under reduced pressure to remove the excess amine. An aqueous 10% HCl (20 mL) solution was added

to the residue, and the resulting mixture was extracted with $CHCl_3$ (10 mL). The combined organic layers were washed with an aqueous saturated $NaHCO_3$ solution (10 mL) and then water (10 mL), dried over anhydrous $MgSO_4$, filtered, and concentrated under reduced pressure. The crude product was purified by column chromatography (50% EtOAc/hexane) to give the amide **23** (0.114 g, 91%) as a colorless oil; ^{13}C NMR ($CDCl_3$, 75.46 MHz): δ 196.7, 149.0, 147.8, 127.4, 121.0, 112.1, 111.1, 55.9, 55.9, 46.8, 45.9, 41.8, 26.1, 24.3; APCI-MS (*m/z*): 250.1 (M+1, 100), 236.1 (18).

(3,4-Dimethoxyphenyl)acetic acid (24).

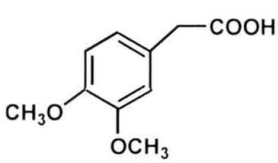

To a solution of 1.0 M HCl (3 mL) and 1,4-dioxane (5 mL) was added amide **23** (0.144 g, 0.576 mmol). The reaction mixture was heated under reflux for 36 h. The resulting mixture was extracted with chloroform (10 mL), and the combined organic layers were dried over $MgSO_4$ and concentrated under reduced pressure. The crude product was purified by column chromatography (40% EtOAc/hexane) to give the acid **24** (0.103 g, 92%) as a yellow solid, mp 98-99 °C; ^1H NMR ($CDCl_3$, 500 MHz): δ 6.80-6.78 (m, 3H), 3.85 (s, 3H), 3.84 (s, 3H), 3.57 (s, 2H); ^{13}C NMR ($CDCl_3$, 125.77 MHz): δ 178.0, 149.4, 148.7, 126.0, 121.9, 112.9, 111.6, 56.3, 56.2, 40.9; GCMS (*m/z*): 196 (M^+, 100), 151 (100), 107 (30).

***N*-((*S*)-α-Methylbenzyl)-(3,4-dimethoxy)phenylacetamide (25a).**

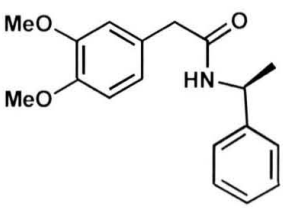

To a stirred solution of oxalyl chloride (2.33 ml, 26.7 mmol) in anhydrous benzene (20 mL) was added 3,4-dimethoxyphenylacetic acid (**24**) (4.37 g, 22.3 mmol) in one batch and DMF (1 drop). The reaction mixture was stirred until the evolution of gas ceased. The benzene was evaporated using a rotary evaporator to give the crude acid chloride, which was used directly in the next step. To a stirred mixture of (*S*)-α-methylbenzylamine (2.75 mL, 22.3 mmol) and CH_2Cl_2/aqueous 5% NaOH (1:1.5, 30.3 ml) was added dropwise a solution of the above crude acid chloride in CH_2Cl_2 (30 mL) at 0 °C. After stirring at room temperature for 1 h, the reaction mixture was extracted with chloroform (30 mL × 3). The organic solution washed with water (20 mL × 3), dried over anhydrous $MgSO_4$, filtered, and the solvent was then evaporated. The residue was purified by flash column chromatography (30% EtOAc/hexane) to afford **25a** (6.14 g, 92%) as a colorless solid, mp 108-110 °C; ^{1}H NMR ($CDCl_3$, 300 MHz): δ 7.32-7.17 (m, 5H), 6.84 (d, *J* = 8.6 Hz, 1H), 6.78 (d, *J* = 1.9 Hz, 1H), 6.10 (dd, *J* = 8.6, 1.9 Hz, 1H), 5.65 (d, *J* = 7.3 Hz, 1H), 5.17-5.11 (m, 1H), 3.89 (s, 3H), 3.84 (s, 3H), 3.53 (s, 2H), 1.41 (d, *J* = 6.9 Hz, 3H); ^{13}C NMR ($CDCl_3$, 75.46 MHz): δ 170.3, 149.2, 148.3, 143.1, 128.6, 127.2, 126.9, 125.9, 121.5, 112.3, 111.5, 55.9, 55.8, 48.6, 43.4, 21.8; APCl-MS (*m/z*): 300.1 (M+1, 100).

Compound **25b:** as in **25a** but with (*R*)-α-methylbenzylamine to afford **25b** as a colorless solid, mp 108-110 °C.

***N*-((*S*)-α-Methylbenzyl)-(3,4-dimethoxy)phenyacetamine (14a).**

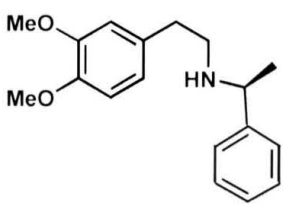

To a solution of **25a** (3.54 g, 11.8 mmol) in anhydrous THF (60 ml) under nitrogen was added $BF_3 \bullet Et_2O$ (0.743 mL, 5.91 mmol). The mixture was heated to gentle reflux and $B_2H_6 \bullet THF$ (29.5 mL, 29.5 mmol) was then added dropwise. The reaction mixture was heated at reflux for 2 h, and then cooled to 0 °C and aqueous 20% HCl (10 mL) was added to the mixture. The reaction mixture, which was stirred at 0 °C for 1 h and then overnight at room temperature, was made basic to pH=13 with aqueous 50% KOH solution. The mixture was then extracted with CH_2Cl_2 (30 mL × 3). The combined organic layers were washed with water (20 mL × 3), dried over anhydrous $MgSO_4$, filtered, and the solvent was evaporated to afford **14a** (2.90 g, 86%) as a viscous oil, which was pure enough to be used directly in the next step without further purification; ^{1}H NMR ($CDCl_3$, 500 MHz): δ 7.31-7.20 (m, 5H), 6.78 (d, J = 8.1 Hz, 1H), 6.70 (dd, J = 8.1, 2.0 Hz, 1H), 6.67 (d, J = 2.0 Hz, 1H), 3.85 (s, 3H), 3.83 (s, 3H), 3.80-3.76 (q, J = 6.5 Hz, 1H), 2.76-2.67 (m, 4H), 1.52 (bs, 1H), 1.32 (d, J = 6.5 Hz, 3H); ^{13}C NMR ($CDCl_3$, 125.77 MHz): δ 149.2, 147.8, 146.0, 133.0, 128.7, 127.2, 126.9, 121.0, 112.3, 111.6, 58.6, 56.3, 56.3, 49.3, 36.3, 24.7; APCI-MS (*m/z*): 284.2 (M^+, 22).

Compound **14b:** as with **14a** but using **25b** to afford **14b;** ^{1}H and ^{13}C NMR spectra and APCI-MS data were identical with **14a**.

***N*-((*S*)-α-Methylbenzyl)-*N*-((3,4-dimethoxy)phenylethyl)-(3-benzyloxy-4-methoxy) phenylacetamide (13a).**

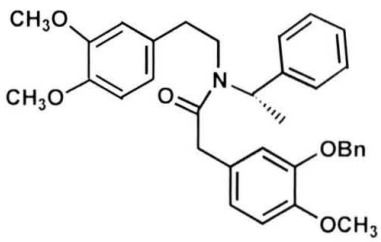

To a stirred solution of oxalyl chloride (1.00 mL, 11.5 mmol) in anhydrous benzene (20 mL) were added **15** (2.62 g, 9.61 mmol) in one batch and DMF (2 drops). The reaction mixture was stirred until the evolution of gas ceased. The benzene was evaporated using a rotary evaporator to give the acid chloride, which was used directly in the next step. To a stirred mixture of **14a** (2.74 g, 9.61 mmol) and CH_2Cl_2/aqueous 5% NaOH (1:1.5, 12.8 mL) was added dropwise a solution of the crude acid chloride in CH_2Cl_2 at 0 °C. After stirring at room temperature for 1 h, the reaction mixture was extracted with chloroform (30 mL × 3), washed with water (20 mL × 3), dried over anhydrous $MgSO_4$, filtered, and the solvent was then evaporated. The residue was purified by flash column chromatography (30% EtOAc/hexane) to afford **13a** (3.73 g, 72%) as a viscous oil whose NMR spectra were complex. APCl-MS (*m/z*): 540.3 (M+1, 100). Compound **13b**: as with **13a** but with **14b** to afford **13b** as colorless oil. APCl-MS (*m/z*): 540.3 (M+1, 100).

1-(*S*)-(3-Benzyloxy-4-methoxybenzyl)-*N*-[(*S*)-α-methylbenzyl]-6,7-dimethoxy-1,2,3,4-tetrahydroisoquinoline (26a).

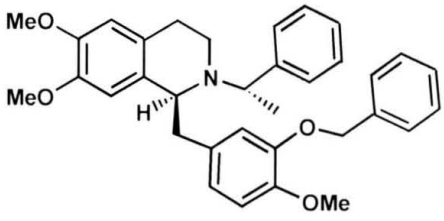

Compound **13a** (2.51 g, 4.66 mmol), $POCl_3$ (8.68 mL, 93.1 mmol) and benzene (50 mL) were combined under argon and heated to reflux at 90 °C. After approximately 12 h, the solvent and excess $POCl_3$ were evaporated on a rotary evaporator and finally on a vacuum pump for 2 h. The resultant residue was re-dissolved in anhydrous MeOH (20 mL) and the solution was cooled to -78 °C in a dry ice bath. To this solution was added $NaBH_4$ (0.881 g, 23.3 mmol) in five portions over 4 h. The reaction was quenched by the addition of aqueous 10% HCl (10 mL), and the mixture was stirred at room temperature for 30 min. The MeOH was evaporated on a rotary evaporator. The residue was basified by adding 20% KOH at 0 °C. Water and CH_2Cl_2 were added in the latter stage to solubilize the postassium salt and the amine. The mixture was extracted with CH_2Cl_2 (3 x 20 mL), the combined organic layers were dried over $MgSO_4$, filtered, and concentrated in *vacuo*. The residue was purified by PLC (30% EtOAc/hexane) to give compound **26a** (1.83 g, 75%) as a colorless oil; ^{1}H NMR ($CDCl_3$, 500 MHz): δ 7.38 (d, J = 7.3 Hz, 2H), 7.33 (t, J = 7.4 Hz, 2H), 7.28-7.19 (m, 4H), 7.14 (d, J = 7.3 Hz, 2H), 6.73 (d, J = 8.1 Hz, 1H), 6.57 (s, 1H), 6.48 (d, J = 2.1 Hz, 1H), 6.46 (dd, J = 8.1 and 2.0 Hz, 1H), 5.79 (s, 1H), 5.00 (AB d, J = 12.2 Hz, 1H), 4.94 (AB d, J = 12.2 Hz, 1H), 3.85 (s, 3H), 3.84 (s, 3H), 3.76 (q, J = 6.2 Hz, 1H), 3.67 (t, J = 6.9 Hz, 1H), 3.48 (s, 3H), 3.26-3.14 (m, 2H), 3.01 (dd, J = 13.3 Hz and 6.0 Hz, 1H), 2.90-2.83 (m, 1H), 2.68-2.63 (m, 1H), 2.43 (dd, J = 16.7 and

2.6 Hz, 1H), 1.35 (d, J = 6.2 Hz, 3H); ^{13}C NMR ($CDCl_3$, 125.77 MHz): δ 148.3, 148.0, 147.5, 146.9, 146.5, 133.1, 129.9, 128.9, 128.6, 128.1, 127.7, 127.7, 126.9, 126.8, 123.0, 115.9, 111.8, 111.7, 111.5, 71.1, 61.1, 59.6, 56.6, 56.1, 55.9, 42.2, 40.2, 24.4, 23.7, 22.4; APCl-MS (*m/z*): 524.3 (M+1, 100).

Compound **26b**: as with **26a** but with **13b** to afford **26b** as a colorless oil; ^{1}H and ^{13}C NMR spectra and APCI-MS data were identical with **26a**.

(*S*)-*N*-Norlaudanidine (6a).

To a solution of compound **26a** (200 mg, 0.382 mmol) in EtOAc (1.5 ml) and EtOH (4.5 mL) was added aqueous 10% HCl (0.83 mL). The resulting solution was hydrogenated over 10% Pd/C for 12 h with stirring. Filtration over Celite followed by evaporation of the solvent afforded a residue, which was dissolved in water (5 mL) and CH_2Cl_2 (5 mL) and basified to pH = 13 with aqueous saturated $NaHCO_3$. The aqueous layer was then acidified to pH = 7 and extracted with CH_2Cl_2 (3 x 20 mL). The combined organic layers were washed with brine, dried over $MgSO_4$, and concentrated in *vacuo* to afforded a brown oil, which was purified by preparative LC (50% EtOAc in hexane) to afford **6a** (90.6 mg, 72%) as a colorless solid, mp 140-141 °C (benzene); ^{1}H NMR ($CDCl_3$, 500 MHz): δ 6.83 (d, J = 1.8 Hz, 1H), 6.79 (d, J = 8.1 Hz, 1H), 6.70 (dd, J = 8.1, 1.8 Hz, 1H), 6.62 (s, 1H), 6.59 (s, 1H), 4.17 (dd, J = 9.6, 4.1 Hz, 1H), 3.86 (s, 3H), 3.85 (s, 3H), 3.82 (s, 3H), 3.24-3.19 (m, 1H), 3.11 (d, J = 4.1 Hz, 1H), 3.09 (d, J = 4.3 Hz, 1H), 2.93-2.88 (m, 1H), 2.80 (dd, J = 9.6, 5.6 Hz, 1H),

2.77-2.66 (m, 2H); ^{13}C NMR ($CDCl_3$, 125.77 MHz): δ 147.9, 147.4, 146.2, 145.9, 132.3, 130.5, 127.4, 121.1, 115.8, 112.2, 111.2, 109.8, 57.1 56.3, 56.2, 42.3, 40.8, 29.6; APCI-MS (*m/z*): 330.1 (M+1, 100). $[\alpha]^{25}_{D}$ +9 (c 0.010, MeOH).

(*R*)-*N*-Norlaudanidine (6b): as with **6a** but with **26b** to afford **6b** as a colorless solid, m.p 140-141 °C (benzene). ^{1}H and ^{13}C NMR spectra and APCI-MS were identical with **6a**. APCI-MS (*m/z*): 330.1 (M^++1, 100); $[\alpha]^{25}_{D}$ -9 (c 0.085, MeOH).

(*S*)-(-)-Corytenchine (34).

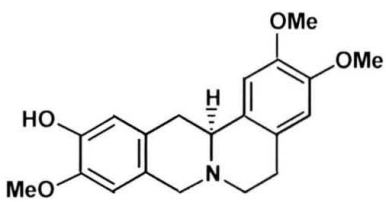

To a stirred solution of **6a** (180 mg, 0.547 mmol) and formalin (37% aq. HCHO, 2.0 mL) in MeCN (3 mL) was added $NaBH_3CN$ (294 mg, 0.892 mmol) at 0 °C. The reaction mixture was stirred for 1 h, and AcOH was then added. After being stirred for 1 h, the reaction was quenched with water, and the solution was neutralized to pH = 8 with saturated aqueous $NaHCO_3$. The mixture was extracted with CH_2Cl_2 (3 x 30 mL). The combined organic layers were dried over $MgSO_4$ and the solvent was evaporated under vacuum to afford **34** (175 mg, 95%) as a colorless solid. mp 257-258 °C; ^{1}H NMR ($CDCl_3$, 500 MHz): δ 6.74 (s, 1H), 6.72 (s, 1H), 6.62 (s, 1H), 6.56 (s, 1H), 3.93 (d, *J* = 14.5 Hz, 1H), 3.90 (s, 1H), 3.87 (s, 1H), 3.86 (s, 1H), 3.67 (d, *J* = 14.5 Hz, 1H), 3.58 (dd, *J* = 11.5, 3.5 Hz, 1H), 3.21 (dd, *J* = 15.5, 3.5 Hz, 1H), 3.17-3.13 (m, 2H), 2.80 (dd, *J* = 15.7, 11.5 Hz, 1H), 2.69-2.60 (m, 2H); ^{13}C NMR ($CDCl_3$, 125.77 MHz): δ 147.9, 147.9, 145.5, 144.5, 130.2, 127.5, 127.1, 126.2, 114.7, 111.8, 109.0, 108.7, 59.3, 60. 3, 58.8,

56.5, 56.4, 51.8, 36.6, 29.5; APCI-MS (*m/z*): 342.1 (M+1, 100); HREI-MS (*m/z*): 341.1627 (calcd for $C_{20}H_{23}NO_4$, 341.1627); $[\alpha]^{25}_{D}$ -271 (c 0.09, MeOH).

(*S*)-(-)-Tetrahydropalmatrubine (33).

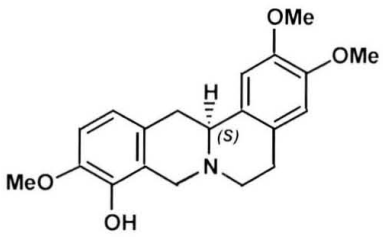

Formalin (37% aq. HCHO, 3.0 mL) was added to a solution of **6a** (250 mg, 0.759 mmol) in MeOH (6.0 mL). After the mixture had been stirred at 25 °C for 3 h, $NaBH_4$ (319 mg, 8.44 mmol) was slowly added. Subsequently, the reaction mixture was stirred at 25 °C for additional 16 h. Then, saturated aqueous NH_4Cl (25 mL) was added, and the mixture was extracted with CH_2Cl_2 (3 x 30 mL). The combined organic layers were dried with $MgSO_4$ and the solvent was evaporated under vacuum to afford a mixture of **33** and **34**, which were separated by preparative TLC (40% EtOAc/ hexane) to give **33** (77.7 mg, 30%) as a colorless prism that slowly develops color on storage, mp 178-179 °C (as the hydrochloride) and **34 (**181 mg, 70%) as a colorless solid, mp 257-258 °C; ^{1}H NMR ($CDCl_3$, 500 MHz): δ 6.75 (d, *J* = 10 Hz, 1H), 6.74 (s, 1H), 6.68 (d, *J* = 10 Hz, 1H), 6.62 (s, 1H), 4.24 (d, *J* = 15 Hz, 1H), 3.89 (s, 3H), 3.87 (s, 6H), 3.58 (dd, *J* = 12, 3.5, 1H), 3.53 (d, *J* = 15 Hz, 1H), 3.26 (dd, *J* = 15.5, 3.5, 1H), 3.23-3.12 (m, 2H), 2.84 (dd, *J* = 15.5, 12 Hz, 1H), 2.96-2.63 (m, 2H); ^{13}C NMR ($CDCl_3$, 125.77 MHz): δ 147.5, 147.4, 144.0, 141.5, 129.8, 128.9, 121.3, 119.3, 111.4, 108.9, 108.6, 59.3, 56.2, 56.1, 55.9, 53.5, 51.4, 36.4, 29.1; APCI-MS (*m/z*): 342.1(M+1,100); HREI-MS (*m/z*): 341.1620 (calcd for $C_{20}H_{23}NO_4$, 341.1614); $[\alpha]^{25}_{D}$ -115 (c 0.09, MeOH) (hydrochloride).

References

(1) Shamma, M. In *The Isoquinoline Alkaloids: Chemistry and Pharmacology*. Blomquist, A. T., Wasseman, H., Eds.; Academic Press: New York, **1972**; pp 44-152.

(2) Brochmann-Hanssen, E.; Furuya, T. *J. Pharm. Sci.* **1964**, *53*, 575-577.

(3) Brochmann-Hanssen, E.; Nielsen, B. *Tetrahedron Lett.* **1965**, *18*, 1271–1274.

(4) Brochmann-Hanssen, E.; Nielsen, B.; Utzinger, G. E. *J. Pharm. Sci.* **1965**, *54*, 1531–1532.

(5) Toske, S. G.; Cooper, S. D.; Morello, D. R.; Hays, P. A.; Casale, J. F.; Casale, E. *J. Forensic Sci.* **2006**, *51*, 308-320.

(6) Lunie, I. S.; Toske, S. G. *J. Chromatogr.* A **2008**, *1188*, 322-326.

(7) Brochmann-Hanssen, E.; Chen, C.; Chen, C. R.; Chiang, H.; Leung, A. Y.; McMurtrey, K. *J. Chem. Soc., Perkin Trans. 1* **1975**, 1531–1537.

(8) Zein, A. L.; Dakhil, O. O.; Dawe, L. N.; Georghiou, P. E. *Tetrahedron Lett.* **2010**, *51*, 177-180.

(9) Brochmann-Hanssen, E.; Hirai, K. *J. Pharm. Sci.* **1968**, *57*, 940-943.

(10) Battersby, A. R.; Binks, R.; Francis, R. J.; McCaldin, D. J.; Ramuz, H. *J. Chem. Soc.* **1964**, 3600-3610.

(11) *See for example*: Ferrari, C.; Deulofeu, V. *Tetrahedron* **1962**, *18*, 419-425.

(12) Chrzanowska, M.; Rozwadowska, M. D. *Chem. Rev.* **2004**, *104*, 3341-3370.

(13) For a recent different approach to the enantioselective synthesis of some benzyltetrahydroisoquinolines via a Bischler-Napieralski approach see Pyo, M. K.; Lee, D. H.; Kim, D. H.; Lee, J. H.; Moon, J. C.; Chang, K. C.; Yun-Choi, H. S. *Bioorg. Med. Chem. Lett.* **2008**, *18*, 4110-4114.

(14) Zein, A. L.; Valluru, V.; Georghiou, P. E. *Studies in Natural Product Chemistry: Bioactive Natural Products* **2011**. Manuscript accepted November 2, 2011.

(15) Wang, Y.; Georghiou, P. E. *Org. Lett.* **2002**, *4*, 2675-2678.

(16) Nagubandi, S.; Fodor, G. *Heterocycles* **1981**, *15*, 165-177.

(17) Fodor, G.; Gal, J.; Phillips, B. *Angew. Chem.Int. Ed. Engl.* **1972**, *11*, 919-920.

(18) Yields in all the steps outlined in the Scheme were not optimized.

(19) Huh, D. H; Jeong, J. S.; Lee, H. B.; Ryu, H.; Kim, Y. G. *Tetrahedron* **2002**, *58*, 9925-9932.

(20) Okawara, T.; Kametani, T. *Heterocycles* **1974**, *22*, 571-574.

(21) Czarnocki, Z.; Mieczkowski, J. B.; Ziolkowski, M. *Tetrahedron Asymm.* **1996**, *7*, 2711-2720.

(22) Iwasa, K.; Cui, W.; Sugiura, M.; Takeuchi, A.; Moriyasu, M.; Takeda, K. *J. Nat. Prod.* **2005**, *68*, 992-1000.

(23) (a) Bhakuni, D. S.; Jain, S. In *The Alkaloids: Chemistry and Pharmacology*; Brossi, A., Ed.; Academic Press: New York, **1986**; Vol. 28, pp 95-181. (b) Sÿantavy´, F. In *The Alkaloids: Chemistry and Physiology*; Manske, R. H. F., Rodrigo, R. G. A., Eds.; Academic Press: New York, **1979**; Vol. 17, 385-544.

(24) Hess, M. *Alkaloids: Nature's Curse or Blessing?:* Wiley-VCH: New York, **2002**.

(25) Memetzidis, G.; Stambach, J. F.; Jung, L.; Schott, C.; Heitz, C.; Stoclet, J. C. *Eur. J. Med. Chem.* **1991**, *26*, 605-611. (b) Suffnees, M.; Cordell, A. C. In *The Alkaloids*; Brossi, A., Ed.; Academic Press: Orlando, FL, **1985**; Vol. 25, pp 3. (c) Cushman, M.; Dekow, F. W.; Jacobsen, L. B. *J. Med. Chem.* **1979**, *22*, 331-333. (d) Wilson, W. D.; Gough, A. N.; Doyle, J. J.; Davison, M. W. *J. Med. Chem.* **1976**, *19*, 1261-1263. (e) Zee-Cheng, R. K. Y.; Cheng, C. C. *J. Med. Chem.* **1976**, *19*, 882-886.

(26) Pictet, A.; Spengler, T. *Ber.* **1911**, *44*, 2030-2036.

(27) Taylor, M. S.; Jacobsen, E. N. *J. Am. Chem. Soc.* **2004**, *126*, 10558-10559.

(28) (a) Mujahidin, D.; Doye, S. *Eur. J. Org. Chem.* **2005**, 2689-2693. (b) Davis, F. A.; Mohanty, P. K. *J. Org. Chem.* **2002**, *67*, 1290-1296. (c) Kametani, T.; Takagi, N.; Toyata, M.; Honda, T.; Fukumoto, K. *J. Chem. Soc., Perkin Trans. 1* **1981**, 2830-2834. (d) Czarnocki, Z.; Arazny, Z. *Heterocycles* **1999**, *51*, 2871-2879.

(29) (a) Enders D.; Boudou, M. *J. Org. Chem.* **2005**, *70*, 9486-9494. (b) Meyers, A. I.; Matulenko, M. A. *J. Org. Chem.* **1996**, *61*, 573-580.

(30) Cheng, J. J.; Yang, Y. S. *J. Org. Chem.* **2009**, *74*, 9225–9228.

(31) Zein, A. L.; Dawe, L. N.; Georghiou, P. E. *J. Nat. Prod.* **2010**, *73*, 1427-1430.

(32) da Silva, M. S.; Tavares, J. F.; Queiroga, K. F.; Agra, M. deF.; Filho, J. M. B.; Almeida, J. R. G. daS.; da Silva, S. A. S. *Quim. Nova.* **2009**, *32*, 1566-1570.

(33) Martinez-Vazquez, M.; Lozano, D. G. C.; Estrada-Reyes, R.; Gonzalez-Lugo, N. M.; Apan, T. R.; Heinze, G. *Fitoterapia* **2005**, *76*, 733-736.

(34) Lu, S. T.; Su, T. L.; Kametani, T.; Ujiie, A.; Ihara, M.; Fukumoto, K. *J. Chem. Soc., Perkin Trans. 1.* **1976**, 63-68.

(35) Kametani, T.; Fukumoto, K.; Agui, H.; Yagi, H.; Kigasawa, K.; Sugahara, H.; Hiiragi, M.; Hayasaka, T.; Ishimaru, H. *J. Chem. Soc. (C)* **1968**, 112-118.

(36) Gellert, E.; Rudzats, R. *Aust. J. Chem.* **1972**, *25*, 2477-2782.

(37) Brochmann-Hanssen, E.; Chiang, H. C. *J. Org. Chem.* **1977**, *42*, 3588-3591.

(38) Kametani, T.; Ihara, M.; Honda, T. *J. Chem. Soc. (C)* **1970**, 1060-1064.

(39) Imaseki, I.; Taguchi, H. *J. Pharm. Soc. Jpn.* **1962**, *82*, 1214-1219.

(40) Cava, M. P.; Nomura, K.; Talaptra, S. K.; Mitchell, M. J.; Schlessinger, R. H.; Buck, K. T.; Beal, J. L.; Douglas, B.; Raffauf, R. F.; Weisbach, J. A. *J. Org. Chem.* **1968**, *33*, 2785-2789.

(41) Telang, S. A.; Bradsher, C. K. *J. Org. Chem.* **1965**, *30*, 752-754.

(42) (a) Kametani, T.; Sugai, T.; Shoji, Y.; Honda, T.; Satoh, F.; Fukumoto, K. *J. Chem. Soc., Perkin Trans. 1* **1977**, 1151-1155. (b) Kametani, T.; Ihara, M.; Honda, T. *J. Chem. Soc., Chem. Commun.* **1969**, 1301.

(43) (a) Bianchi, D. A.; Kaufman, T. S. *Can. J. Chem.* **2000**, *78*, 1165-1169. (b) Bianchi, D. A.; Kaufman, T. S. *Synlett* **2000**, *6*, 801-804.

(44) Kametani, T.; Fukumoto, K.; Ihara, M.; Ujiie, A.; Koizumi, H. *J. Org. Chem.* **1975**, *40*, 3280-3283.

Supplementary Spectral Data for Chapter 2:

^{1}H and ^{13}C NMR spectra are presented in the following sequence for compound numbers:

17, 18, 19, 15, 21, 22, 23, 24, 25a, 25b, 14a, 14b, 13a, 26a, 26b, 6a, 6b, 34, 33

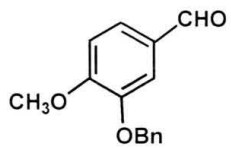

17

$CDCl_3$, NMR 300 MHz

1-az-28

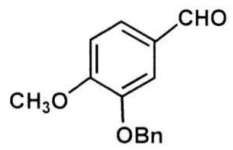

17

$CDCl_3$, NMR 75.46 MHz

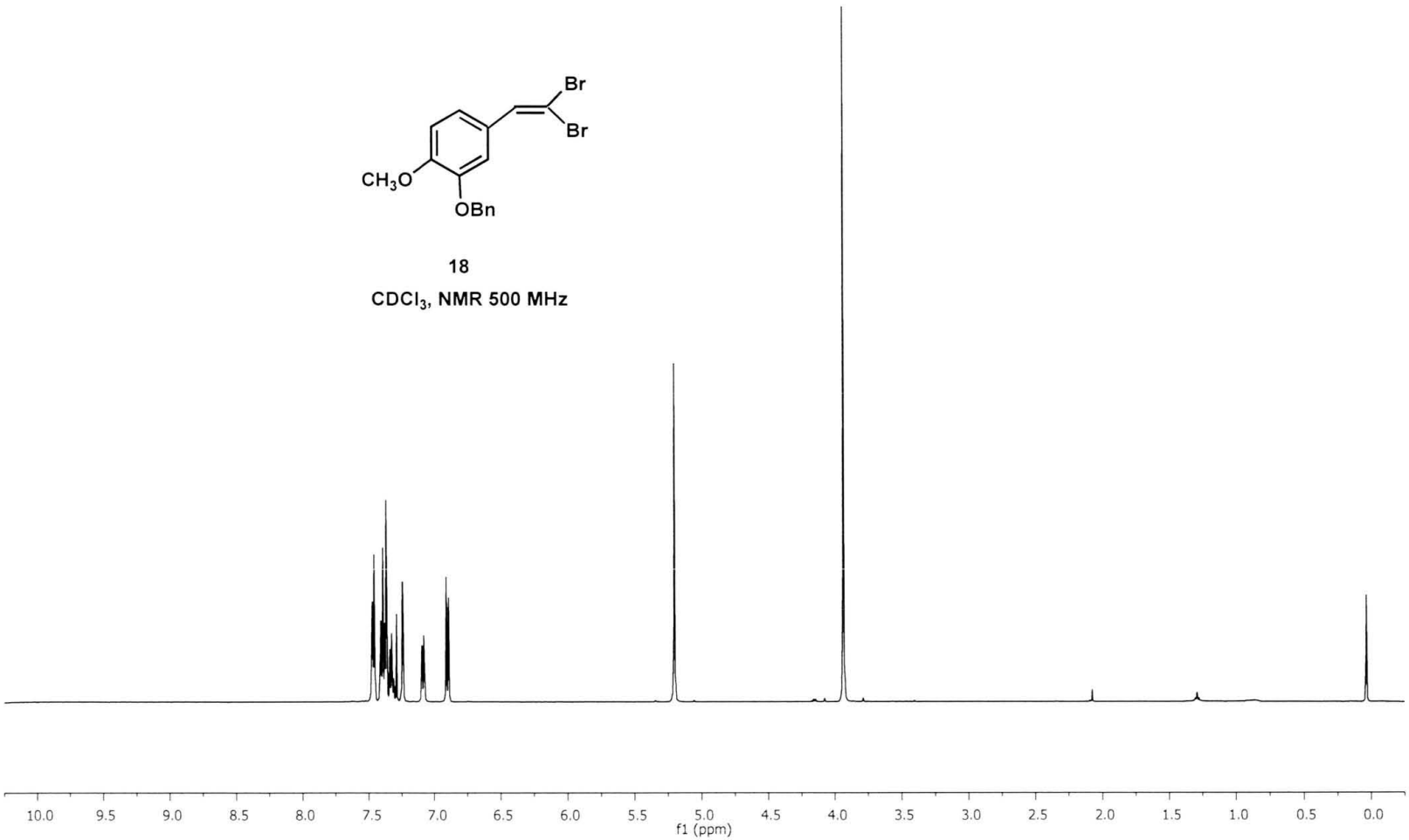
Br
Br
CH3O
OBn
18
CDCl3, NMR 500 MHz
10.0
9.5
9.0
8.5
8.0
7.5
7.0
6.5
6.0
5.5
5.0
4.5
4.0
3.5
3.0
2.5
2.0
1.5
1.0
0.5
0.0
f1 (ppm)

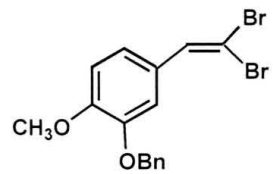

18

$CDCl_3$, NMR 125.77 MHz

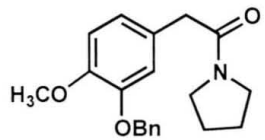

19

$CDCl_3$, NMR 300 MHz

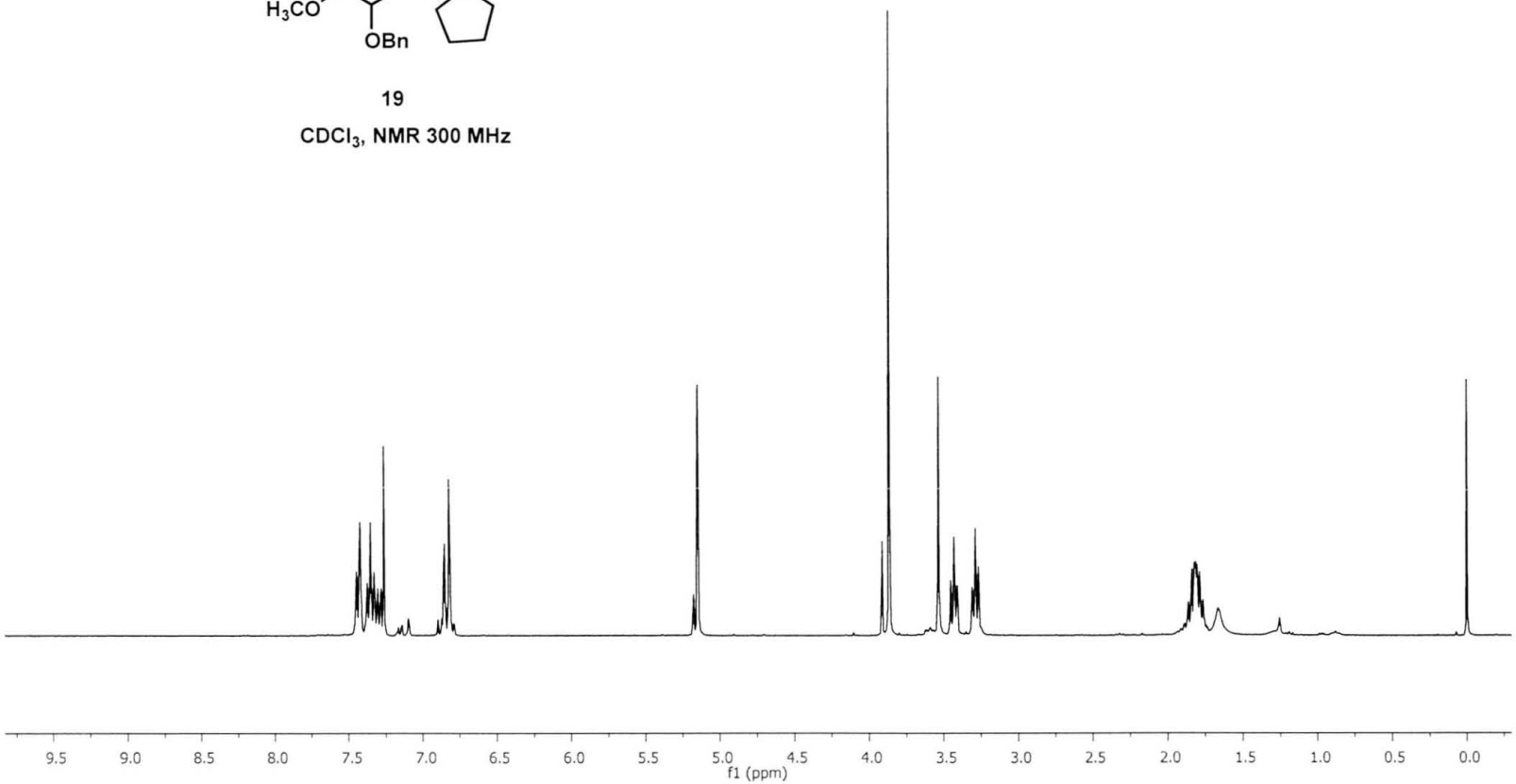

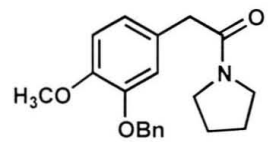

19

$CDCl_3$, NMR 75.46 MHz

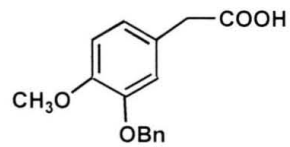

15

$CDCl_3$, NMR 500 MHz

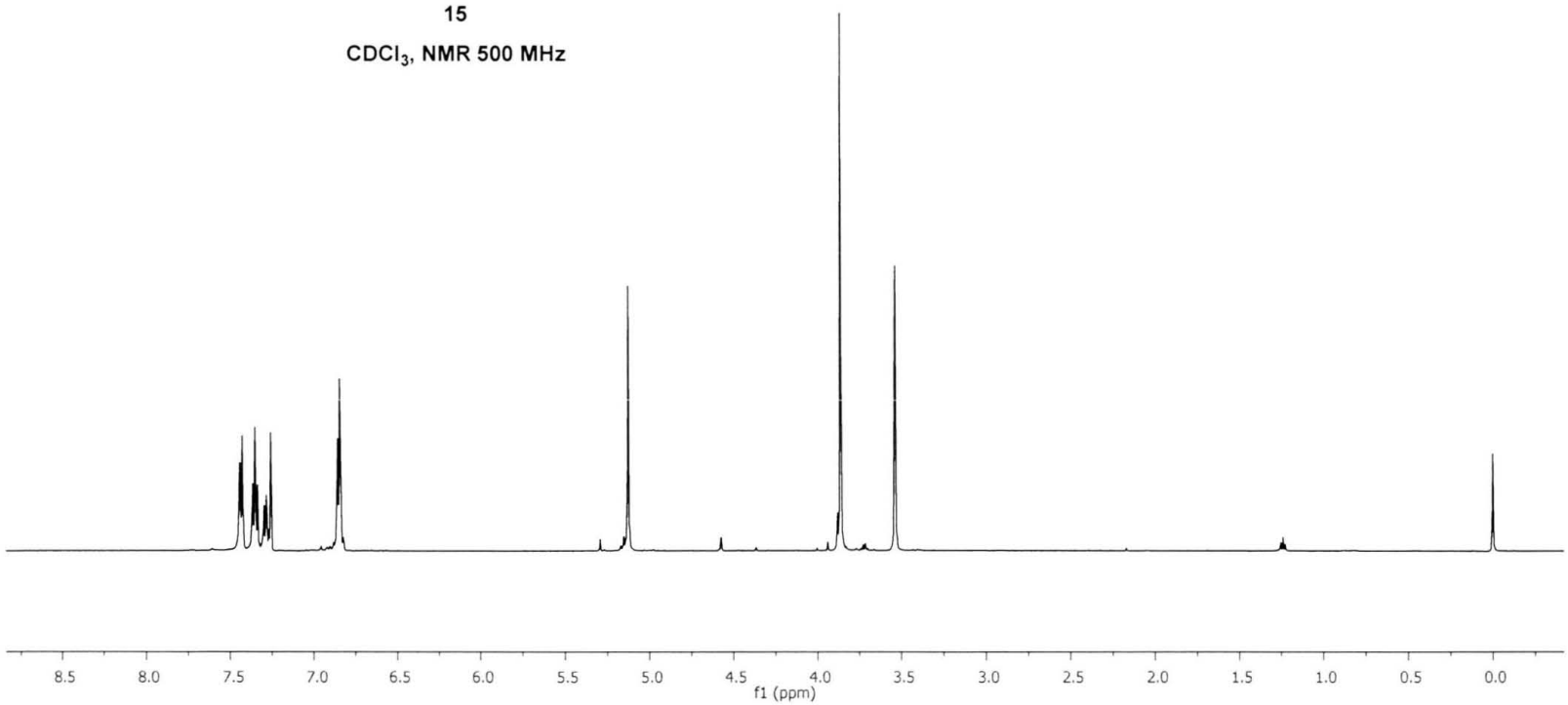

az3010b/1

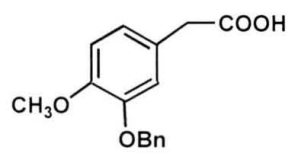

15

$CDCl_3$, NMR 125.77 MHz

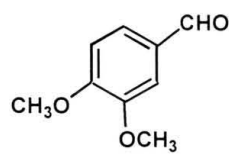

21

$CDCl_3$, NMR 300 MHz

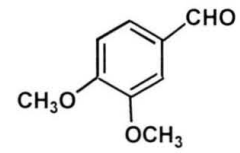

21

$CDCl_3$, NMR 75.46 MHz

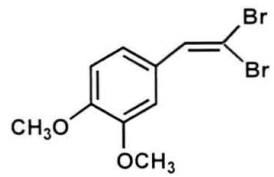

22

$CDCl_3$, NMR 500 MHz

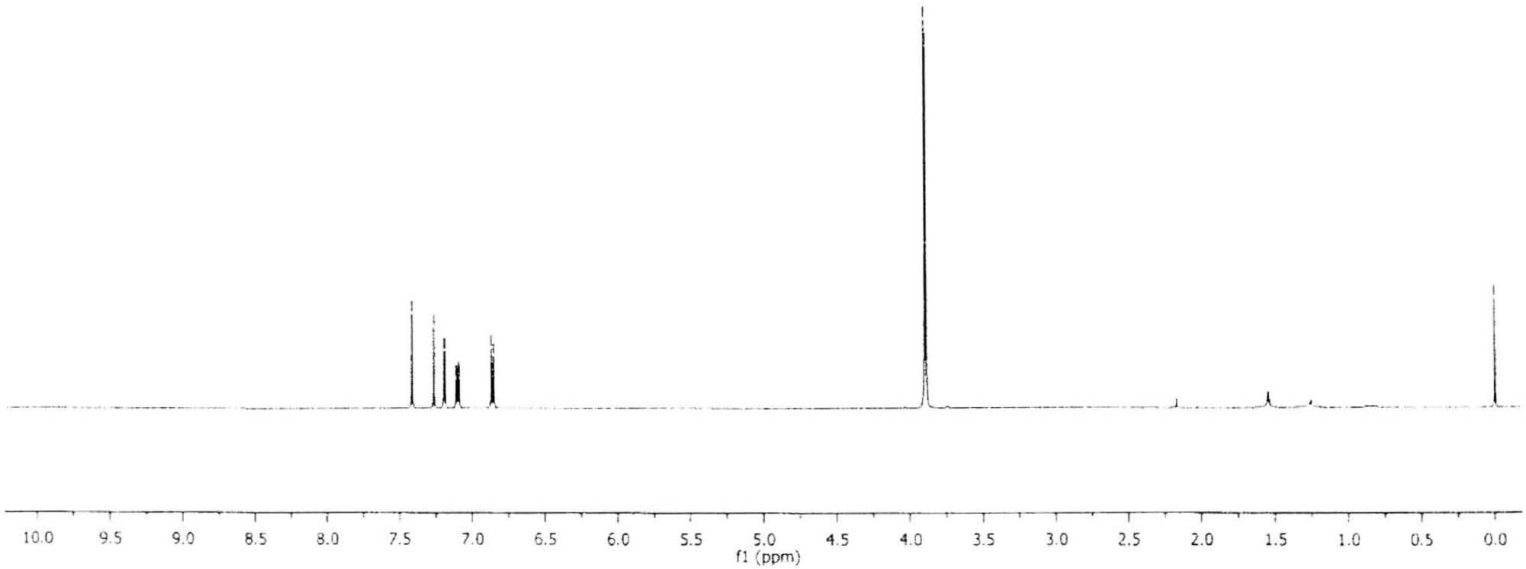

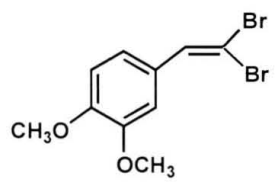

22

$CDCl_3$, NMR 125.77 MHz

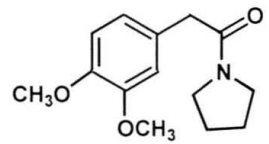

23

$CDCl_3$, NMR 75.46 MHz

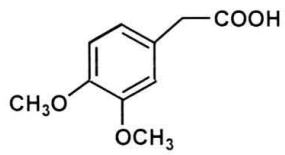

24

$CDCl_3$, NMR 500 MHz

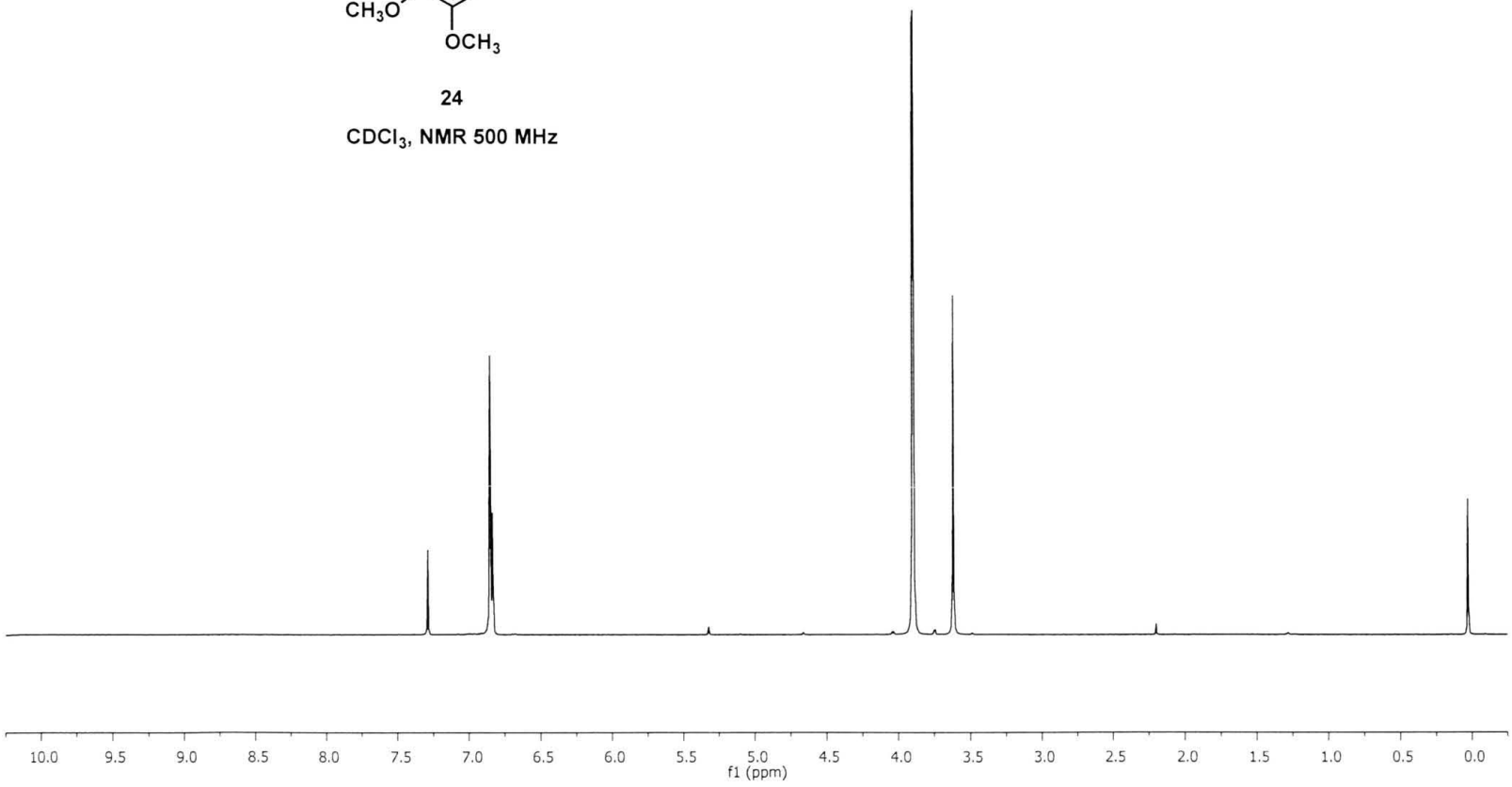

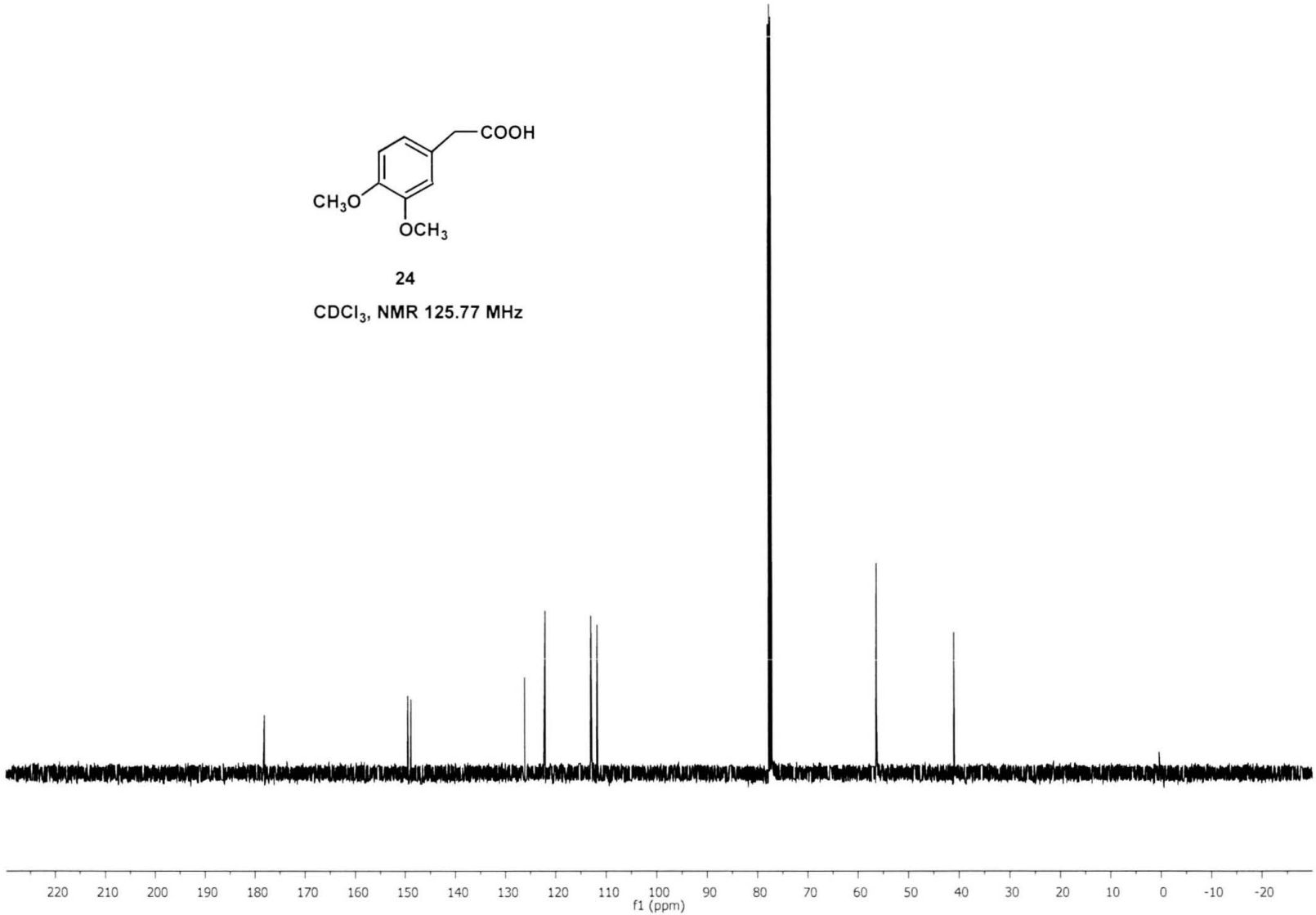
COOH
CH3O
OCH3
24
CDCl3, NMR 125.77 MHz
220 210 200 190 180 170 160 150 140 130 120 110 100 90 80 70 60 50 40 30 20 10 0 -10 -20
f1 (ppm)

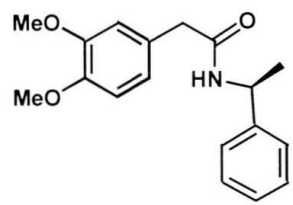

25a

$CDCl_3$, NMR 300 MHz

1-az-53

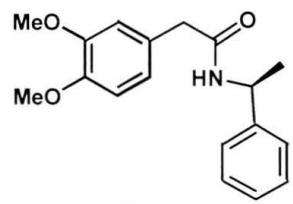

25a

$CDCl_3$, NMR 75.46 MHz

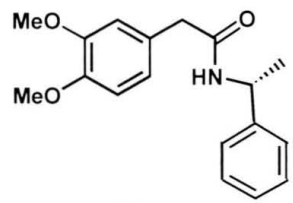

25b

$CDCl_3$, NMR 300 MHz

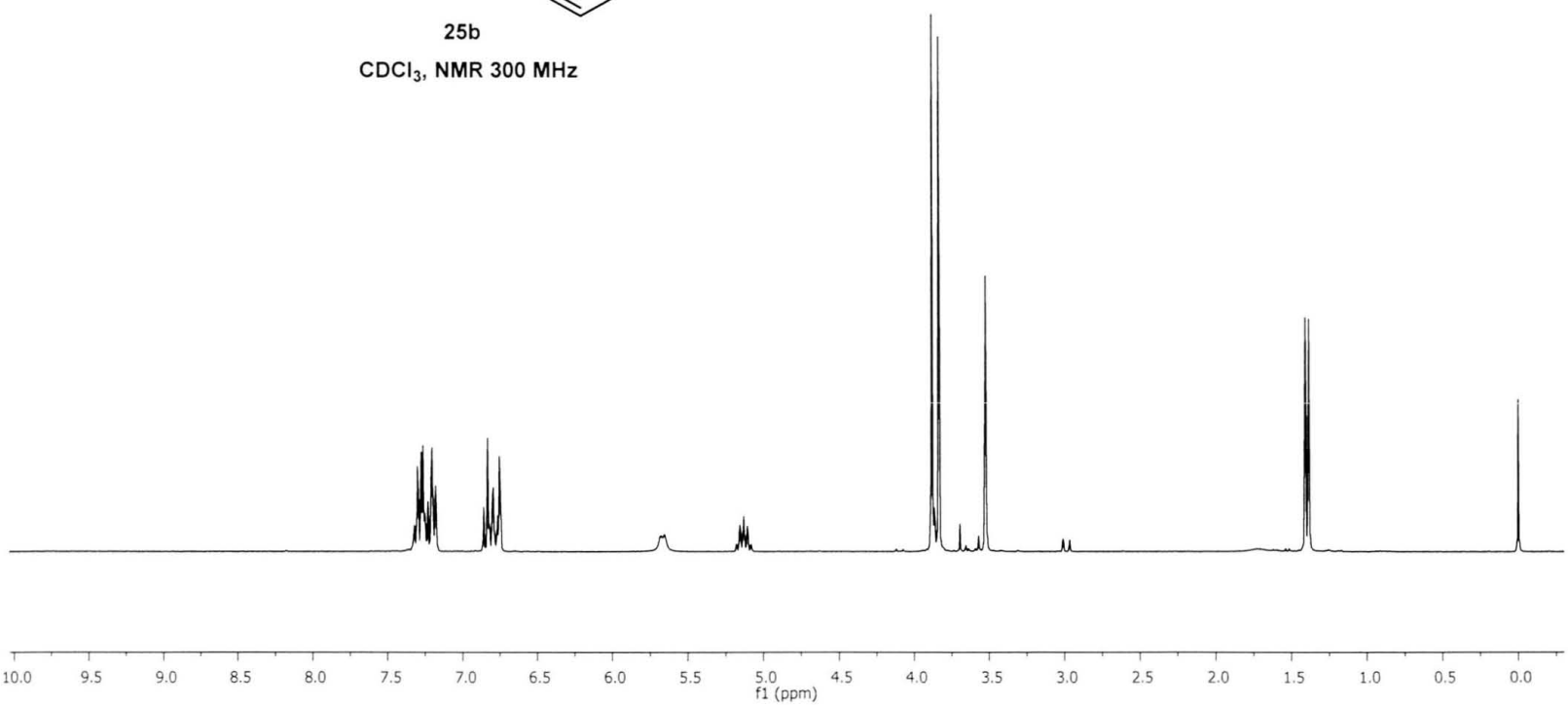

az-41

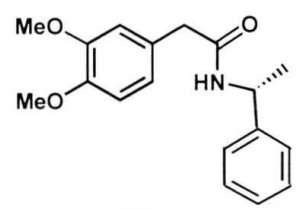

25b

$CDCl_3$, NMR 75.46 MHz

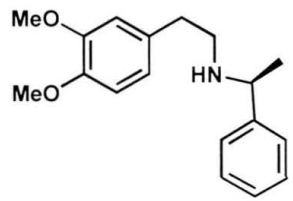

14a

$CDCl_3$, NMR 300 MHz

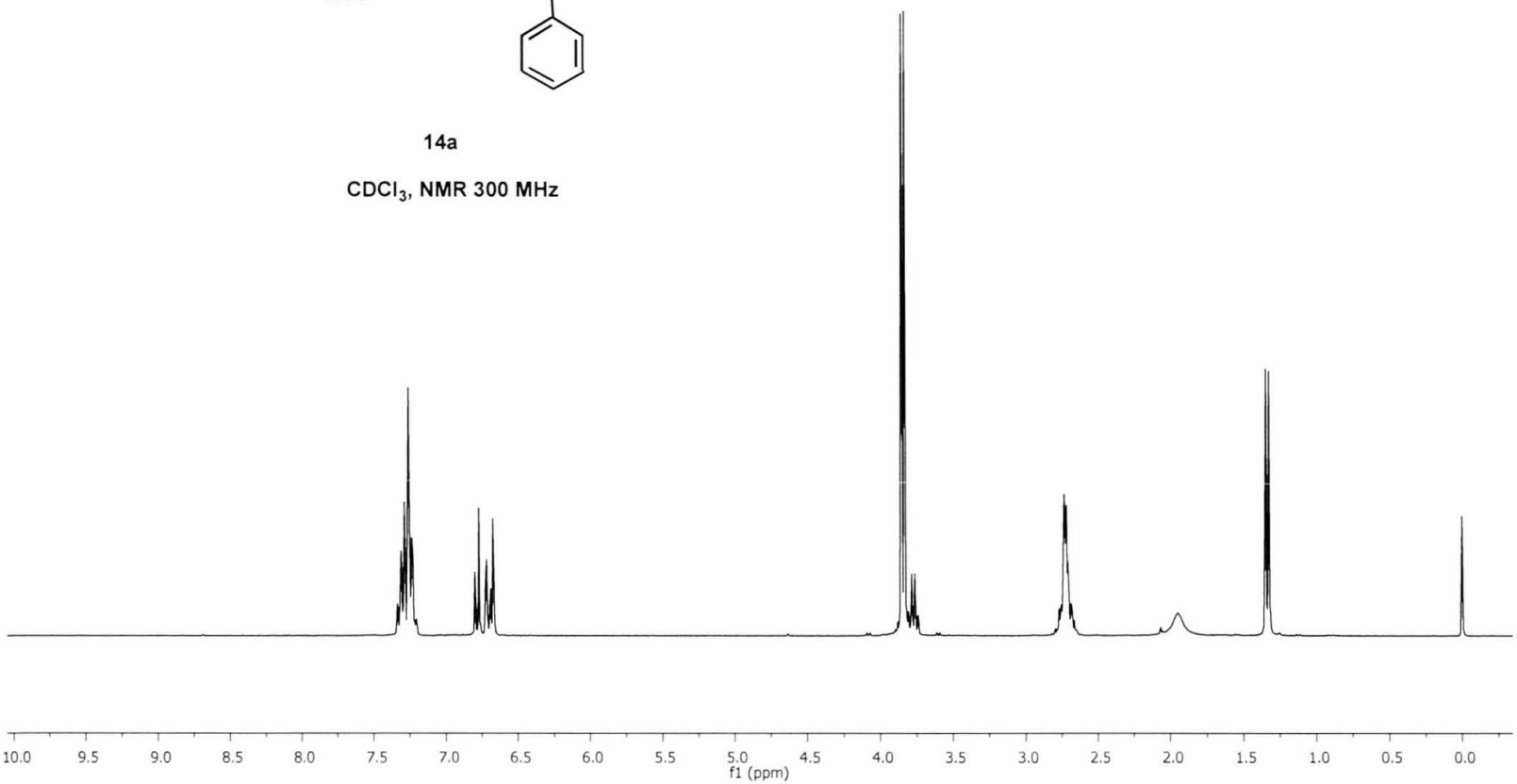

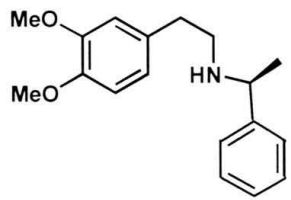

14a

$CDCl_3$, NMR 125.77 MHz

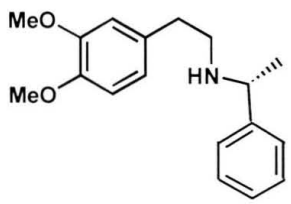

14b

$CDCl_3$, NMR 500 MHz

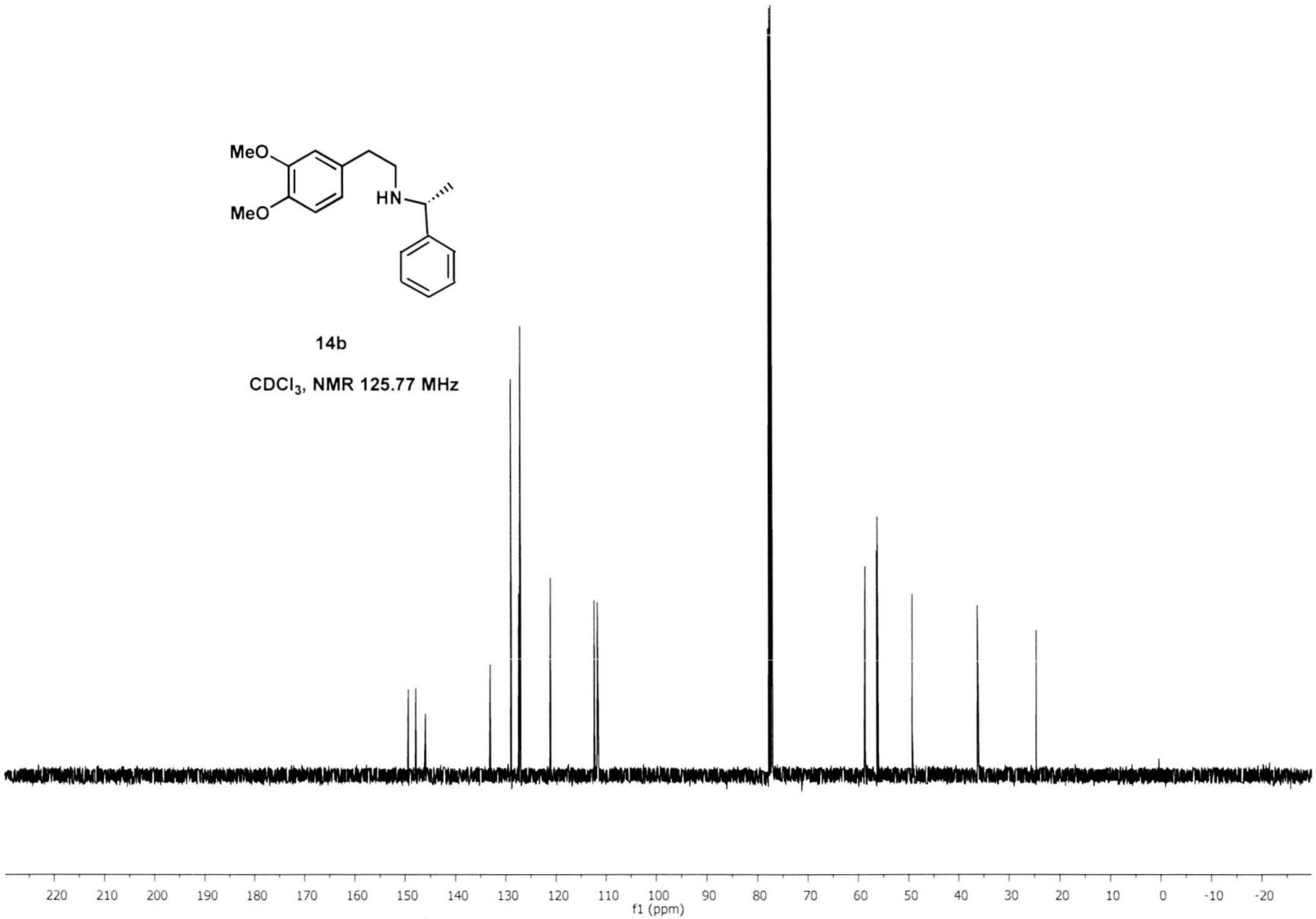
MeO
MeO
HN
14b
CDCl3, NMR 125.77 MHz
220 210 200 190 180 170 160 150 140 130 120 110 100 90 80 70 60 50 40 30 20 10 0 -10 -20
f1 (ppm)

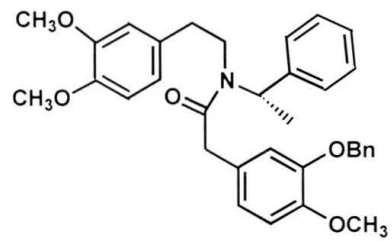

13a

$CDCl_3$, NMR 500 MHz

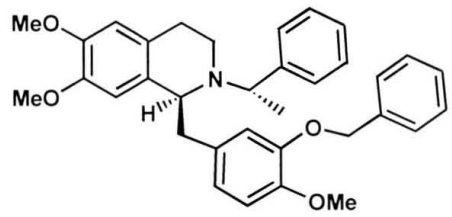

26a

$CDCl_3$, NMR 500 MHz

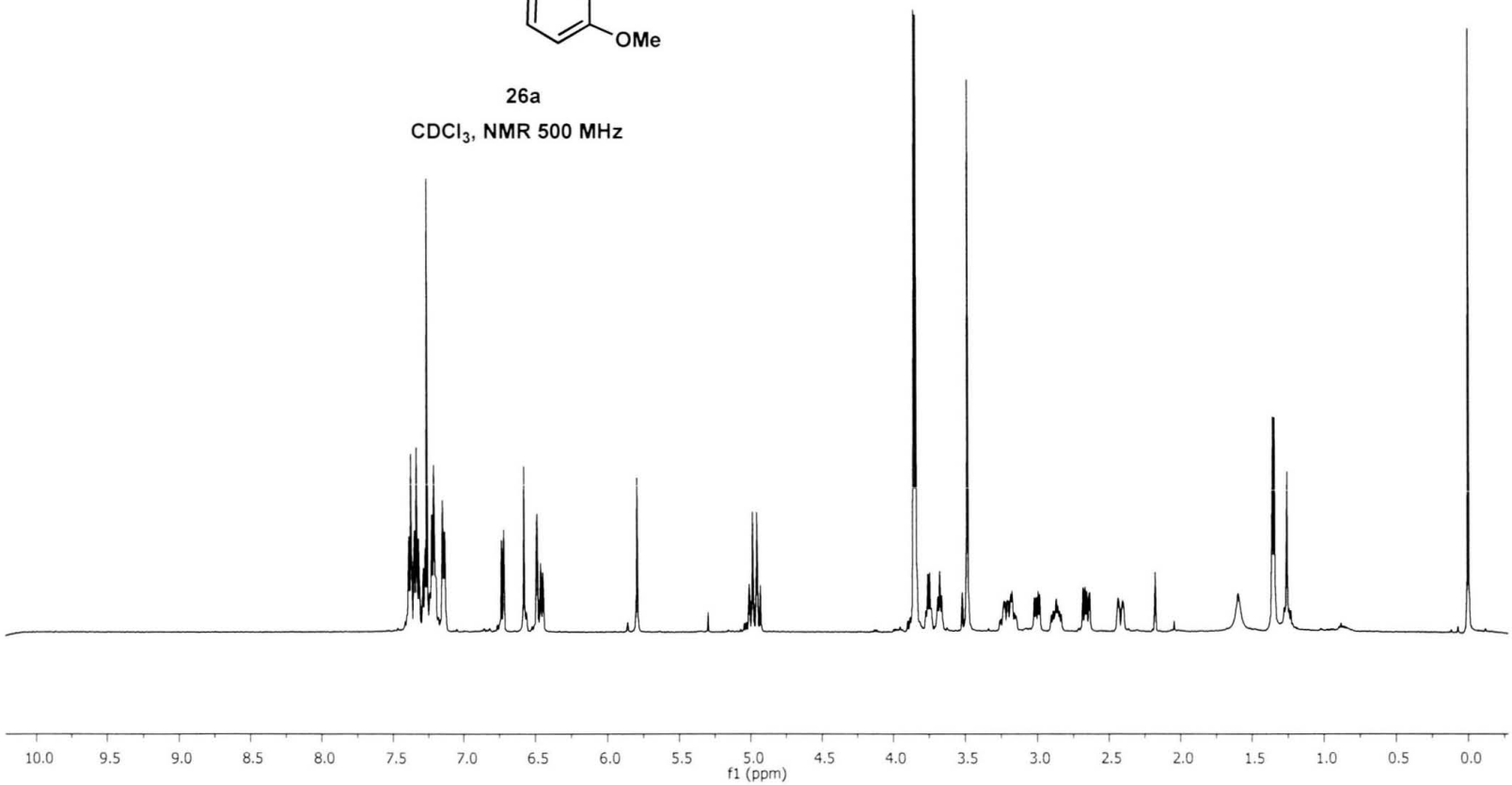

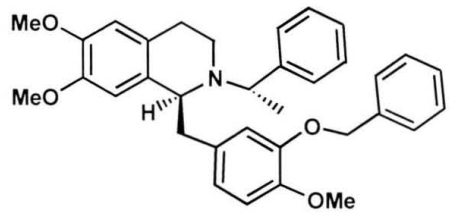

26a

$CDCl_3$, NMR 125.77 MHz

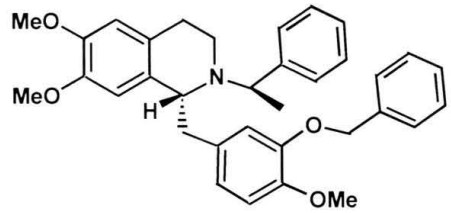

26b

$CDCl_3$, NMR 500 MHz

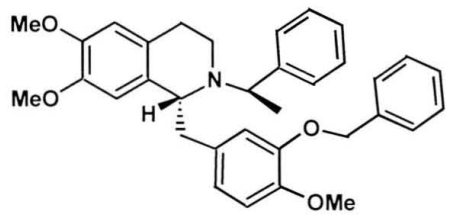

26b

$CDCl_3$, NMR 125.77 MHz

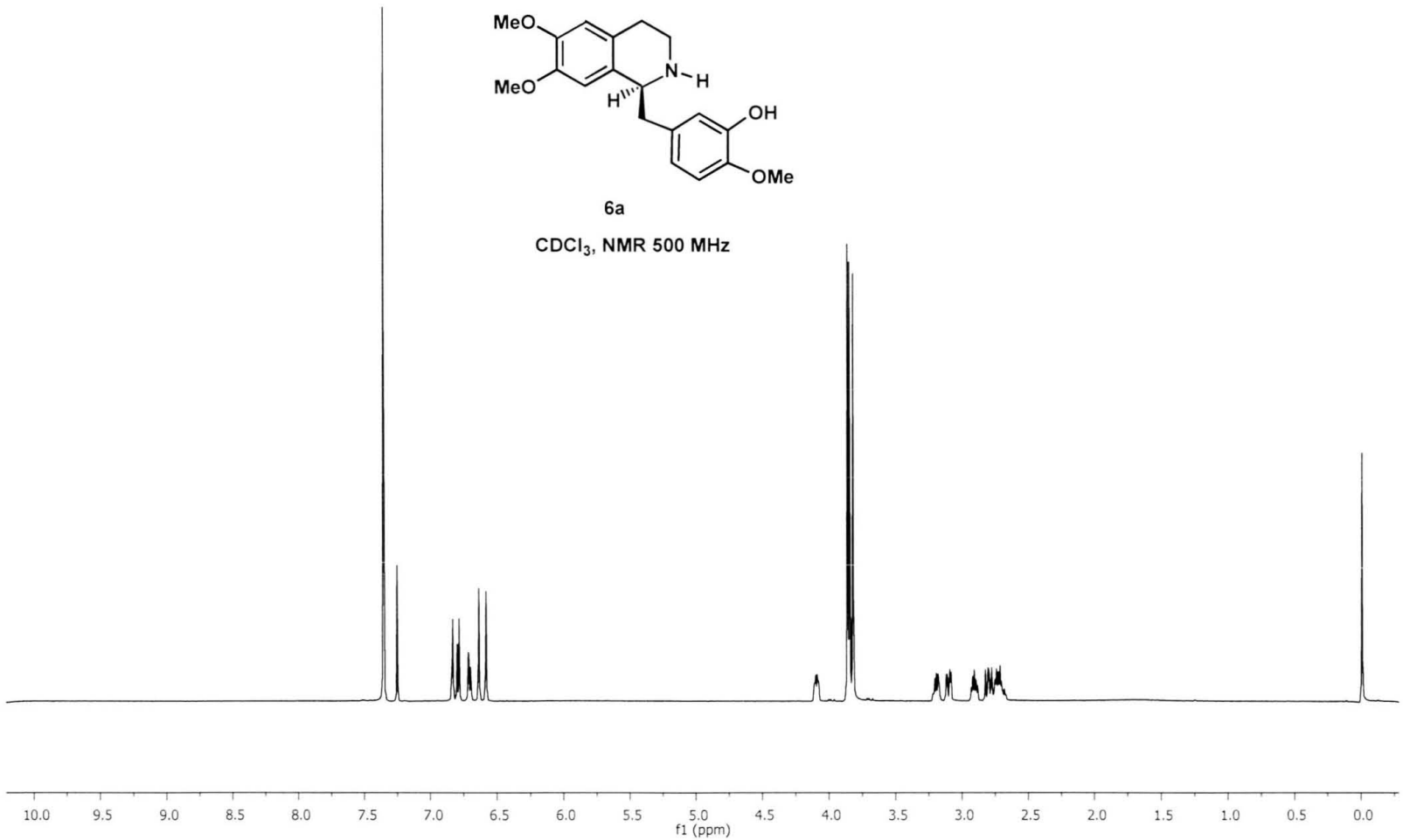
MeO
MeO
N
H
H
OH
OMe
6a
CDCl3, NMR 500 MHz
10.0
9.5
9.0
8.5
8.0
7.5
7.0
6.5
6.0
5.5
5.0
4.5
4.0
3.5
3.0
2.5
2.0
1.5
1.0
0.5
0.0
f1 (ppm)

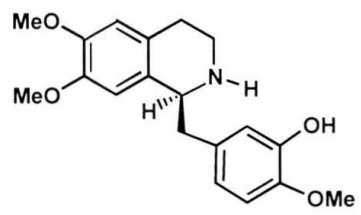

6a

$CDCl_3$, NMR 125.77 MHz

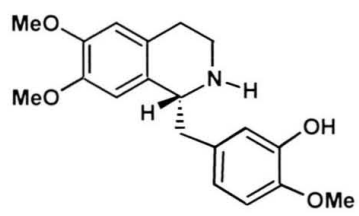

6b

$CDCl_3$, NMR 500 MHz

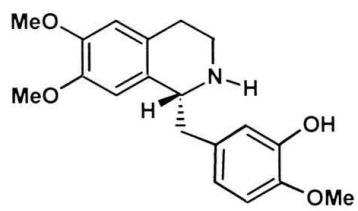

6b

$CDCl_3$, NMR 125.77 MHz

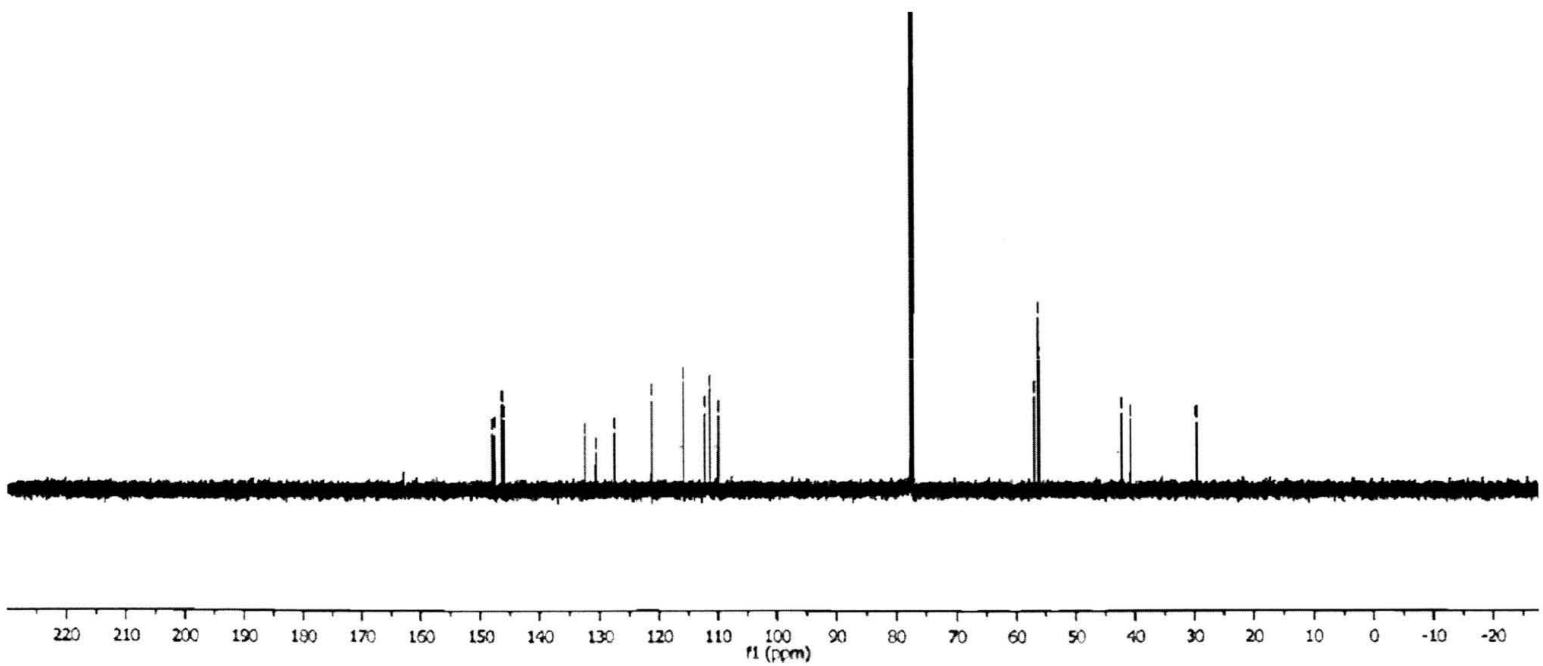

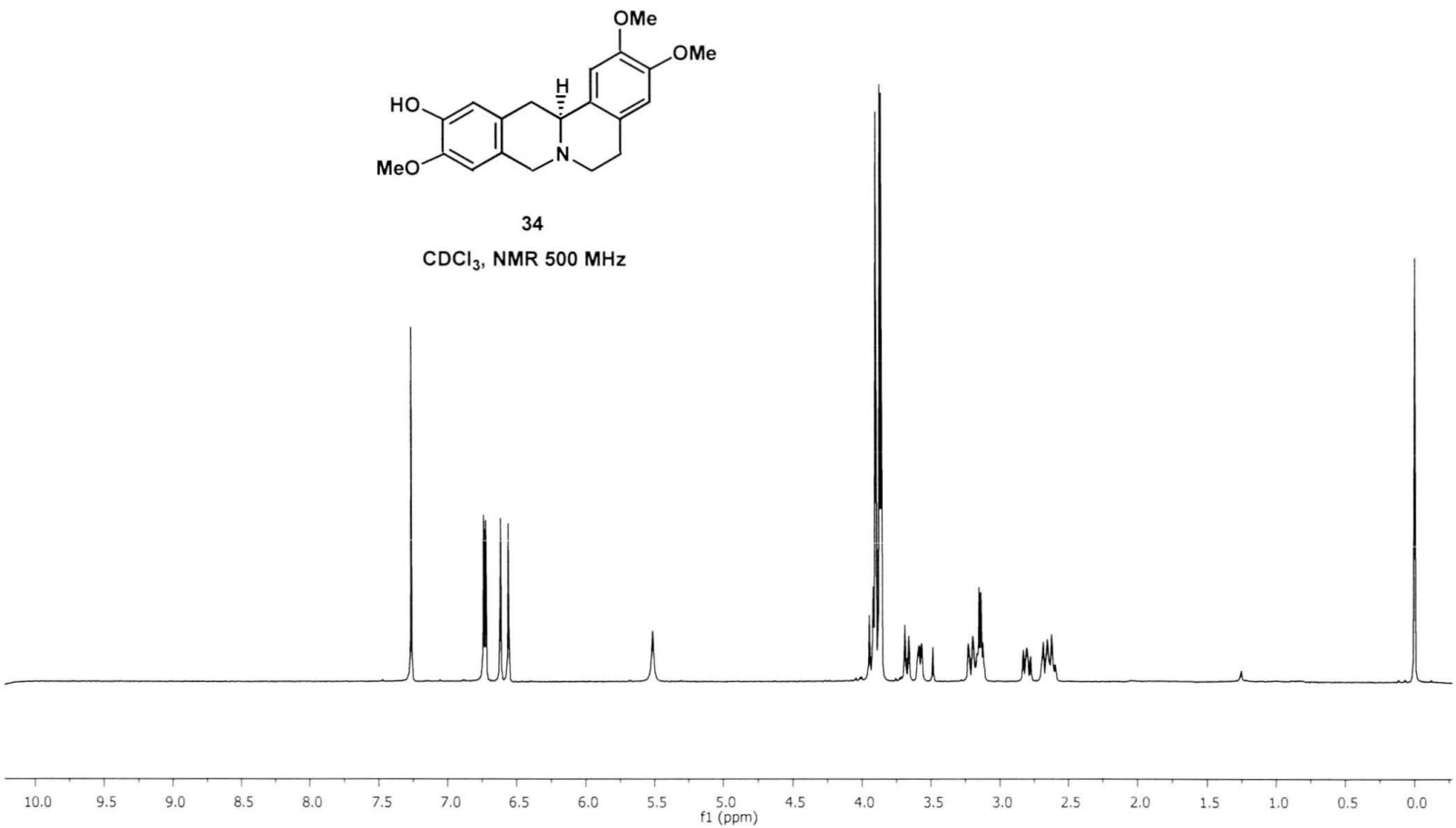
OMe
OMe
HO
H
N
MeO
34
CDCl3, NMR 500 MHz
10.0
9.5
9.0
8.5
8.0
7.5
7.0
6.5
6.0
5.5
5.0
4.5
4.0
3.5
3.0
2.5
2.0
1.5
1.0
0.5
0.0
f1 (ppm)

az2999e/1

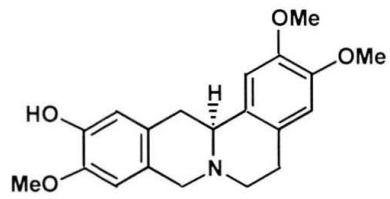

34

$CDCl_3$, NMR 125.77 MHz

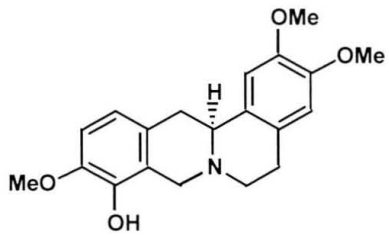

33

$CDCl_3$,NMR 500 MHz

az3161a/1

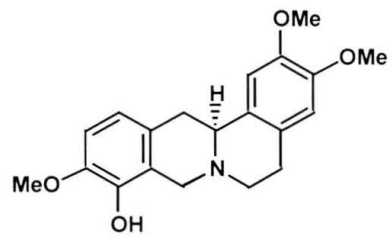

33

$CDCl_3$,NMR 125.77 MHz

Chapter 3

Enantioselective Total Synthesis of (1*R*, 1′*S*)-Temuconine, a Bisbenzyltetrahydroisoquinoline Alkaloid

Part of the work described in this chapter has been published in

Acta Cryst. **2010**, *E66*, o2646

Chapter 3

Enantioselective Total Synthesis of (1*R*, 1′*S*)-Temuconine, a Bisbenzyltetrahydroisoquinoline Alkaloid

3.1 Definition and Structural Classification of BBIQs.

The bisbenzyltetrahydroisoquinoline ("BBIQ") family of alkaloids is one of the most important groups of isoquinoline alkaloids that exist in many plant species, particularly in members of *Menispermaceae*, *Berberidaceae*, *Ranunculaceae*, *Annonaceae*, and *Monimiaceae*.[1] The most important common structural characteristic of BBIQ alkaloids is that there are two benzylisoquinoline subunits in each molecule. Classically, the BBIQs are divided into three categories based on the benzylisoquinoline units from which they are derived: biscoclaurines, coclaurine-reticulines, and bisreticulines.[2] Most of the bisbenzyltetrahydroisoquinolines are formed through the condensation of two *N*-methylcoclaurin units, and a much smaller group are derived from the bonding of one *N*-methylcoclaurin unit with a reticuline unit. Most recently, dimers have been found which are formed through the condensation of two reticuline units.

According to Guha and Shamma[1,3] the BBIQs can be classified into five groups, depending on the nature of the bridges, the number of the oxygen substituents on the aromatic ring, the number of linkages between the two benzylisoquinoline units, and finally, the site at which the bonds exist between the two benzylisoquinoline units. According to this classification, the two moieties are usually bound by one diaryl ether bridge or more, such as is found in magnoline (**1**) and antioquine (**3**). Other types of

bonding motifs can also be found, including the carbon-carbon bridges such as is found in pisopowine (**2**), or a methylene-dioxy bridge such as is found in medelline (**6**). When the linkage involves two benzyl groups, it is called a "tail-to-tail" linkage such as in **1**; however the linkage between one isoquinoline and one benzyl group is called "head-to tail" linkage such as that found in cycleanine (**4**). There may also be different numbers of diaryl ether linkages in different BBIQs. Figure 3.1 shows some BBIQ alkaloids having one, two or three diarylether linkages.[4]

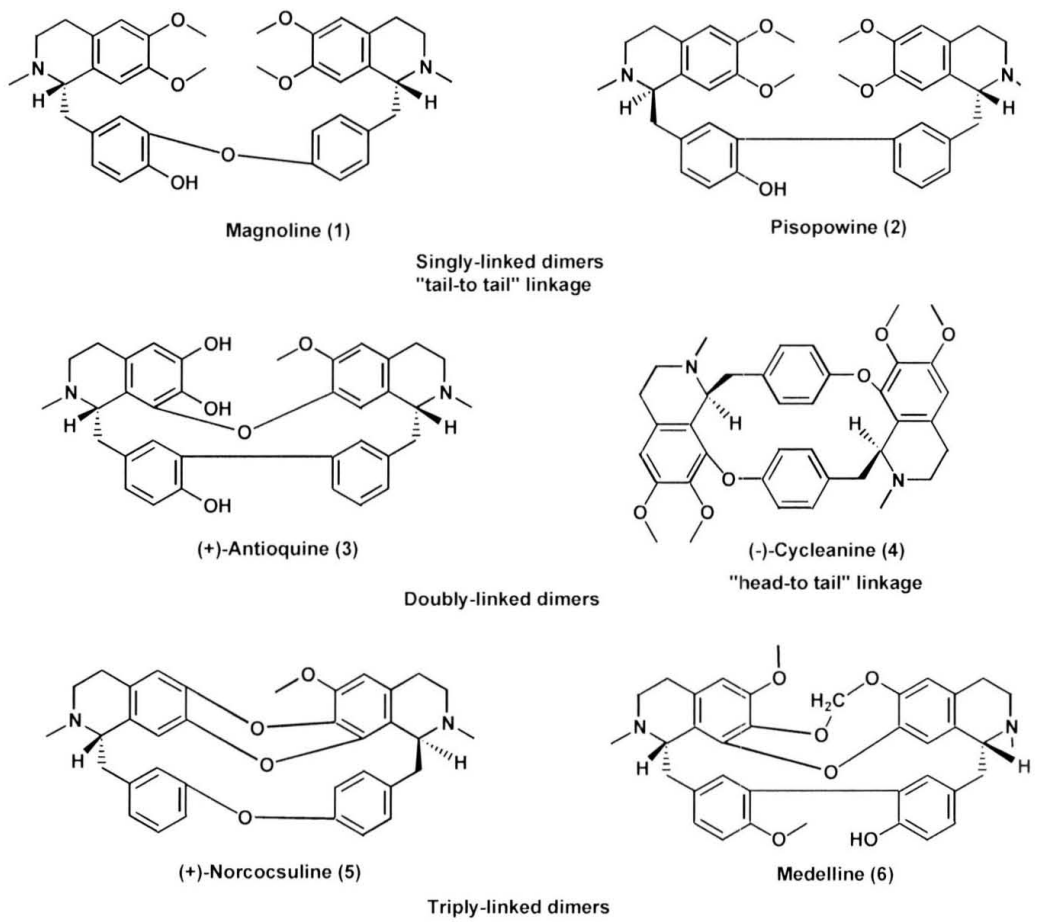

Figure 3.1. Examples of BBIQ alkaloids.

In each subgroup, the members differ by the nature of their oxygenated substituents (*e.g* OH, OMe, OCH_2O), the degree of unsaturation of the heterocyclic rings, the nature of the substituents on the two nitrogen atoms (*e.g* NH, NMe, NMe_2), and the stereochemistry of their two chiral centers, C-1 and C-1′ with either the same, or opposite absolute configurations.

The numbering system is as indicated in Figure 3.2. The right-hand tetrahydroisoquinoline unit is assigned the "prime" superscript and the substituents in the C and C′ rings are always numbered to assign the smallest number to these substituents. In some cases, and for the purpose of simplification, simple Roman numerals are also used for the different types of BBIQs.[3]

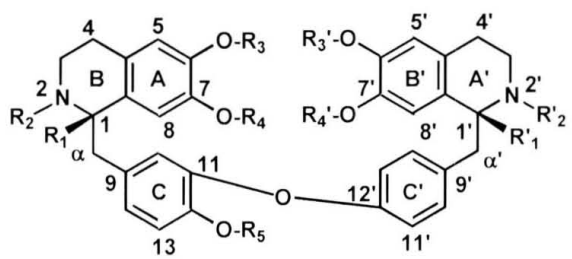

Figure 3.2. Numbering of BBIQ.

3.2 Botanical Sources of BBIQ Alkaloids.

BBIQ alkaloids have been isolated from a variety of plant sources and the amounts and nature of the BBIQs found in plants are affected by ecological factors.[1] In general, different groups of BBIQs are normally found in different genera and some BBIQs could be found as the major component, and also as minor components. For

example, from *Dapkizaizdra micraittha* Benth, collected from New South Wales, micranthine (**7**) (Type XXIII) was separated as the minor constituent; however the major alkaloids were daphnandrine and daphnoline (Type VI) (**8** and **9**, respectively, Figure 3.3).[5]

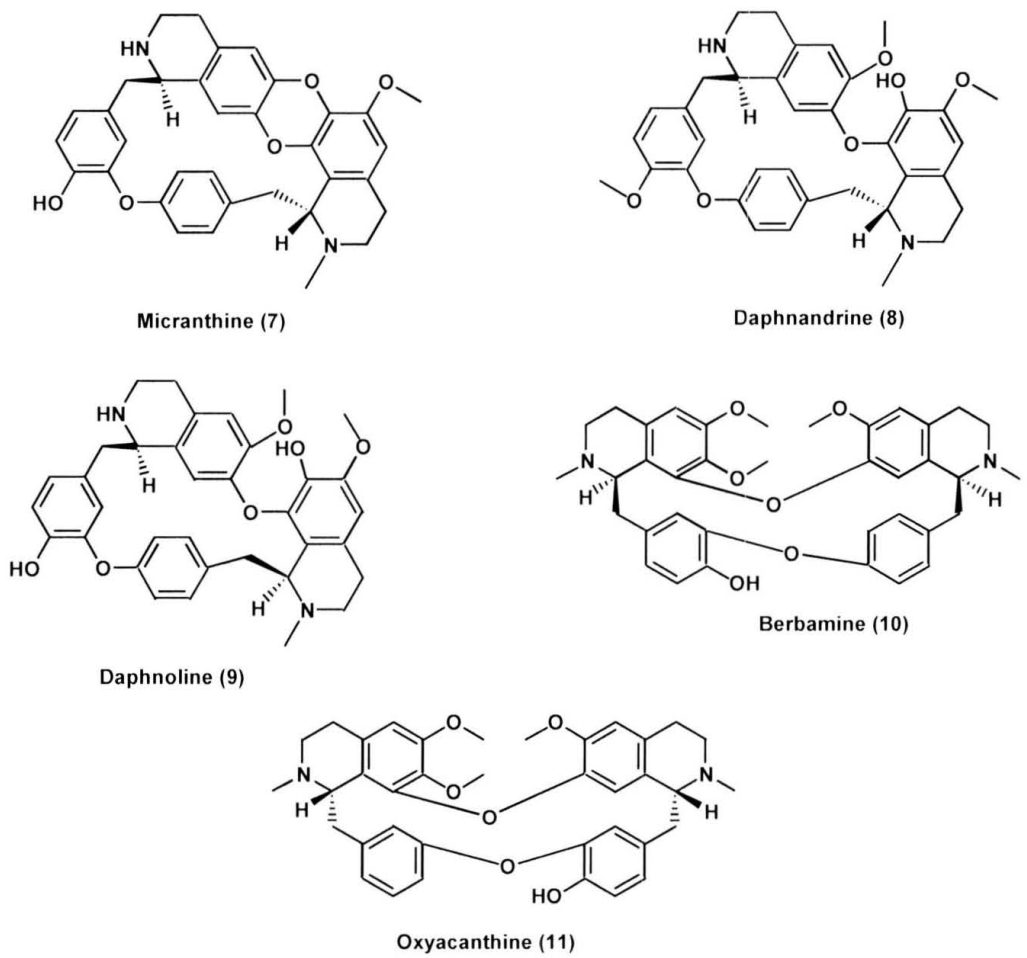

Figure 3.3. Structures of some BBIQs.

Moreover, the alkaloids differ in their proportions in different parts of the plant.[1] For example, the *Mahoriia fortuiiei* Fedde leaves do not contain any BBIQ alkaloids however the trunk is found to have berbamine (**10**) and oxyacanthine (**11**).[6] Also, the

leaves of *Menispermum canadense* Linn were found not to have any alkaloids but the stem, roots, and the rhizome contain alkaloids of Type I.[7] Table 3.1 shows some botanical sources of some BBIQ alkaloids.

Table 3.1. Botanical sources of some bisbenzyltetrahydroisoquinoline.[1]

Name of the plant	**Plant parts**	**alkaloids**
B. lschonoskyana Regel[1]	Stem	Obaberine, Obamegine, Oxyacanthine
C. platiphyllum Miers[8]	Leaf Stem, root and leaf Root and leaf	Chondroioline (-)-Curine Isochondodendrine
C. laurifoliirs DC[9]	Bark and trunk	Isotrilboine, Triboine
C. *leaeba* DC[10,11]	Root Leaf	Oxyacanthine (**11**) Menisarine
C. pareira Linn[12, 13]	Whole plant Root and leaf	Cissampareine Cycleanine (**4**)
T. patens Oliv[14,15]	Root and steam Leaf	Cocsuline Aromoline

3.3 Pharmacological Activity of BBIQ Alkaloids.

BBIQ have been widely demonstrated to possess a number of interesting biological activities, such as anti-tumor, anti-inflammatory, antibiotic, antihypertensive and antiplasmodial activities.[16] The pharmacological activity of several BBIQs is outlined in Table 3.2, which shows that the anti-inflammatory action is common to each of the compounds and the individual alkaloids usually have multiple pharmacological activities.

Table 3.2. Selective BBIQ with pharmacological activity.[6]

Alkaloid	**Structural Type**	**Pharmacological activity**
Tetrandrine (**12**)	VIII	Antiplasmodial,[17] anti-inflammatory[18,19,20,21]
Oxyacanthine (**11**)	VI	anti-inflammatory,[22] antioxidant[23] antiproliferative[18]
Berbamine (**10**)	VIII	Antiplasmodial,[17] anti-inflammatory,[23] antiproliferative,[19] antioxidant [23]
Cepharanthine (**13**)	VIII	anti-inflammatory,[24] analgesic[25]
Cycleanine (**4**)	VI	Muscle relaxant, anti-inflammatory[25]
Fangchinoline (**14**)	VIII	Antiplasmodial, anti-inflammatory[26]
(-)-Repandine (**15**)	X	Antiplasmodial,[18] anti-inflammatory[23]

It is presumed that the chirality and the substitution patterns play a role in determination of the pharmacological activity,[27] however, there is no firm conclusion that

has been made about how exactly these features of BBIQ alkaloids influence the biological activity.

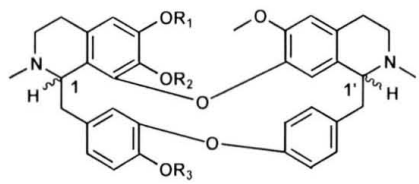

(10) (1*R*, 1'*S*)-Berbamine $R_1 = CH_3$ $R_2 = CH_3$ $R_3 = H$
(12) (1*S*, 1'*S*)- Tetrandrine $R_1 = CH_3$ $R_2 = CH_3$ $R_3 = CH_3$
(14) (1S, 1'*S*)-Fangchinoline $R_1 = CH_3$ $R_2 = H$ $R_3 = CH_3$

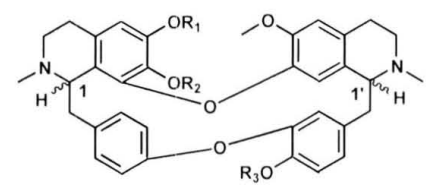

(13) (1*R*, 1'*S*)-Cepharanthine $R_1 = CH_3$ $R_2 = CH_3$ $R_3 = CH_3$
(11) (1S, 1'*S*)-Oxyacanthine $R_1 = CH_3$ $R_2 = CH_3$ $R_3 = H$
(15) (1S, 1'*S*)-Repandine $R_1 = CH_3$ $R_2 = CH_3$ $R_3 = H$

Figure 3.4. Examples of some alkaloids having pharmacological activity.

An example of how the chirality can affect the biological activities can be illustrated by comparison of the three alkaloids tetrandrine (**12**), phaeanthine (**16**) and isotetrandrine (**17**) (Figure 3.5). Although these alkaloids have the same structures, with the only differences in their configurations being at the sterogenic center, these three BBIQs possess different pharmacological activities.[28,29]

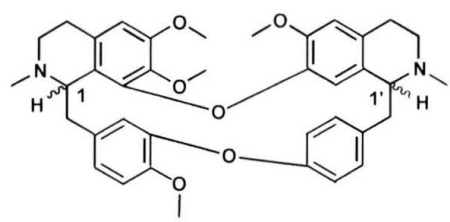

(+)-(1*S*, 1'*S*)-Tetrandrine (12)
(-)- (1*R*, 1'*R*)- Phaeanthine (16)
(+)-(1*R*, 1'*S*)-Isotetrandrine (17)

Figure 3.5. Structure of tetrandrine (**12**), phaeanthine (**16**) and isotetrandrine (**17**).

The two BBIQ alkaloids oxyacanthine (**11**) and berbamine (**10**), isolated from *Mahonia aquifolium*, show that their chirality and substitution patterns have also been

found to affect the biological activity. These two alkaloids differ in their substitution patterns and have opposite configuration at C-1 and C-1′ and have different biological activity (Table 3.2).

3.4 History of Temuconine.

(-)-Temuconine is a bisbenzyltetrahydroisoquinoline ("BBIQ") alkaloid isolated from *Aristolochia elegans* of Egyptian origin, by Shamma *et al.* [30] It was proposed to be the enantiomer of a compound previously obtained from Chilean *Berberis valdiviana.*[31] In 1999 Angerhofer *et al.*[17] reported that (-)-temuconine has potent antiplasmodial activities but the structure which they depicted, **18**, is not the same as **19** which was reported earlier by Shamma *et al.*[30]

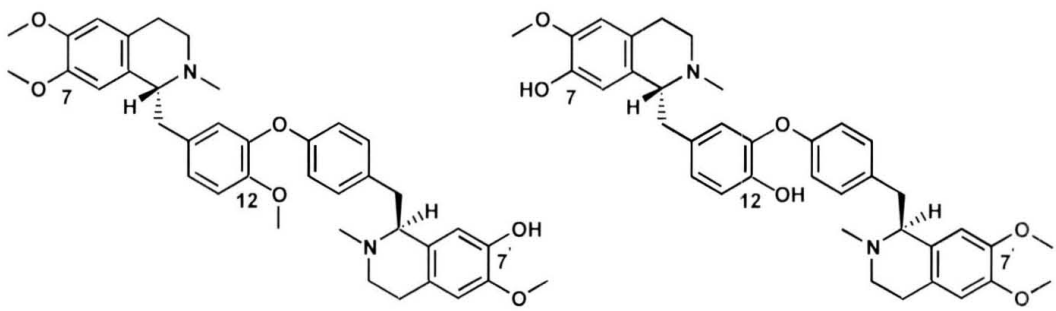

Figure 3.6. Structures proposed for temuconine.

In 1989 Shamma showed that temuconine has two hydroxyl groups at C-7 and C-12 and a methoxy group at C-7′. Angerhofer however showed that temuconine has two

methoxy groups at C-7 and C-12 and a hydroxyl group at C-7′. Shamma and Angerhofer were in agreement that temuconine has two sterogenic centers, *R* at C-1 and *S* at C-1′.

Temuconine has the simplest representative structure of a BBIQ alkaloid which has a "tail-to-tail" linkage and, according to Shamma and Guha's classification, it is a Type I of group A alkaloid. Angerhofer *et al.*[17] recently reported on the antiplasmodial activity and cytotoxicity against mammalian cells for 53 bisbenzylisoquinoline alkaloids. The most selective alkaloids were (-)-cycleanine (**4**), (+)-cycleatjehine (**20**), (+)-cycleatjehenine (**21**), (+)-malekulatine (**22**), (-)-repandine (**15**), and (+)-temuconine (**18**). Moreover, among the BBIQ alkaloids, temuconine had the lowest reported cytotoxic activity towards KB cells (human oral epidermoid carcinoma).

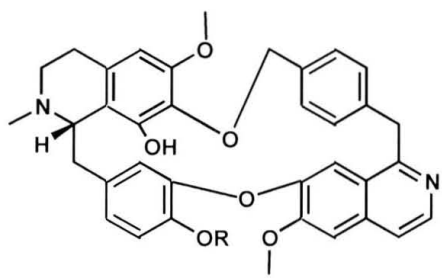

(20) (+)-Cycleatjehine R = H
(21) (+)-Cycleatjehenine R = CH_3

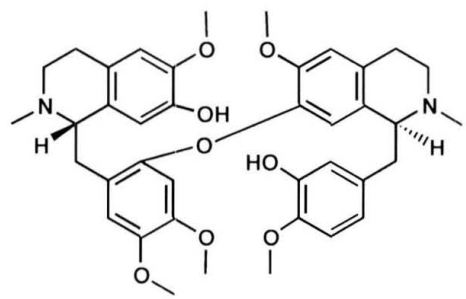

(22) (+)-Malekulatine

Figure 3.7. Structures of (+)-cycleatjehine (**20**), (+)-cycleatjehenine (**21**), (+)-malekulatine (**22**).

(1*S*,1′*S*)-Thalibrine (**23**), which was isolated from *Thalictrum reaolutum* DC, is known to be the diastereomer of (1*R*,1′*S*)-temuconine.[17] Methylation of the hydroxyl

group at C-7′ produces the BBIQs *O*-methylthalibrine (**24**) which is used as a folk medicine in central Asia.[32]

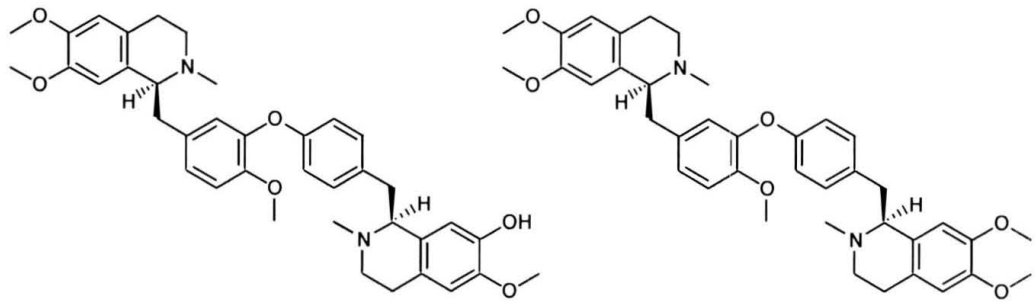

Figure 3.8. Structures of thalibrine (**23**) and *O*-methylthalibrine (**24**).

3.5 Results and Discussion.

The unsymmetrical structure for temuconine and the two stereogenic centers, in addition to the complexity of the substituents on the tetrahydroisoquinoline subunits and the diaryl ether bridge, when taken into consideration, make temuconine a synthetically challenging target. It was decided to aim for the synthesis of **18**, the structure reported by Angerhofer *et al.*

3.5.1 Initial proposal for the synthesis of (1*R*, 1′*S*)-temuconine.

As indicated before, there are two main steps for preparing the BBIQ alkaloids. First is the stereoselective construction of the tetrahydroisoquinoline unit, and second is the efficient formation of the diaryl ether linkage. The tetrahydroisoquinoline unit had previously been synthesized with well-controlled stereoselectivity as shown in Chapter 2

for the syntheses of (*S*)-and (*R*)-*N*-norlaudanidine, using a chiral auxiliary-assisted Bischler-Napieralski cyclization (BNC)/reduction reaction. Outlined in Scheme 3.1 is the initial retrosynthetic analysis undertaken for (1*R*,1′*S*)-temuconine (**18**).

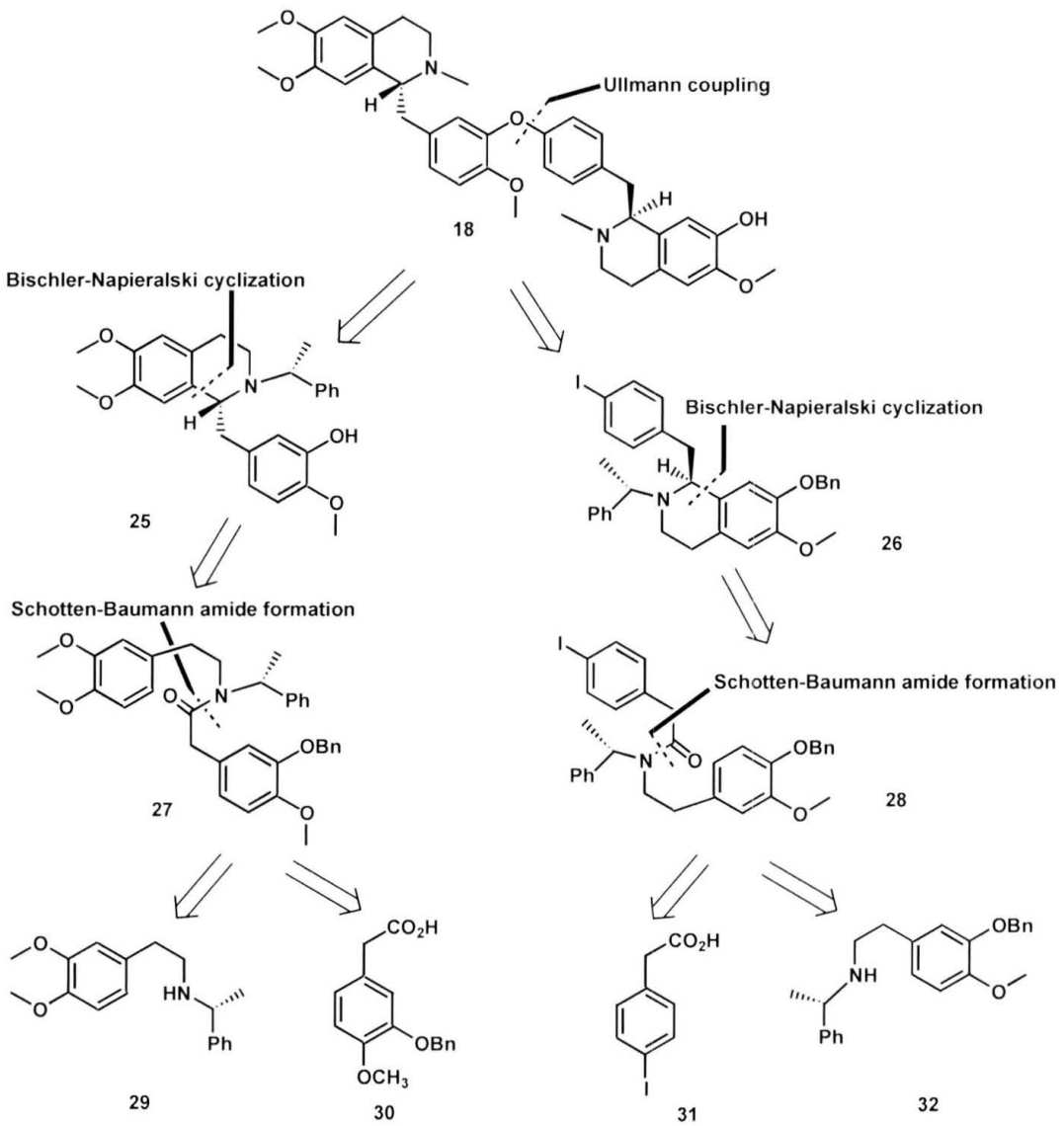

Scheme 3.1. The first retrosynthetic analysis for (1*R*,1′*S*)-temuconine (**18**).

As shown in this Scheme classical Ullmann coupling diaryl ether formation is one of the key methodologies applied in this approach. If such a coupling methodology were to be used, the first retrosynthetic disconnection gives the iodo- and the phenolic hydroxyl synthons. The two tetrahydrosioquinoline units **25** and **26** could be constructed using a chiral auxiliary-assisted Bischler-Napieralski cyclization (BNC)/reduction reaction of the amides **27** and **28**, respectively. This regioselectivity for ring closure in the BNC reaction is due to the presence of only one site which is *para* to the electron-donating methoxy group. Compound **25** should be derived from compound **27**, which had been synthesized in Chapter 2 in our syntheses of both (*S*)-and (*R*)-*N*-norlaudanidine after selective removal of the benzyl protecting group without affecting the chiral auxiliary. Vanillin would be the logical starting material for **29**. The second disconnection dissects the amide **28** into the key intermediates, carboxylic acid **31,** and the chiral auxiliary-protected amine **32,** having the chiral auxialry, (*S*)-α-methylbenzylamine. These two intermediates are required for the Schotten-Baumann reaction to afford the amide **28**.

3.5.2 Synthesis of the key intermediate tetrahydroisoquinoline unit 25.

In order to effect the Ullman diaryl ether coupling step, selective removal of the benzyl group is needed first from compound **33** (the intermediate that was used in the syntheses for both (*S*)-and (*R*)-*N*-norlaudanidine) to form **25**. In general, Pd/C-catalyzed hydrogenolysis is one of the main methods to cleave the benzyl group.[33,34] Catalytic hydrogenation using 10 % Pd/C, ethanol, EtOAc, $HCl_{(aq)}$, and stirring for 24 h under H_2

however removed both the chiral auxiliary and the benzyl group (Scheme 3.2), as noted before in Chapter 2 .

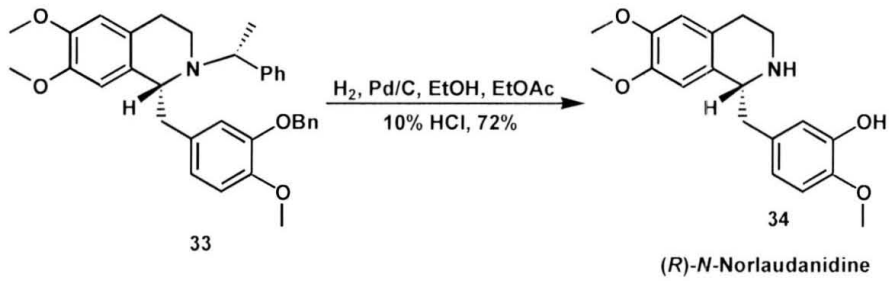

Scheme 3.2. Catalytic hydrogenation for **33**.

Attention was then directed towards the use of an alternative mild condition, using Raney nickel in MeOH to achieve the debenzylation without affecting the chiral auxiliary.[35] When this condition was employed on compound **33**, the reaction produced the desired product **25** in 33% yield, but along with (*R*)-*N*-norlaudanidine (**34**) in 15% yield and the unreacted starting material, **33** (Scheme 3.3).

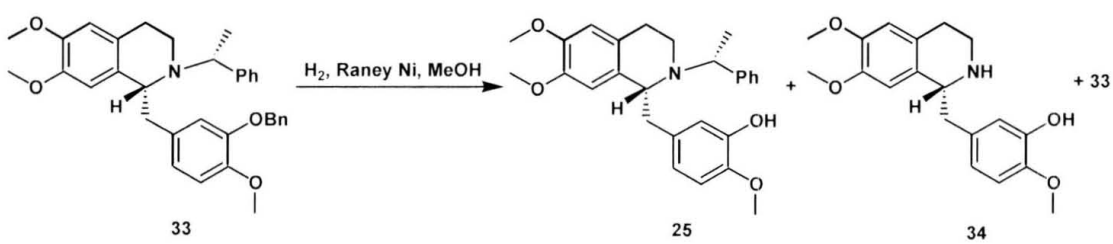

Scheme 3.3. Hydrogenation of compound **33** using Raney nickel.

Using milder hydrogenation conditions, in anhydrous CH_2Cl_2, the desired product was obtained but in a very low yield, and some starting material was also recovered.

Increasing the reaction time, or hydrogen pressure, led to the removal of the chiral auxiliary and formation of compound **34** in 25% yield, along with compound **25** in 31% yield as shown in Scheme 3.4.

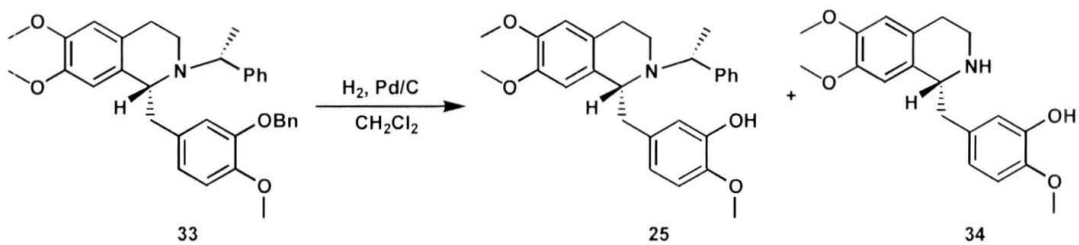

Scheme 3.4. Hydrogenation of compound **33** using mild conditions.

Finally, a debenzylation procedure developed by Hori and Mukai's group[36,37] using the Lewis acid $TiCl_4$, in dry CH_2Cl_2 afforded the desired product in a reasonable yield without affecting the chiral auxiliary (Scheme 3.5).

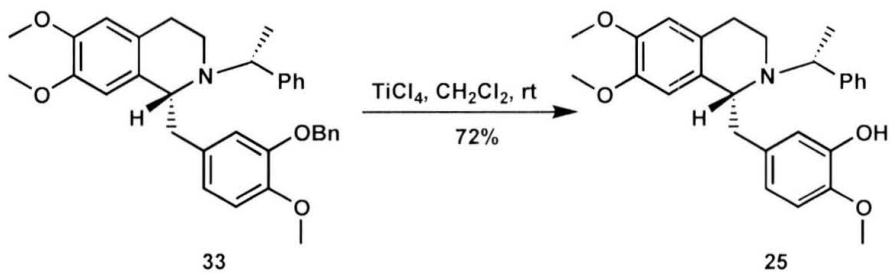

Scheme 3.5. Debenzylation of compound **33** using $TiCl_4$.

Crystals of **25** were obtained from methanol and a single-crystal X-ray structure was determined. Figure 3.9 shows the X-ray structure of compound **25** having the *R* configuration at C-1.

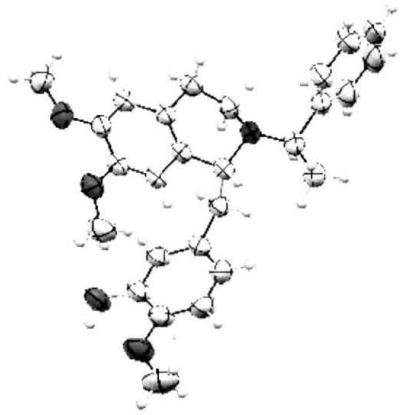

Figure 3.9. X-ray structure of compound **25** with 50% probability ellipses.

3.5.3 Synthesis of the key intermediate benzyltetrahydroisoquinoline 26.

In order to synthesize the key intermediate benzyltetrahydroisoquinoline **26**, it is important that both chiral auxiliary-protected amine **32**, and the benzyl component **31**, be synthesized in good yield. The chiral auxiliary-protected amine **32** was synthesized as outlined in Scheme 3.6. Protection of the phenolic group on the commercially-available vanillin (**35**) as the benzyl ether **36** using benzyl bromide was achieved in 98% yield. Reduction of the aldehyde group to the corresponding primary alcohol **36** was accomplished using sodium borohydride to furnish the alcohol **36** in a 94% yield. Treating compound **36** with $SOCl_2$ gave the benzyl chloride **37** in 88% yield. Cyanation in DMSO resulted in the formation of **38** in a 91% yield which was subjected to hydrolysis using NaOH/EtOH to form the corresponding phenylacetic acid **39** in 95% yield. Reaction of the phenyl acyl chloride, formed *in situ* from phenylacetic acid **39**, with (*S*)-α-methylbenzylamine under Schotten-Baumann conditions resulted in the

formation of the amide **40** (88%). Reduction of **40** to the corresponding secondary amine **32** was accomplished in 83% yield via BF_3•etherate-mediated reaction with B_2H_6 in THF.

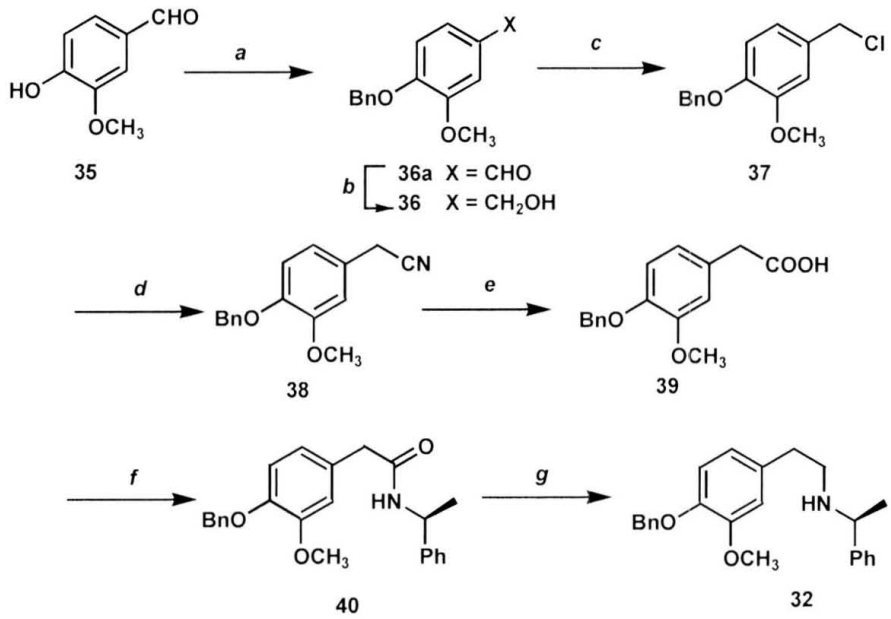

a: BnBr, K_2CO_3, DMSO, 98%, **36a**; ***b:*** $NaBH_4$, THF, MeOH, 94%, **36**; ***c:*** $SOCl_2$, benzene, pyridine, rt, 88%; ***d:*** NaCN, DMSO, benzene, 91%; ***e:*** 4N NaOH, EtOH, 95%; ***f:*** 1. $(COCl)_2$, benzene; 2. (*S*)-α-methylbenzylamine, 5% NaOH(aq), CH_2Cl_2, 88%; ***g:*** B_2H_6, THF, BF_3•Et_2O, 83%.

Scheme 3.6. Synthesis of the chiral auxiliary-protected amine **32**.

The synthesis of the other benzyl component, 4-iodophenylacetic acid (**31**), was achieved in a relatively smooth way using 4-iodotoluene (**41**) as the starting material. A radical reaction takes place when **41** is treated with NBS as a bromination reagent to produce *p*-iodobenzylbromide (**42**). Cyanation resulted in the formation of 4-iodoacetonitrile (**43**) in an 88% yield which was followed by hydrolysis with NaOH/EtOH to form the desired 4-iodophenylacetic acid (**31**) in 93% yield (Scheme 3.7).

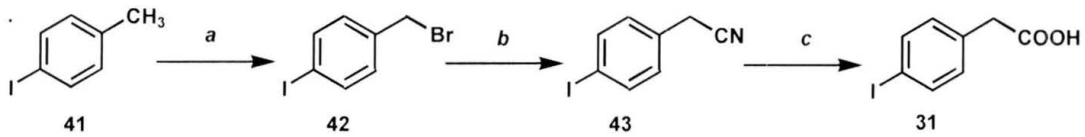

a: NBS, *hv*, CH_2Cl_2, 95%; ***b:*** NaCN, DMSO, benzene, 88%; ***c:*** 4N NaOH, EtOH, 93%.

Scheme 3.7. Preparation of the carboxylic acid **31**.

With both the amine **32** and the benzyl component **31** in hand, amide **28** was synthesized by employing Schotten-Baumann conditions. Bischler-Napieralski cyclization-$NaBH_4$ reduction of the amide **28** afforded the benzyltetrahydroisoquinoline **26**, with *ca.* 96% *de*, as determined from its ^{1}H-NMR spectrum (Scheme 3.8).

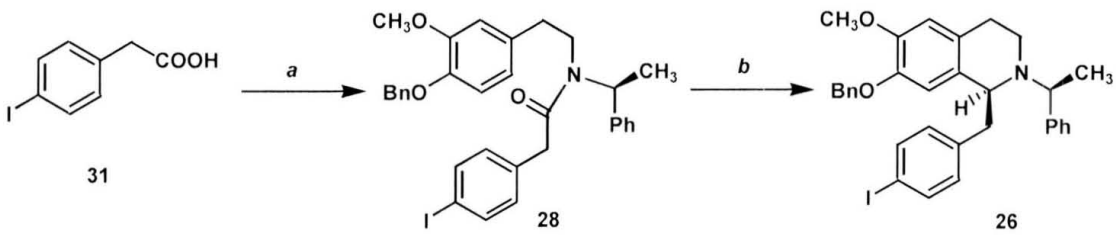

a: 1. $(COCl)_2$, benzene; 2. **32,** 5% NaOH(aq), CH_2Cl_2, 72%; ***b:*** 1. $POCl_3$, benzene; 2. $NaBH_4$, MeOH, 71%, (96% *de*).

Scheme 3.8. Synthesis of the benzyltetrahydroisoquinoline unit **26**.

3.5.4 Diaryl ether formation.

As mentioned before, the second key step for preparing the BBIQ alkaloids is to use an efficient method for formation of the diaryl ether linkage. There are two synthetic strategies which can be envisioned for construction of the diaryl ether. These are by either joining the two aryl moieties together (Route I), or by an intramolecular ether formation of a tethered diaryl system which contains both an electron-donor and acceptor (Route II).[38]

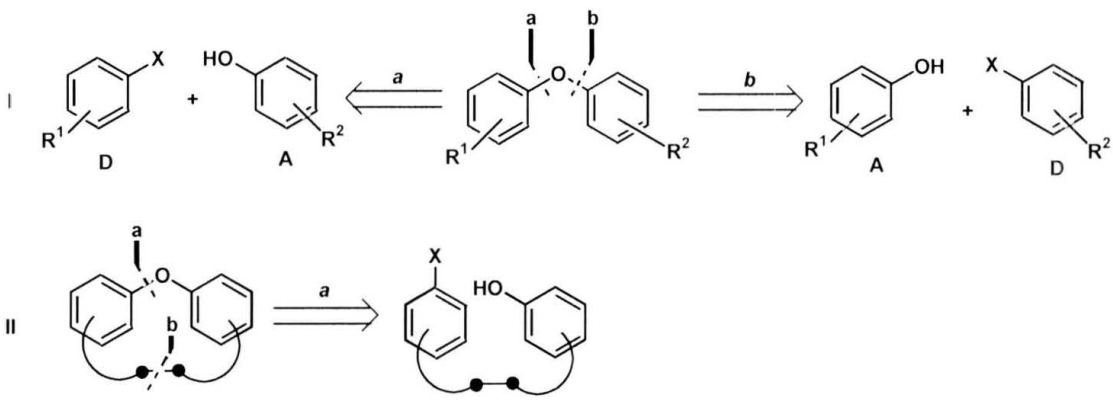

Scheme 3.9. Retrosynthetic analysis showing routes I and II which could be used for diaryl ether formation. A = aryl acceptor and D = aryl donor.[38]

Many methods have been developed to achieve such diaryl ether bridge formation and among these methods are the metal-mediated arylation of phenols, nucleophilic aromatic substitution reactions, and oxidative coupling of phenols. The position and type of the aryl substituents play a role in the rate and yield of the diaryl ether formed. Ullmann-type coupling is one of the most important methods that has been used to achieve diaryl coupling. [39] Its general synthetic scheme is shown below (Scheme 3.10).

Fair to good yields are obtained when electron-rich phenols and electron-poor aryl halides are used. As well, aryl iodides are more reactive than the aryl bromides. The presence of a base such as potassium or cesium carbonate is required and pyridine is commonly used as a solvent. The classic Ullmann biaryl coupling method has been extended by using Cu-based catalysts to permit the reaction of alcohols with aryl halides and has become one of the most well-known methods for the preparation of diaryl ethers. This type of coupling is known as the Ullmann-type condensation.

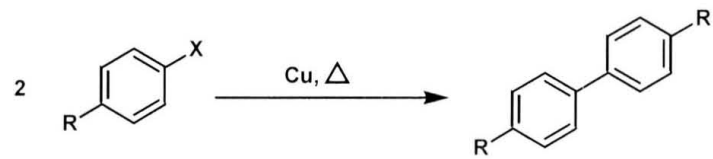

The Ullmann Reaction
Where R = NO_2, CHO, CO_2Me, etc.
X = Br, I

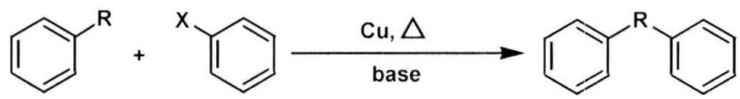

The Ullmann Condensation
Where R = NH_2, OH
X = Br, I

Scheme 3.10. Schematic representation of the Ullmann reaction and the Ullmann condensation.

The exact mechanism for the Ullmann coupling is not known but the most widely accepted mechanism suggests that the aryl halide couples with an excess of copper to form the activated copper (I) intermediate. This species undergoes oxidative addition with the second equivalent of the halide, followed by reductive elimination and formation

of the aryl-aryl carbon bond. Ullmann-type condensation undergoes the same mechanism to produce the diaryl ether and copper halide as a byproduct.

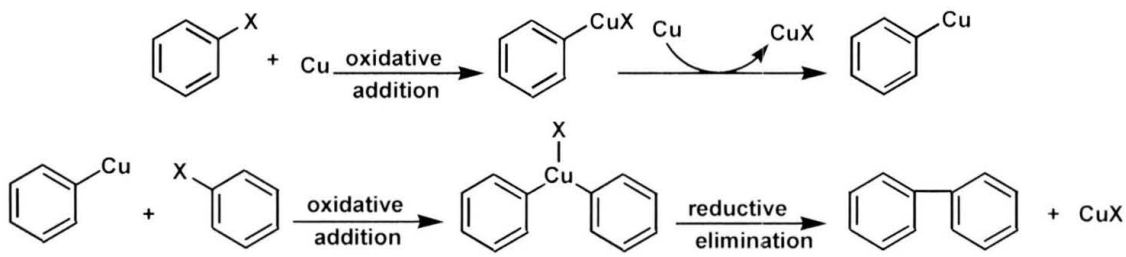

Scheme 3.11. Mechanism of the Ullmann reaction.[40]

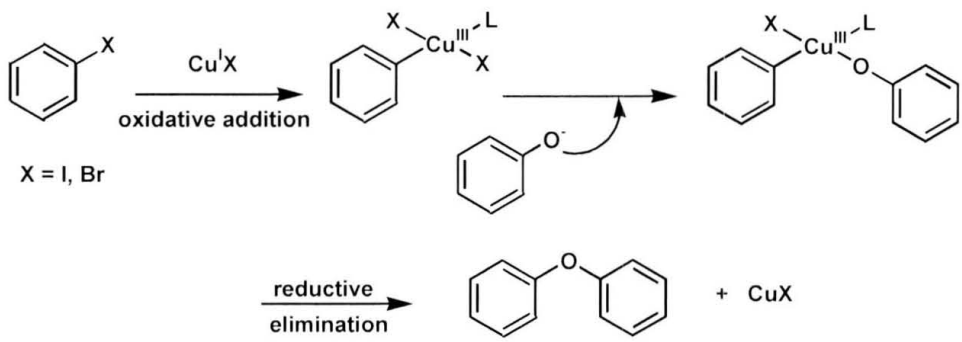

Scheme 3.12. Mechanism of the Ullmann condensation reaction.[41]

However, the Ullmann-type coupling has limitation, and in most cases it is only used with structurally simple phenols and aryl halides due to the harsh reaction conditions required such as the high temperature, and the use of superstoichiometric amounts of copper.[38]

An improvement to the classic Ullmann coupling has been reported by Buchwald using a palladium catalyst.[42] However, the high cost of palladium and the cost of the

ligands have caused many researchers turn their attention again towards copper-mediated cross-coupling reactions. The successful development and the breakthrough in such catalytic versions have resulted in what are generally known as "modified Ullmann reactions", in which the key step is the addition of suitable ligands to the copper catalyst in order to increase the solubility of the copper precursor. This improvement has lead to the use of mild reaction conditions such as low temperature, low catalyst loading and an increase in the reactivity.[43]

Buchwald *et al.*[42] have used copper (II) triflate salts as catalysts with cesium carbonate base at low temperature and in a non-polar solvent to carry out these reactions in good yields under milder conditions with a wide variety of substrates (Scheme 3.13).

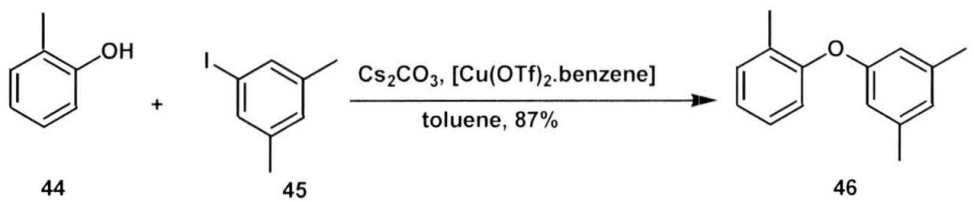

Scheme 3.13. Formation of diaryl ether **46**.

Due to the high cost of copper triflate and its air sensitivity, other types of ligands for copper have been used; these include pyridine-type ligands and phosphine-type ligands which are found to be soluble in most organic solvents such as dichloromethane, toluene, DMF, NMP, and chloroform. Cu(phen)(PPh_3)Br (**47**) and Cu(neocup)(PPh_3)Br (**48**) were examined to act as catalysts. It was reported that aryl bromides can be coupled with phenols to form diaryl ethers in good yields using 10 mol % of **48** as a catalyst and

Cs_2CO_3 as a base in toluene at 110 °C (Scheme 3.14). However, yields of diaryl ethers are substantially lower for aryl bromides bearing *ortho*-substituents.[44]

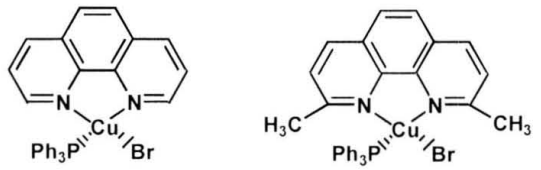

Cu(Phen)(PPh_3)Br (47) Cu(neocup)(PPh_3)Br (48)

Figure 3.10. Structures of Cu(phen)(PPh_3)Br (**47**) and Cu(neocup)(PPh_3)Br (**48**).

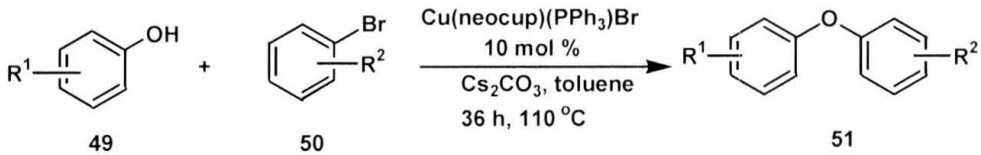

Scheme 3.14. Formation of diaryl ether linkage.

Buck *et al.*[45]reported the use of 2,2,6,6-tetramethylheptane-3,5-dione (TMHD) to improve the Ullmann coupling reaction and allowing it to occur at moderate temperatures. In general, Ullmann-type couplings do not work with aryl halides with strong electron-donating groups and phenols with electron-withdrawing groups. Nevertheless, this methodology has shown significant improvement over the classical methods, and desired products are formed in good yields (Scheme 3.15).

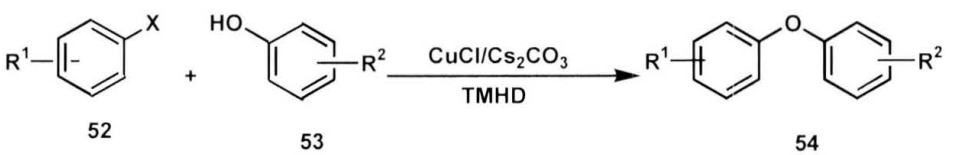

Scheme 3.15. Formation of diaryl ether linkage.

In order to accelerate Ullmann-type coupling, α- and β-amino acids can be used. It has recently been reported that CuI/L-proline (or CuI/*N*-methylglycine) is an efficient catalytic system to permit Ullmann-type aryl amination to work at the lowest temperature reported (Scheme 3.16);[46] however, the use of this amino acid formed the products in low yield due to the formation of *N*-(4-methoxyphenyl)-*N*-methylglycine as a side-product.

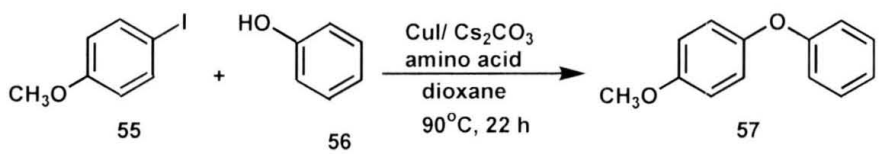

Scheme 3.16. Formation of diaryl ether linkage using amino acid co-catalyst.

However using *N,N*-dimethylglycine instead, from Table 3.3 it can be seen that the yield of the model diaryl ether product increases. These authors showed that the diaryl ethers can be efficiently synthesized using their conditions.[47]

Table 3.3. Coupling reaction of 4-iodoanisole with phenol under the catalysis of copper salts and *N*-methylglycine, L-proline, and *N,N*-dimethylglycine.[47]

Copper salt	**Amino acid**	**Yield %**
CuI	$MeNHCH_2CO_2H$	37
CuI	L-proline	35
CuI	$Me_2NCH_2CO_2H.HCl$	85
CuBr	$Me_2NCH_2CO_2H.HCl$	83
$Cu(OAc)_2$	$Me_2NCH_2CO_2H.HCl$	73
$CuSO_4$	$Me_2NCH_2CO_2H.HCl$	85

3.5.5 First attempts toward the diaryl ether coupling.

In order to conserve valuable intermediates **25** and **26** and test the reactivity of the reagents, model reactions using *p*-cresol and 4-iodotoluene were first conducted (Scheme 3.17).

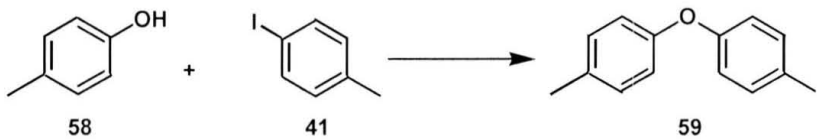

58 41 59

Scheme 3.17. A model reaction for the Ullmann coupling.

Table 3.4. Yields of diaryl ether products using different Ullmann coupling conditions.

Conditions	**Yield %**
BaO, $CuCl_2$, DMF, 150°C.[48]	no reaction
K_2CO_3, CuO, pyridine, 130 °C.[49]	33
Cs_2CO_3, CuI, TMHD, 120 °C.[45,50]	45
Cs_2CO_3, 0.25 % mol $(CuOTf)_2$. PhH, toluene, 5 mol % EtOAc, 96 °C.[42]	50
Cs_2CO_3, CuI, NMP, MW, 195 °C.	40
Cs_2CO_3, CuI, *N,N*-dimethyl glycine HCl, dioxane, 90 °C.[47]	55

As shown in Table 3.4 the yields of the diarylether compound varied under the conditions examined. Buchwald's[42] and Ma's[47] methodologies gave the highest yields for the model reaction, and it was decided to apply these two methods first with the valuable intermediates **25** and **26**. Considering the lower temperature used, Ma's method[47] was first tried using the two intermediates, phenol **25**, and iodo **26** as reactants, in the

presence of Cs_2CO_3, copper catalyst, and *N,N*-dimethylglycine salt in anhydrous dioxane at 90 °C under argon for 35 h (Scheme 3.18). The desired product was detected by mass spectrometry, however, subsequent attempts at purification of this product failed (Entry 1, Table 3.5).

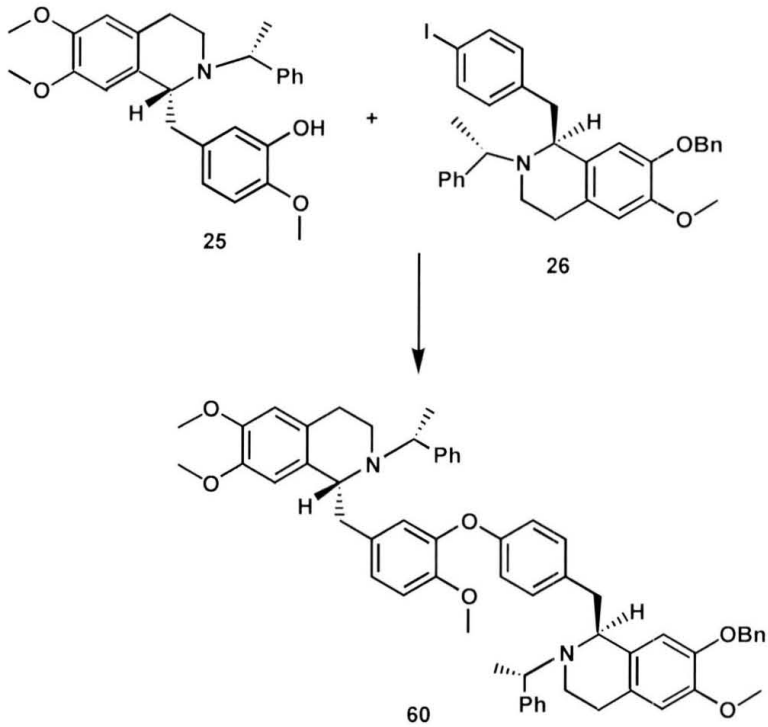

Scheme 3.18. The first attempt toward the diaryl ether coupling.

When Buchwald's method[42] was applied using 0.25 mol% copper triflate as a catalyst and Cs_2CO_3 as base in toluene at 96 °C, no changes in the starting materials were observed and only unreacted starting material were recovered (Entry 2, Table 3.5). Buck's method [45] using TMHD to improve the Ullmann coupling reaction was then tried using the copper catalyst, which was added to anhydrous NMP, and the mixture was

warmed to 120 °C under argon for 24 h. Analysis by APCI-MS showed that no new products were formed. Using microwave heating as a final attempt with copper iodide as catalyst and NMP as solvent for 1 h, the desired product was again detected by mass spectroscopy, however, subsequent attempts at purification of this product also failed to afford clean ^{1}H NMR and ^{13}C NMR spectra.

Table 3.5. Yields of diaryl ether products using different Ullmann coupling conditions.

Conditions	**Yield %**
Cs_2CO_3, CuI, *N,N*-dimethyl glycine HCl, 1,4-dioxane, 90 °C.	the product detected by mass spectrometry
Cs_2CO_3, 0.25 % mol $(CuOTf)_2$. PhH, toluene, 5 mol % EtOAc, 1-naphthoic acid, 90 °C.	no reaction
K_2CO_3, CuO, pyridine, 130 °C.	no reaction
Cs_2CO_3, CuI, NMP, MW, 195 °C.	the product detected by mass spectrometry
Cs_2CO_3, CuI, TMHD, DMF, 120 °C.	no reaction

As mentioned before, Ullmann-type coupling has limitation and in most cases is only used with structurally simple phenols and aryl halides due to the harsh reaction conditions required such as high temperatures, and the use of a stoichiometric amount of copper.[38] It is also possible that in our case, the actual yields for the products obtained in our reactions were very low, due to the use of very small reaction scales. Thus, all of these factors directed attention to use of the second proposal for the synthesis of (1*R*,1′*S*)-

temuconine using a copper acetate-mediated coupling reaction instead, as presented below.

3.5.6 Second proposal for the synthesis of (1*R*,1′*S*)-temuconine (18).

The second strategy employed to prepare the (1*R*,1′*S*)-temuconine **(18)** was to set up the diaryl ether bridge first before installing the second tetrahydroisoquinoline unit. A modified Ullmann-type coupling using a copper acetate-mediated reaction was employed.

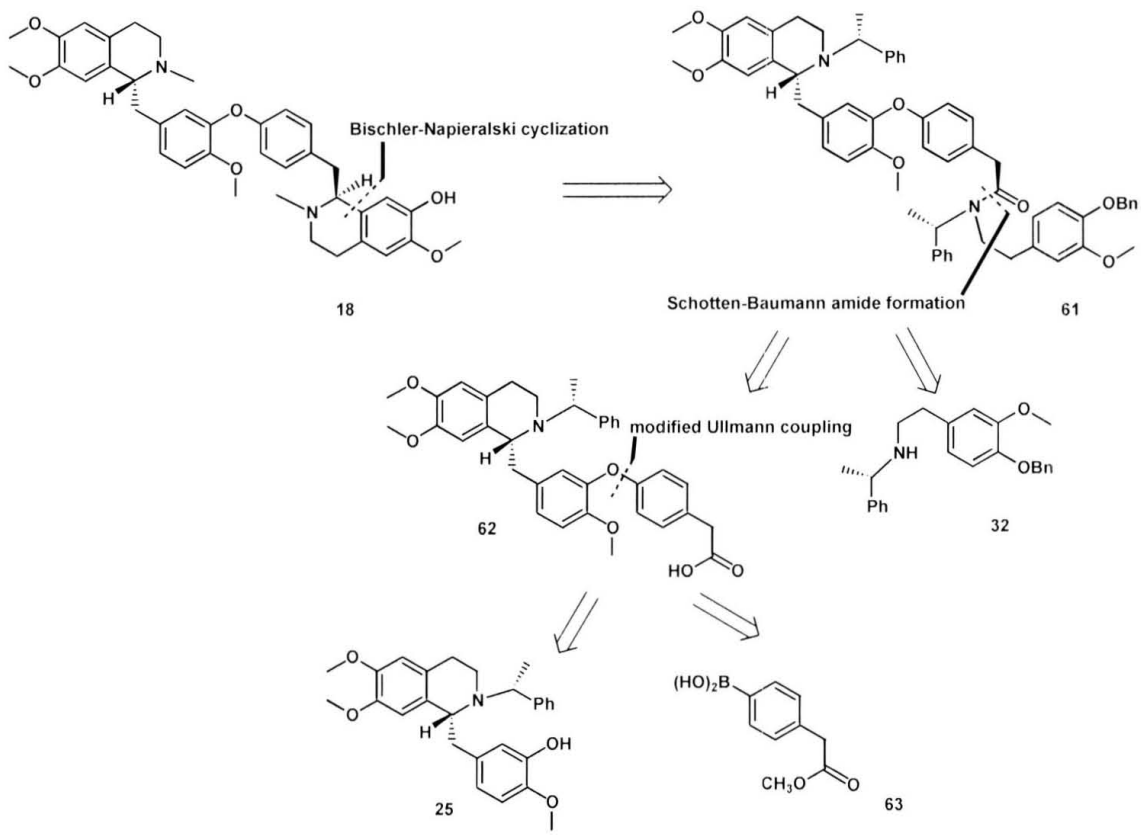

Scheme 3.19. The second retrosynthetic analysis for (1*R*,1′*S*)-temuconine (**18**).

Even though the first attempt did not reach the final target, this strategy was still very useful as most of these intermediates could be used in the next strategy. Scheme 3.19 outlines the retrosynthetic analysis for (1*R*,1'*S*)-temuconine (**18**) showing that the first retrosynthetic cut gives the amide **61** which undergoes Bischler-Napieralski cyclization-$NaBH_4$ reduction to produce the temuconine backbone. This ring closure for the amide is expected to be a regioselective reaction due to the presence of only one site for ring closure (*para* to the electron-donating methoxy group). This amide was prepared using Schotten-Baumann reaction conditions between the diaryl ether acid **62** and the chiral auxiliary-protected amine **32** which was used previously in the first strategy described earlier. A further retrosynthetic cut dissects the acid **62** into the benzyltetrahydroisoquinoline unit **25**, and the aryl boronic acid **63** as a precursor to the $Cu(OAc)_2$-mediated coupling step.

3.5.7 Preparation of the arylboronic acid 63.

The arylboronic acid **63** was synthesized via the commercially-available 4-hydroxyphenylacetic acid (**64**). Esterification of the carboxylic acid using thionyl chloride in methanol gave the methyl (4-hydroxyphenyl)acetate **65a** in 95% yield, followed by activation of the phenolic group as the triflate **65** using triflic anhydride in pyridine. This activation is necessary for the palladium-catalyzed borylation step.[51] $PdCl_2$(dppf)-catalyzed coupling of triflate **65** with bis(pinacolato)diboron afforded the intermediate arylboronate **66** in 75% yield. Without any purification, this aryl boronate **66** converted into the corresponding cyclic aminoboronate intermediate **67** with

diethanolamine using a procedure similar to that described by Jung and Lazarova.[52] The cyclic aminoboronate intermediate **67** could be more easily hydrolyzed to **63** than **66**, under acidic conditions (Scheme 3.20).

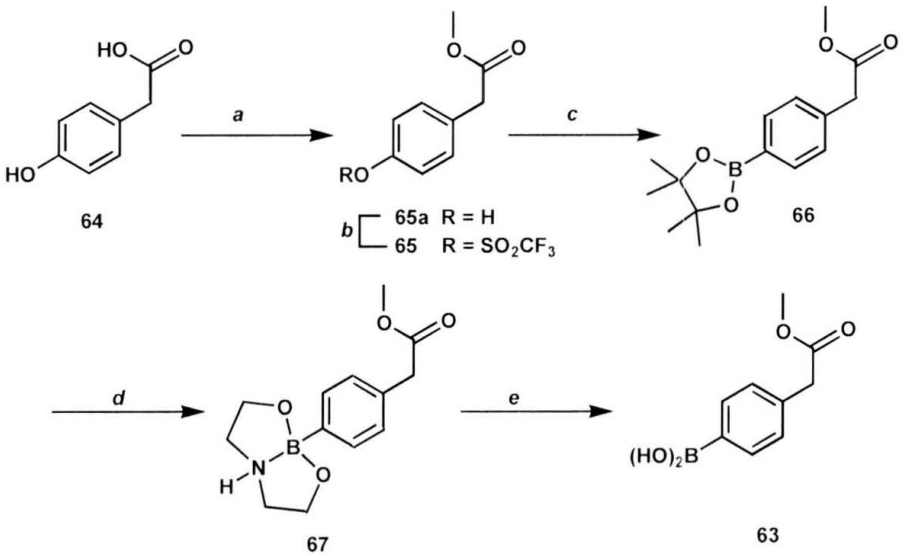

a: $SOCl_2$, MeOH, reflux, 95%, **65a**; *b:* Tf_2O, pyridine, 0 °C, 98%, **65**; *c:* 4,4,5,5-tetramethyl-1,3,2-dioxaborolane, $PdCl_2(dppf)$, Et_3N, dioxane, 100 °C, 90%; *d:* diethanolamine, 2-propanol, 77%; *e:* aq 1 M HCl, THF, 85%.

Scheme 3.20. Preparation of arylboronic acid **63**.

On the way to arylboronic acid **63**, the X-ray structure of the cyclic amino-arylboronate compound **67** was obtained. There has been only one previously reported X-ray crystallographic study of the structure of a diethanolamine ester of a phenylboronic acid. The X-ray structure of this compound, **68**, which was named as *B*-phenyl-*diptych*oboroxazolidine was measured on a diffractometer with Cu *Ka* radiation and it was revealed to be non-centrosymmetric and in the *P*21 space group.[53]

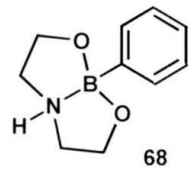

68

Figure 3.11. Structure of a diethanolamine ester of a phenylboronic acid **68**.

With our compound **67**, crystals were obtained in the non-centrosymmetric space group *P*212121. However in our case, data collection was performed using molybdenum radiation, and the absolute configuration could not be determined due to the lack of an atom with significant anomalous dispersion.

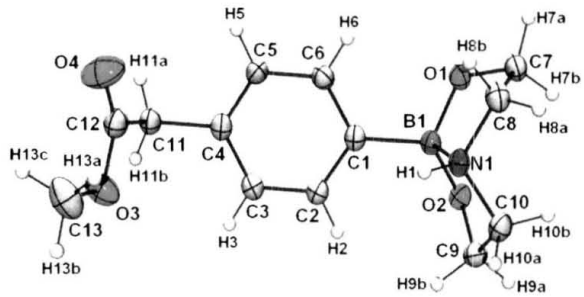

Figure 3.12. The molecular structure of (**67**), with atom labels and 50% probability displacement ellipsoids for non-H atoms.

Intermolecular hydrogen bonding between N1—H1···O2^{i} (N1···O2^{i} = 2.921 (2) Å) and C—H···π interactions between C10—H10B···*Cg*3^{ii} (C10···*Cg*3^{ii}= 3.618 (2); where *Cg*3 is the centroid of C1—C6) leads to the pair-wise association of molecules (Figure 3.12). These molecular associates are related *via* the twofold screw axes in the crystal structure.[54]

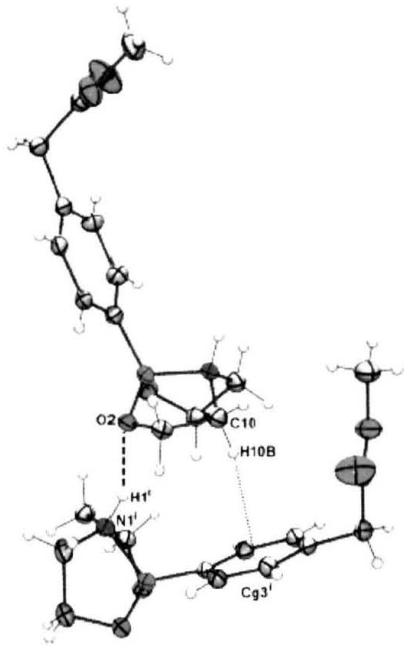

Figure 3.13. Intermolecular hydrogen bonds (long dashes) and C—H···π interactions (short dashes) between two associated molecules.

3.5.8 The second attempt toward the diaryl ether coupling.

In 1998, Evans *et al.*[41] synthesized diaryl ethers by the copper-promoted arylation of phenols with arylboronic acids which produced the corresponding diaryl ethers in high yields at room temperature. Evans reported a number of structurally- and electronically-diverse substrates and in most cases yields were generally good, especially with the electron-rich phenols which underwent arylation more efficiently. Evans pointed out that *ortho*-substituted phenols were arylated in good yield but yields were depressed with *ortho*-heteroatom substituted boronic acids using their conditions.

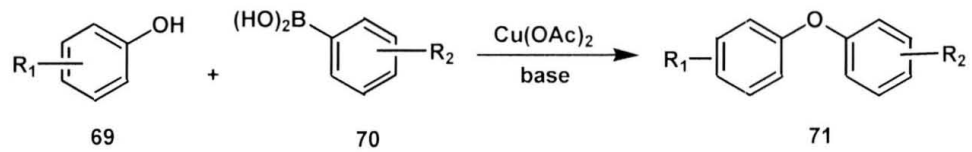

Scheme 3.24. General scheme for diaryl ether formation using copper acetate-mediated coupling.

It was noted that addition of powdered 4Å molecular sieves increased the product yields as the formation of phenol and diphenyl ether side-products which were generated even under anhydrous conditions was prevented. The selection of the optimal base (triethylamine or pyridine) for a given reaction has been empirical and the amine could have a dual role as both a base and/or ligand for one of the organocopper intermediates.

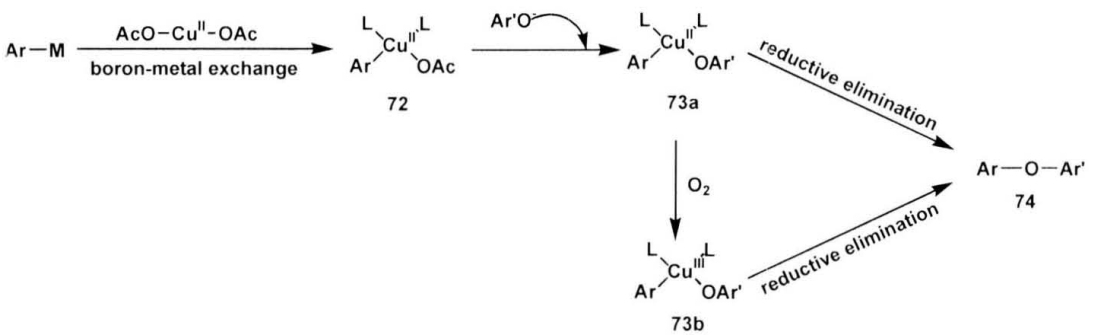

Scheme 3.21. General mechanism for copper acetate-mediated coupling.[41]

The mechanism proposed starts with a boron-metal exchange of the arylboronic acid with the copper acetate to afford arylcopper(II) complex **72**.[41] This complex reacts with the phenoxide ion to prduce the arylcopper(II) phenoxide intermediate **73a** which undergoes subsequent reductive elimination to the diaryl ether **74,** or could be oxidized to

arylcopper(III) phenoxide intermediate **73b** under the reaction conditions prior to reductive elimination (Scheme 3.21).

Again, and to conserve valuable intermediate **25** and test the reactivity of the reagents, model reactions were first conducted using the two model compounds methyl(4-hydroxyphenyl)acetate **75** and the arylboronic acid **63** (Scheme 3.22). After stirring **75** and **63** with $Cu(OAc)_2$, pyridine, and 4Å molecular sieves in dichloromethane for 48 h at room temperature, the diaryl ether compound was formed in reasonably good yield (72%).

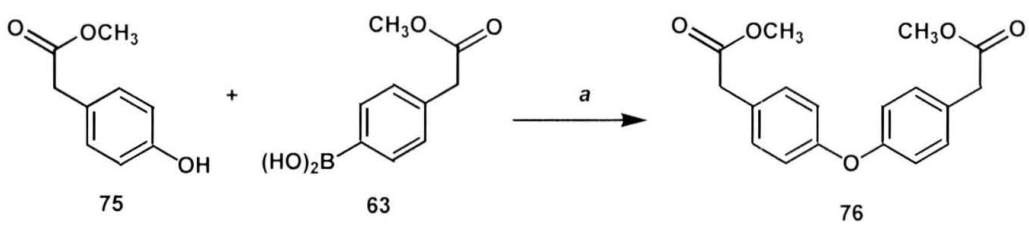

a: $Cu(OAc)_2$, pyridine, 4 Å molecular sieves, CH_2Cl_2, rt, 48 h, 72%.

Scheme 3.22. Model reaction for copper acetate mediated coupling.

With pure benzyltetrahydroisoquinoline compound **25** in hand and the arylboronic acid **63**, an attempt to form the corresponding diaryl ether compound using Evan's method was tried. The reaction was monitored by TLC and HPLC. After 48 h, monitoring of the reaction showed the formation of our desired product, however, the starting material was not fully consumed. The reaction was therefore stirred for 6 days in total, to afford the desired diaryl ether compound with complete consumption of the starting material (Scheme 3.23).

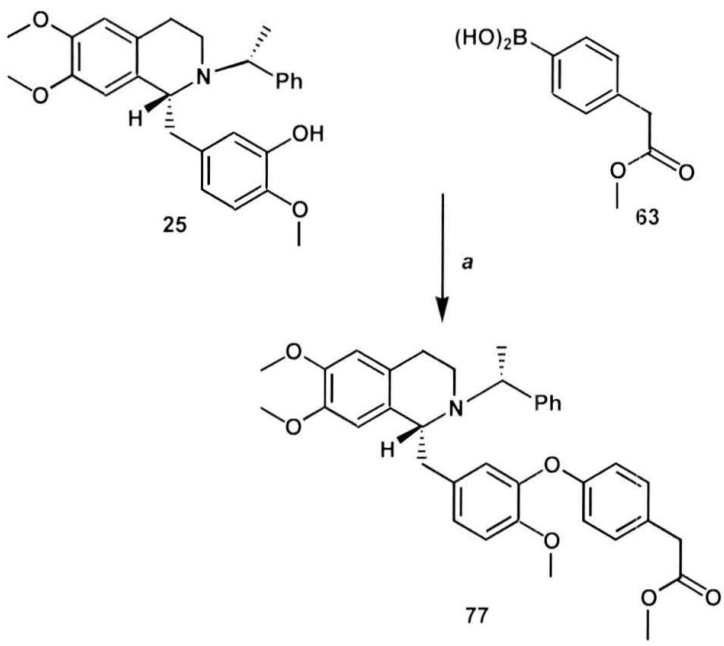

a: $Cu(OAc)_2$, pyridine, 4Å molecular sieves, CH_2Cl_2, rt, 6 days, 63%.

Scheme 3.23. Second attempt toward the diaryl ether coupling.

3.5.9 Completion of the total synthesis of (1*R*,1′*S*)-temuconine (18).

To complete the total synthesis of (1*R*,1′*S*)-temuconine (**18**), the ester **77** was hydrolyzed to the free carboxylic acid **62**, using conditions which would not affect the other protecting groups. The compound was stirred for 2 h with lithium hydroxide in tetrahydrofuran and water to afford **62** in 82% yield (Scheme 3.24).

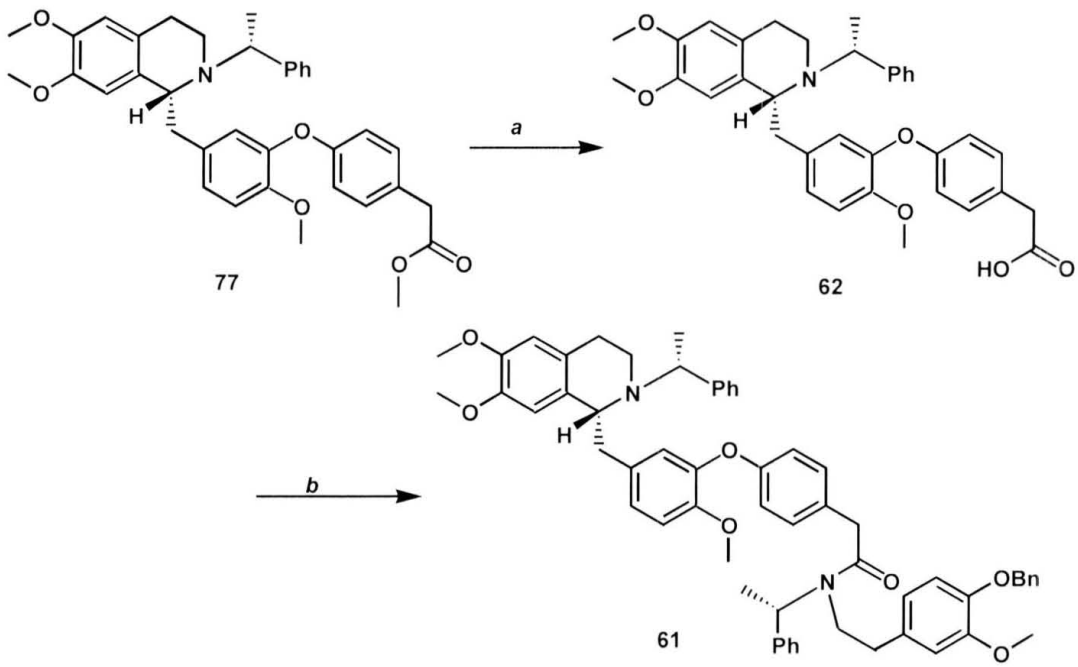

a: LiOH, THF-H_2O, 82%; ***b:*** 1. $(COCl)_2$, benzene; 2. **32**, 5% NaOH(aq), CH_2Cl_2, 69%.

Scheme 3.24. Installation for the second benzyltetrahydroisoquinoline unit **61**.

The amine **32** was then condensed smoothly with **62** using Schotten-Baumann reaction conditions to form amide **61**. The ^{1}H- and ^{13}C-NMR spectra of **61** in $CDCl_3$ showed a doubling of the majority of the signals. This is possibly due to the presence of different conformations which have restricted mobility. There are several studies which have reported that different atropisomers exist with bistetrahydroisoquinolines.[55]

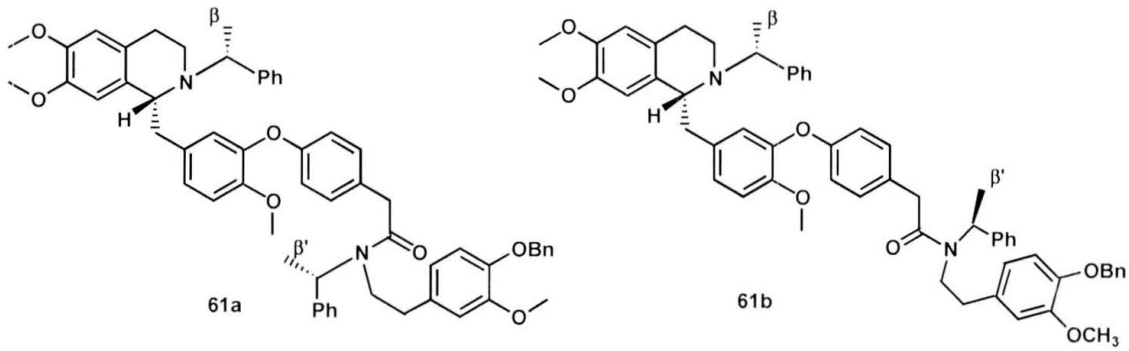

Figure 3.14. Two possible conformations for **61**.

The ^{1}H-NMR spectrum for compound **61** showed that the H-β and -β′ signals appeared as four doublets at δ 1.34, 1.44, 1.47 and 1.53 ppm. On the other hand two methoxy groups appeared as two peaks at 3.80, and 3.83 ppm with integration of 6-protons due to overlap.

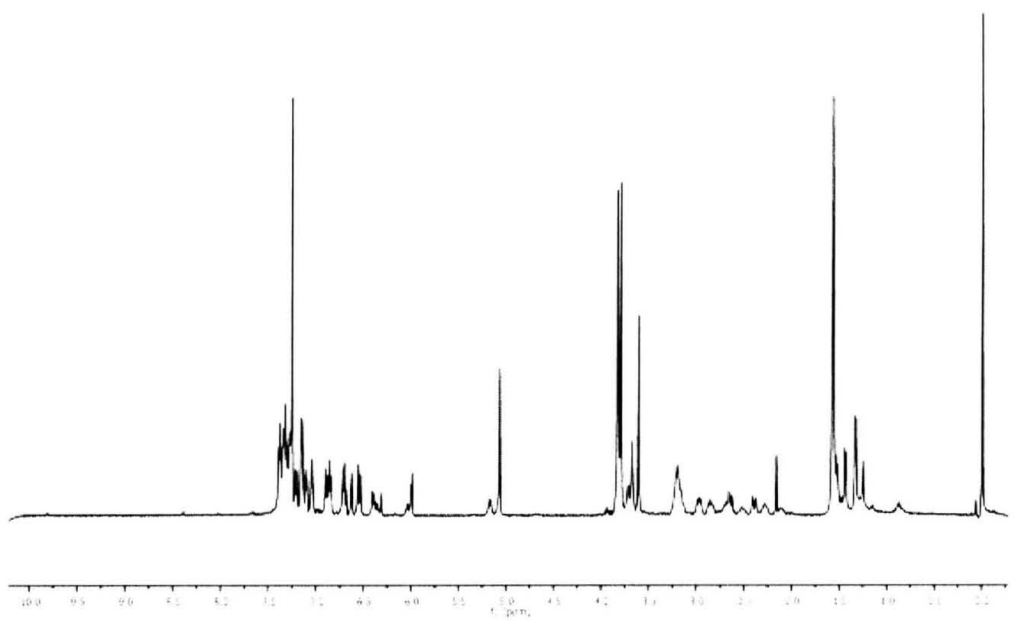

Figure 3.15. The ^{1}H-NMR spectrum of **61**.

Cyclization of **61** using typical Bischler-Napieralski conditions, with $POCl_3$ in benzene, followed by $NaBH_4$ reduction afforded the temuconine back-bone **60** in 54% yield and 86% *de*, as determined from its ^{1}H-NMR spectrum (Scheme 3.25).

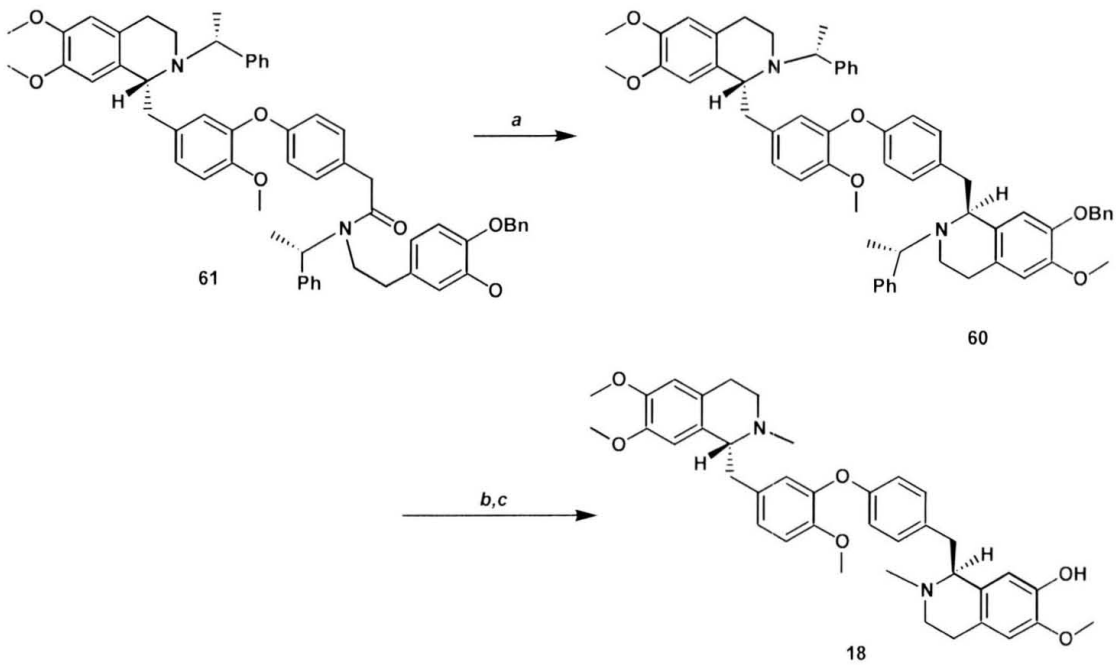

a: 1. $POCl_3$, benzene; 2. $NaBH_4$, MeOH, 54%, (86% *de*); ***b:*** H_2, 10% Pd/C, EtOH, 10% HCl(aq); ***c:*** 1. HCHO, CH_3CN; 2. $NaBH_3CN$; CH_3CO_2H.

Scheme 3.25. Completion of the total synthesis of temuconine (**18**).

Pd/C-catalyzed hydrogenation effected smooth removal of both the chiral auxiliary and the benzyl groups. The secondary amine of the tetrahydroisoquinoline was then selectively methylated using formaldehyde in acetonitrile followed by addition of $NaBH_3CN$ at room temperature. By mass spectrometry, a mass corresponding to that

temuconine could be detected, but at the time of writing the thesis the desired compound was not isolated in sufficiently pure form for spectral and spectroscopic analysis.

3.6 Conclusions.

The enantioselective synthesis of (1*R*,1′*S*)-temuconine, a bisbenzyltetrahydroisoquinoline alkaloid, has been achieved using the chiral auxiliary-mediated Bischler-Napieralski cyclization-reduction reactions. The use of either (*R*)- and (*S*)-α-methylbenzylamine as a chiral auxiliary/reagent, again has proven to be convenient and effective in the cyclization step to enantioselectively form the (-)-temuconine back-bone.

The synthesis started by using the intermediate previously used to prepare (*R*)-*N*-norlaudanidine, and a modified Ullmann-type coupling, using a copper acetate-mediated reaction was employed to set up the diaryl ether bridge first before installing the second tetrahydroisoquinoline unit in 54% yield and 86% *de*. Temuconine has been detected by mass spectrometry, and attempts at purification of this product to afford clean ^{1}H- and ^{13}C-NMR spectra are in progress at the time of writing this thesis.

On the way to our synthesis, the X-ray structure of the intermediate cyclic amino-arylboronate compound **67** was obtained with a non-centrosymmetric space group *P*212121. There has been only one previously reported X-ray crystallographic study of the structure of a diethanolamine ester of a phenylboronic acid.

Experimental

1-(*R*)-(3-Hydroxy-4-methoxybenzyl)-*N*-[(*R*)-α-methylbenzyl]-6,7-dimethoxy-1,2,3,4-tetrahydroisoquinoline (25).

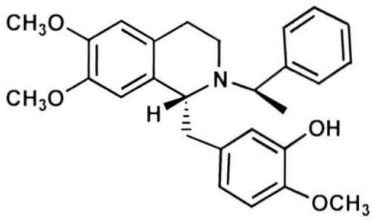

To a solution of **33** (0.530 g, 1.01 mmol) in anhydrous CH_2Cl_2 was added dropwise $TiCl_4$ (0.167 mL, 1.52 mmol) at 0 °C. The solution was warmed to room temperature and stirred for 5 h. The reaction solution was poured into cooled aqueous saturated $NaHCO_3$. The combined mixture was filtered through a Celite pad, and the organic layer was isolated. The aqueous layer was extracted with CH_2Cl_2 (10 mL x 3). The combined organic layers were washed with brine (5 mL x 3), dried over $MgSO_4$, filtered and the solvent was removed over on a rotary evaporator. The residue obtained was crystallized from methanol to give colorless crystals mp 141-142 °C (0.316 g, 72%); ^{1}H NMR ($CDCl_3$, 300 MHz): δ 7.21-7.11 (m, 5H), 6.70 (d, J = 8.2 Hz, 1H), 6.58 (s, 1H), 6.57 (d, J = 2.0 Hz, 1H), 6.38 (dd, J = 8.2, 2.0 Hz, 1H), 5.90 (s, 1H), 5.53 (bs, 1H), 3.86 (s, 3H), 3.84 (s, 3H), 3.79-3.70 (m, 2H), 3.54 (s, 3H), 3.31-3.14 (m, 2H), 3.02 (dd, J = 13.3 Hz, 6.4 Hz, 1H), 2.94-2.82 (m, 1H), 2.65 (dd, J = 13.3 Hz, 7.7 Hz, 1H), 2.44 (dd, J = 16.8, 3.1 Hz, 1H), 1.38 (d, J = 6.5 Hz, 3H); ^{13}C NMR ($CDCl_3$, 75.46 MHz): δ 147.2, 146.4, 146.2, 145.1, 144.8, 133.5, 129.7, 128.1, 127.3, 126.6, 126.4, 121.5, 116.0, 111.5, 111.2, 110.2, 60.5, 59.2, 56.1, 55.7, 55.5, 41.3, 39.8, 24.2, 22.1. APCl-MS (*m/z*): 434.2 (M+1, 100).

1-(*R*)-(3-Hydroxy-4-methoxybenzyl)-*N*-[(*R*)-α-methylbenzyl]-6,7-dimethoxy-1,2,3,4-tetrahydroisoquinoline (25), and (*R*)-*N*-norlaudanidine (34).

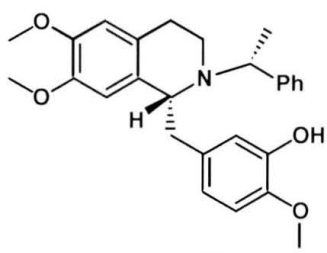

25

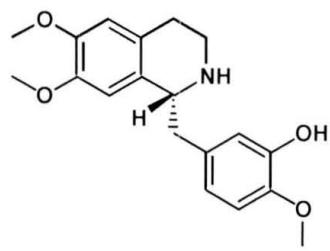

34

A solution of compound **33** (0.102 g, 0.195 mmol) in anhydrous CH_2Cl_2 (5 mL) was hydrogenated over 10% Pd/C (0.501 mg) for 12 h with vigorous stirring. Filtration over Celite, followed by evaporation of solvent afforded a residue which was dissolved in water (10 mL) and CH_2Cl_2 (10 mL) and basified to pH = 8 with aqueous saturated $NaHCO_3$. The aqueous layer was then acidified to pH = 7, and extracted with CH_2Cl_2 (20 mL x 3). The combined organic layers were washed with brine, dried over $MgSO_4$, filtered, and concentrated in *vacuo* to afford a brown oil which was purified by preparative TLC (30% EtOAc/hexane) to afford **25** (13.1 mg, 31%) as a colorless solid, mp 141-142 °C, and **34** (8.03 mg, 25%) as a colorless solid, mp 140-141 °C. The ^1H NMR and ^{13}C NMR spectra for compound **34** were presented in Chapter 2.

1-(*R*)-(3-Hydroxy-4-methoxybenzyl)-*N*-[(*R*)-α-methylbenzyl]-6,7-dimethoxy-1,2,3,4-tetrahydroisoquinoline (25), and (*R*)-*N*-norlaudanidine (34).

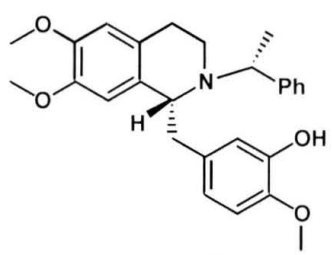

25

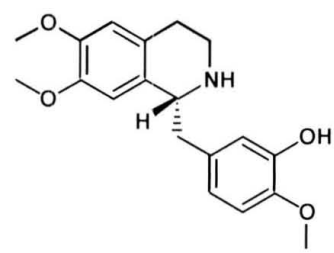

34

A solution of compound **33** (300 mg, 0.143 mmol) in MeOH (5 mL) at 0 °C was treated with Raney nickel, and the reaction mixture was stirred under an atmosphere of H_2 for 15 h. The mixture was then filtered over Celite followed by evaporation of solvent to afford a residue, which was dissolved in water (5 mL) and EtOAc and basified to pH = 8 with aqueous saturated $NaHCO_3$. The aqueous layer was then acidified to pH = 7, and extracted with EtOAc (20 mL x 3). The combined organic layers were washed with brine, dried over $MgSO_4$, filtered, and concentrated in *vacuo* to afford a brown oil which was purified by preparative TLC (30% EtOAc/hexane) to afford **25** (27.3 mg, 33%) as a colorless solid, mp 141-142 °C, and **34** (9.45 mg, 15%) as a colorless solid, mp 140-141 °C. Starting material was also recovered in a low yield. Spectroscopic data for those products were identical to those obtained previously.

4-Benzyloxy-3-methoxybenzaldehyde (36a).

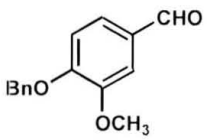

To a suspension of anhydrous potassium carbonate (12.1 g, 87.4 mmol) in DMSO (40 mL) was added 4-hydroxy-3-methoxybenzaldehyde (**35**) (5.32 g, 35.0 mmol) and benzyl bromide (5.00 mL, 42.0 mmol). After stirring for 4 h, water was added and the mixture was extracted with EtOAc (50 mL x 3). The combined organic extracts were washed with brine (15 mL x 3), dried over anhydrous $MgSO_4$, filtered, and the solvent was evaporated to afford **36a** (8.30 g, 98%) as a colorless solid, mp 59-60 °C; ^{1}H NMR ($CDCl_3$, 500 MHz): δ 9.83 (s, 1H, CHO), 7.44-7.43 (m, 3H), 7.39-7.36 (m, 3H), 7.32 (t, J = 7.3 Hz, 1H), 6.99 (d, J = 8.2 Hz, 1H), 5.24 (s, 2H), 3.94 (s, 3H); ^{13}C NMR ($CDCl_3$, 75.46 MHz): δ 190.9, 153.6, 150.1, 136.0, 130.3, 128.7, 128.2, 127.2, 126.6, 112.4, 109.3, 70.9, 56.0; GCMS (*m/z*): 242 (M^+, 100), 91 (100), 65 (65), 51 (20).

4-Benzyloxy-3-methoxybenzyl alcohol (36).

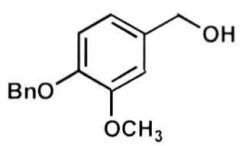

To a solution of **36a** (7.26 g, 30.0 mmol) in MeOH (75 mL) and THF (75 mL) was added $NaBH_4$ (0.567 g, 15.0 mmol) in portions over a period of 3 h. The solution was stirred at room temperature for 11 h, followed by removal of the solvent on the rotary evaporator. The colorless solid was dissolved with aqueous 10% HCl (75 mL) and the solution was transferred to a separatory funnel. The aqueous layer was extracted with EtOAc (50 mL x 3), dried over $MgSO_4$, filtered, and the solvent was evaporated to give a colorless solid (6.88 g, 94%), mp 67-68 °C; ^{1}H NMR ($CDCl_3$, 500 MHz): δ 7.43 (d, J = 7.3 Hz, 2H), 7.35 (t, J = 7.7 Hz,

2H), 7.30 (d, J = 7.3 Hz, 1H), 6.94 (d, J = 2.0 Hz, 1H), 6.85 (d, J = 8.1 Hz, 1H), 6.81 (dd, J = 8.1 and 2.0 Hz, 1H), 5.15 (s, 2H), 4.60 (s, 2H), 3.89 (s, 3H); ^{13}C NMR ($CDCl_3$, 75.46 MHz): δ 149.8, 147.7, 137.1, 134.1, 128.5, 127.8, 127.2, 119.3, 114.0, 111.0, 71.1, 65.3, 56.0; GCMS (*m/z*): 244 (M^+, 100), 91 (100), 65 (40).

4-Benzyloxy-3-methoxybenzyl chloride (37).

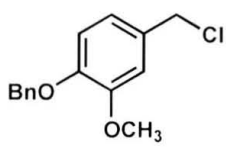

To a solution of **36** (6.43 g, 26.3 mmol) in anhydrous benzene (50 mL) was added pyridine (2.6 mL) followed by dropwise addition of thionyl chloride (2.29 mL, 31.6 mmol) at 0 °C. The mixture was then stirred at room temperature overnight, and then quenched by addition of water (20 mL). The mixture was extracted with EtOAc (20 mL x 3) and washed with aqueous saturated $NaHCO_3$ (10 mL x 3), water (20 mL), dried over $MgSO_4$ and filtered. The solvent was evaporated to give a yellow solid (6.09 g, 88%), mp 55-56 °C; ^{1}H NMR ($CDCl_3$, 300 MHz): δ 7.42 (d, J = 7.1 Hz, 2H), 7.37 (t, J = 7.6 Hz, 2H), 7.30 (d, J = 7.1 Hz, 1H), 6.93 (d, J = 1.7 Hz, 1H), 6.87-6.83 (m, 2H), 5.15 (s, 2H), 4.54 (s, 2H), 3.90 (s, 3H); ^{13}C NMR ($CDCl_3$, 75.46 MHz): δ 149.7, 148.3, 136.9, 130.5, 128.5, 127.9, 127.2, 121.0, 113.7, 112.2, 71.0, 65.0, 56.6; GCMS (*m/z*): 262 (M^+, 30), 227 (20), 91 (100), 65 (20).

4-Benzyloxy-3-methoxyphenylacetonitrile (38).

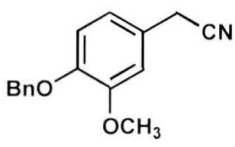

To a solution of **37** (5.62 g, 21.4 mmol) in DMSO (40 mL) and benzene (20 mL) was added NaCN powder (2.10 g, 42.8 mmol) in 4 portions. After stirring for 2 h at room temperature, the reaction mixture was poured into

water (40 mL) and extracted with EtOAc (20 mL x 3). The combined organic layers were washed with brine (20 mL x 3), dried over $MgSO_4$, filtered, and the solvent was evaporated to give a yellow solid (4.93 g, 91%), mp 61-62 °C; ^{1}H NMR ($CDCl_3$, 500 MHz): δ 7.42 (d, *J* = 7.2 Hz, 2H), 7.36 (t, *J* = 7.4 Hz, 2H), 7.30 (d, *J* = 7.2 Hz, 1H), 6.85 (d, *J* = 8.2 Hz, 1H), 6.83 (d, *J* = 2.1 Hz, 1H), 6.75 (dd, *J* = 8.2, 2.1 Hz, 1H), 5.14 (s, 2H), 3.89 (s, 3H), 3.67 (s, 2H); ^{13}C NMR ($CDCl_3$, 75.46 MHz): δ 150.1, 147.9, 136.8, 128.6, 127.9, 127.2, 122.7, 120.2, 114.3, 111.5, 71.1, 65.1, 23.2; GCMS (*m/z*): 253 (M^+, 70), 91 (100), 65(45).

4-Benzyloxy-3-methoxybenzoic acid (39).

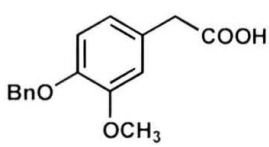

A solution of **38** (4.24 g, 16.67 mmol) in ethanol (25 mL) and aqueous 4.0 M NaOH (7.0 mL) was heated at reflux for 20 h. The reaction mixture was then cooled to room temperature and diluted with water (10 mL) and then acidified to pH = 1 to form a precipitate which was filtered and washed with water to give a yellow solid (4.33 g, 95%), mp 104-105 °C; ^{1}H NMR ($CDCl_3$, 500 MHz) : δ 7.42 (d, *J* = 7.3 Hz, 2H), 7.35 (t, *J* = 7.5 Hz, 2H), 7.28 (d, *J* = 7.3 Hz, 1H), 6.83 (d, *J* = 8.1 Hz, 1H), 6.82 (d, *J* = 2.1 Hz, 1H), 6.75 (dd, *J* = 8.2, 2.0 Hz, 1H), 5.13 (s, 2H), 3.87 (s, 3H), 3.56 (s, 2H); ^{13}C NMR ($CDCl_3$, 125.77 MHz): δ 176.9, 149.6, 147.5, 137.1, 128.5, 127.8, 127.2, 126.2, 121.5, 114.0, 113.0, 71.0, 56.0, 40.5; GCMS (*m/z*): 272 (M^+, 30), 91 (100).

***N*-((*S*)-α-Methylbenzyl)-(4-benzyloxy-3-methoxy)phenylacetamide (40).**

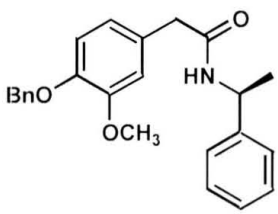

To a stirred solution of oxalyl chloride (0.769 mL, 8.95 mmol) in anhydrous benzene (10 mL) **39** (2.03 g, 7.46 mmol) was added in one batch, and DMF (2 drops). The reaction mixture was stirred until the evolution of the gas ceased. The benzene was evaporated using a rotary evaporator to give a crude acid chloride **39a**, which was used directly in the next step without any further purification. The crude acid chloride was re-dissolved in anhydrous CH_2Cl_2 (4.0 mL) at 0 ^{o}C and the resulting solution was added dropwise to a stirred mixture of (*S*)-α-methylbenzylamine (0.961 mL, 7.46 mmol) and CH_2Cl_2/aqueous 5 % NaOH (1:1.5, 10.5 mL). After stirring at room temperature for 1 h, the reaction mixture was extracted with EtOAc (20 mL x 3), washed with water (15 mL x 3), dried over anhydrous $MgSO_4$, filtered, and the solvent was evaporated to give a yellow solid (2.46 g, 88%), mp 115-116 ^{o}C; ^{1}H NMR ($CDCl_3$, 500 MHz) : δ 7.43 (d, *J* = 7.5 Hz, 2H), 7.36 (t, *J* = 7.5 Hz, 2H), 7.31-7.21 (m, 4H), 7.18 (d, *J* = 7.3 Hz, 2H), 6.84 (d, *J* = 8.2 Hz, 1H), 6.77 (d, *J* = 1.8 Hz, 1H), 6.70 (dd, *J* = 8.2, 1.8 Hz, 1H), 5.61 (d, *J* = 7.6 Hz, 1H), 5.14 (s, 2H), 5.16 (q, *J* = 7.0 Hz, 1H), 3.84 (s, 3H), 3.50 (s, 2H), 1.39 (d, *J* = 7.0 Hz, 3H); ^{13}C NMR ($CDCl_3$, 75.46 MHz): δ 170.2, 150.0, 147.4, 143.1, 137.0, 128.6, 128.5, 127.9, 127.9, 127.3, 125.9, 121.5, 114.4, 112.8, 56.0, 48.6, 43.5, 21.8; APCl-MS (*m/z*): 376.1 (M+1, 100).

***N*-((*S*)-α-Methylbenzyl)-(4-benzyloxy-3-methoxy)phenylacetamine (32).**

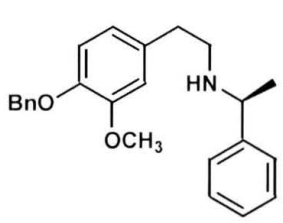

To a solution of chiral amide **40** (2.12 g, 5.66 mmol) in anhydrous THF (50 mL) was added $BF_3 \bullet Et_2O$ (0.355 mL, 2.83 mmol) under argon. The mixture was heated to gentle reflux and $B_2H_6 \bullet THF$ (1.0 M solution in THF, 14.1 mL, 14.1 mmol) was then added dropwise. The reaction mixture was refluxed for 2 h, and then was cooled to 0 °C and aqueous 20% HCl (20 mL) was added to the mixture. The reaction mixture which was stirred at 0 °C for 1 h and then overnight at room temperature, was made basic to pH = 13 with aqueous 50% KOH solution. The mixture was then extracted with CH_2Cl_2 (20 mL x 3), dried over anhydrous $MgSO_4$, filtered and the solvent was evaporated to afford **32** (1.70 g, 83%) as a colorless oil, which was pure enough to be used in the next step; ^{1}H NMR ($CDCl_3$, 500 MHz): δ 7.42 (d, J = 7.3 Hz, 2H), 7.34 (t, J = 7.7 Hz, 2H), 7.30-7.20 (m, 6H), 6.78 (d, J = 8.1 Hz, 1H), 6.98 (d, J = 2.0 Hz, 1H), 6.63 (dd, J = 8.1, 2.0 Hz, 1H), 5.11 (s, 2H), 3.83 (s, 3H), 3.75 (q, J = 6.6 Hz, 1H), 2.75-2.65 (m, 4H), 1.32 (d, J = 6.6 Hz, 3H); ^{13}C NMR ($CDCl_3$, 75.46 MHz): δ 149.6, 146.5, 145.5, 137.3, 133.2, 128.5, 128.4, 127.7, 127.3, 126.9, 126.5, 120.6, 114.3, 112.5, 71.2, 58.2, 55.9, 48.8, 35.9, 24.2; APCl-MS (*m/z*): 362.5 (M+1, 100).

4-Iodobenzyl bromide (42).

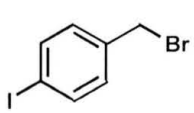

To a solution of 4-iodotoulene (**41**) (2.22 g, 10.0 mmol) and a few crystals of dibenzoyl peroxide in CH_2Cl_2 was added NBS (1.81 g, 10.0 mmol). The mixture was stirred under the light of a 100-watt lamp at a gentle reflux.

After 1 h, the reaction was stopped; brine (8 mL) with KI (0.25 g) was added to the reaction mixture. Then aqueous $Na_2S_2O_3$ solution (20 mL) was added to remove the produced I_2. The organic layer was separated and the aqueous layer was extracted by CH_2Cl_2 (10 mL x 3). The combined organic layers were washed with brine (10 mL), dried over anhydrous $MgSO_4$, filtered and the solvent was evaporated to afford **42** which was further purified by crystallization by using EtOH to afford **42** (2.87 g, 95%) as a colorless crystals, mp 77-78 °C; ^{1}H NMR ($CDCl_3$, 500 MHz): δ 7.67 (d, J = 8.4 Hz, 2H), 7.13 (d, J = 8.4 Hz, 2H), 4.41 (s, 2H); ^{13}C NMR ($CDCl_3$, 75.46 MHz) : δ 137.9, 137.4, 130.8, 94.1, 32.5; GCMS (*m/z*): 298 (M+1, 100), 217 (100), 127 (30), 90 (100), 63 (68).

4-Iodophenylacetonitrile (43).

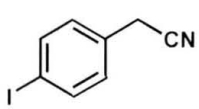

To a solution of **42** (2.53 g, 8.53 mmol) in DMSO (40 mL) and benzene (20 mL) was added NaCN powder (0.836 g, 17.1 mmol) in 4 portions. After stirring for 2 h at room temperature, the reaction mixture was poured into water (40 mL) and extracted with EtOAc (20 mL x 3). The combined organic layers were washed with brine (20 mL x 3), dried over $MgSO_4$, filtered, and the solvent was evaporated to give a yellow solid (1.82 g, 88%), mp 52-53 °C; ^{1}H NMR ($CDCl_3$, 300 MHz): δ 7.71 (d, J = 8.3 Hz, 2H), 7.08 (d, J = 8.3 Hz, 2H), 3.69 (s, 2H); ^{13}C NMR ($CDCl_3$, 75.46 MHz): δ 138.2, 129.8, 117.4, 129.5, 93.6, 23.3; GCMS (*m/z*): 243 (M+1, 100), 116 (85), 89 (42).

4-Iodophenylacetic acid (31).

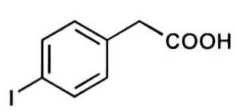

A solution of **43** (1.53 g, 6.30 mmol) in ethanol (25 mL) and aqueous 4.0 M NaOH (4 mL) was heated at reflux for 20 h. The reaction mixture was then cooled to room temperature and diluted with water (10 mL) and then acidified to pH = 1 to form a precipitate which was filtered and washed with water to give a colorless solid (1.54 g, 93%), mp 126-127 °C; ^{1}H NMR ($CDCl_3$, 300 MHz): δ 7.66 (d, J = 8.2 Hz, 2H), 7.03 (d, J = 8.2 Hz, 2H), 3.59 (s, 2H); ^{13}C NMR ($CDCl_3$, 75.46 MHz): δ 176.7, 137.7, 132.8, 131.3, 93.0, 40.4; GCMS (*m/z*): 261 (M^+, 92), 217 (100), 91 (21).

***N*-((*S*)-α-methylbenzyl)-*N*-((4-benzyloxy-3-methoxy)phenethyl)-4-iodophenylacetamide (28).**

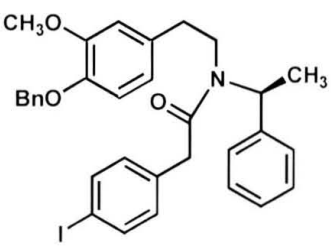

To a stirred solution of oxalyl chloride (0.520 mL, 6.05 mmol) in anhydrous benzene (8 mL) were added 4-iodophenylacetic acid (**31**) (1.32 g, 5.04 mmol) in one batch and DMF (2 drops). The reaction mixture was stirred until the evolution of gas ceased. The benzene was evaporated using a rotary evaporator to give the crude acid chloride, which was used directly in the next step. To a stirred mixture of **32** (1.82 g, 5.04 mmol) and CH_2Cl_2/aqueous 5% NaOH (1:1.5, 6.7 mL) was added dropwise a solution of the crude acid chloride in CH_2Cl_2 at 0 °C. After stirring at room temperature for 1 h, the reaction mixture was extracted with CH_2Cl_2 (30 mL × 3), washed with water (20 mL × 3), dried over anhydrous $MgSO_4$, filtered, and the solvent

was then evaporated. The residue was purified by flash column chromatography (50 % EtOAc/hexane) to afford **28** (2.20 g, 72%) as a viscous oil whose NMR spectrum was complex. APCI-MS (*m/z*): 606.2 (M+1, 100), 502.1 (8), 480.2 (15).

1-(*S*)-7-benzyloxy- (4-Iodobenzyl)-*N*-((*S*)-α-methylbenzyl)-6-methoxy-1,2,3,4-tetra-hydroisoquinoline (26).

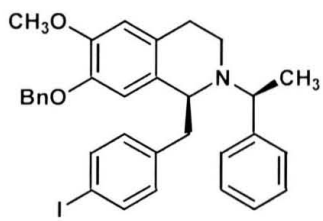

Compound **28** (0.741 g, 1.22 mmol), $POCl_3$ (2.28 mL, 24.4 mmol) and benzene (50 mL) were combined and heated to reflux at 90 °C under argon. After approximately 12 h, the solvent and excess $POCl_3$ were evaporated on a rotary evaporator and finally on a vacuum pump for 2 h. The resultant residue was re-dissolved in anhydrous MeOH (8 mL) and the solution was cooled to -78 °C in a dry-ice bath. To this solution was added $NaBH_4$ (0.231 g, 6.12 mmol) in five portions over 4 h. The reaction was quenched by the addition of aqueous 10% HCl (4 mL), and the mixture was stirred at room temperature for 30 min. The MeOH was evaporated on a rotary evaporator and the residue was basified by adding 20% KOH at 0 °C. The mixture was extracted with CH_2Cl_2 (10 mL x 3), the combined organic layers were dried over $MgSO_4$, filtered and the solvent was evaporated on a rotary evaporator. The residue was purified by preparative TLC (20% EtOAc/hexane) to give compound **26** (0.512 g, 71%) as a colorless oil; ^{1}H NMR ($CDCl_3$, 500 MHz): δ 7.52 (d, J = 8.0 Hz, 2H), 7.36-7.26 (m, 5H), 7.18-7.11 (m, 3H), 6.96 (d, J = 6.8 Hz, 2H), 6.65 (d, J = 7.8 Hz, 2H), 6.61 (s, 1H), 6.01 (s, 1H), 4.85 (d, J = 12.2 Hz, 1H), 4.82 (d, J = 12.2 Hz, 1H), 3.85 (s, 3H), 3.67 (q, J = 6.5

Hz, 1H), 3.59 (t, J = 7.1 Hz, 1H), 3.28-3.18 (m, 2H), 2.93 (dd, J = 13.4, 7.5 Hz, 1H), 2.89-2.83 (m, 1H), 2.57 (dd, J = 13.4, 6.6 Hz, 1H), 2.42 (dd, J = 16.4, 2.6 Hz, 1H), 1.33 (d, J = 6.5 Hz, 3H); ^{13}C NMR ($CDCl_3$, 125.77 MHz): δ 148.0, 145.9, 145.6, 139.8, 137.1, 136.8, 132.0, 129.2, 128.4, 128.1, 127.6, 127.3, 127.2, 126.5, 114.2, 111.8, 90.8, 70.8, 60.3, 58.9, 55.9, 41.6, 39.5, 23.7, 21.8. APCI-MS (m/z): 590.2 (M+1, 100).

Bis(4-methylphenyl)ether (59).

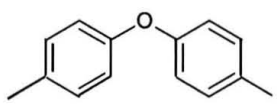

A flask was charged with 4-iodotoluene (**41**) (165 mg, 0.757 mmol), *p*-cresol (**58**) (123 mg, 1.14 mmol), Cs_2CO_3 (0.493 mg, 1.51 mmol), copper iodide (28.8 mg, 0.0151 mmol), *N,N*-dimethylglycine hydrochloride salt (0.0317 mg, 0.227 mmol), and dioxane (8 mL) was heated at 90 °C under a nitrogen atmosphere. After the reaction monitored by TLC was complete, the mixture was extracted with EtOAc. The organic layer was separated and washed with brine, dried over $MgSO_4$, and concentrated in *vacuo*. The residual oil was purified by flash column chromatography (10 % EtOAc/hexane) to afford the product as colorless oil (82.6 mg, 55%); ^{1}H NMR ($CDCl_3$, 500 MHz): δ 7.11 (d, J = 8.2 Hz, 4H), 6.89 (d, J = 8.2 Hz, 4H), 2.32 (s, 6H); GCMS (m/z): 198 (M^+, 100), 155 (15), 91 (65), 65 (21).

Methyl (4-hydroxyphenyl) acetate (65a).

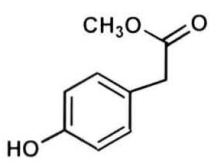

To methanol (50 mL), which was pre-cooled to 0 °C, was added dropwise thionyl chloride (5.19 mL, 71.1 mmol). 4-Hydroxyphenylacetic acid **64** (7.21 g, 47.4 mmol) was then added in

one batch. The cooling bath was removed, and the mixture was refluxed for 3 h. The reaction was quenched by addition of water (30 mL), and then the mixture was extracted with EtOAc (20 mL x 3). The combined organic layers were washed with water (20 mL x 3), dried over $MgSO_4$, filtered, and the solvent was evaporated to give **65a** (7.48 g, 95%) as a colorless solid, mp 53-54 °C; ^{1}H NMR ($CDCl_3$, 300 MHz): δ 7.12 (d, J = 8.5 Hz, 2H), 6.75 (d, J = 8.5 Hz, 2H), 5.31 (s, 1H), 3.69 (s, 3H), 3.55 (s, 2H); ^{13}C NMR ($CDCl_3$, 75.46 MHz): δ 172.8, 154.8, 130.4, 125.9, 115.5, 52.1, 40.3; GCMS (*m/z*): 166 (M^+, 30), 107 (100), 77 (15).

Methyl 4-(trifluoromethanesulfonato)phenylacetate (65).

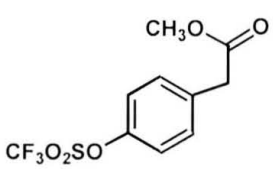

To a solution of **65a** (7.33 g, 44.1 mmol) in pyridine (50 mL), which was pre-cooled to -40 °C (dry ice in acetone), was added dropwise trifluoromethane-sulfonic anhydride (14.8 mL, 88.0 mmol). After stirring for 2 h, water was added (40 mL) and the mixture was extracted with EtOAc (30 mL x 3). The combined organic phases were washed with water (20 mL x 3), dried over $MgSO_4$, filtered, and the solvent was evaporated to give **65** (12.9 g, 98%) as a colorless semi-solid, mp < 40 °C; ^{1}H NMR ($CDCl_3$, 300 MHz): δ 7.37 (d, J = 8.6 Hz, 2H), 7.24 (d, J = 8.6 Hz, 2H), 3.71 (s, 3H), 3.65 (s, 2H); ^{13}C NMR ($CDCl_3$, 75.46 MHz): δ 171.1, 148.6, 134.5, 131.1, 121.4, 52.2, 40.3; GCMS (*m/z*): 298 (M^+, 100), 239 (100), 175 (100), 109 (45), 78 (100), 59 (100).

Methyl 4-(4,4,5,5-tetramethyl-1,3,2-dioxaborolan-2-yl)phenylacetate (66)

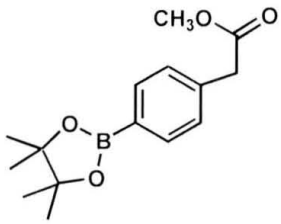

To a solution of $PdCl_2$(dppf) (160 mg, 0.180 mmol) in dioxane (24 ml) was added **65** (1.58 g, 5.93 mmol), Et3N (2.49 ml, 17.8 mmol) and 4,4,5,5-tetramethyl-1,3,2-dioxaborolane (1.30 ml, 8.9 mmol). After stirring for 20 h at 100 °C, the reaction mixture was diluted with benzene (50 mL) and the mixture was transferred to a separatory funnel. The aqueous layer was extracted with benzene (20 mL x 3) and the combined organic layers were washed with brine (20 mL x 2), dried over $MgSO_4$, filtered, and the solvent was evaporated. The residue was purified by flash column chromatography (10% EtOAc/hexanes) to afford the arylboronate **66** (3.7 g, 90%) as a colorless oil; ^{1}H NMR ($CDCl_3$, 500 MHz): δ 7.78 (d, J = 7.8 Hz, 2H), 7.29 (d, J = 7.8 Hz, 2H), 3.67(s, 3H), 3.63 (s, 2H), 1.33 (s, 12H); ^{13}C NMR ($CDCl_3$, 125.77 MHz): δ 171.8, 137.2, 135.2, 128.8, 83.9, 68.0, 52.2, 41.5, 24.9; GCMS (*m/z*): 276 (M^+, 50), 261 (70), 217 (30), 190 (85), 177 (100), 117 (45).

[2,2'-Iminodiethanolato(2-)-κ^3*O,N,O'*][4-(methoxycarbonylmethyl)phenyl]boron (67).

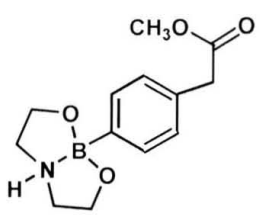

To a solution of the arylboronate (1.47 g, 5.33 mmol) in diethyl ether (53 mL) was added diethanolamine (0.566 mL, 5.86 mmol) in 2-propanol (10 mL). The resulting mixture was stirred at room temperature for 72 h, the reaction mixture was then filtered, and the solid was washed with diethyl ether to give cyclic aminoarylboronate **67** (1.08 g,

77%) as a colorless powder. Crystals suitable for X-ray diffraction analysis were obtained by crystallization from EtOAc; ^{1}H NMR ($CDCl_3$, 500 MHz): δ 7.41 (d, J = 7.8 Hz, 2H), 7.14 (d, J = 7.8 Hz, 2H), 5.83 (s, 1H), 3.64-3.75 (m, 4H), 3.62 (s, 3H) 3.58 (s, 2H), 2.90-3.01 (m, 2H), 2.43-2.47 (m, 2H); ^{13}C NMR ($CDCl_3$, 125.77 MHz): δ 172.6, 132.8, 132.7, 128.3, 63.1, 51.8, 51.1, 41.0.

Arylboronic Acid (63).

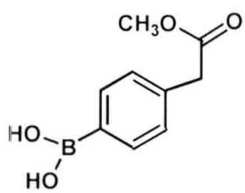

To a solution of **67** (720 mg, 2.74 mmol) in THF (20 mL) was added aqueous 1.0 M HCl (20 mL), and the resulting reaction mixture was stirred for 1 h at room temperature. The reaction mixture was then diluted with water (20 mL) and extracted with EtOAc (30 mL x 3). The combined organic extract was washed with brine, dried over $MgSO_4$, filtered, and the solvent was evaporated to give crude arylboronic acid **63** (452 mg, 85%) as colorless powder which was directly used in the next step, m.p 168-169 °C; ^{1}H NMR ($(CD_3)_2CO$, 300 MHz): δ 7.83 (d, J = 7.8 Hz, 2H), 7.28 (d, J = 7.8 Hz, 2H), 3.65 (s, 2H), 3.64 (s, 3H); ^{13}C NMR ($(CD_3)_2CO$, 75.46 MHz): δ 172.1, 137.6, 135.1, 129.3, 52.0, 41.4; APCI-MS (m/z): 527 ($M^+_{\text{trimers}} - 3\ H_2O$).

Bis (4,4'-dimethylesterdiphenyl) ether (76).

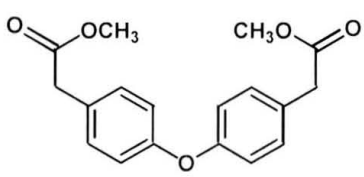

A flask was charged with methyl (4-hydroxyphenyl) acetate (**65a**) (0.260 g, 1.57 mmol), $Cu(OAc)_2$ (0.284 g, 1.57 mmol), arylboronic acid **63** (0.607 g, 3.13 mmol), and powdered 4 Å molecular sieves in CH_2Cl_2 (8 mL), and pyridine (0.63 mL, 7.8 mmol) was added. After stirring for 48 h at room temperature under nitrogen, the resulting slurry was dissolved in diethyl ether, then filtered and the solvent was evaporated. The residue was purified by flash column chromatography (10% EtOAc/hexane) to afford the diaryl ether **76** (0.354 g , 72%) as a colorless oil; ^{1}H NMR ($CDCl_3$, 500 MHz): δ 7.23 (d, J = 8.4 Hz, 4H), 6.96 (d, J = 8.4 Hz, 4H), 3.70 (s, 6H), 3.60 (s, 4H); ^{13}C NMR ($CDCl_3$, 75.46 MHz) δ 172.1, 156.3, 130.6, 128.8, 118.9, 52.0, 40.3; APCI-MS (*m/z*): 313.2 ((M-1, 90), 255.1 (100).

1-(*R*)-(3-{*O*-(Methyl-4-phenylacetate)}-4-methoxybenzyl)-*N*-[(*R*)-α-methylbenzyl]-6,7-dimethoxy-1,2,3,4-tetrahydroisoquinoline (77).

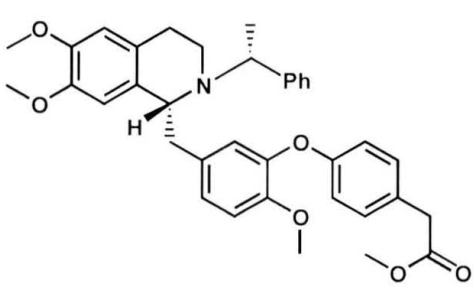

A flask was charged with **25** (0.107 g, 0.247 mmol), $Cu(OAc)_2$ (0.0449 g, 0.247 mmol), arylboronic acid **63** (0.0959 g, 0.494 mmol), and powdered 4 Å molecular sieves in CH_2Cl_2 (5 mL), and pyridine (0.10 mL, 1.24 mmol) was added. After stirring for 6 days at room temperature under nitrogen, the resulting slurry was dissolved in diethyl ether, then filtered, and the solvent was evaporated. The residue

was purified by flash column chromatography (20% EtOAc/hexane) to afford the diaryl ether **77** (0.906 g, 63%) as a colorless oil; ^{1}H NMR ($CDCl_3$, 500 MHz): δ 7.17-7.15 (m, 5H), 7.06 (d, *J* = 3.6 Hz, 2H), 6.85-6.83 (m, 3H), 6.72 (d, *J* = 8.1 Hz, 1H), 6.61 (d, *J* = 8.1 Hz, 1H), 6.57 (s, 1H), 5.99 (s, 1H), 3.84 (s, 6H), 3.81 (s, 3H), 3.77-3.73 (m, 1H), 3.68 (s, 3H), 3.61 (s, 2H), 3.58 (t, *J* = 13.4 Hz, 1H), 3.27-3.14 (m, 2H), 2.98 (dd, *J* = 13.4, 7.2 Hz, 1H), 2.88-2.85 (m, 1H), 2.65 (dd, *J* = 13.4, 7.2 Hz, 1H), 2.40 (d, *J* = 14.5 Hz, 1H), 1.35 (d, *J* = 6.3 Hz, 3H); APCI-MS (*m/z*): 582.3 ((M+1, 100).

1-(*R*)-6,7-dimethoxy-(3-{*O*-4-phenylaceticacid}-4-methoxybenzyl)-*N*-[(*R*)-α-methyl-benzyl]-1,2,3,4-tetrahydroisoquinoline (62).

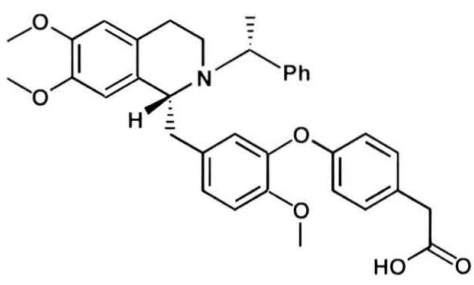

To a solution of **77** (92.7 mg, 0.159 mmol) in THF-H_2O (4 mL, 3:1) was added powdered LiOH (9.56 mg, 0.398 mmol). The reaction mixture was stirred at room temperature for 3 h, and quenched by the cautions addition of aqueous 10% HCl and adjusted pH = 7. The reaction mixture was then diluted with water (20 mL) and extracted with EtOAc (30 mL x 3), dried over $MgSO_4$, filtered, and the solvent was evaporated to afford a foam which was purified by preparative TLC (50% EtOAc/hexane) to give a colorless foam **62** (74.2 mg, 82%); ^{1}H NMR ($CDCl_3$, 500 MHz): δ 7.18-7.16 (m, 5H), 7.08 (dd, *J* = 7.5, 3.9 Hz, 2H), 6.84 (d, *J* = 8.4 Hz, 2H), 6.81 (d, *J* = 8.4 Hz, 2H), 6.67 (dd, *J* = 8.3, 2.1 Hz, 1H), 6.57 (s, 1H), 6.56 (d, *J* = 2.1 Hz, 1H), 5.87 (s, 1H), 3.83 (s, 3H), 3.79 (s, 3H), 3.75 (q, *J* = 6.5 Hz, 1H), 3.69 (t, *J* = 6.9 Hz, 1H),

3.85 (s, 2H), 3.56 (s, 3H), 3.32-3.22 (m, 2H), 3.05 (dd, J = 13.5, 6.7 Hz, 1H), 2.91-2.84 (m, 1H), 2.64 (dd, J = 13.5, 7.5 Hz, 1H), 2.47 (dd, J = 16.6, 2.6 Hz, 1H), 1.39 (d, J = 6.5 Hz, 3H); ^{13}C NMR ($CDCl_3$, 75.46 MHz): δ 176.2, 157.0, 149.8, 147.5, 146.4, 144.2, 132.6, 130.4, 128.3, 128.2, 127.5, 127.0, 126.2, 125.8, 122.8, 116.8, 112.4, 111.2, 60.7, 59.5, 56.1, 55.7, 55.6, 41.0, 39.8, 23.5, 21.3; APCI-MS (*m/z*): 568.2 ((M+1, 100), 448.1 (30).

1-(*R*)-[3-O-{*N'*-((*S*)-α-Methylbenzyl)-*N'*-(4'-benzyloxy-3'-methoxy)-phenylethyl) phenylactamido}-4-methoxybenzyl]-*N*-((*R*)-α-methylbenzyl)-6,7-dimethoxy-1,2,3,4-tetrahydroisoquinoline (61).

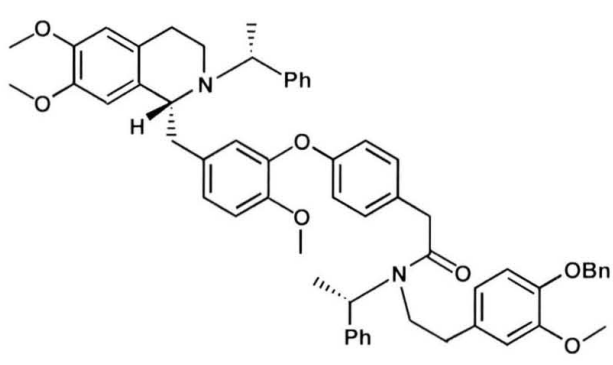

To a stirred solution of oxalyl chloride (0.0728 mL, 0.834 mmol) in anhydrous benzene (8 mL) were added **62** (0.158 g, 0.278 mmol) in one batch and DMF (2 drops). The reaction mixture was stirred until the evolution of gas ceased. The benzene was evaporated using a rotary evaporator to give acid chloride, which was used directly in the next step. A stirred mixture of **32** (0.101 g, 0.278 mmol) and CH_2Cl_2/aqueous 5% NaOH (1:1.5, 0.5 mL) was added dropwise to a solution of the crude acid chloride in CH_2Cl_2 at 0 °C. After stirring at room temprature for 4 h, the reaction mixture was extracted with CH_2Cl_2 (30 mL × 3), washed with water (20 mL × 3), dried over anhydrous $MgSO_4$, filtered, and the solvent was then evaporated.

The residue was purified by preparative TLC (25% EtOAc/hexane) to give a viscous oil **61** (0.175 g, 69%); ^{1}H NMR ($CDCl_3$, 500 MHz): δ 7.39 (d, *J* = 7.6 Hz, 3H), 7.35-7.27 (m, Ar-5H), 7.22 (d, *J* = 8.3 Hz, 1H), 7.16 (d, *J* = 5.0 Hz, 4H), 7.11 (d, *J* = 7.3 Hz, 1H), 7.05 (bs, 2H), 6.90 (d, *J* = 8.3 Hz, 2H), 6.86 (t, *J* = 7.0 Hz, 1H), 6.73-6.69 (m, 2H), 6.63 (bs, 1H), 6.55 (d, *J* = 8.3 Hz, 2H), 6.41-6.32 (m, 2H), 6.01 (d, *J* = 6.8 Hz, 1H), 5.07 (s, 2H), 3.83 (two s, 6H), 3.80 (two s, 3H), 3.73-3.68 (m, 3H), 3.61 (s, 3H), 3.21-3.13 (m, 4H), 3.00-2.95 (m, 1H), 2.89-2.82 (m, 1H), 2.72-2.61 (m, 2H), 2.56-2.49 (m, 1H), 2.41-2.38 (bd, 1H), 2.17 (d, *J* = 1.15 Hz, 1H), 1.53 (d, *J* = 7.5 Hz, 2H), 1.45 (d, *J* = 6.8 Hz, 2H), 1.34 (d, *J* = 6.5 Hz, 3H); ^{13}C NMR ($CDCl_3$, 75.46 MHz): δ 170.9, 157.0, 156.9, 149.6, 149.4, 147.2, 146.2, 144.1, 140.0, 137.3, 133.2, 132.8, 129.8, 129.7, 128.6, 128.5, 128.4, 128.1, 128.0, 127.8, 127.7, 127.7, 127.3, 127.2, 127.1, 126.5, 126.5, 120.5, 117.3, 116.9, 114.0, 112.4, 112.4, 111.3, 71.0, 60.4, 59.0, 56.1, 55.9, 55.7, 55.6, 55.5, 41.2, 41.0, 39.5, 34.4, 23.8, 22.0, 17.8, 16.6; APCI-MS (*m/z*): 911.5 (M^+, 100), 657 (10), 448.2 (15).

1-(*R*)-[3-O-{1′-(*S*)-Benzyl-*N*′-((*S*)-α-methylbenzyl)-7′-benzyloxy-6′-methoxy-1′,2′,3′,4′-tetrahydroisoquinolinyl}-4-methoxybenzyl]-*N*-((*R*)-α-methylbenzyl)-6,7-dimethoxy-1,2,3,4-tetrahydroisoquinoline (60).

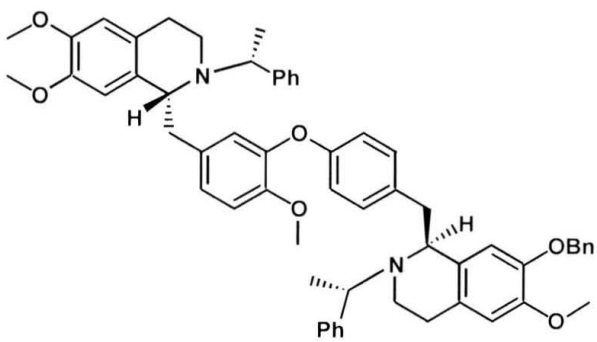

Compound **61** (0.714 g, 0.784 mmol), $POCl_3$ (1.46 mL, 15.7 mmol) and benzene (20 mL) were combined under argon and heated to reflux at 90 °C. After approximately 12 h, the solvent and excess $POCl_3$ were evaporated on a rotary evaporator and finally on a vacuum pump for 2 h. The resultant residue was re-dissolved in anhydrous MeOH (8 mL), and the solution was cooled to -78 °C in a dry ice bath. To this solution was added $NaBH_4$ (0.148 g, 3.92 mmol) in five portions over 4 h. The reaction was quenched through the addition of aqueous 10% HCl (4 mL), and the mixture was stirred at room temperature for 30 min. The MeOH was evaporated on a rotary evaporator. The residue was basified by adding 20% KOH at 0 °C. The mixture was extracted with CH_2Cl_2 (10 mL x 3), the combined organic layers were dried over $MgSO_4$, filtered and the solvent was evaporated on a rotary evaporator. The residue was purified by preparative TLC (30% EtOAc/hexane) to give compound **60** (0.379 g, 54%) as a colorless oil; ^{1}H NMR ($CDCl_3$, 500 MHz): δ 7.34 (d, J = 7.0 Hz, 2H), 7.29 (t, J = 7.3 Hz, 3H), 7.16-7.12 (m, 6H), 7.06-7.04 (m, 2H), 6.99-6.97 (m, 2H), 6.86 (d, J = 8.2 Hz, 1H), 6.81 (d, J = 8.6 Hz, 2H), 6.77 (d, J = 8.6 Hz, 1H), 6.71 (dd, J = 8.2, 2.0 Hz, 1H), 6.64 (d, J = 2.0 Hz, 1H), 6.60 (s, 1H), 6.56 (s, 1H), 6.06 (s, 1H), 5.97 (s, 1H), 4.88 (d, J = 12.3 Hz, 2H), 4.82 (d, J

= 12.3 Hz, 2H), 3.85 (s, 3H), 3.83 (s, 3H), 3.79 (s, 3H), 3.75-3.66 (m, 4H), 3.61 (t, J = 7.5 Hz, 2H), 3.57 (s, 3H), 3.29-3.12 (m, 4H), 2.99-2.95 (m, 2H), 2.90-2.82 (m, 2H), 2.65-2.58 (m, 2H), 2.43-2.37 (m, 2H), 1.34 (d, J = 3.0 Hz, 3H), 1.32 (d, J = 3.0 Hz, 3H); APCl-MS (m/z): 895.3 (M^+, 100), 614 (18), 538.2 (22).

References

(1) Guha, K.; Mukherjee, B. *J. Nat. Prod.* **1979**, *42*, 1-84.

(2) Guinaudeau, H.; Freyer A. J.; Shamma M. *Nat. Prod. Rep.* **1986**, 3, 477-488.

(3) Shamma, M.; Moniot, J. L. *Heterocycles* **1976**, *4*, 1817-1824.

(4) Paul, L.; Schiff, Jr. *J. Nat. Prod.* **1997**, *60*, 934-953.

(5) BICK, I. C.; Todd, A. R. *J. Chem. Soc.* **1950**, 1606-1612.

(6) Cui, J. *M. Sc. Thesis*, Memorial University of Newfoundland, **2003**.

(7) Manske, R. H. F. *Can. J. Res.* **1943**, *21B*, 17-20.

(8) King, H. *J. Chem. Soc.* **1940**, *737-746.*

(9) Tomita, M.; Kusuda, F. *Pharm. Bull.* **1953**, *1*, 1-5.

(10) Sinha, A. *J. Proc. Inst. Chem. (India)* **1960**, *32*, 250-252.

(11) Beauquesene, L. *Bull. Sci. Pharmacol.* **1938**, *45*, 7-14.

(12) Kupchan, S. M.; Patel, A. C.; Fujita, E. *J. Pharm. Sci.* **1965**, *54*, 580-583.

(13) Roychoudhury, A. *Sci. Culture* **1972**, *38*, 358-359.

(14) Tackie, A. N.; Okarter, T.; Knapp, J. E. *Lloydia* **1974**, *37*, 1-5.

(15) Dwuma-Badu, D.; Ayim, J. S. K.; Tackie, A. N.; Knapp, J. E.; Slaktin, D. J.; Schiff, P. L. *Phytochemistry* **1975**, *14*, 2524-2525.

(16) (a) Wright, C.; Marshall, S.; Russell, P.; Anderson, M.; Phillipson, J.; Kirby, G.; Warharst, D.; Schiff Jr., P. *J. Nat. Prod.* **2000**, *63*, 1638-1640. (b) Kupeli, E.; Kosar, M.; Yesilada, E.; Husnu, K.; Baser, C. *Life Sci.* **2002**, *72*, 645–657. (c) Tomita, M.; Shingu, T.; Fujitani, K.; Furukawa, H. *Chem. Pharm. Bull.* **1965**, *13*, 921-926. (d) Quevedo, R.; Valderrama, K.; Moreno-Murillo, B.; Laverde, M.; Fajardo, V. *Biochem. Syst. Ecol.* **2008**, *36*, 812–814. (e) Kaur, K.; Jain, M.; Kaur, T.; Jain, R. *Bioorg. Med. Chem.* **2009**, *17*, 3229–3256.

(17) Angerhofer, C. K.; Guinaudeau, H.; Wongpanich, V.; Pezzuto, J. M.; Cordell, G. A. *J. Nat. Prod.* **1999**, *62*, 59-66.

(18) Teh, B. S.; Seow, W. K.; Li, S. Y.; Thong, Y. H. *Int. J. Immunopharmacol.* **1996**, *11*, 321-326.

(19) Si-Ying, L.; Li-Hua, L.; Teh, B. S.; Seow, W. K.; Thong, Y. H. *Int. J. Immunopharmacol.* **1989**, *11*, 395-401.

(20) Seow, W. K.; Ferrante, A.; Si-Ying, L; Thong, Y. H. *Clin. Exp. Immunol.* **1989**, *75*, 47-51.

(21) Wong, C. W.; Seow, W. K.; O'Callaghan, J. W.; Thong, Y. H. *Agents and Actions* **1992**, *36*, 112-118.

(22) Ivanovska, N.; Philipov, S. *Int. J. Immunopharmacol.* **1996**, *18*, 553-561.

(23) Müller, K.; Ziereis, K. *Planta Med.* **1994**, *60*, 421-424.

(24) Seow, W. K.; Nakamura, K.; Sugimura, Y., Sugimoto, Y.; Yamada, Y.; Fairlie, D. P.; Thong, Y. H. *Mediators Inflamm.* **1993**, *2*, 199-203.

(25) Schiff, P. L. *J. Nat. Prod.* **1987**, *50*, 529-599.

(26) Pan, J. X.; Lam, Y. K.; Huang, L. Y.; Garcia, M. L.; King, V. F.; Kaczorowski, G. J. *J. Beijing Med. Univ.* **1987**, *19*, 177-178.

(27) Wright, J. S.; Johnson, E. R.; DiLabio, G. A. *J. Am. Chem. Soc.* **2001**, *123*, 1173-1183.

(28) Shamma, M.; Moniot, J. L. *Isoquinoline Alkaloids Research*; Plenum Press: New York, **1972**; pp. 71-100.

(29) Shamma, M. In *Isoquinoline Alkaloids*: *The Bisbenzylisoquinolines*; Academic Press: New York, **1972**; Vol. 25, pp. 115-150.

(30) El-Sebakhy, N.; Richomme, P.; Taaima, S.; Shamma, M. *J. Nat. Prod.* **1989**, *52*, 1374-1375.

(31) Guinaudeau, H.; Cassels, B. K.; Shamma, M. *Heterocycles* **1982**, *19*, 1009-1012.

(32) Naito, Y.; Tanabe, T.; Kawabata, Y.; Ishikawa Y.; Nishiyama, S. *Tetrahedron Lett.* **2010**, *51*, 4776-4778.

(33) Felix, A. M.; Heimer, E. P.; Lambros, T. *J. Org. Chem.* **1978**, *43*, 4194-4196.

(34) Barrero, A. F.; Alvarez-Manzaneda, E. J.; Chahboun, R. *Tetrahedron Lett.* **1997**, *38*, 8101-8104.

(35) Crowley, B.; Boger, L. D. *J. Am. Chem. Soc.* **2006**, *128*, 2885-2892.

(36) Hori, H.; Nishida, Y.; Meguro, H. *J. Org. Chem.* **1989**, *54*, 1346-1353.

(37) Mukai, C.; Hirai, S.; Hanaoka, M. *J. Org. Chem.* **1997**, *62*, 6619-6626.

(38) Pitsinos, N. E.; Vidali, P. V.; Couladouros A. E. *Eur. J. Org. Chem.* **2011**, *7*, 1207–1222.

(39) For reviews, see: (a) Lindley, J. *Tetrahedron* **1984**, *40*, 1433-1456. (b) Sawyer, J. S. *Tetrahedron* **2000**, *56*, 5045-5065.

(40) http://www.organic-chemistry.org/namedreactions/ullmann-reaction.shtm.

(41) Evans, D. A.; Katz, J. L.; West, T. R. *Tetrahedron Lett.* **1998**, *39*, 2937-2940.

(42) Marcoux, J. F.; Doye, S.; Buchwald, S. L. *J. Am. Chem. Soc.* **1997**, *119*, 10539-10540.

(43) Sperotto, E.; Klink, G.; Koten, G.; and De Vries, J. *Dalton Trans.* **2010**, *39*, 10338–10351.

(44) Gujadhur, R. K.; Bates, C. G.;Venkataraman, D. *Org. Lett.* **2001**, *3*, 4315-4317.

(45) Buck, E.; Song, Z. J.; Tschaen, D.; Dormer, P. G.; Volante, R. P.; Reider, R. P. *Org. Lett.* **2002**, *4*, 1623-1626.

(46) Ma, D.; Cai, Q.; Zhang, H. *Org. Lett.* **2003**, *5*, 2453-2455.

(47) Ma, D.; Cai, Q. *Org. Lett.* **2003**, *5*, 3799-3802.

(48) Torii, S.; Tanaka, H.; Siroi, T.; Akada, M. *J. Org. Chem.* **1979**, *44*, 3305-3310.

(49) Fürstner, A.; Müller, C. *Chem. Commun.* **2005**, 5583-5585.

(50) Pospíšil, J.; Müller, C.; Fürstner A. *Chem. Eur. J.* **2009**, *15*, 5956-5958.

(51) Murata, M.; Oyama, T.; Watanabe, S.; Masuda, Y. *J. Org. Chem.* **2000**, *65*, 164-168.

(52) Jung, M. E.; Lazarova, T. I. *J. Org. Chem.* **1999**, *64*, 2976-2977.

(53) Rettig, S., J.; Trotter, J. *Can. J. Chem.* **1975**, *53*, 1393-1401.

(54) Zein, A. L.; Dawe, L. N.; Georghiou, P. E. *Acta Crys.* **2010**, *E66*, o2646.

(55) Jansa, P.; Macháček, V.; Nachtigall, p.; Wsól, V.; Svobodová, M. *Molecules* **2007**, *12*, 1064-1079.

Supplementary Spectral Data for Chapter 3:

^{1}H and ^{13}C NMR spectra are presented in the following sequence for compound numbers:

25, 36a, 36, 37, 38, 39, 40, 32, 42, 43, 31, 26, 59, 65a, 65, 67, 63, 76, 77, 62, 661, 60

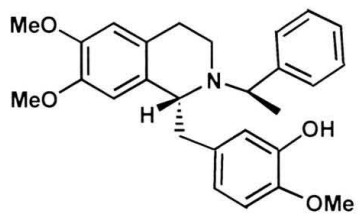

25

$CDCl_3$, NMR 300 MHz

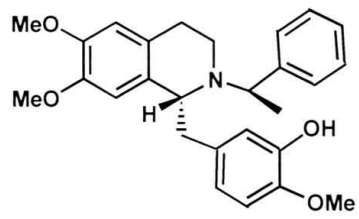

25

$CDCl_3$, NMR 75.46 MHz

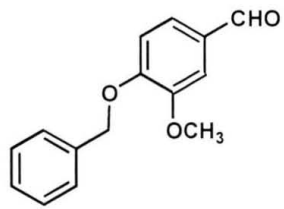

36a

$CDCl_3$, NMR 500 MHz

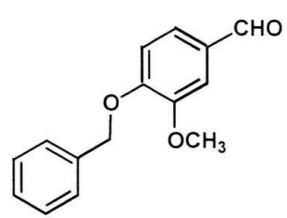

36a

$CDCl_3$, NMR 75.46 MHz

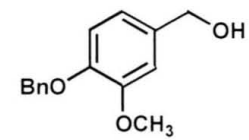

36

$CDCl_3$, NMR 500 MHz

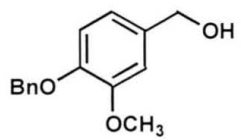

36

$CDCl_3$, NMR 75.46 MHz

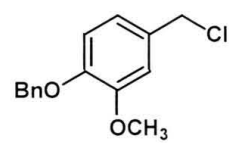

37

$CDCl_3$, NMR 300 MHz

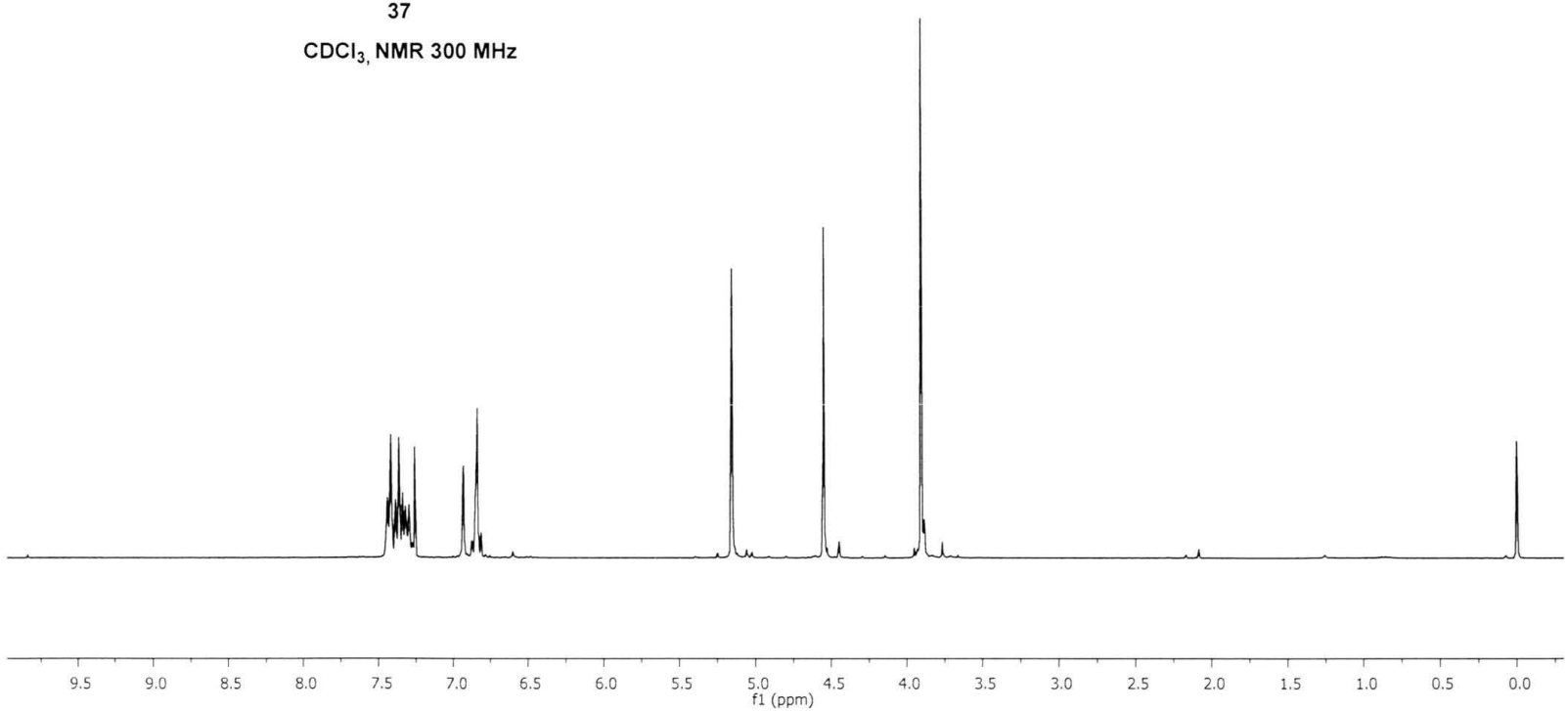

az-63

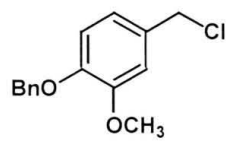

37

$CDCl_3$, NMR 75.46 MHz

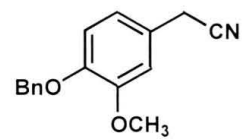

38

$CDCl_3$, NMR 500 MHz

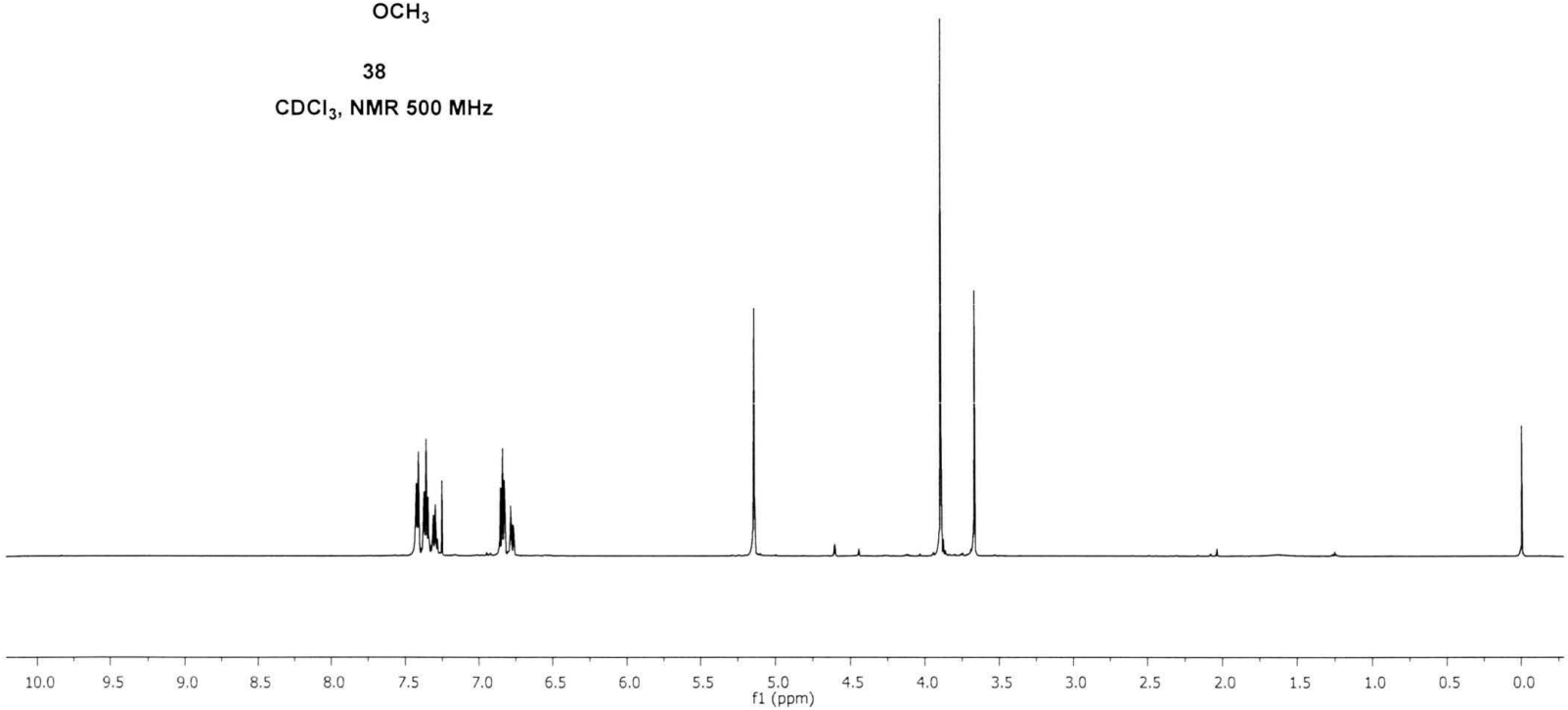

az-66

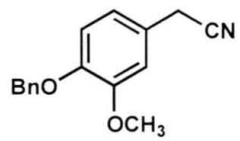

38

$CDCl_3$, NMR 75.46 MHz

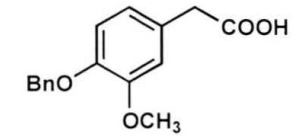

39

$CDCl_3$, NMR 500 MHz

az3160c/1

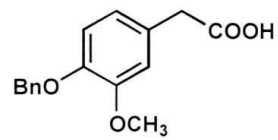

39

$CDCl_3$, NMR 125.77 MHz

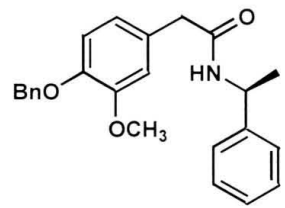

40

$CDCl_3$, NMR 500 MHz

az-86

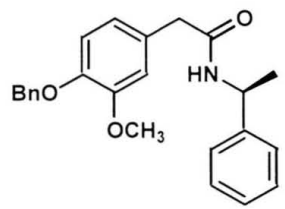

40

$CDCl_3$, NMR 75.46 MHz

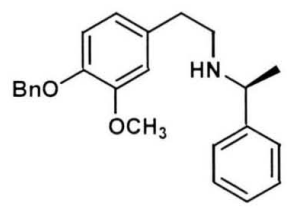

32

$CDCl_3$, NMR 500 MHz

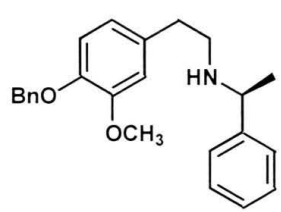

32

$CDCl_3$, NMR 75.46 MHz

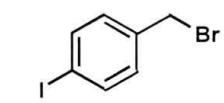

42

$CDCl_3$, NMR 500 MHz

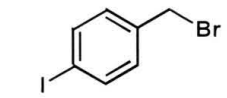

42

$CDCl_3$, NMR 75.46 MHz

2-az-154

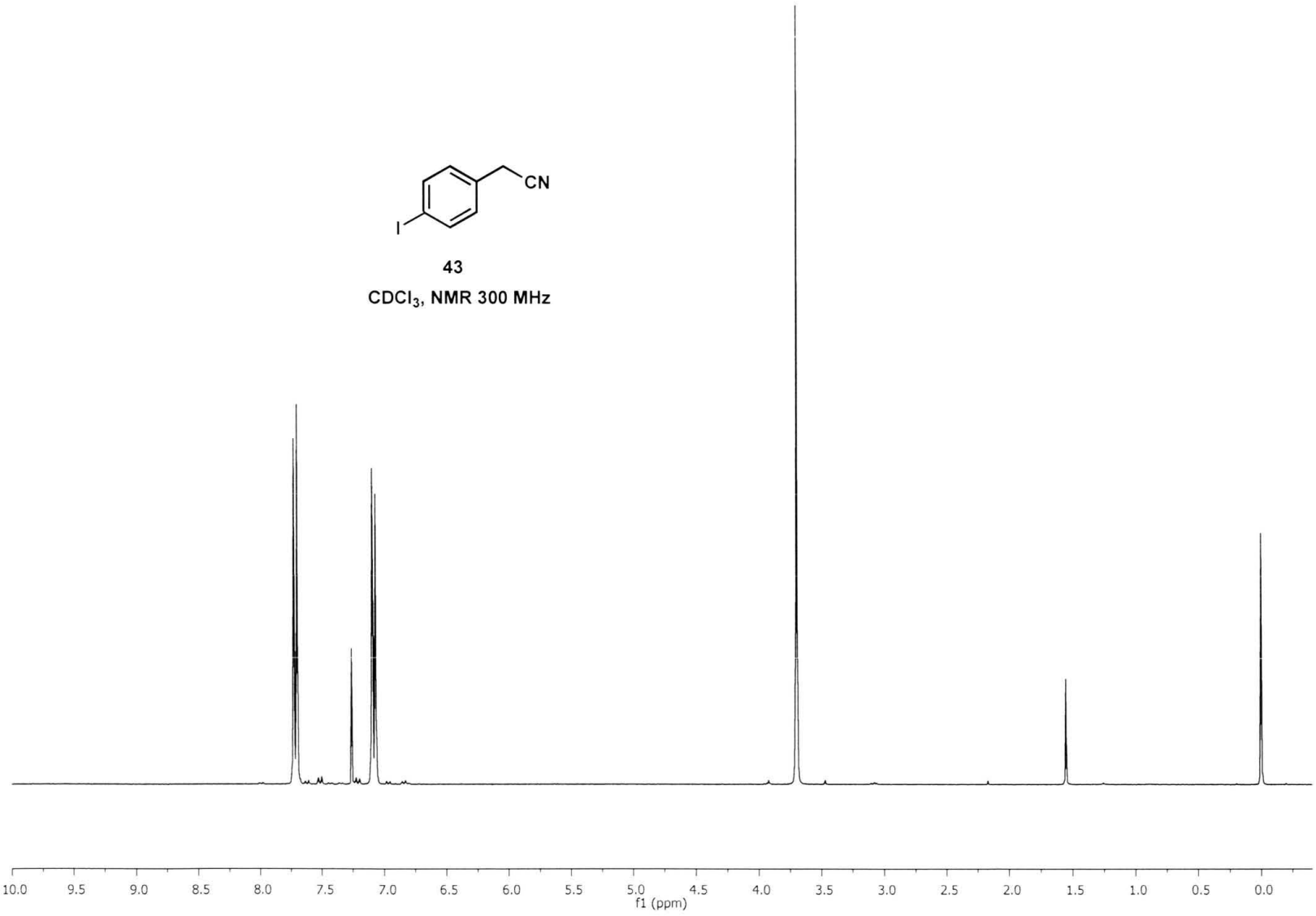
CN
I
43
CDCl3, NMR 300 MHz
10.0
9.5
9.0
8.5
8.0
7.5
7.0
6.5
6.0
5.5
5.0
4.5
4.0
3.5
3.0
2.5
2.0
1.5
1.0
0.5
0.0
f1 (ppm)

2-az-154

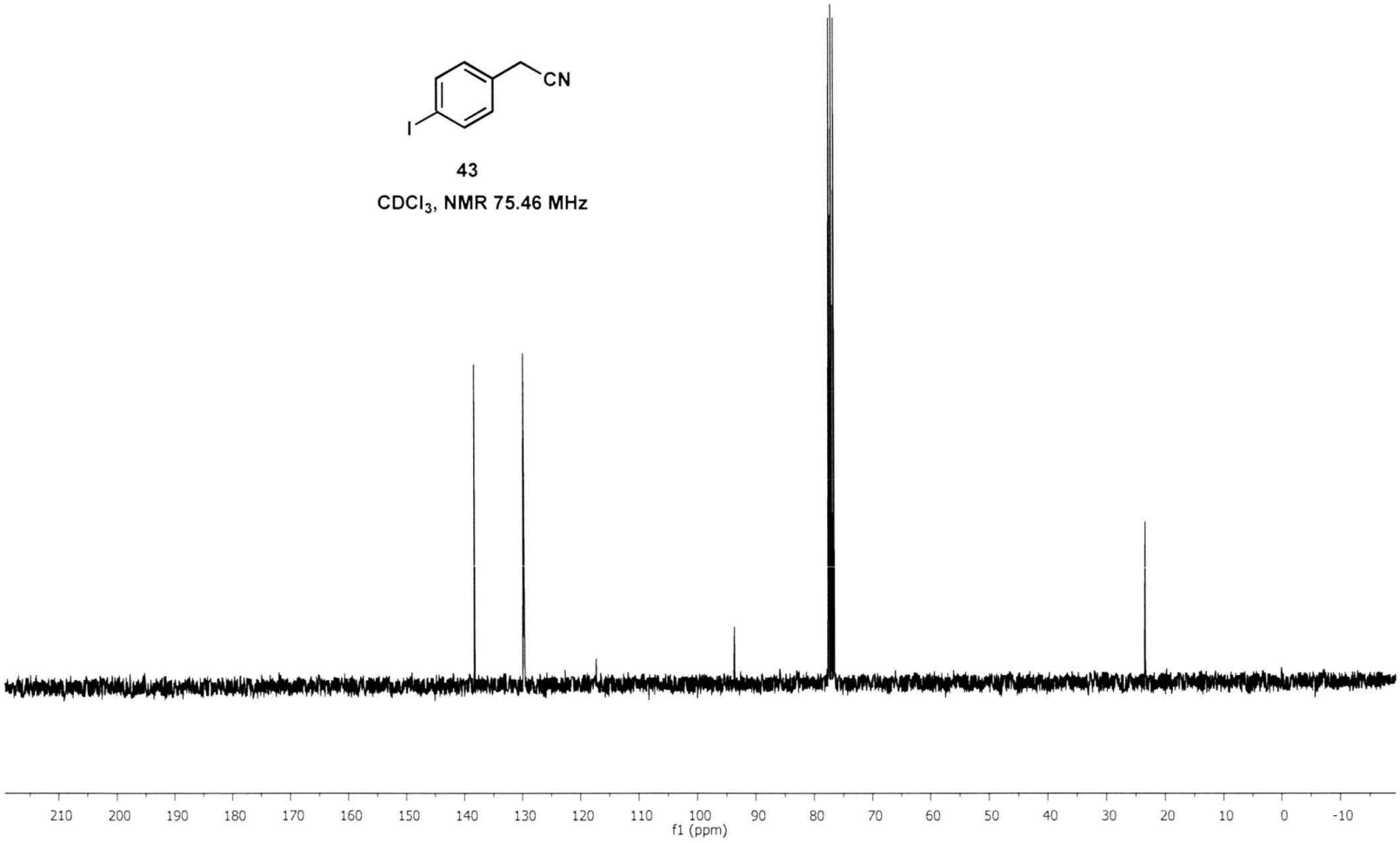
CN
I
43
CDCl3, NMR 75.46 MHz
210 200 190 180 170 160 150 140 130 120 110 100 90 80 70 60 50 40 30 20 10 0 -10
f1 (ppm)

31

$CDCl_3$, NMR 300 MHz

2-az-155

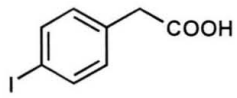

31

$CDCl_3$, NMR 75.46 MHz

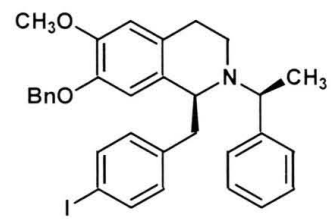

26

$CDCl_3$, NMR 500 MHz

az3076d/1

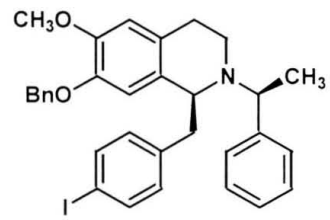

26

$CDCl_3$, NMR 125.77 MHz

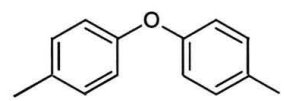

59

$CDCl_3$, NMR 500 MHz

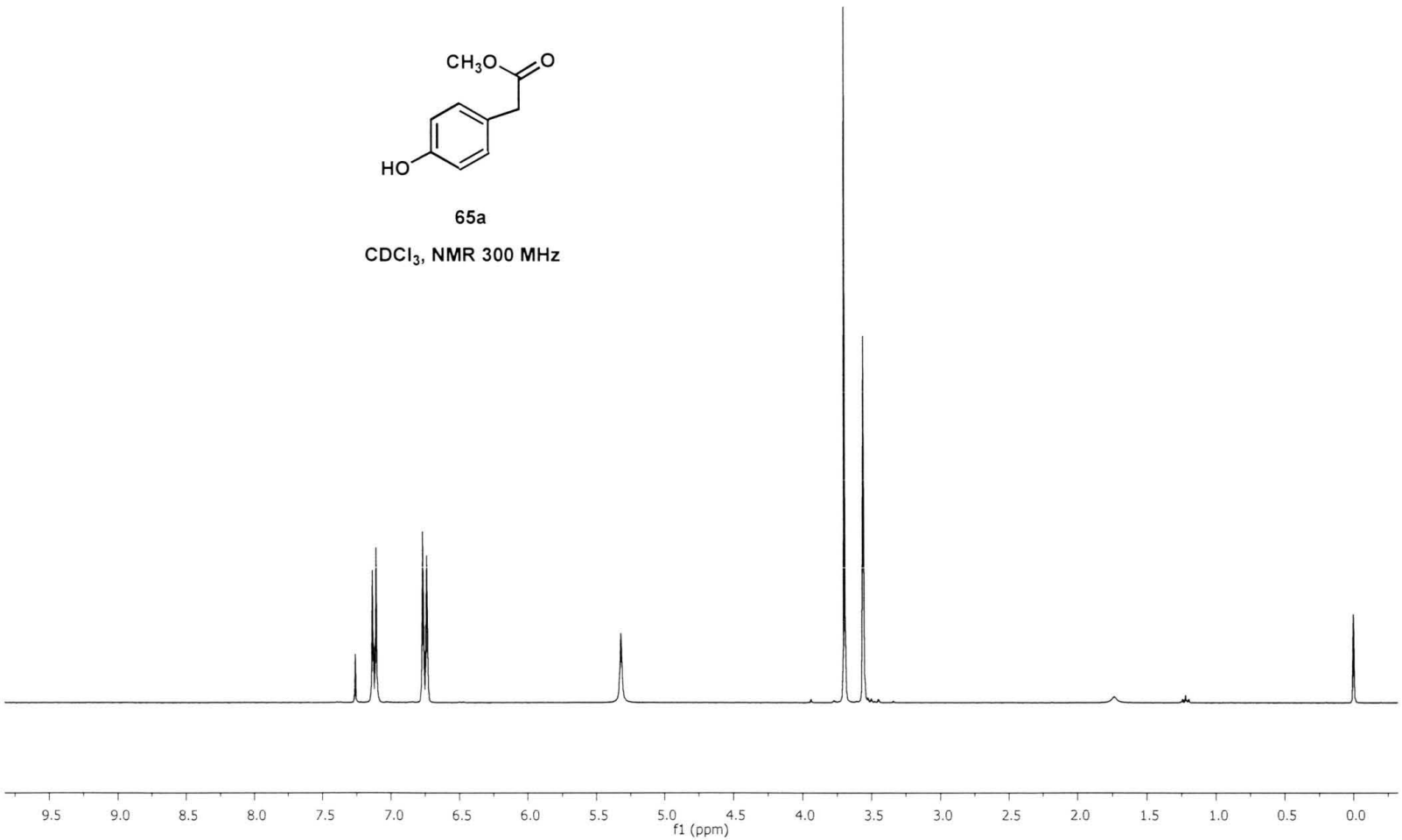
CH3O
O
HO
65a
CDCl3, NMR 300 MHz
9.5
9.0
8.5
8.0
7.5
7.0
6.5
6.0
5.5
5.0
4.5
4.0
3.5
3.0
2.5
2.0
1.5
1.0
0.5
0.0
f1 (ppm)

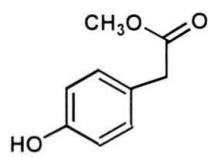

65a

$CDCl_3$, NMR 75.46 MHz

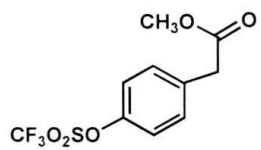

65

$CDCl_3$, NMR 300 MHz

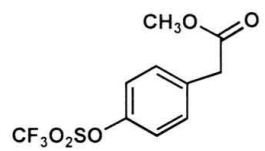

65

$CDCl_3$, NMR 75.46 MHz

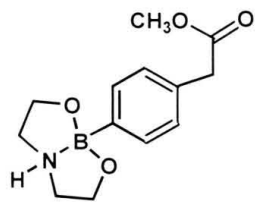

67

$CDCl_3$, NMR 500 MHz

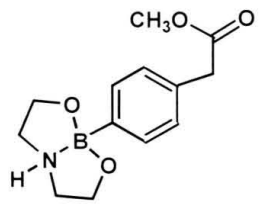

67

$CDCl_3$, NMR 125.77 MHz

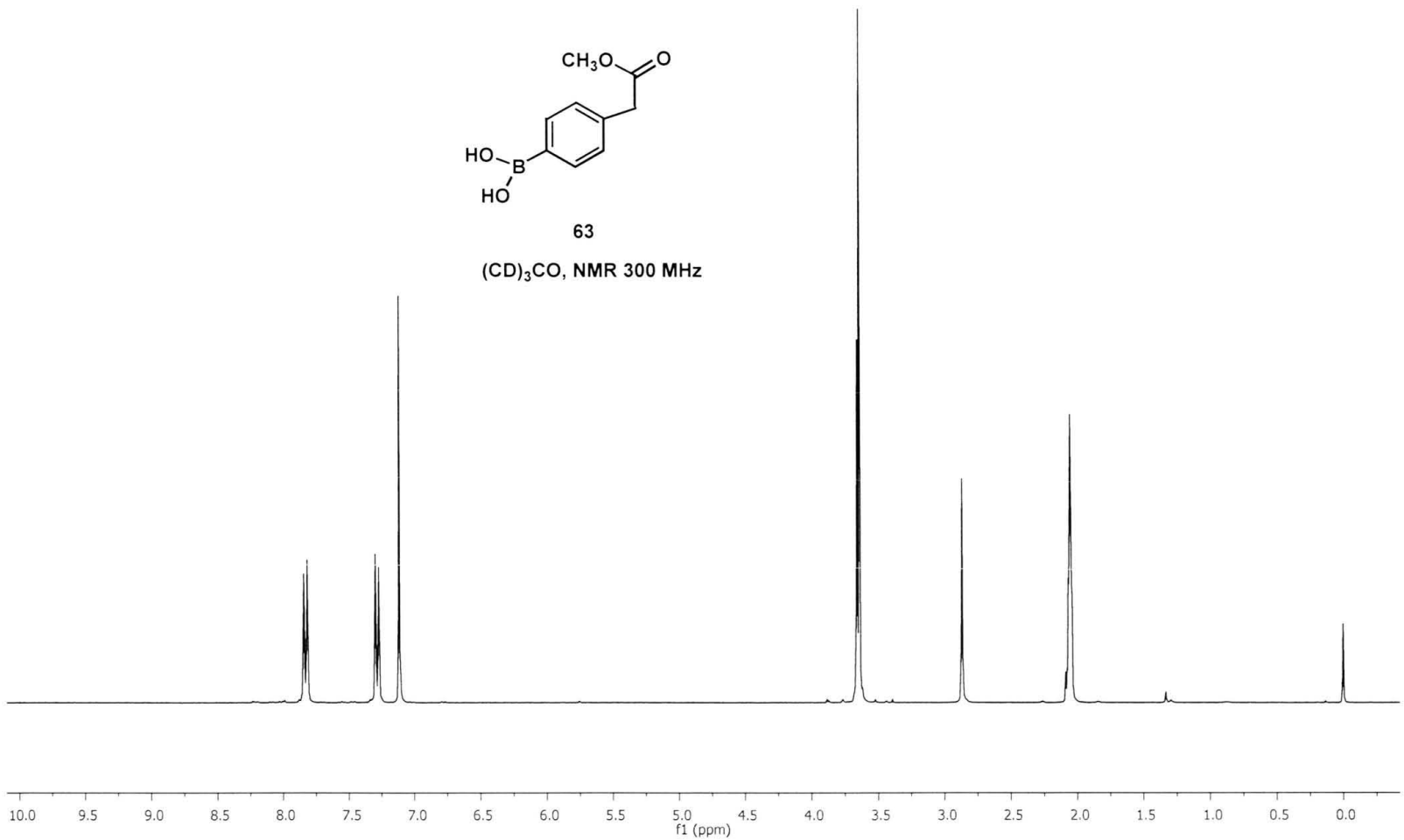
CH3O
O
HO
B
HO
63
(CD)3CO, NMR 300 MHz
10.0
9.5
9.0
8.5
8.0
7.5
7.0
6.5
6.0
5.5
5.0
4.5
4.0
3.5
3.0
2.5
2.0
1.5
1.0
0.5
0.0
f1 (ppm)

2-az-102

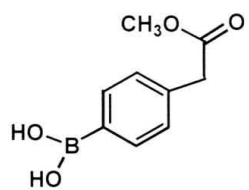

63

$(CD)_3CO$, NMR 75.46 MHz

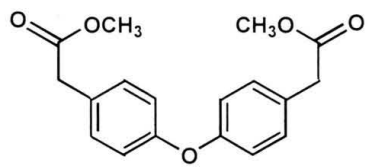

76

$CDCl_3$, NMR 500 MHz

2-az-147 c13
diester

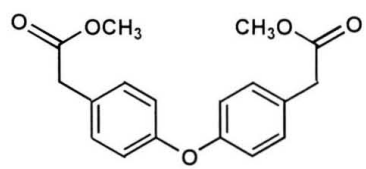

76

$CDCl_3$, NMR 75.46 MHz

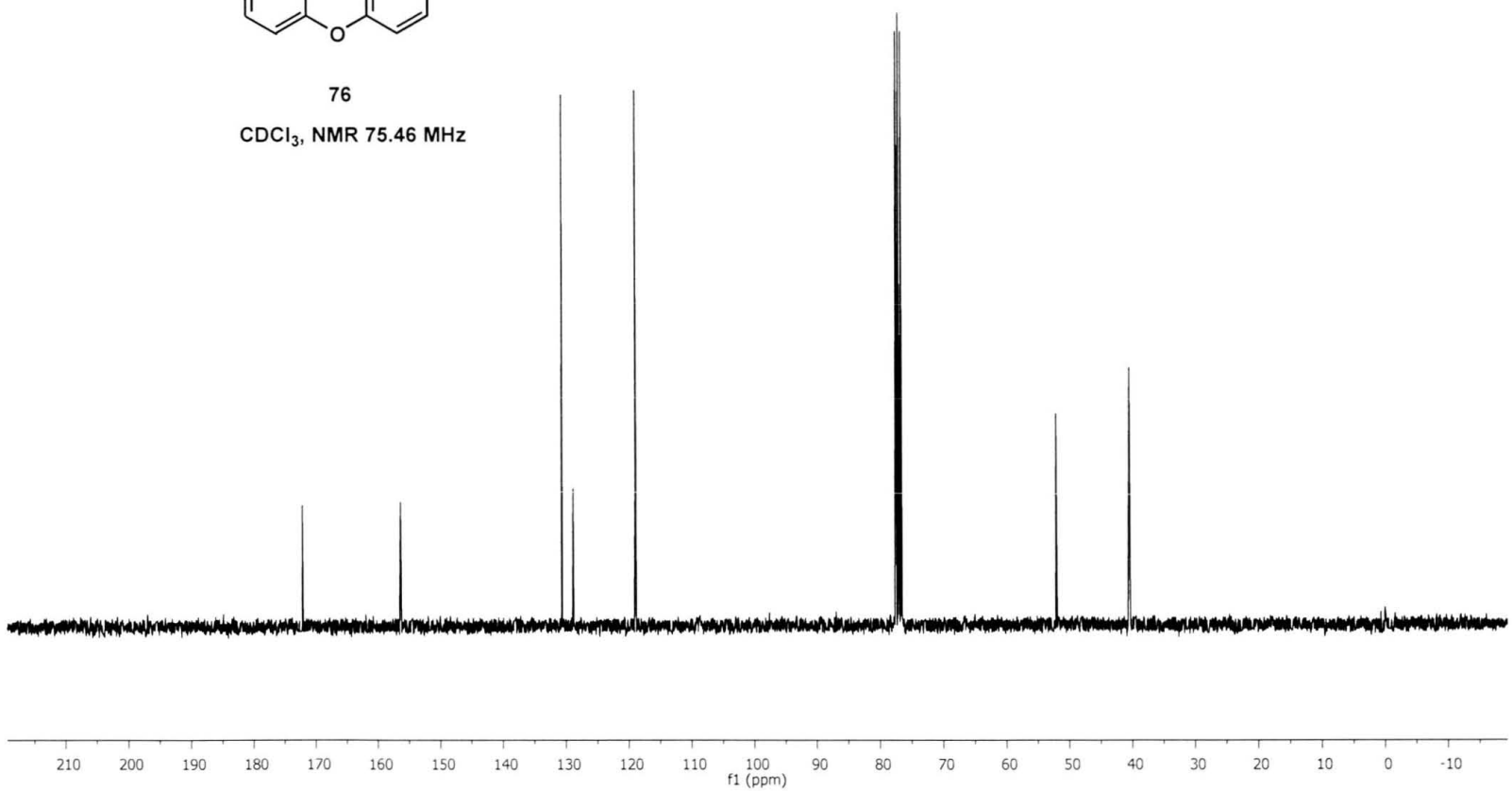

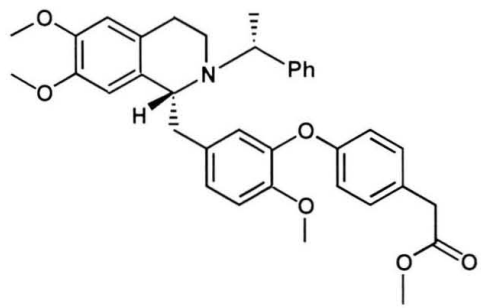

77

CDCl3, NMR 500 MHz

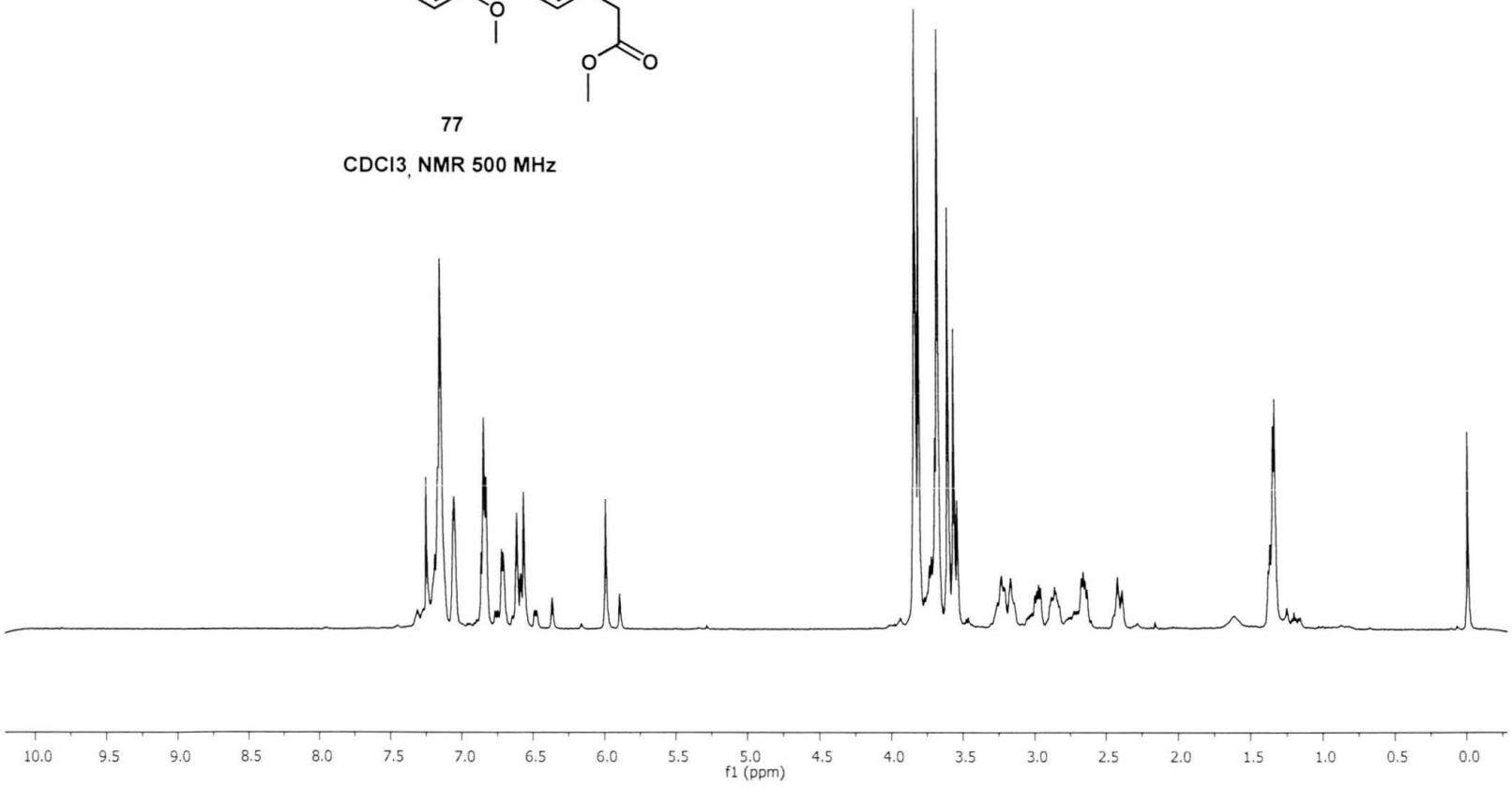

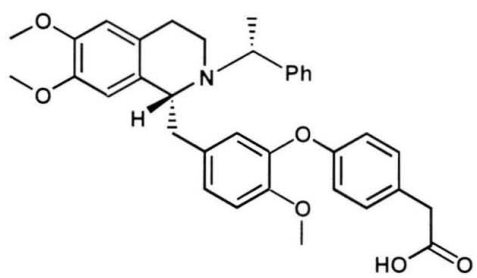

62

$CDCl_3$, NMR 500 MHz

2-az-130
c13 for az-130

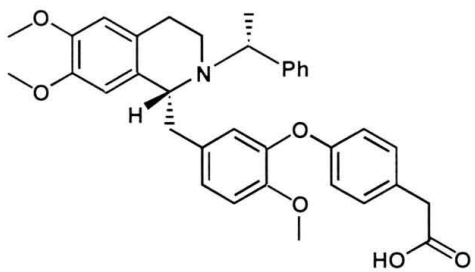

62

$CDCl_3$, NMR 75.46 MHz

az3799/1

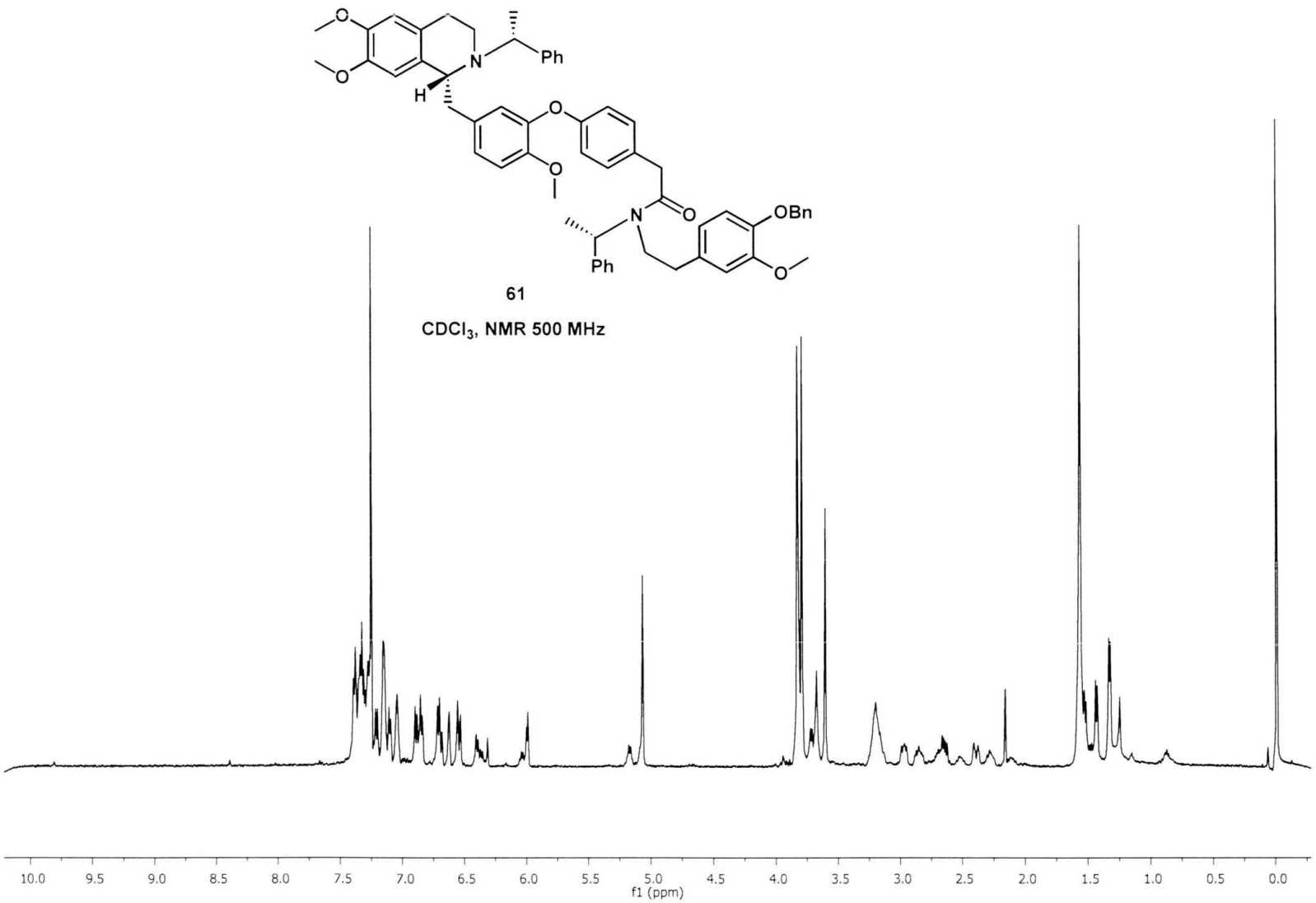
O
O
N
Ph
H
O
O
O
N
O
OBn
Ph
O
61
CDCl3, NMR 500 MHz
10.0
9.5
9.0
8.5
8.0
7.5
7.0
6.5
6.0
5.5
5.0
4.5
4.0
3.5
3.0
2.5
2.0
1.5
1.0
0.5
0.0
f1 (ppm)

2-az-134-3

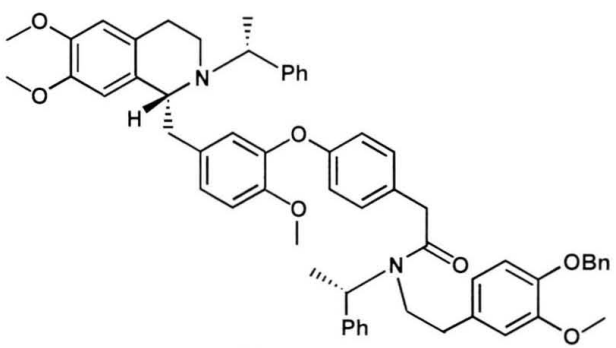

61

$CDCl_3$, NMR 75.46 MHz

az3824/2

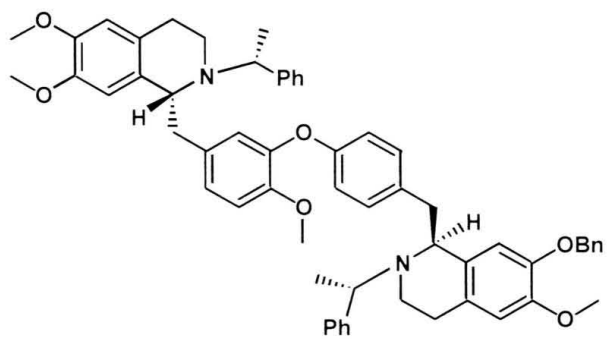

60

$CDCl_3$, NMR 500 MHz

Chapter 4

Synthesis of Anthrax Lethal Factor Inhibitors Containing Tetrahydroisoquinoline Units

Chapter 4

Synthesis of Anthrax Lethal Factor Inhibitors Containing Tetrahydroisoquinoline Units

4.1 Definition and Classification of Anthrax.

Anthrax is an acute infectious disease that normally affects animals, especially ruminants (such as goats, cattle, sheep, and horses). It is caused by the *B. anthracis* bacterium. Some other animals however are very resistant to anthrax and these include for example, dogs, cats, and rats.[1] Anthrax does not spread from person to person under natural conditions. However, anthrax can be transmitted to humans by contact with infected animals or their products. Recently, anthrax infection gained a great deal of attention as it has become clear that the infection can also be used in a bioterrorist attack.[2]

In 1876, Dr. Robert Koch, a German physician and scientist, described the life cycle of the anthrax bacillus and its relationship to anthrax disease, and he proved that the anthrax bacterium was the cause of a disease that affected farm animals in his community. *B. anthracis* bacteria are rod-like in appearance. However, in soil they exist as spores in an inactive (dormant) state. These spores are very hardy, are difficult to destroy, and have been known to survive in soil for as long as 48 years.[3,4]

Depending on the way in which a spore infects the body, anthrax disease has been divided into three types:[5]

(a) Cutaneous anthrax, which causes skin infection with ugly sores. The symptoms may also include muscle aches and pain. These symptoms can usually be effectively treated using antibiotics and in some other cases, the infected organism's immune system eliminates the spore by itself.

(b) Gastrointestinal and oropharyngeal forms of anthrax, in which humans and animals can ingest anthrax from spore-contaminated meat. Even though it is a very rare form of anthrax, the infection spreads throughout the body and causes serious disease.

(c) Inhalation anthrax, which is the most dangerous form in which the spores of anthrax enter the host via aerosols, and are then carried into the lymph glands in the chest where they proliferate, spread, and produce toxins. In most cases this kind of anthrax often causes death.

In 2001, *B. anthracis* spores were sent in a letter by mail causing the death of several postal workers. This event was achieved by causing airborne numbers of spores to far exceed a natural exposure, resulting in inhalation anthrax affecting a large number of people. These facts have led to recent efforts towards improving anthrax vaccines.[2]

4.1.1 Lethality of *B. anthracis* and anthrax toxin.

The virulence factor of *B. anthracis* can be attributed to two main factors: the capsule, and the toxin.[5] The capsule which contains poly-γ-D-glutamic acid (γDPGA) (**1**), is an essential virulence factor of *B. anthracis* as it reduces the natural host defence

mechanism through its antiphagocytic action.[6] Although γDPGA by itself is weakly immunogenic and does not induce booster response, it stimulates the production of serum antibodies when covalently bound to a carrier protein.[7]

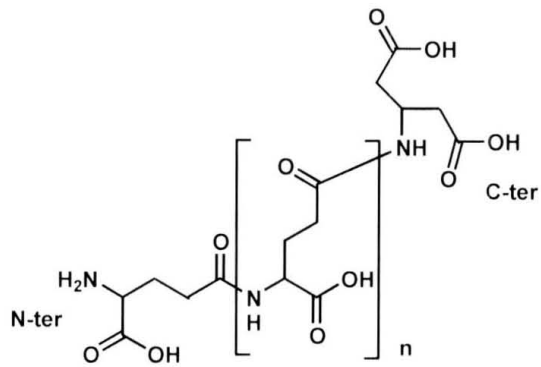

1

Figure 4.1. Structure of poly-γ-D-glutamic acid.

The toxin, which contains three proteins, is the second factor that determines the virulence of *B. anthracis*. These three proteins are referred to as: protective antigen (PA), and two other enzyme components, namely, lethal factor (LF), and edema factor (EF).[8] None of these individual proteins is toxic; however, when a mixture of PA and LF are injected together, a lethal shock is caused in experimental animals. Also, a mixture of PA and EF causes edema at the site of injection.

Anthrax toxin is a new type of "AB" toxin that is found in the form A_2B, where the two enzymes, EF and LF, are the *A* components and PA is the *B* component. In this case the PA protein carries EF and LF through the plasma membrane into the cytosol, where they may then exert their lethal effect. Early infection by anthrax toxin is detectable in low concentration either on the surface of receptor-bearing cells or in

solution, however, the cell-surface pathway is likely to be physiologically more important.[9]

It is presumed that the combination of the three proteins PA, LF, and EF kills the host macrophages and decreases or eliminates the host immune system which, in turn, increases the progress of the disease. Thereby, inhalation anthrax leads to the death of the host organism if untreated.[10]

4.1.2 Detection and inhibition of ALF.

Anthrax lethal factor (ALF) is a zinc-dependent endopeptidase and a constituent of the anthrax toxin that cleaves MAPKK and causes cell death. The identification and preparation of potent inhibitors against LF and understanding its unusual mode of action has become the focus of several studies.[11,12,13,14] Many different small molecules have been reported to develop an effective and inexpensive vaccine against the anthrax lethal factor, and most of these inhibitors are centered on zinc-binding groups such as hydroxamate and thiazolidine.[11,15] On the other hand, some other molecules which have been effective as lethal factor inhibitors, such as guanidinylated compounds, do not possess the prototypical zinc-binding groups.[16,17,18]

Panchal *et al.*[12] identified 19 compounds with more than 50% LF inhibition (at 20 μM inhibitor concentration) from the NCI Diversity Set screen. These included the NSC 12155 (**2**) and NSC 357756 (**3**), which were used in 3D database mining studies to identify additional LF inhibitors.

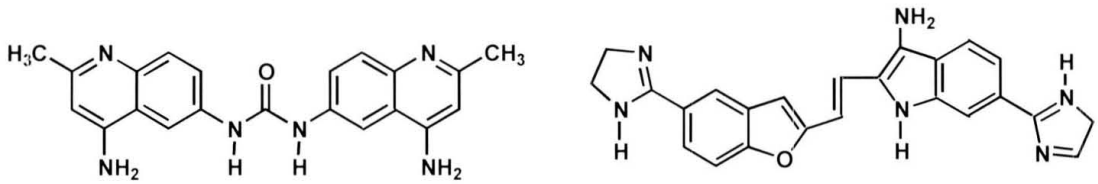

Figure 4.2. Structure of NSC 12155 (**2**) and NSC 357756 (**3**).

Among the 19 compounds, the crystal structure of the most potent inhibitor, NSC 12155 complex, with LF was determined. The urea moiety of the NSC 12155 binds to the catalytic site of LF close to the catalytic Zn atom (within 4 Å). One of the quinoline rings shows strong electron density near the side-chain of His690, showing a π-stacking interaction between histidine's side-chain imidazole and the quinoline ring (Figure 4.3).

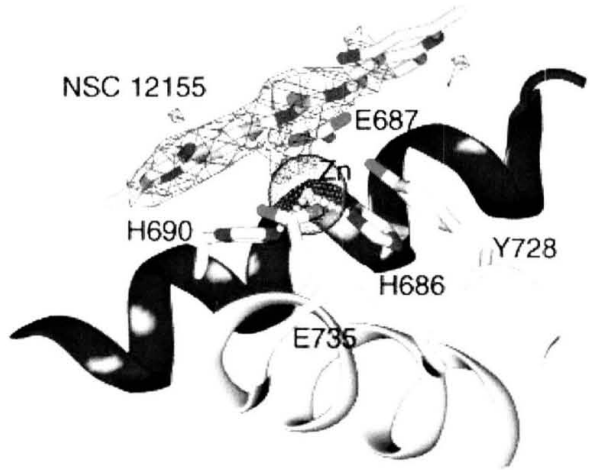

Figure 4.3. Inhibitor NSC 12155 (**2**) bound in the active site of LF (Figure adapted from reference 12).

Similar basic and cationic compounds with a detailed computational investigation have been reported by Bavari *et al.* in 2007.[19]

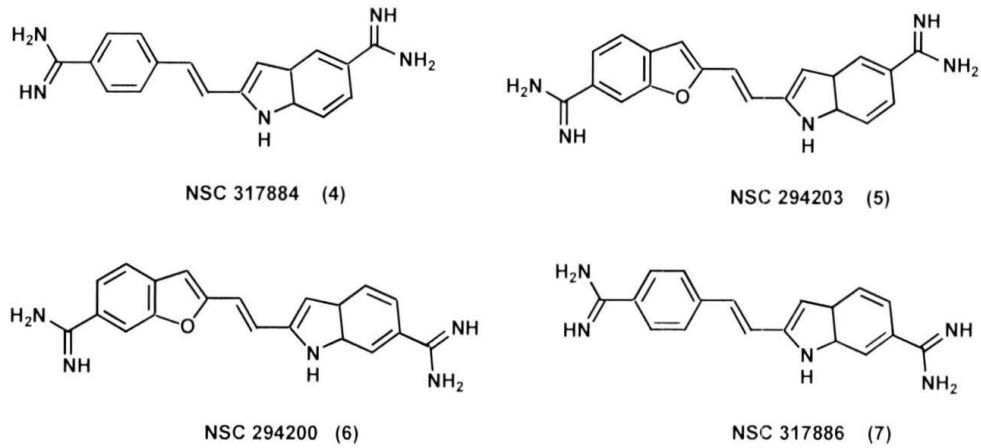

Figure 4.4. Chemical structures for some LF inhibitors.

It was determined by HPLC-based enzymatic assays that carbamimidolyl-aryl-vinyl-indole-carboxamidine compounds **4-7**, are dose-independent with an average % LF inhibition of 89-92% at 20 μm, 59-88% at 10 μm, and by 21-69% at 5 μm. Also, the experimental results showed that compounds **4-7** bind at the LF active site, although these compounds do not posses identifiable zinc binding groups. They are, however, characterized by a common indol-attached amidine moiety and a stable Zn-N(amidine) bond with an atom-atom distance of 2.02 Å and bond angle of 138.8°.

A series of phenylfuran-2-ylmethylenerhodanineacetic acid derivatives of LF inhibitors were designed in 2005 by Forino *et al.*[20] These compounds showed highly potent activity against LF in both *in vitro* tests and cell-based, assays especially in the presence of phenyl groups having small electronegative groups in the R_1 position and a

carboxylic acid moiety in position R_2 (Figure 4.5) It was also noted that the presence of multiple substituents increases the reactivity.

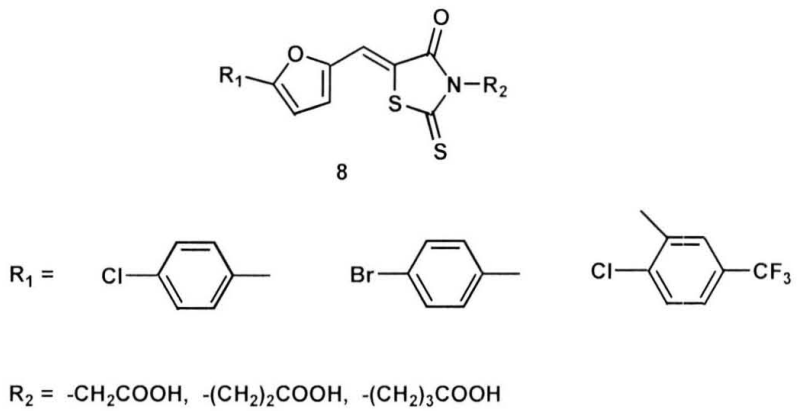

Figure 4.5. Derivatives of compound **8**.

The crystal structure of the LF-inhibitor zinc-complex shows the interaction between the zinc atom in the LF active site and the inhibitor molecule via an S atom, in addition, greater interaction is mainly found between the hydrophobic aromatic ring of the inhibitors, and the hydrophobic side chain of the LF.

The galloyl (3,4,5-trihydroxybenzoyl) derivatives (**9**) found in green tea have been described as powerful inhibitors of LF-metalloproteolytic activity (Figure 4.6). The main catechins of green tea, CG (**11**) and EGCG (**13**), have been found to be effective inhibitors for anthrax LF and macrophage cytotoxicity.[21]

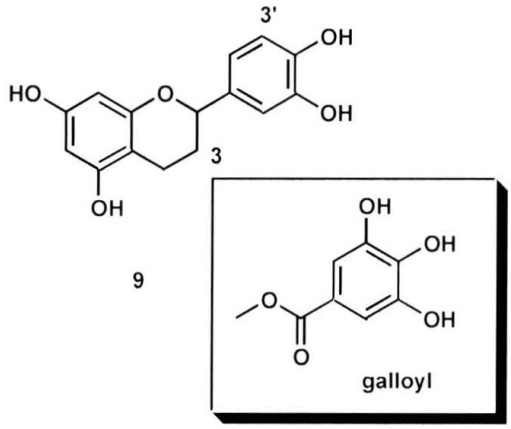

		3	3'
EC	(10)	OH	-
CG	(11)	galloyl	-
EGC	(12)	OH	OH
EGCG	(13)	galloyl	OH

Figure 4.6. Examples for some anthrax lethal factor inhibitors derivatives.

Based on this study, Wong tried to identify more potent LF inhibitors containing the same polyphenolic motif.[22] Ten commercial compounds were tested to confirm the importance of the gallate motif in the inhibition of LF, these including alizarin (**14**), purpurin (**15**), and purpurogallin (**16**) (Figure 4.7).

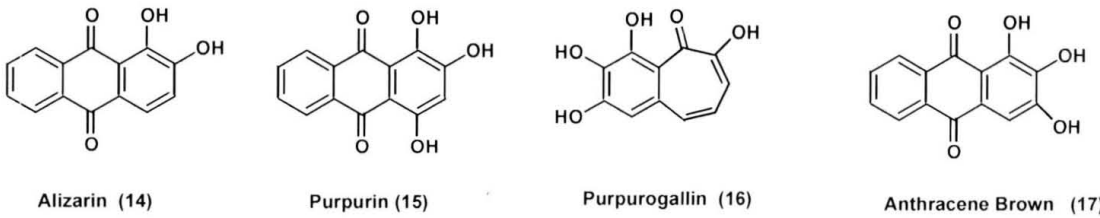

Figure 4.7. Structures of alizarin (**14**), purpurin (**15**), and purpurogallin (**16**).

Although these three compounds have very strong structural similarity to anthracene brown (**17**), they did not however show any LF inhibition, even though anthracene brown itself was identified as an inhibitor against anthrax lethal factor.

Due to the presence of the 3,4,5-trihydroxy motif, 5-hydroxydopamine hydrochloride was chosen as a core reagent to react with fifty-nine structurally-diverse aldehydes, and seven dialdehydes to prepare gallate-like tetrahydroisoquinoline derivatives using the Pictet-Spengler reaction (Scheme 4.1).[22]

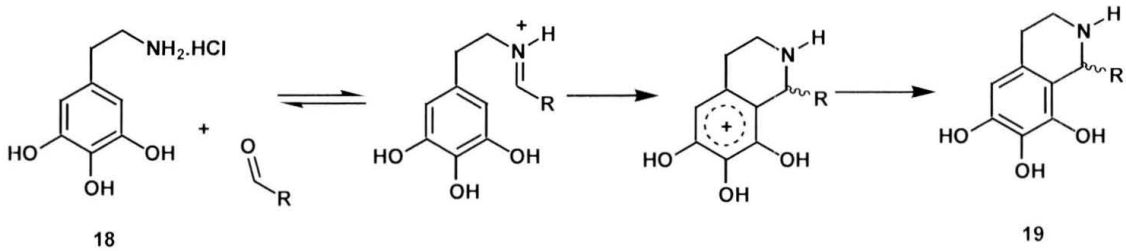

Scheme 4.1. Mechanism for formation gallate-like tetrahydroisoquinoline polyphenols.

It was noted that the reaction with dialdehydes produces compounds **20-22** having high lethal factor inhibition values and that the potency of these compounds (which were purified by preparative HPLC) is dependent on the ionic strength of the assay conditions.

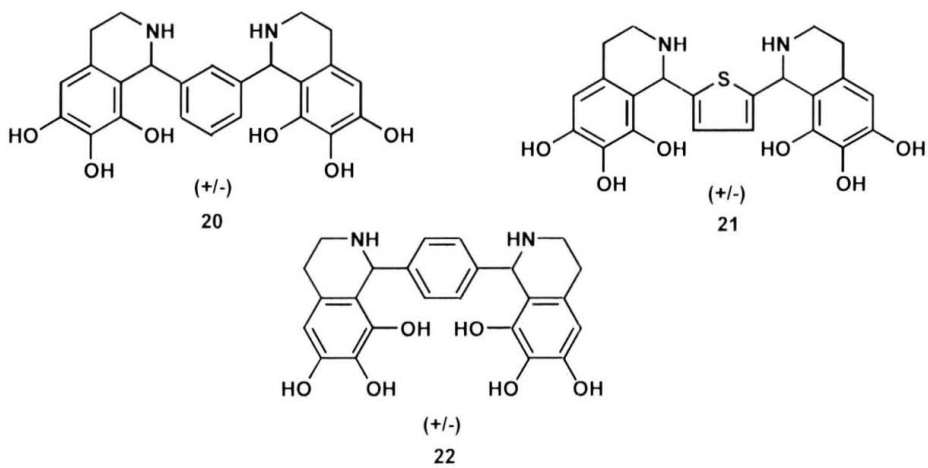

Figure 4.8. Structures of bis(tetrahydroisoquninoline) compounds.

It was also noted that under a physiological salt concentration the *meso* (1*S*,1'*R*), compound **23**, shows a highly potent non-competitive inhibition with a K_i value = 4.3 ± 1.8 μM as compared to its racemic mixture, which shows a K_i value = 51.8 ± 1.2 μM.

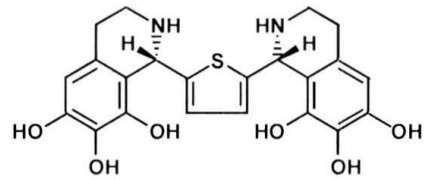

23

Ki = 4.3 ± 1.8 μM

Figure 4.9. Structure of the *meso* compound **23**.

Wong also suggested that analogues of tetrahydroisoquinolines, such as dihydroisoquinolines and isoquinolines, can also be considered as potentially interesting targets for the identification of new potent LF inhibitors. However, the actual potencies of the individual enantiomers tested are still unknown. These studies piqued our interest to see whether some of the intermediates obtained in the course of our on-going studies towards the enantioselective synthesis of (-)-cycleanine, a bisbenzyltetrahydroisoquinoline alkaloid, could be employed as anthrax LF inhibitors. Thus compounds **24a,b** and **25a,b** were targeted (Figure 4.10).

Since the *meso* compound **23** in Wong's studies showed highly potent non-competitive LF inhibition, chiral-auxiliary double Bischler-Napieralski cyclization reactions were employed to enantioselectively synthesize these compounds **24a,b** and **25a,b**.

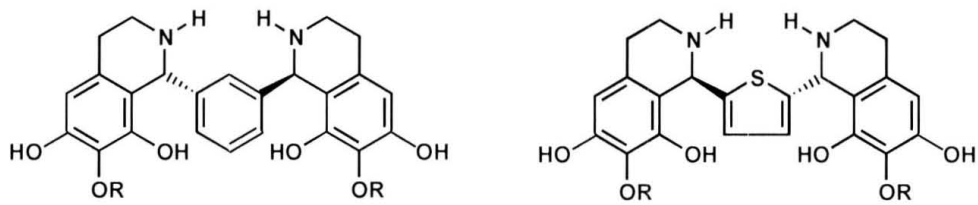

24a,b 25a,b

Figure 4.10. Structures of target compounds **24a,b** and **25a,b**.

4.2 Results and Discussion.

As discussed in Chapter 2, the chiral auxiliary-assisted Bischler-Napieralski cyclization reduction reaction was found to be one of the most effective reactions for the syntheses of tetrahydroisoquinolines from β-ethylamides of electron-rich arenes affording high stereoselectivity in position C-1 when the chiral auxiliary (*S*)-or (*R*)-α-methylbenzylamine is used. In this Chapter, trials are described toward the enantioselective synthesis of compounds **24a** and **25a**, which are the diastereomers of those previously reported by Wong and coworkers in their formal synthesis without any stereoselectivity. In addition, two other new analogues, **24b** and **25b,** containing a methoxy group at C-7 instead of the hydroxyl group, were also targeted for the synthesis using the Bischler-Napieralski cyclization reaction.

Outlined in Scheme 4.2 is an initial retrosynthetic analysis for the enantioselective synthesis of each of these compounds, **24a** and **24b.**

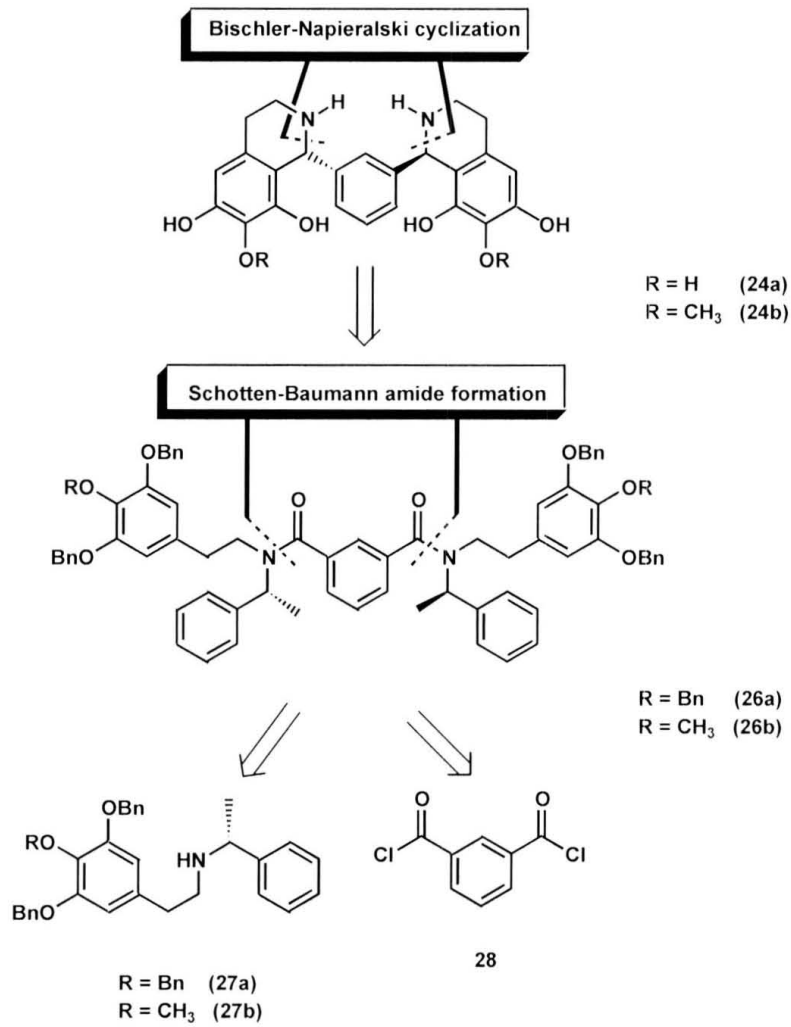

Scheme 4.2. Retrosynthetic analysis of **24a** and **24b**.

The first retrosynthetic disconnection gives the amides **26a,b** which undergo a double-BNC-reduction reaction to produce the two stereogenic centers (1*R*,1′*R*). The second retrosynthetic dissects the amide **26a** (or **26b**) into the key intermediates: the commercially-available isophthaloyl chloride **28** and the chiral auxiliary-protected amine **27a** or **27b** having either a methoxy or benzyloxy group in position 4. These two

intermediates are required for the Schotten-Baumann reaction to afford the amide **26a** or **26b**, respectively.

4.2.1 Synthesis of the CA-protected amine 27a.

The chiral auxiliary-protected amine **27a** was synthesized as outlined in Scheme 4.6.

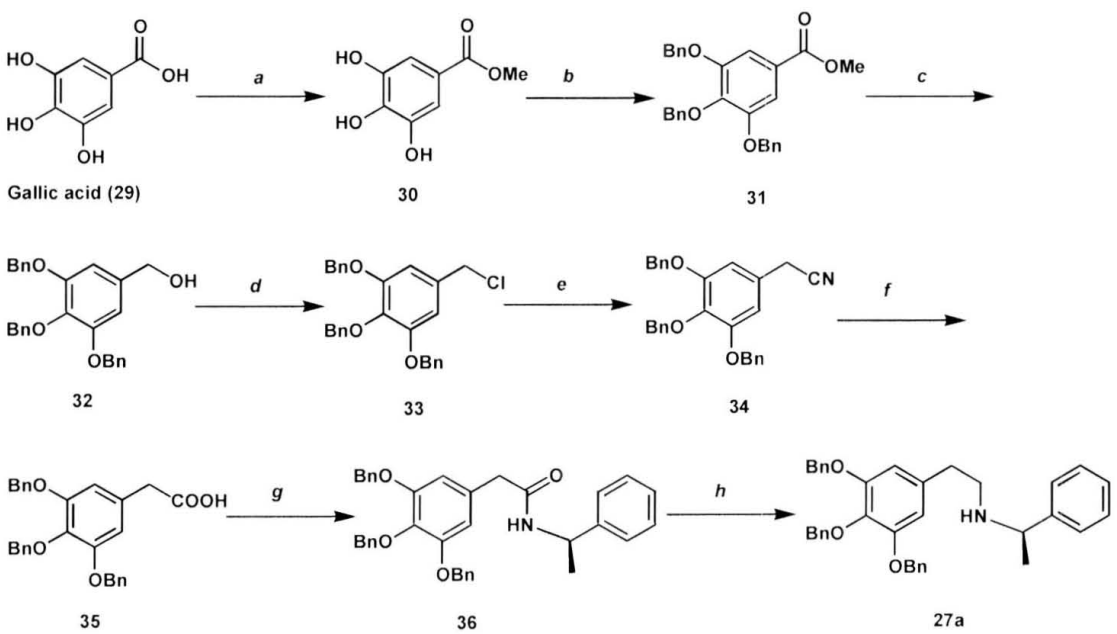

a: $SOCl_2$, MeOH, 94%, ***b:*** BnBr, K_2CO_3, DMSO, 97%; ***c:*** $LiAlH_4$, THF, 89%; ***d:*** $SOCl_2$, pyridine, benzene, 86%; ***e:*** NaCN, DMSO, benzene, 90%; ***f:*** NaOH, ethanol, 95%; ***g:*** 1. $(COCl)_2$, benzene; 2. (*R*)-α – methylbenzylamine, NaOH, CH_2Cl_2, 96%; ***h:*** BF_3•Et_2O, BH_3•THF, 89%.

Scheme 4.3. Synthesis of the CA-protected amine **27a**.

Gallic acid (**29**) was chosen to be the starting material as it contains three hydroxyl groups which can be easily protected as their benzyl ethers. Esterification of the carboxylic acid group using thionyl chloride in methanol gave methyl gallate **30** in 94%

yield, followed by protection of the phenolic groups as the benzyl ethers using 3 (mol equiv) of benzyl bromide. The protected ester **31** was achieved in 97% yield. Reduction of the ester group to the corresponding primary alcohol **32** was accomplished using lithium aluminum hydride to produce the alcohol **32** in 89% yield. In order to elongate the side-chain, compound **32** was treated with $SOCl_2$ to furnish the benzyl chloride **33** in 86% yield. Cyanation in DMSO followed by hydrolysis using NaOH/EtOH form the corresponding phenylacetic acid **35** in 95% yield. Schotten-Baumann Reaction between the phenylacyl chloride, formed *in situ* from phenylacetic acid **35**, with (*R*)-α-methylbenzylamine resulted in the formation of the chiral auxiliary-protected amide **36** in 96% yield. Reduction of the amide **36** to the corresponding secondary chiral auxiliary-protected amine **27a** was achieved in 89% yield via BF_3•etherate-mediated reduction with B_2H_6 in THF.

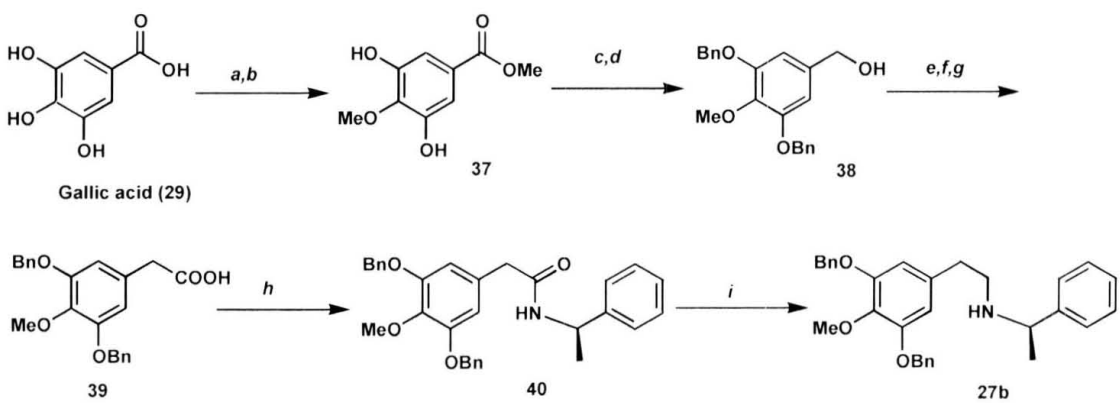

a: $SOCl_2$, MeOH, 97%; ***b:*** $(CH_3)_2SO_4$, K_2CO_3, acetone, 61%; ***c:*** BnBr, K_2CO_3, acetone, 95%; ***d:*** $LiAlH_4$, THF, 94%; ***e:*** $SOCl_2$, pyridine, benzene, 85%; ***f:*** NaCN, DMSO, benzene, 89%; ***g:*** NaOH, ethanol, 88%; ***h :*** 1. $(COCl)_2$, benzene; 2. (*R*)-α–methylbenzylamine, NaOH, CH_2Cl_2, 79%; ***h:*** BF_3•Et_2O, BH_3•THF, 85%.

Scheme 4.4. Synthesis of the CA-protected amine **27b**.[23]

The second chiral-auxiliary protected amine **27b** was prepared with the same method used for **27a** with the only difference being the selective methylation for the *p*-hydroxy group of the gallic acid starting material as shown in Scheme 4.4.[24]

4.2.2 Synthesis of the ALF inhibitors.

Double amidation using a Schotten-Baumann reaction between 1 mol equiv of the chiral auxiliary-protected amine **27a** and 0.5 mol equiv of the commercially available 1,3-isophthaloyl chloride **28** afforded a good yield of the desired product, as shown in Scheme 4.5. The ^{1}H-NMR and ^{13}C-NMR data showed an unexpected result especially in the ^{13}C-NMR spectrum. It is understandable that rotation about the amide bond of some tetrahydroisoquinolines leads to the interconversion of the two rotamers, and as a result the ^{1}H-NMR signals become broad and the ^{13}C-NMR signals are duplicated. However, the ^{13}C-NMR spectra showed a lesser number of peaks in both the aliphatic and aromatic region, although the TLC showed it to be a single spot and the APCI-MS gave the expected exact mass.

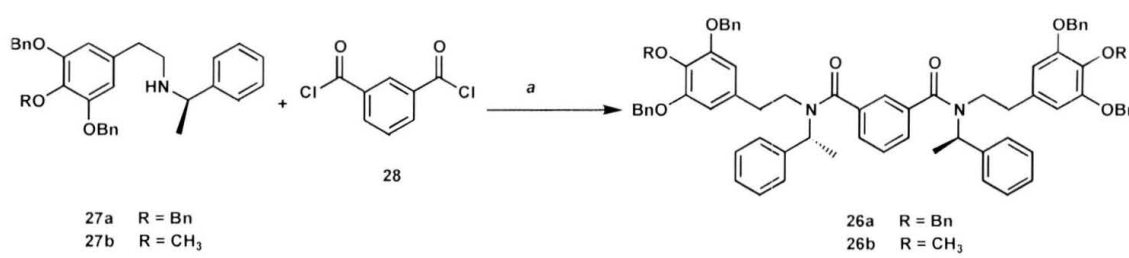

a: 5% NaOH, CH_2Cl_2, rt, 75%.

Scheme 4.5. Preparation of the chiral amide **26a** and **26b**.

With the only difference being the choice of the starting material used, commercially available 2,5-thiophene-dicarbonyl dichloride (**41**) was used to synthesize the second set of the ALF inhibitors (Scheme 4.6). Schotten-Baumann reaction between 1 (mol equiv) of the chiral auxiliary protected-amine **27a** or **27b** and 0.5 (mol equiv) of 2,5-thiophene-dicarbonyl dichloride (**41**) afforded a good yield of the desired products **42a** or **42b**, respectively, as shown in Scheme 4.6, with the same observations being noted for the ^{1}H-NMR and ^{13}C-NMR spectrum.

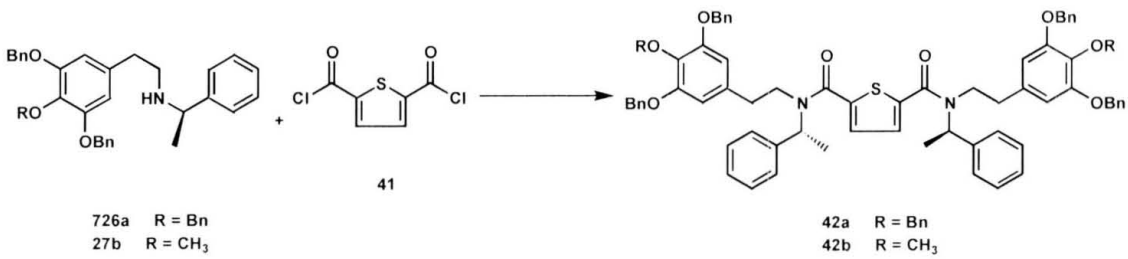

a: 5% NaOH, CH_2Cl_2, rt, 72%.

Scheme 4.6. Preparation of the chiral amide **41a** and **41b**.

Cyclization of these diamide compounds using typical Bischler-Napieralski conditions, with $POCl_3$ in benzene, followed by $NaBH_4$ reduction afforded the anthrax LF inhibitor backbone **43a** and **43b** which ranged between 10-13% in overall yield (Scheme 4.7).

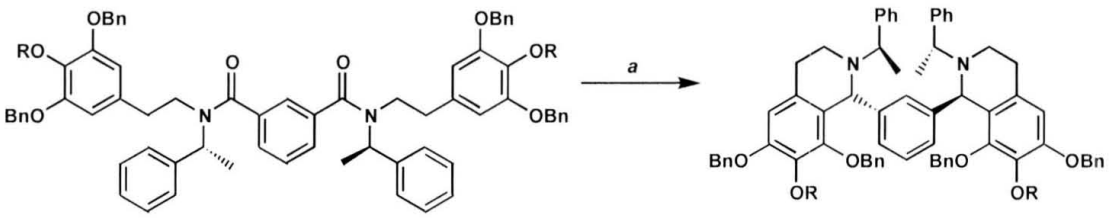

26a R = Bn
26b R = CH_3

43a R = Bn
43b R = CH_3

a: 1. $POCl_3$, benzene, reflux, 72 h; 2. $NaBH_4$, MeOH, -78 °C, 10%.

Scheme 4.7. Cyclization of the diamide **26a** and **26b**.

Although clean ^{1}H-NMR and ^{13}C-NMR data for the desired diasteromeric compounds were obtained, attempts to increase the yield by changing the solvent or using microwave conditions failed. As a result, the next step, which included catalytic hydrogenation to remove the benzyl groups and the chiral auxiliary to produce anthrax LF inhibitors as shown in Scheme 4.8, were not completed at the time of writing this thesis.

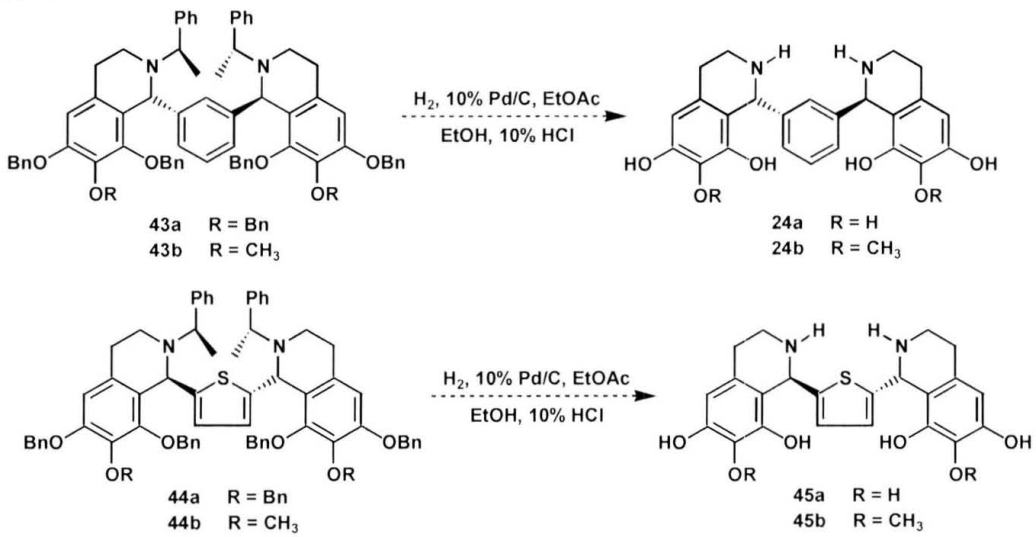

43a R = Bn
43b R = CH_3

24a R = H
24b R = CH_3

44a R = Bn
44b R = CH_3

45a R = H
45b R = CH_3

Scheme 4.8. Removal of the chiral auxiliaries and benzyl groups.

4.3 Conclusions.

A second set of tetrahydroisoquinoline-containing synthetic targets which are of interest and are potential ALF inhibitors have been investigated. Enantioselective synthesis of these compounds using the chiral auxiliary-mediated strategy, previously employed in our group, successfully afforded some chiral tetrahydroisoquinoline intermediate compounds, and pure diastereoisomers of these compounds could be isolated. Attempts to remove the chiral auxiliaries and the protecting groups were not succeeded and the low yields which were obtained in Bischler-Napieralski cyclization-reduction reactions limited the experimental efforts. Increasing the yield in the Bischler-Napieralski cyclization step is therefore essential. This can in principle be done by changing the solvent or the conditions used and future work will be required in order to produce some tetrahydroisoquinoline unit-containing compounds that could be effective anthrax LF inhibitors.

Experimental

Methyl gallate (30).

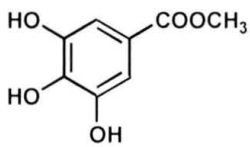

To a solution of gallic acid **29** (8.21 g, 48.3 mmol) in methanol (75 mL) was added dropwise thionyl chloride (4.22 mL, 57.9 mmol) at 0 °C. The solution was allowed to warm to room temperature before it was heated to reflux for 3 h. The reaction was quenched by addition of water (30 mL), and then the mixture was extracted with EtOAc (20 mL x 3). The combined organic layers were washed with water (20 mL x 3), dried over $MgSO_4$, filtered, and the solvent was evaporated to afford **30** (8.35 g, 94%) as a colorless solid, mp 204-205 °C; ^{1}H NMR ($(CD_3)_2CO$, 500 MHz): δ 8.13 (bs, 2H), 7.11 (s, 2H), 3.79 (s, 3H); ^{13}C NMR ($(CD_3)_2CO$, 125.77 MHz): δ 166.6, 145.5, 138.1, 121.3, 109.3, 51.3; APCI-MS (*m/z*): 182.7 (M-1, 100).

Methyl 3,4,5-tris(benzyloxy)benzoate (31).

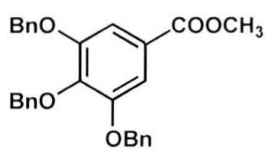

To a suspension of anhydrous potassium carbonate (16.9 g, 122 mmol) in DMSO (90 mL) was added methyl gallate (**30**) (7.50 g, 40.7 mmol) and benzyl bromide (14.5 mL, 122 mmol). After being stirred for overnight, water was added and the mixture was extracted with EtOAc (50 mL x 3). The combined organic extracts were washed with brine (15 mL x 3), dried over anhydrous $MgSO_4$, filtered, and the solvent was evaporated to afford **31** (18.0 g, 97%) as a colorless solid, mp 99-100 °C; ^{1}H NMR ($CDCl_3$, 300 MHz): δ 7.45-7.32 (m,

Ar-14H), 7.25-7.24 (m, Ar-3H), 5.13 (s, 4H), 5.11 (s, 2H), 3.88 (s, 3H); ^{13}C NMR ($CDCl_3$, 75.46 MHz): δ 166.6, 152.5, 137.4, 136.6, 128.5, 128.5, 128.1, 128.0, 127.9, 127.5, 125.2, 109.0, 75.1, 71.2, 52.2; APCI–MS (*m/z*): 455.2 (M+1, 100), 317.2 (80), 181.1 (79).

3,4,5-Tris(benzyloxy)benzyl alcohol (32).

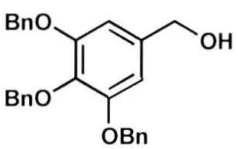

To a suspension of $LiAlH_4$ (0.624 g, 16.4 mmol) in THF (20 mL) was added a solution of compound **31** (6.23 g, 13.7 mmol) in THF (45 mL). The solution was stirred under nitrogen for 4 h. The resulting solution was quenched with aqueous 10% HCl, filtered, and dissolved in EtOAc (100 mL). The aqueous layer was separated and extracted with EtOAc (50 mL x 3). The combined organic extracts were washed with brine (15 mL x 3), dried over anhydrous $MgSO_4$, filtered, and the solvent was evaporated to afford **32** (5.20 g, 89%) as a colorless solid, m.p 103-104 °C; ^{1}H NMR ($CDCl_3$, 300 MHz): δ 7.43-7.40 (bd, 6H), 7.39-7.31 (m, 6H), 7.26 (d, J = 2.5 Hz, 3H), 6.66 (s, 2H), 5.10 (s, 4H), 5.04 (s, 2H), 4.56 (s, 2H); ^{13}C NMR ($CDCl_3$, 75.46 MHz): δ 153.0, 137.8, 137.7, 137.1, 136.6, 128.6, 128.5, 128.1, 127.8, 127.8, 127.4, 106.4, 75.2, 71.2, 65.4; APCI-MS (*m/z*): 427.2 (M+1, 20), 317.2 (100), 229.1 (50), 181.1 (50).

3,4,5-Tris(benzyloxy)benzyl chloride (33).

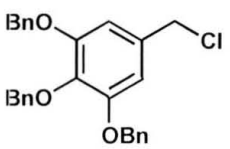

To a solution of **32** (5.01 g, 11.8 mmol) in anhydrous benzene (75 mL) was added pyridine (1.43 mL) followed by dropwise addition of

thionyl chloride (1.28 mL, 17.6 mmol). After stirring at room temperature overnight, the reaction was quenched by addition of water (20 mL), and the mixture was extracted with EtOAc (20 mL x 3). The combined extracts were washed with aqueous saturated $NaHCO_3$ (10 mL x 3), water (20 mL), dried over $MgSO_4$, filtered, and the solvent was evaporated to afford **33** (4.50 g, 86%) as a yellow solid, mp 102-103 °C; ^{1}H NMR ($CDCl_3$, 300 MHz): δ 7.43-7.32 (m, 12H), 7.26 (d, J = 2.2 Hz, 3H), 6.69 (s, 2H), 5.10 (s, 4H), 5.04 (s, 2H), 4.49 (s, 2H); ^{13}C NMR ($CDCl_3$, 75.46 MHz): δ 152.9, 137.7, 136.9, 132.9, 128.5, 128.5, 128.1, 127.9, 127.8, 127.4, 108.3, 75.2, 71.3, 46.7; APCI-MS (*m/z*): 445.2 (M+1, 20), 409.2 (40), 317.2 (100).

3,4,5-Tris(benzyloxy)phenylacetonitrile (34).

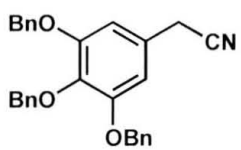

To a solution of **33** (4.23 g, 9.51 mmol) in DMSO (30 mL) and benzene (15 mL) was added NaCN powder (0.932 g, 19.0 mmol) in 4 portions. After stirring for 2 h at room temperature, the reaction mixture was poured into water (40 mL) and extracted with EtOAc (20 mL x 3). The combined organic layers were washed with brine (20 mL x 3), dried over $MgSO_4$, filtered, and the solvent was evaporated to give a yellow solid **34** (3.73 g, 90%), mp 90-91 °C; ^{1}H NMR ($CDCl_3$, 300 MHz): δ 7.42-7.26 (m, 15H), 6.58 (s, 2H), 5.09 (s, 4H), 5.04 (s, 2H), 3.63 (s, 2H); ^{13}C NMR ($CDCl_3$, 75.46 MHz): δ 153.2, 138.1, 137.6, 136.7, 128.6, 128.5, 128.2, 128.0, 127.9, 127.4, 125.2, 117.8, 107.6, 75.2, 71.3, 23.7; APCI-MS (*m/z*): 436.2 (M+1, 35), 268.1 (100), 181.1 (45).

3,4,5-Tris(benzyloxy)benzoic acid (35).

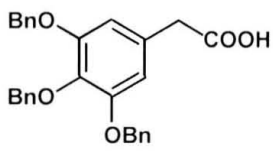

A solution of **34** (3.22 g, 7.39 mmol) in ethanol (20 mL) and aqueous 4.0 M NaOH (4 mL) was heated at reflux for 20 h. The reaction mixture was then cooled to room temperature and diluted with water (10 mL) and then acidified to pH = 1 to form a precipitate which was filtered, and washed with water to give a yellow solid **35** (3.19 g, 95%), mp 103-104 ^{0}C; ^{1}H NMR ($CDCl_3$, 300 MHz): δ 7.42-7.24 (m, 15H), 6.60 (s, 2H), 5.08 (s, 4H), 5.02 (s, 2H), 3.45 (s, 2H); ^{13}C NMR ($CDCl_3$, 75.46 MHz): δ 176.7, 152.9, 137.9, 137.8, 137.0, 128.7, 128.5, 128.4, 128.1, 127.9, 127.7, 127.5, 127.4, 109.1, 75.2, 71.2, 41.1; APCI-MS (*m/z*): 455.2 (15), 423.2 (100), 287.1 (40).

***N*-((*R*)-α-Methylbenzyl)-(3,4,5-tribenzyloxy)phenylacetamide (36).**

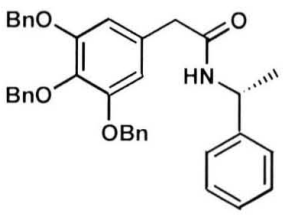

To a stirred solution of oxalyl chloride (1.51 mL, 17.3 mmol) in anhydrous benzene (35 mL) was added **35** (6.54 g, 14.4 mmol) in one batch and DMF (2 drops). The reaction mixture was stirred until the evolution of the gas ceased. The benzene was evaporated using a rotary evaporator to give a crude acid chloride, which was used directly in the next step without any further purification. The crude acid chloride was re-dissolved in anhydrous CH_2Cl_2 (12 mL) at 0 ^{0}C and the resulting solution was dropwise added to a stirred mixture of (*R*)-α-methylbenzylamine (1.79 mL, 14.4 mmol) and CH_2Cl_2/aqueous 5 % NaOH (1:1.5, 19.5 mL). After stirring at room temperature for 1 h, the reaction mixture was extracted with EtOAc (20 mL x 3), washed with water (15 mL x

3), dried over anhydrous $MgSO_4$, filtered and the solvent was evaporated to give a colorless solid **36** (7.70 g, 96%), mp 148-149 °C; ^{1}H NMR ($CDCl_3$, 300 MHz): δ 7.41 (d, J = 3.5 Hz, 2H), 7.36 (d, J = 1.7 Hz, 4H), 7.35 (s, 2H), 7.32-7.22 (m, 10H), 7.16 (d, J = 1.2 Hz, 1H), 7.14 (bs, 1H), 6.50 (s, 2H), 5.56 (d, J = 7.8 Hz, 1H), 5.10 (q, J = 7.0 Hz, 1H), 5.08 (s, 2H), 5.05 (s, 4H), 3.44 (s, 2H), 1.34 (d, J = 7.0 Hz, 3H); ^{13}C NMR ($CDCl_3$, 75.46 MHz): δ 169.8, 153.1, 143.1, 137.7, 137.5, 136.8, 130.4, 128.6, 128.6, 128.5, 128.1, 127.9, 127.8, 127.3, 125.9, 108.8, 75.1, 71.1, 48.7, 44.1, 21.8; APCl-MS (*m/z*): 558.5 (M+1, 100).

***N*-((*R*)-α-Methylbenzyl)-(3,4,5-tribenzyloxy)phenylacetamine (27a).**

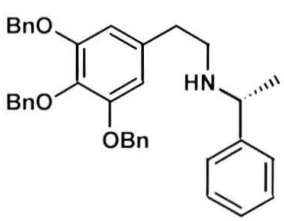

To a solution of chiral amide **36** (6.09 g, 10.9 mmol) in anhydrous THF (75 mL) was added BF_3•Et_2O (0.686 mL, 5.46 mmol) under nitrogen. The mixture was heated to gentle reflux and B_2H_6•THF (1.0 M solution in THF, 27.3 mL, 27.3 mmol) was then added dropwise. The reaction mixture was refluxed for 2 h, and then the reaction mixture was cooled to 0 °C and aqueous 20% HCl (10 mL) was added to the mixture. The solution was stirred at 0 °C for 1 h and then at room temperature overnight was basified to pH = 13 with aqueous 50% KOH solution. The mixture was then extracted with CH_2Cl_2 (20 mL x 3), dried over anhydrous $MgSO_4$, filtered and the solvent was evaporated to afford **27a** (5.28 g, 89%) as a colorless oil, which was pure enough to be used in the next step; ^{1}H NMR ($CDCl_3$, 300 MHz): δ 7.42-7.23 (m, 20H), 6.44 (s, 2H), 5.05 (s, 4H), 5.02 (s, 2H), 3.71 (q, J = 6.5 Hz, 1H), 2.70-2.62 (m, 4H), 1.29 (d, J = 6.5

Hz, 3H); ^{13}C NMR ($CDCl_3$, 75.46 MHz): δ152.7, 138.0, 137.2, 136.8, 135.7, 128.5, 128.4, 128.4, 128.1, 127.8, 127.7, 127.4, 126.9, 126.5, 108.3, 75.2, 71.2, 58.2, 36.4, 24.3; APCl-MS (*m/z*): 544.4 (M+1, 100).

1,3-Dicarbonyl-bis[*N*-((*R*)-α-methylbenzyl)-*N*-(3,4,5-tribenzyloxy)phenylethyl] benzene (26a).

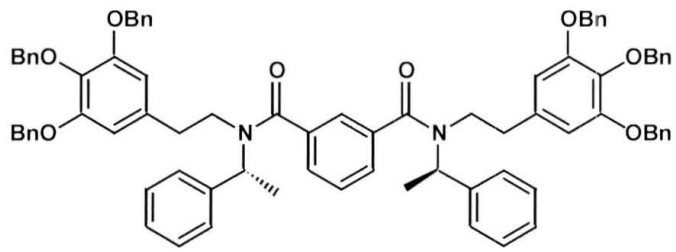

To a stirred solution of **27a** (0.550 g, 1.01 mmol) in CH_2Cl_2/aqueous 5 % NaOH (1:1.5, 1.5 mL) at 0 °C was added dropwise a solution of isophthaloyl chloride (**28**) (0.103 g, 0.506 mmol) in CH_2Cl_2. After stirring at room temperature overnight, the reaction mixture was extracted with EtOAc (20 mL x 3), washed with water (15 mL x 3), dried over anhydrous $MgSO_4$, filtered, and the solvent was evaporated to give a yellow oil which was purified by flash column chromatography (30% EtOAc/hexane) to afford **26a** (0.924 g, 75%) as a viscous oil whose ^{1}H NMR spectrum was complex; ^{13}C NMR ($CDCl_3$, 125.77 MHz): δ 152.7, 137.9, 137.2, 137.0, 128.6, 128.5, 128.4, 128.1, 127.7, 127.7, 127.4, 75.1, 71.2; APCI-MS (*m/z*): 1217.4 (M^+, 100).

1,3-Dicarbonyl-bis[*N*-(*R*)-α-methylbenzyl)-*N*-(3,5-dibenzyloxy-4-methoxy)phenyl-ethyl] benzene (26b).

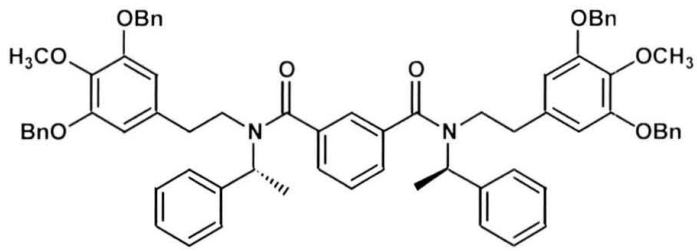

To a stirred solution of **27b** (0.563 g, 1.20 mmol) in CH_2Cl_2/aqueous 5 % NaOH (1:1.5, 1.6 mL) at 0 °C was added dropwise a solution of isophthaloyl chloride (**28**) (0.122 g, 0.602 mmol) in CH_2Cl_2. After stirring at room temperature overnight, the reaction mixture was extracted with EtOAc (20 mL x 3), washed with water (15 mL x 3), dried over anhydrous $MgSO_4$, filtered, and the solvent was evaporated to give a yellow oil which was purified by flash column chromatography (30% EtOAc/hexane) to afford **26b** (0.949 g, 74%) as a viscous oil whose ^1H NMR spectrum was complex; ^{13}C NMR ($CDCl_3$, 125.77 MHz): δ 152.4, 138.0, 137.2, 137.1, 128.6, 128.5, 128.4, 127.7, 127.2, 127.2, 124.4, 71.0, 60.9; APCI-MS (*m/z*): 1066.7 (M+1, 100).

2,5-Dicarbonyl-bis[*N*-(*R*)-α-methylbenzyl)-*N*-(3,4,5-tribenzyloxy)phenylethyl] thiophene (42a).

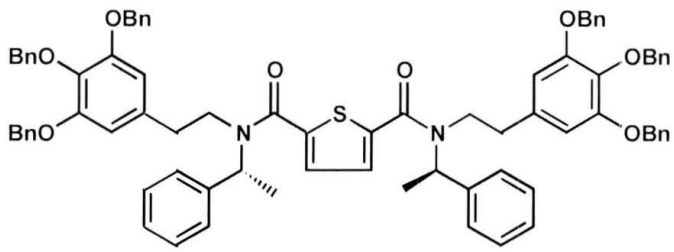

To a stirred solution of **27a** (0.538 g, 0.990 mmol) in CH_2Cl_2/aqueous 5 % NaOH (1:1.5, 2.5 mL) at 0 °C was added dropwise a solution of 2,5-thiophene dicarbonyl dichloride (**41**) (0.103 g, 0.494 mmol) in CH_2Cl_2. After stirring at room temperature overnight, the reaction mixture was extracted with EtOAc (20 mL x 3), washed with water (15 mL x 3), dried over anhydrous $MgSO_4$, filtered, and the solvent was evaporated to give a yellow oil which was purified by flash column chromatography (30% EtOAc/hexane) to afford **42a** (0.872 g, 72%) as a colorless oil; ^{1}H NMR ($CDCl_3$, 300 MHz): δ 7.42-7.22 (m, 42H), 6.30 (bs, 4H), 5.58 (bs, 2H), 5.02 (s, 8H), 4.99 (s, 4H), 3.46-3.36 m, 2H), 3.18 (bs, 2H), 2.77 (bs, 2H), 2.45 (bs, 2H), 1.59 (bs, 2H), 1.51 (d, J = 6.8 Hz, 6H); ^{13}C NMR ($CDCl_3$, 75.46 MHz): δ 164.0, 152.7, 140.3, 139.7, 139.9, 137.1, 137.0, 128.7, 128.5, 128.4, 128.1, 127.9, 127.8, 127.7, 127.4, 108.4, 75.2, 71.1; APCl-MS (*m/z*): 1223.3 (M^+, 100).

1,3-Dicarbonyl-bis[*N*-(*R*)-α-methylbenzyl)-*N*-(3,5-dibenzyloxy-4-methoxy)phenyl-ethyl]thiophene (42b).

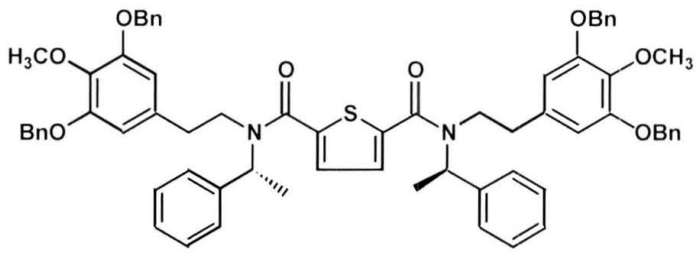

To a stirred solution of **27b** (0.502 g, 1.07 mmol) in CH_2Cl_2/aqueous 5 % NaOH (1:1.5, 2.5 mL) at 0 ^{0}C was added dropwise a solution of 2,5-thiophene dicarbonyl dichloride (**41**) (0.112 g, 0.537 mmol) in CH_2Cl_2. After stirring at room temperature overnight, the reaction mixture was extracted with EtOAc (20 mL x 3), washed with water (15 mL x 3), dried over anhydrous $MgSO_4$, filtered, and the solvent was evaporated to give a yellow oil which was purified by flash column chromatography (30% EtOAc/hexane) to afford **42b** (0.805 g, 70%) as a colorless oil; ^{1}H NMR ($CDCl_3$, 300 MHz): δ 7.44-7.23 (m, 32H), 6.27 (bs, 4H), 5.58 (bs, 2H), 5.05 (s, 8H), 3.84 (s, 6H), 3.39-3.16 (m, 2H), 2.73 (bs, 2H), 2.42 (bs, 2H), 2.22 (bs, 2H), 1.57 (bs, 2H), 1.52 (d, J = 6.8 Hz, 6H); ^{13}C NMR ($CDCl_3$, 75.46 MHz): δ 164.0, 152.4, 140.3, 139.7, 138.0, 137.2, 128.7, 128.4, 128.3, 127.9, 127.7, 127.6, 127.2, 108.4, 71.0, 60.9; APCl-MS (*m/z*): 1071.2 (M^+, 100).

1,3-bis-[1-(*R*)-*N*-((*R*)-α-Methylbenzyl)-6,7,8-tribenzyloxy-1,2,3,4-tetrahydro-isoquinolinyl]benzene (43a).

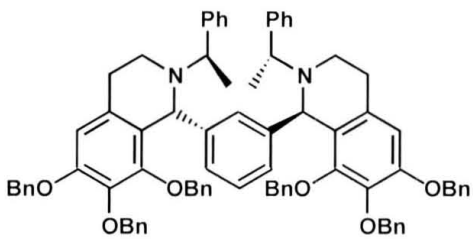

Compound **26a** (0.200 g, 0.164 mmol), $POCl_3$ (0.612 mL, 6.57 mmol) and anhydrous benzene (20 mL) were combined under nitrogen and heated to reflux at 90 °C. After approximately 72 h, the solvent and excess $POCl_3$ were evaporated on a rotary evaporator and finally on a vacuum pump for 2 h. The resultant residue was re-dissolved in anhydrous MeOH (8 mL) and the solution was cooled to -78 °C in a dry ice bath. To this solution was added $NaBH_4$ (0.0621 g, 1.64 mmol) in portions, then the reaction was stirred overnight. The reaction was quenched through the addition of aqueous 10% HCl (2 mL), and the mixture was stirred at rt for 30 min. The MeOH was evaporated on a rotary evaporator. The residue was basified by adding 20% KOH at 0 °C. The mixture was extracted with CH_2Cl_2 (10 mL x 3), the combined organic layers were dried over $MgSO_4$, filtered and the solvent was evaporated on a rotary evaporator. The residue was purified by preparative TLC (20% EtOAc/hexane) to give compound **43a** (0.0195 g, 10%) as a colorless oil; ^{1}H NMR ($CDCl_3$, 500 MHz): δ 7.46 (d, J = 8.0 Hz, 4H), 7.40-7.35 (m, 6H), 7.32-7.28 (m, 8H), 7.24-7.19 (m, 9H), 7.13 (t, J = 7.5 Hz, 2H), 7.07-6.99 (m, 6H), 6.93 (t, J = 7.5 Hz, 2H), 6.75 (d, J = 8.1 Hz, 2H), 6.70 (d, J = 7.5 Hz, 4H), 6.56 (s, 2H), 5.08 (ABq, J = 10.6 Hz, 4H), 5.02 (s, 2H), 4.90 (ABq, J = 10.5 Hz, 4H), 4.37 (d,

J = 10.5 Hz, 2H), 4.23 (d, J = 10.5 Hz, 2H), 3.67 (q, J = 6.5 Hz, 2H), 2.87-2.81 (m, 4H), 2.40-2.36 (m, 2H), 1.33 (d, J = 6.5 Hz, 6H); APCI-MS (*m/z*): 1186.4 (M+1, 100).

1,3-Bis-[1-(*R*)-*N*-((*R*)-α-methylbenzyl)-3,5-dibenzyloxy-4-methoxy-1,2,3,4-tetra-hydroisoquinolinyl]benzene (43b).

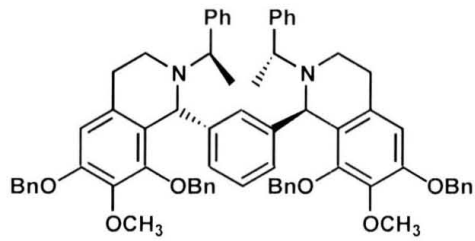

Compound **26b** (0.203 g, 0.191 mmol), $POCl_3$ (0.710 mL, 7.62 mmol) and anhydrous benzene (20 mL) were combined under nitrogen and heated to reflux at 90 °C. After approximately 72 h, the solvent and excess $POCl_3$ were evaporated on a rotary evaporator and finally on a vacuum pump for 2 h. The resultant residue was re-dissolved in anhydrous MeOH (8 mL) and the solution was cooled to -78 °C in a dry ice bath. To this solution was added $NaBH_4$ (0.0721 g, 1.91 mmol) in portions, then the reaction was stirred overnight. The reaction was quenched through the addition of aqueous 10% HCl (2 mL), and the mixture was stirred at rt for 30 min. The MeOH was evaporated on a rotary evaporator. The residue was basified by adding 20% KOH at 0 °C. The mixture was extracted with CH_2Cl_2 (10 mL x 3), the combined organic layers were dried over $MgSO_4$, filtered and the solvent was evaporated on a rotary evaporator. The residue was purified by preparative TLC (20% EtOAc/hexane) to give compound **43b** (0.022 g, 11%) as a colorless oil; ^{1}H NMR ($CDCl_3$, 500 MHz): δ 7.50 (d, J = 8.0 Hz, 4H), 7.46-7.33 (m,

8H), 7.30 (d, J = 8.1 Hz, 4H), 721 (t, J = 7.5 Hz, 4H), 7.14-7.06 (m, 6H), 6.95 (t, J = 7.5 Hz, 2H), 6.82 (d, J = 8.1 Hz, 2H), 6.78 (d, J = 7.5 Hz, 4H), 6.54 (s, 2H), 5.15-5.10 (m, 4H), 5.01 (s, 2H), 4.39 (d, J = 10.5 Hz, 2H), 4.22 (d, J = 10.5 Hz, 2H), 3.75 (s, 6H), 3.66 (q, J = 6.5 Hz, 2H), 2.83-2.74 (m, 4H), 2.38-2.34 (m, 2H), 1.38 (d, J = 6.5 Hz, 6H); ^{13}C NMR ($CDCl_3$, 125.77 MHz): δ 151.3, 150.6, 146.1, 142.9, 140.9, 137.7, 137.3, 131.3, 128.5, 128.3, 127.9, 127.8, 127.7, 127.4, 127.3, 127.2, 126.7, 123.7, 109.1, 74.2, 70.9, 60.9, 58.1, 57.6, 38.7, 24.7, 20.1; APCI-MS (m/z): 1034.4 (M+1, 100).

References

(1) Gates, C. C.; Elkin, B. T.; Dragon, D. C. *Can. J. Vet. Res.* **1995**, *59*, 256–264.

(2) Puhar, A.; Montecucco, C. *Trends Microbiol.* **2007**, *15*, 477-482.

(3) Gainer, R.S.; Saunders, R. *Can. Vet. J.* **1989**, *30*, 953-956.

(4) Smith, K. L.; De Vos, V.; Price, L. B.; Hugh-Jones, M. E.; Keim, P. *J. Clin. Microbiol.* **2000**, *38*, 3780-3784.

(5) Collier, R. J.; Young, J. A. T. *Annu. Rev. Cell Dev. Biol.* **2003**, *19*, 45-70.

(6) Green, B. D.; Battist, I. L.; Koehler, T. M.; Thorne, C. B.; Ivins, B. E. *Infect. Immun.* **1985**, *49*, 291-297.

(7) Kubler, J.; Liu, T-Y.; Mocca, C.; Majadly, F.; Robbins, J. B.; Schneerson, R. *Infect. Immun.* **2006**, *74*, 4744-4749.

(8) Smith, H.; Keppie, J. *Nature* **1954**, *173*, 869-870.

(9) Ezzell, J. W.; Abshire, T. G. *J. Gen. Microbio.* **1992**, *138*, 543-549.

(10) Gujraty, K.; Sadacharan, S.; Frost, M.; Poon, V.; Kane, S.; Mogridge, *J. Mol. Pharmaceutics* **2005**, *2*, 367-372.

(11) Lee, L. V.; Bower, K. E.; Liang, F. S.; Shi, J.; Wu, D.; Sucheck, S. J.; Vogt, P. K.; Wong, C. H. *J. Am. Chem. Soc.* **2004**, *126*, 4774-4775.

(12) Panchal, R. G.; Hermone, A. R.; Nguyen, T. L.; Wong, T. Y.; Schwarz**enba**cher, R.; Schmidt, J.; Lane, D.; McGrath, C.; Turk, B. E.; Burnett, J.; Aman, M. J.; Little, S.; Sausville, E. A.; Zaharevitz, D. W.; Cantley, L. C.; Liddington, R. C.; Gussio, R.; Bavari, S. *Nat. Struct. Mol. Biol.* **2004**, *11*, 67-72.

(13) Turk, B. E.; Wong, T. Y.; Schwarzenbacher, R.; Jarrell, E. T.; Leppla, S. H.; Collier, R. J.; Liddington, R. C.; Cantley, L. C. *Nat. Struct. Mol. Biol.* **2004**, *11*, 60-66.

(14) Min, D. H.; Tang, W. J.; Mrksich, M. *Nat. Biotechnol.* **2004**, *22*, 717-720.

(15) Shoop, W. L.; Xiong, Y.; Wiltsie, J.; Woods, A.; Guo, J.; Pivnichny, J. V.; Felcetto, T.; Michael, B. F.; Bansal, A.; Cummings, R.T.; Cunningham, B. R.; Friedlander, A. M.; Douglas, C. M.; Patel, S. B.; Wisniewski, D.; Scapin, G.;

Salowe, S. P.; Zaller, D. M.; Chapman, K. T.; Scolnick, E. M.; Schmatz, D. M.; Bartizal, K.; MacCoss, M.; Hermes, J. D. *Proc. Natl. Acad. Sci. USA* **2005**, *102*, 7958-7963.

(16) Jiao, G. S.; Cregar, L.; Goldman, M. E.; Millis, S. Z.; Tang, C. *Bioorg. Med. Chem. Lett.* **2006**, *16*, 1527-1531.

(17) Jiao, G. S.; Simo, O.; Nagata, M.; O'Malley, S.; Hemscheidt, T.; Cregar, L.; Millis, S. Z.; Goldman, M. ; Tang, E. C. *Bioorg. Med. Chem. Lett.* **2006**, *16*, 5183-5189.

(18) Puerta, D. T.; Cohen, S. M. *Curr. Top. Med. Chem.* **2004**, 4, 1551-1573.

(19) Nguyen, T.; Panchal, R.; Topol, I.; Lane, D.; Kenny, T.; Burnett, J.; Hermone, A.; McGrath, C.; Burt, S.; Gussio, R.; Bavari, S. *J. Mol. Struct.* **2007**, *821*, 139-144.

(20) Forino, M.; Johnson, S.; Wong, T. Y.; Rozanov, D. V.; Savinov, A. Y.; Li, W.; Fattorusso, R.; Becattini, B.; Orry, A. J.; Jung, D.; Abagyan R. A.; Smith, J. W.; Alibek, K.; Liddington, R. C.; Strongin, A. Y.; Pellecchia, M. *PNAS.* **2005**, *102*, 9499-9504.

(21) Dell'Aica, I.; Dona, M.; Tonello, F.; Piris, A.; Mock, M.; Montecucco, C.; Garbisa, S. *EMBO Rep.* **2004**, *5*, 418-422.

(22) Numa, M. D.; Lee, L. V.; Hsu, C.; Bower, K. E.; Wong, C. *Chem. Bio. Chem.* **2005**, *6*, 1002-1006.

(23) For the synthesis and the spectral data for compound **27b**, see: Dakhil, O. *M. Sc. Thesis*, Memorial University of Newfoundland, **2009**.

Supplementary Spectral Data for Chapter 4:

^{1}H and ^{13}C NMR spectra are presented in the following sequence for compound numbers:

30, 31, 32, 33, 34, 35, 36, 27a, 26a, 26b, 42a, 42b, 26a, 26b, 42a, 42b, 43a, 43b

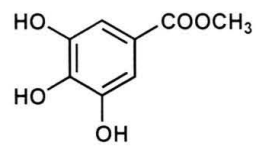

30

$(CD_3)_2CO$, NMR 500

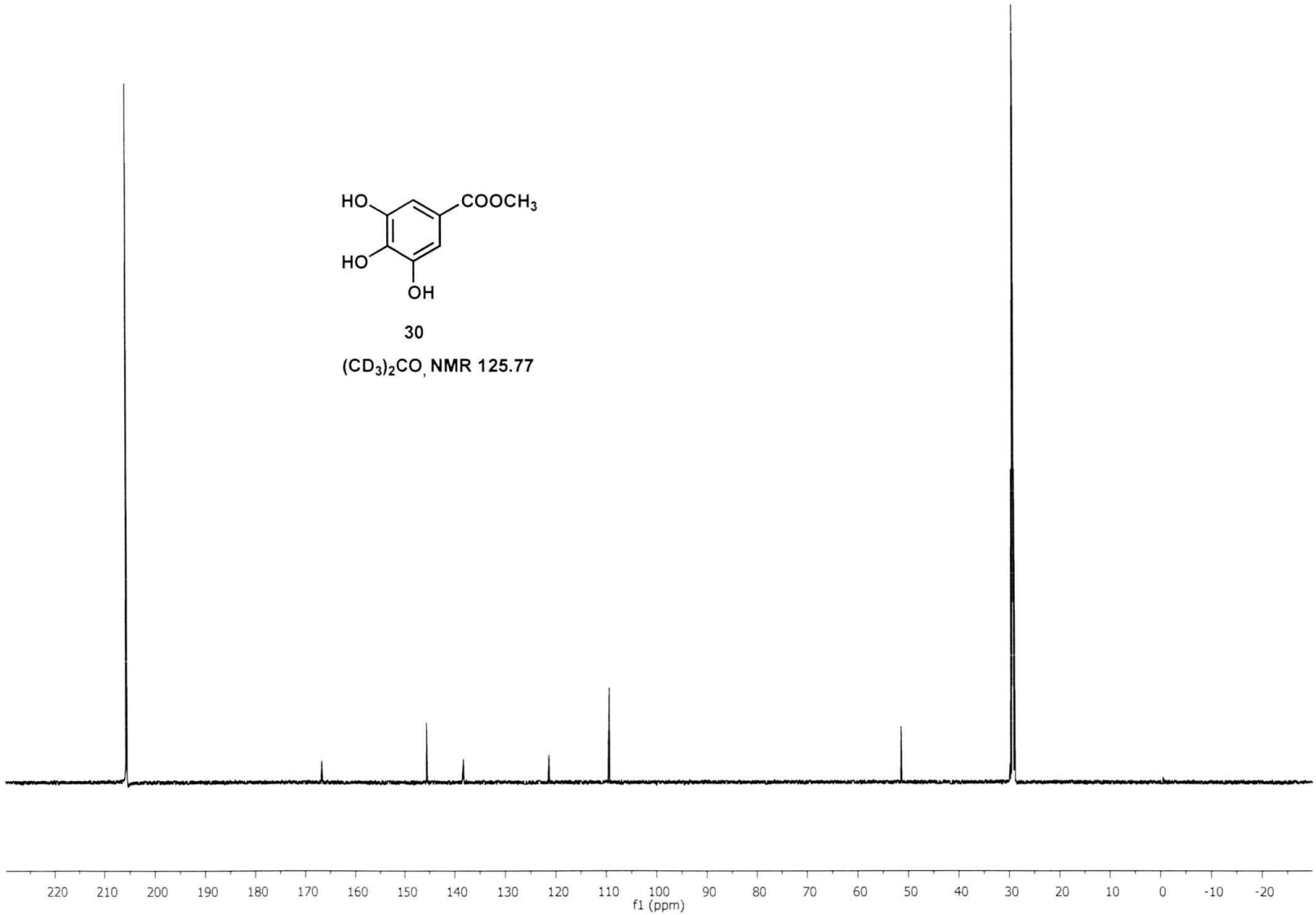
HO
COOCH3
HO
OH
30
(CD3)2CO, NMR 125.77
220 210 200 190 180 170 160 150 140 130 120 110 100 90 80 70 60 50 40 30 20 10 0 -10 -20
f1 (ppm)

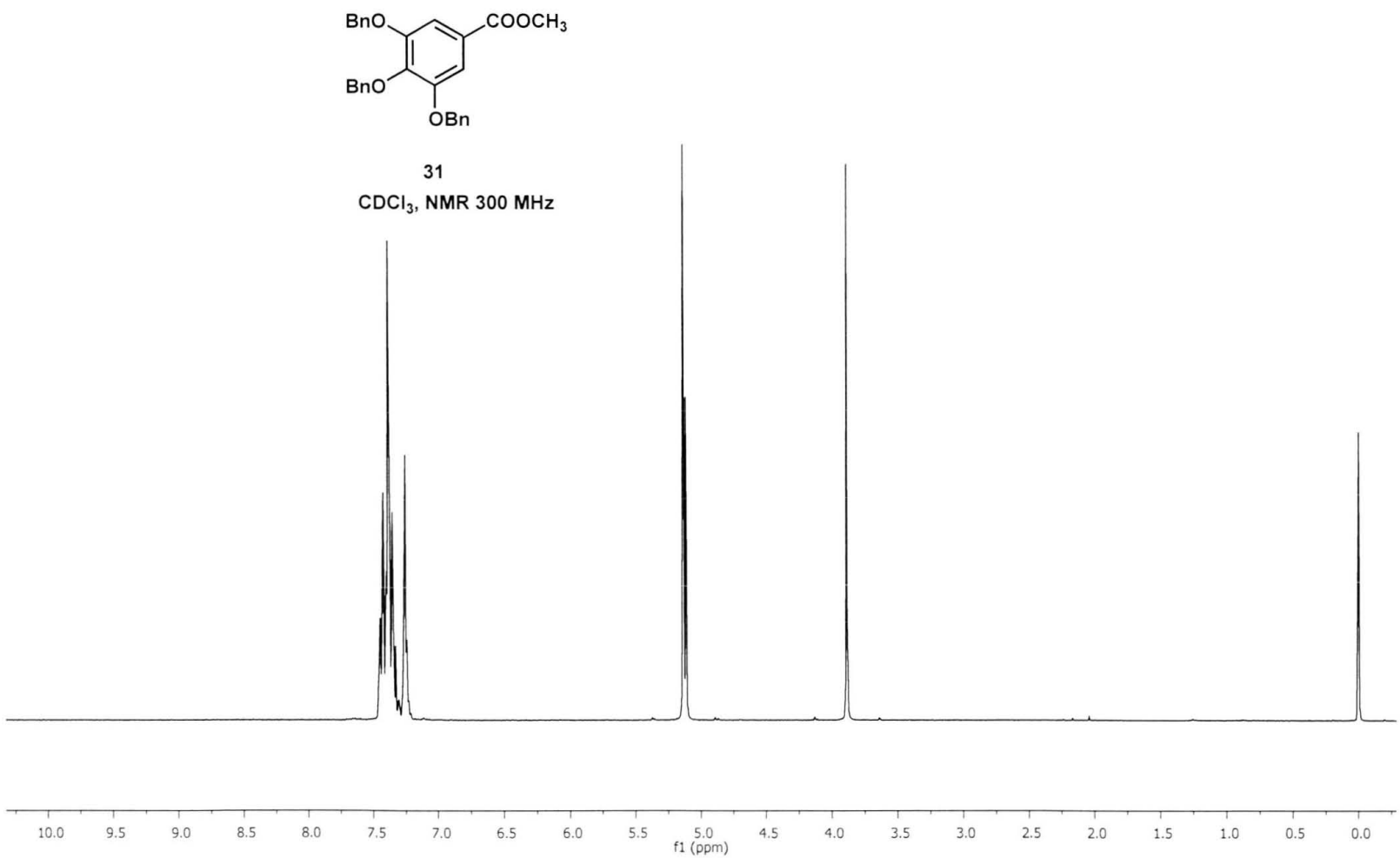
BnO
COOCH3
BnO
OBn
31
CDCl3, NMR 300 MHz
10.0
9.5
9.0
8.5
8.0
7.5
7.0
6.5
6.0
5.5
5.0
4.5
4.0
3.5
3.0
2.5
2.0
1.5
1.0
0.5
0.0
f1 (ppm)

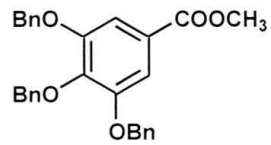

31

$CDCl_3$, NMR 75.46 MHz

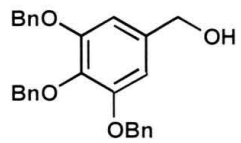

32

$CDCl_3$, NMR 300 MHz

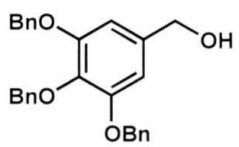

32

$CDCl_3$, NMR 75.46 MHz

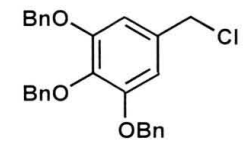

33

$CDCl_3$, NMR 300 MHz

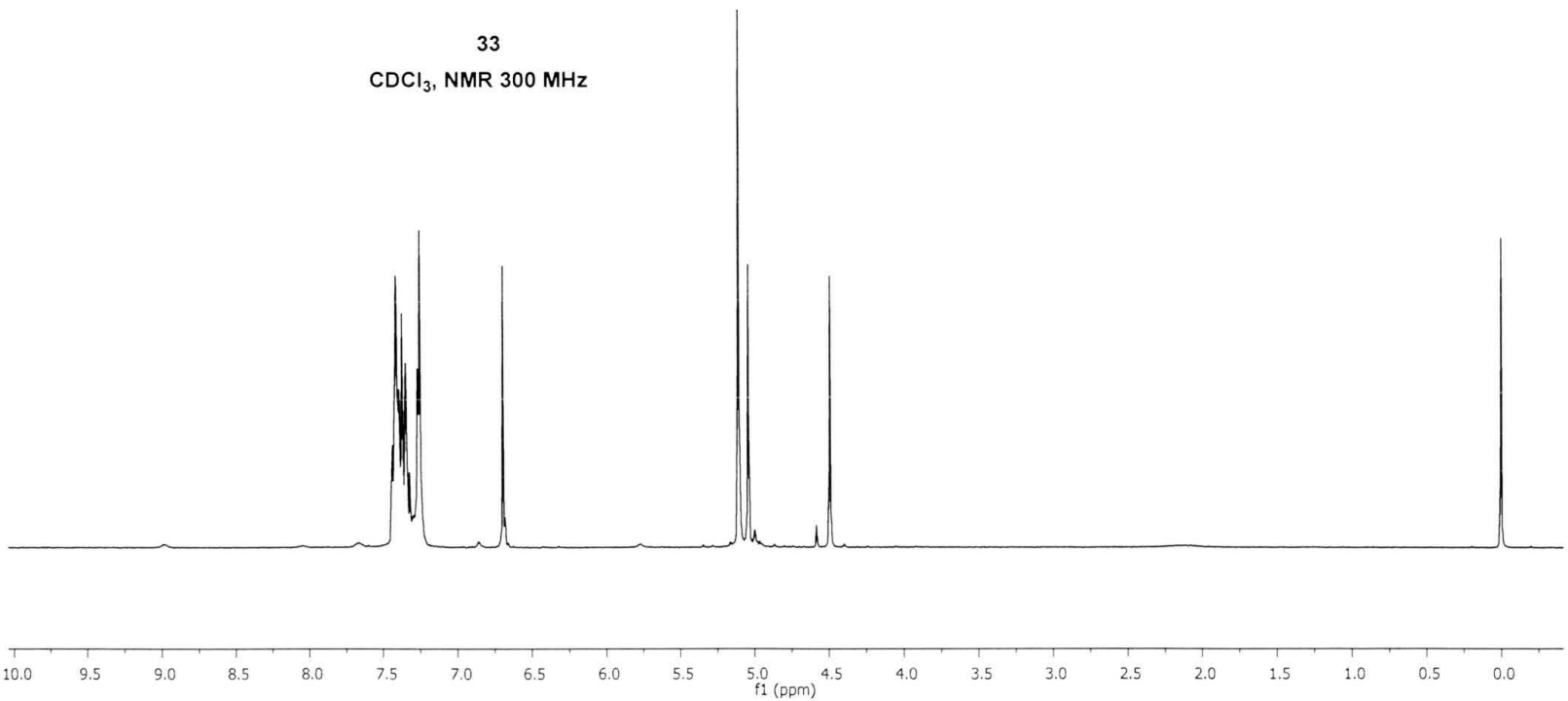

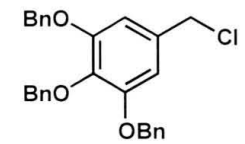

33

$CDCl_3$, NMR 75.46 MHz

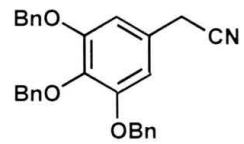

34

$CDCl_3$, NMR 300 MHz

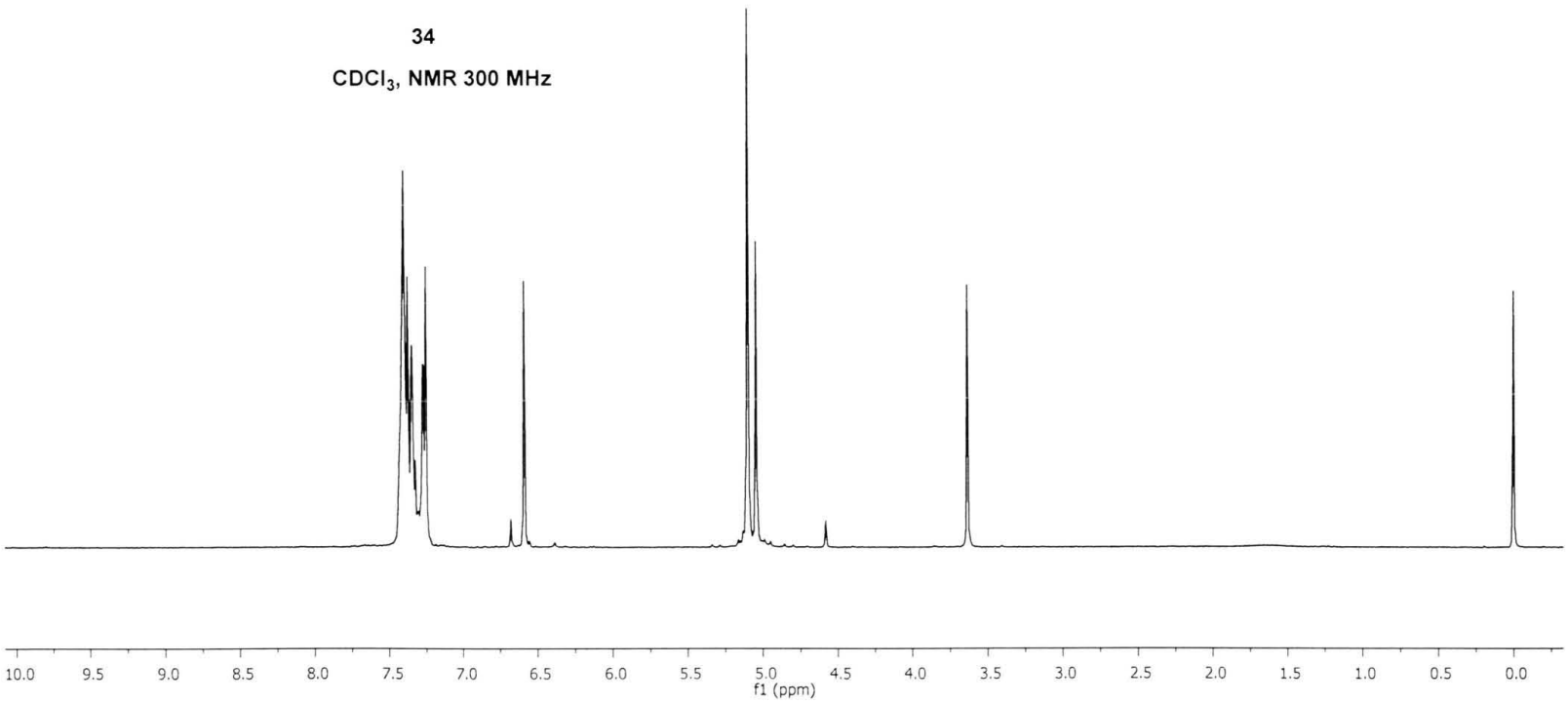

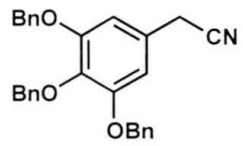

34

$CDCl_3$, NMR 75.46 MHz

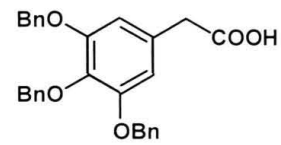

35

$CDCl_3$, NMR 300 MHz

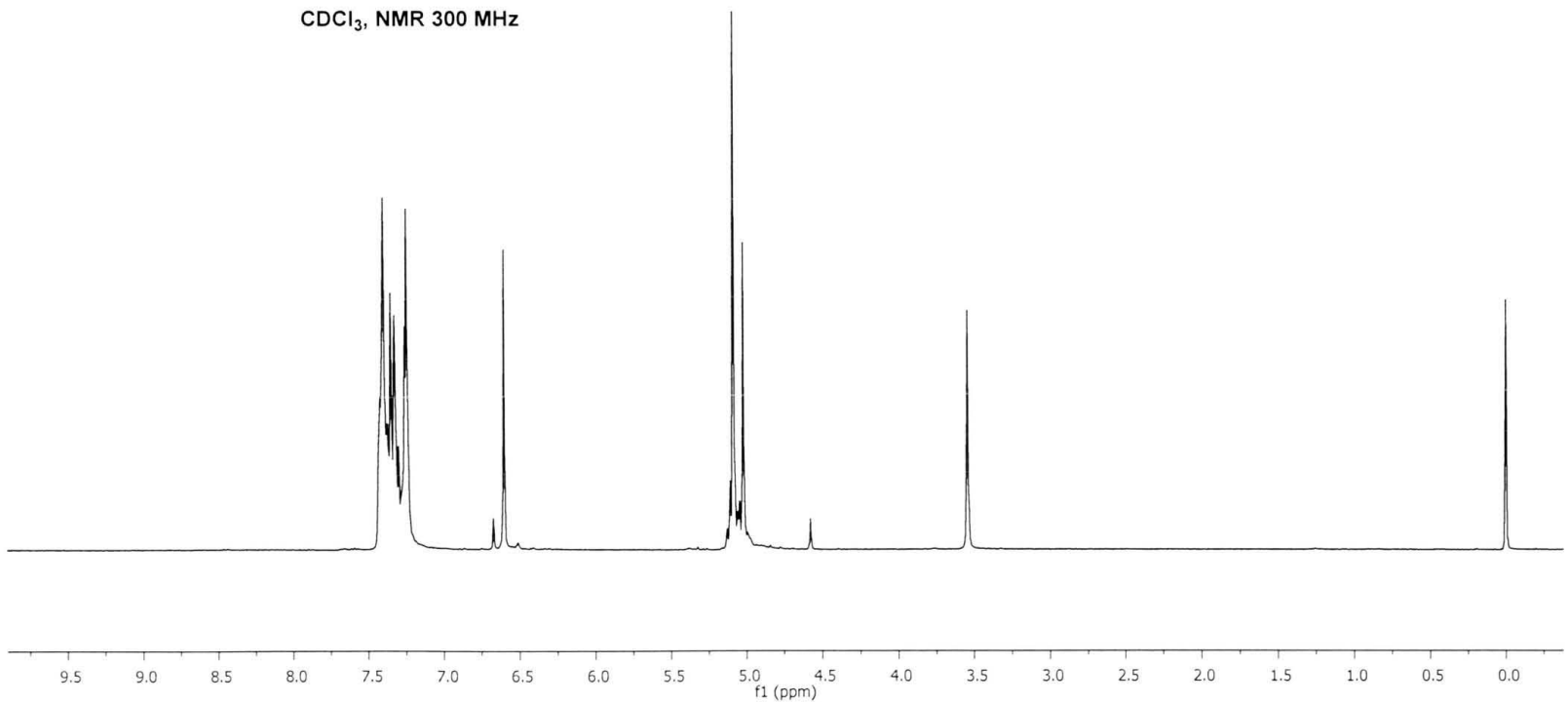

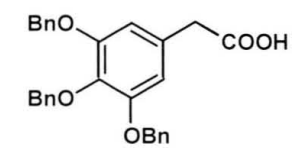

35

$CDCl_3$, NMR 75.46 MHz

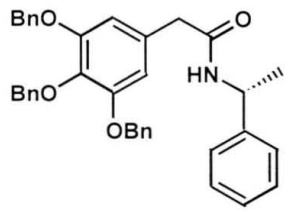

36

$CDCl_3$, NMR 300 MHz

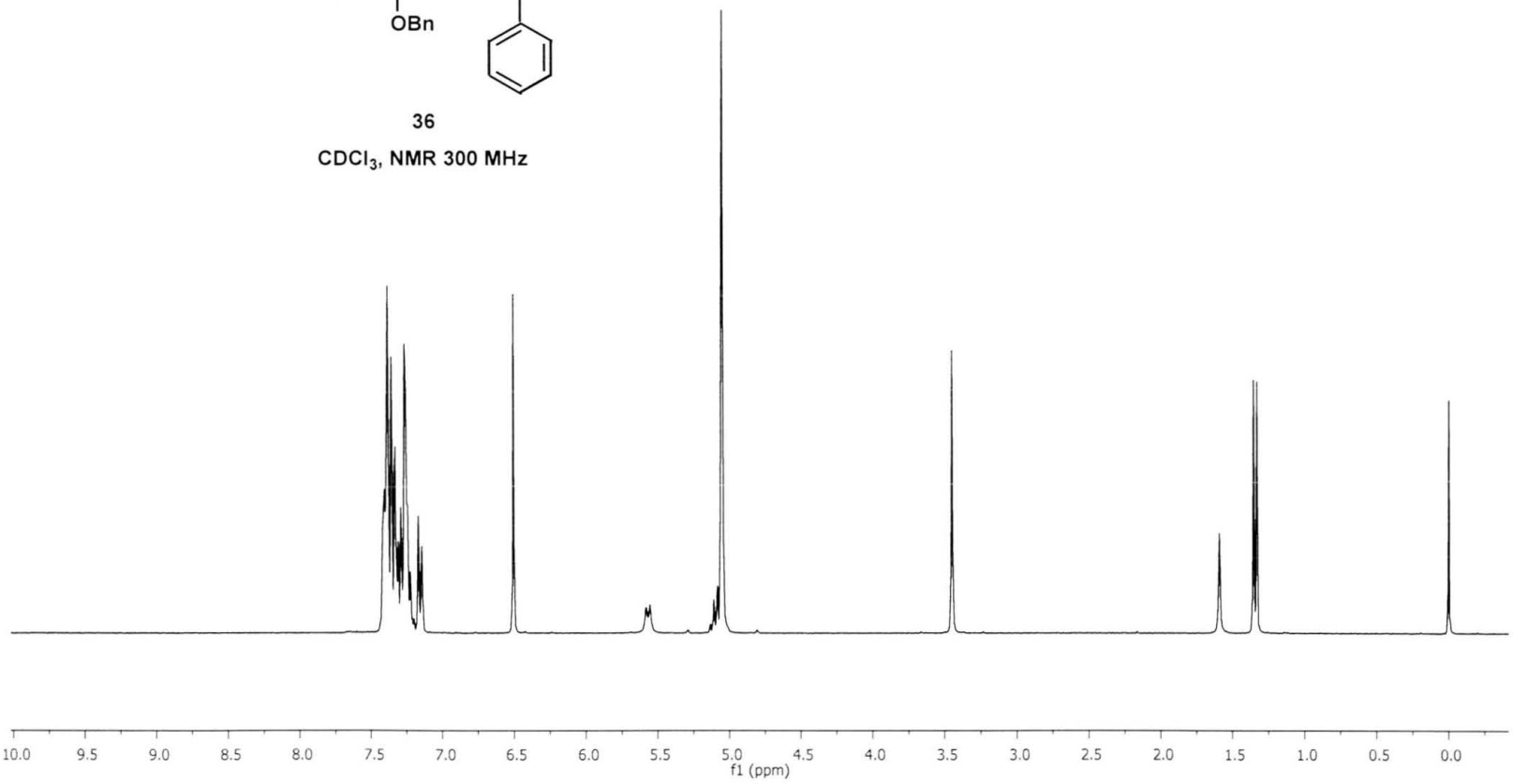

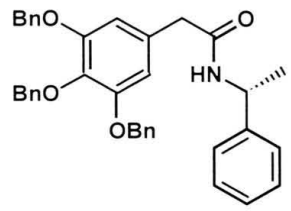

36

$CDCl_3$, NMR 75.46 MHz

2-az-115

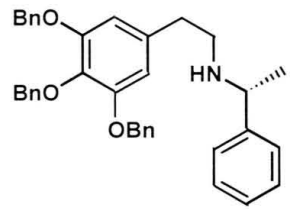

27a

$CDCl_3$, NMR 300 MHz

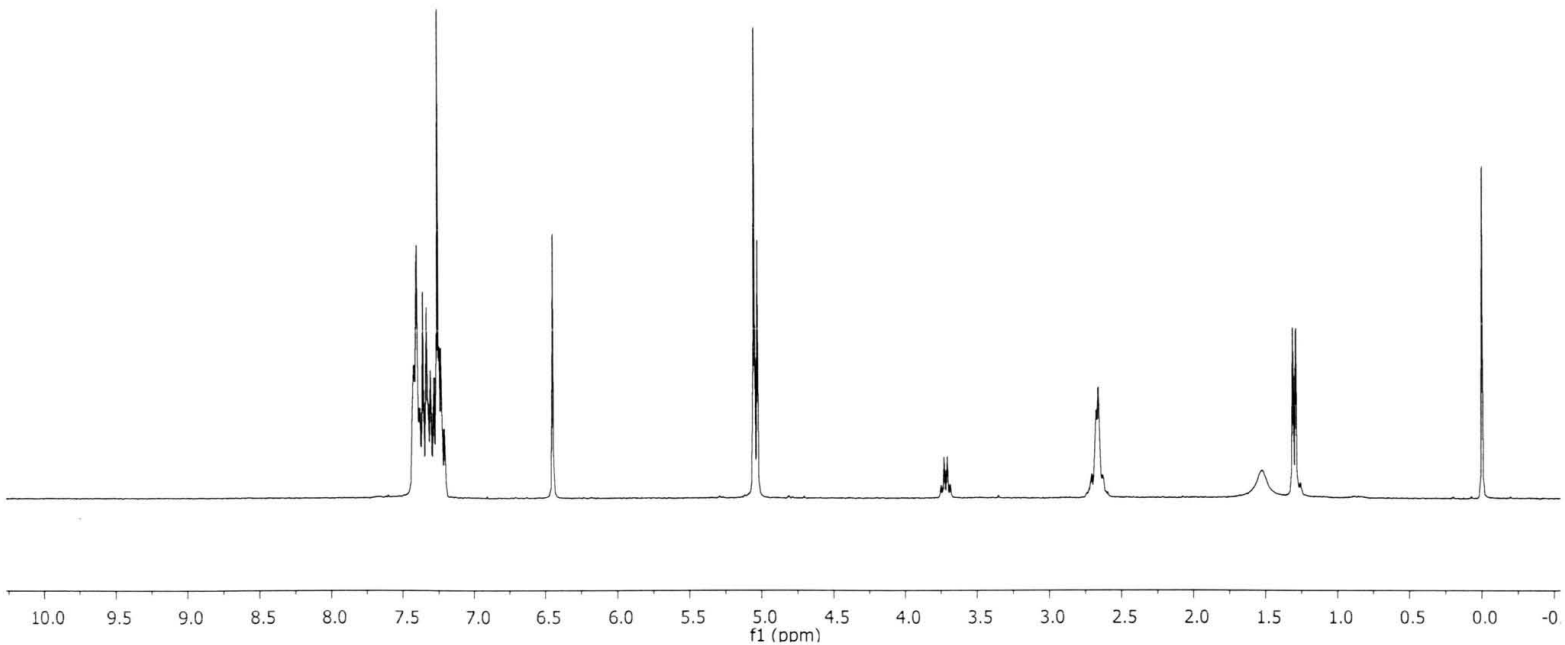

2-az-115-2

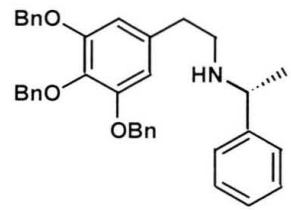

27a

$CDCl_3$, NMR 75.46 MHz

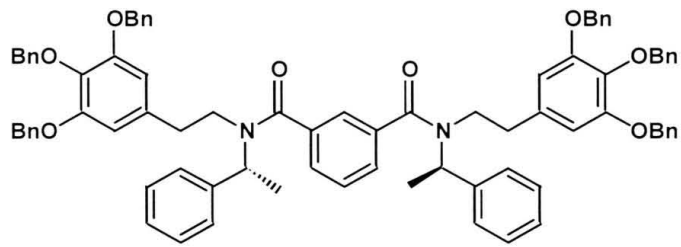

26a

$CDCl_3$, NMR 500 MHz

az3180a/1

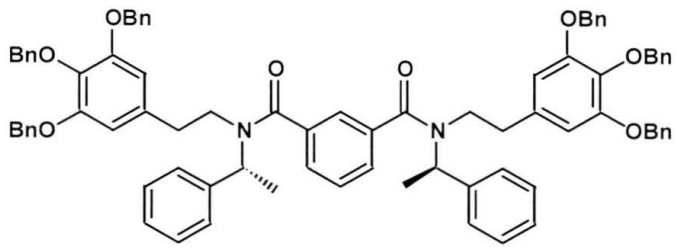

26a

$CDCl_3$, NMR 125.77 MHz

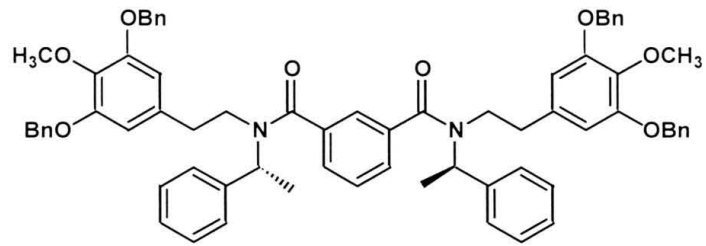

26b

$CDCl_3$, NMR 500 MHz

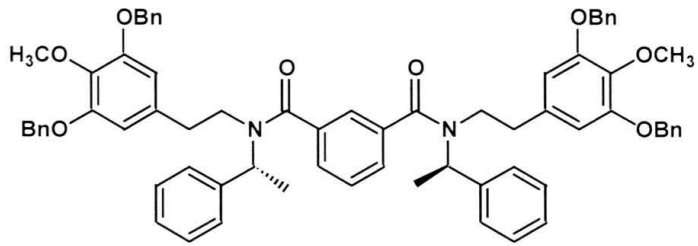

26b

$CDCl_3$, NMR 125.77 MHz

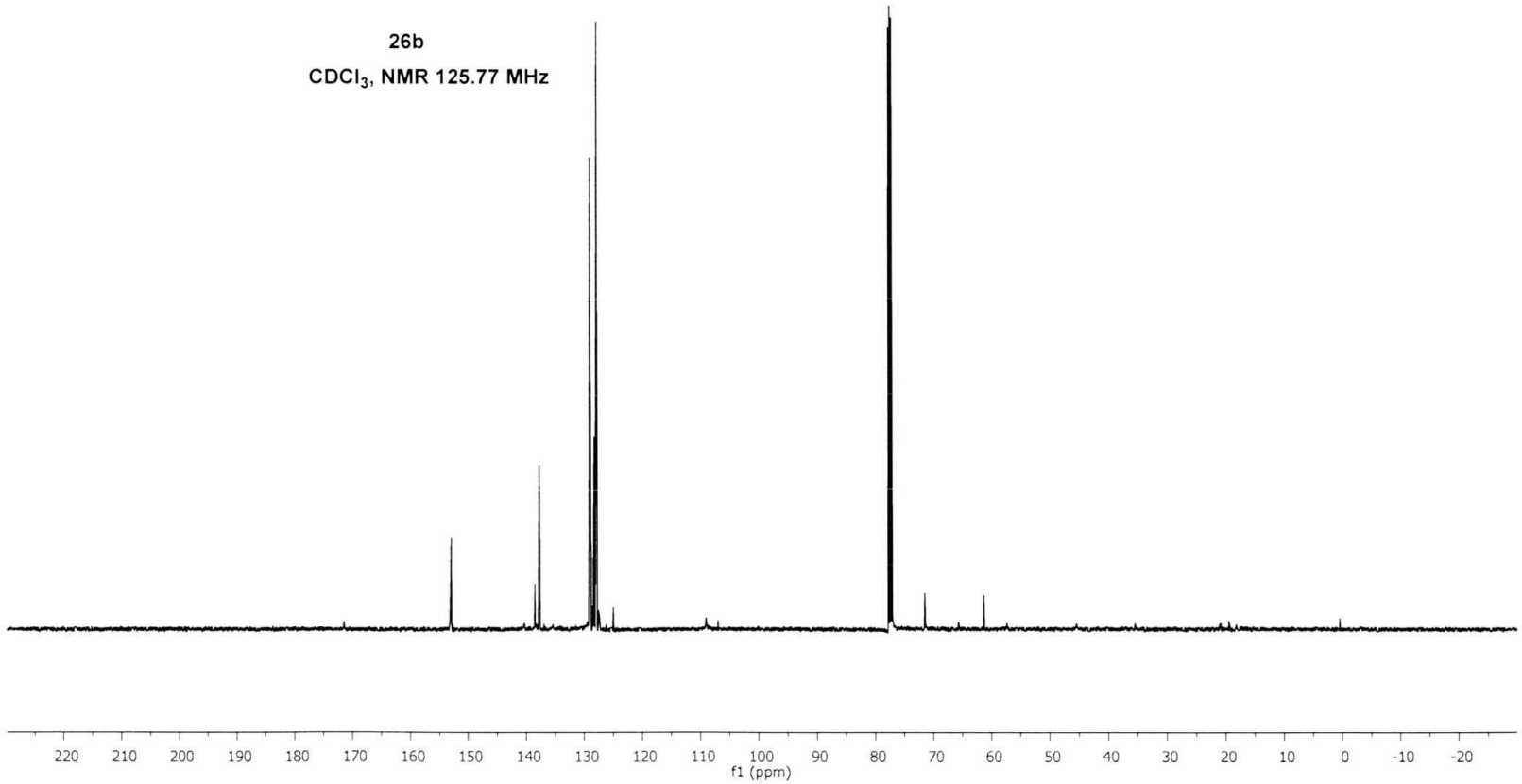

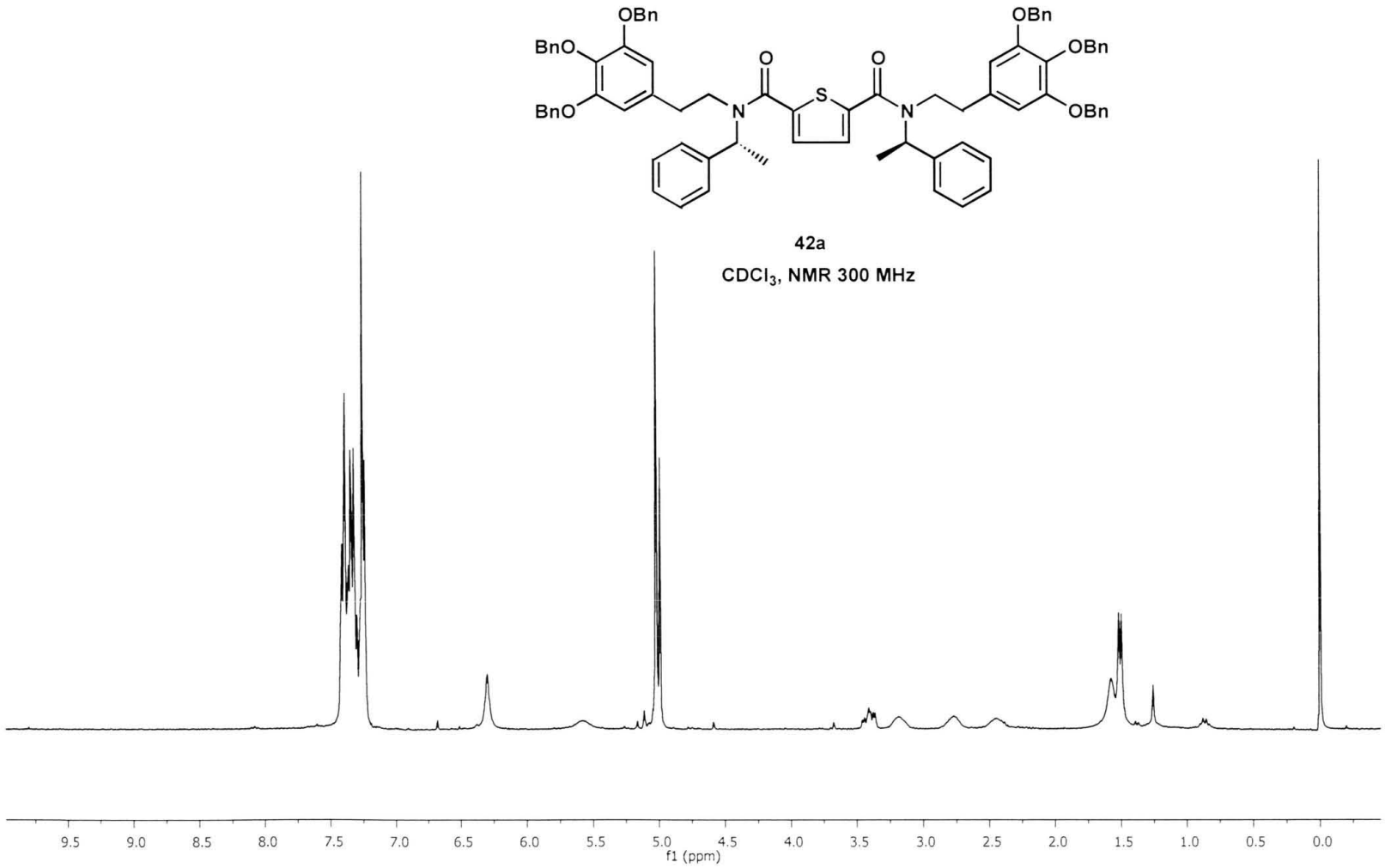
OBn
BnO
BnO
O
O
S
N
N
OBn
OBn
OBn
42a
CDCl3, NMR 300 MHz
9.5
9.0
8.5
8.0
7.5
7.0
6.5
6.0
5.5
5.0
4.5
4.0
3.5
3.0
2.5
2.0
1.5
1.0
0.5
0.0
f1 (ppm)

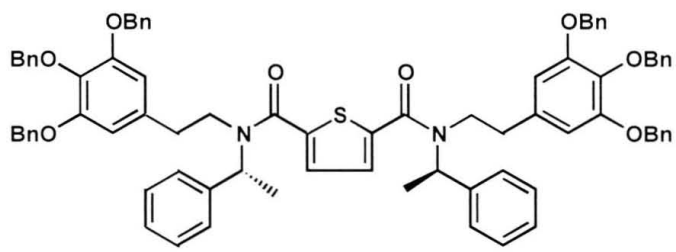

42a

$CDCl_3$, NMR 75.46 MHz

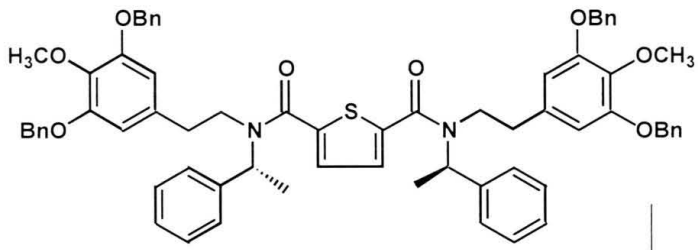

42b

$CDCl_3$, NMR 300 MHz

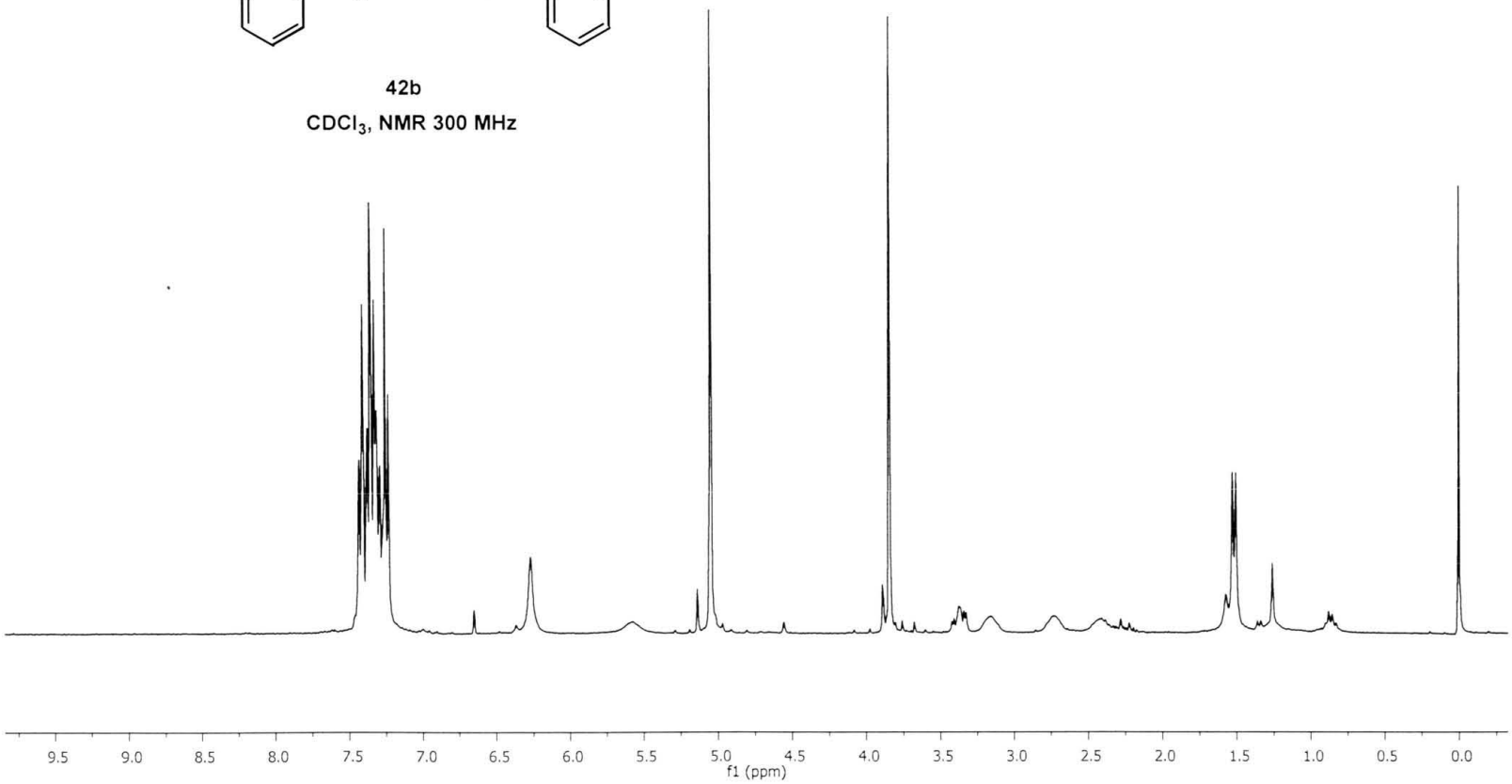

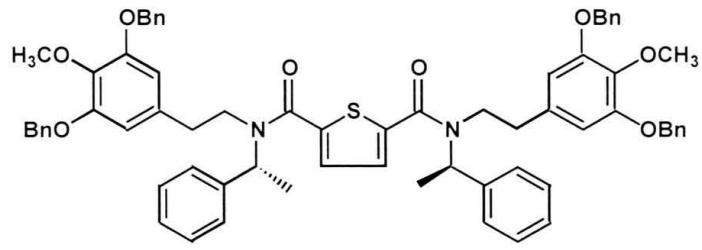

42b

$CDCl_3$, NMR 75.46 MHz

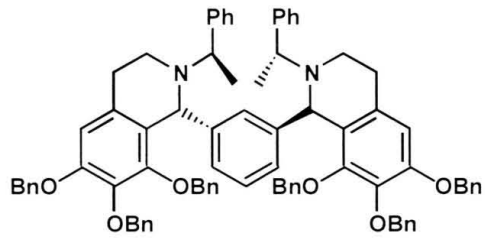

43a

$CDCl_3$, NMR 500 MHz

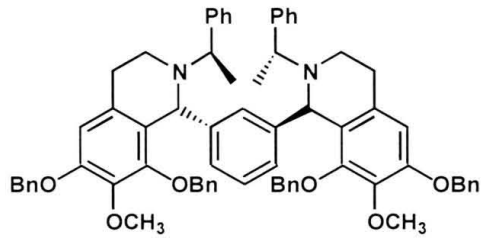

43b

$CDCl_3$, NMR 125.77 MHz

2-az-118

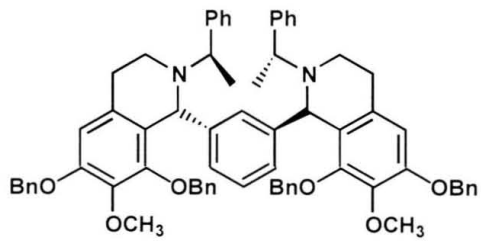

43b

$CDCl_3$, NMR 125.77 MHz

Appendix 1:

X-ray crystallographic data for compound **6a**

(Chapter 2)

Sample: 6a

X-ray Structure Report

for
Dr. P. E. Georghiou

Prepared by

Louise N. Dawe, PhD

Centre for Chemical Analysis, Research and Training (C-CART)
Department of Chemistry
Memorial University of Newfoundland
St. Johns, NL, A1B 3X7
(709) 737-4556 (X-Ray Laboratory)

June 23, 2009

Introduction

Collection, solution and refinement proceeded normally. H (13, 18, 36 and 41) were initially introduced in difference map positions with thermal parameters fixed at 1.2 times that of their bonding partners, and were refined on (x,y,z). In the final round of least square analysis they were refined on the riding model. All other hydrogen atoms were introduced in calculated positions with isotropic thermal parameters set twenty percent greater than those of their bonding partners. They were refined on the riding model. All other atoms were refined anisotropically.

Platon's ADDSYM detects a (pseudo) centre of symmetry, however, this is a chiral molecule and is therefore incompatible with an inversion centre. Solution in the ADDSYM suggested possible pseudo/new space-group did not yield a result that could be refined. The two molecules contained in the asymmetric unit have angles between ring planes that differ by approximately 10 degrees.

Friedel mates were not collected, consequently, the Flack x parameter value deviates from zero. The Friedel pairs that were inadvertently collected were not merged since the chirality of the molecule was confirmed by other methods (synthetic, spectroscopic and by structural comparison to the enantiomer.)

Acknowledgement for Julie L. Collins for data collection.

Experimental

Data Collection

A colorless block crystal of $C_{19}H_{23}NO_4$ having approximate dimensions of 0.15 x 0.12 x 0.10 mm was mounted on a low temperature diffraction loop. All measurements were made on a Rigaku Saturn CCD area detector equipped with a Rigaku SHINE optic, and Mo-Kα radiation.

Indexing was performed from 300 images that were exposed for 15 seconds. The crystal-to-detector distance was 40.06 mm.

Cell constants and an orientation matrix for data collection corresponded to a primitive monoclinic cell with dimensions:

a = 8.364(3) Å
b = 10.005(4) Å β = 93.282(8)^o
c = 20.210(9) Å
V = 1688.5(12) Å^3

For Z = 4 and F.W. = 329.39, the calculated density is 1.296 g/cm^3. Based on the systematic absences of:

0k0: k ± 2n

packing considerations, a statistical analysis of intensity distribution, and the successful solution and refinement of the structure, the space group was determined to be:

$P2_1$ (#4)

The data were collected at a temperature of -150 ± 1^{o}C to a maximum 2θ value of 61.8^o. A total of 762 oscillation images were collected. A sweep of data was done using ω scans from -75.0 to 75.0^o in 0.5^o step, at χ=45.0^o and ϕ = 0.0^o. The exposure rate was 30.0 [sec./^{o}]. The detector swing angle was 14.93^o. A second sweep was performed using ω scans from -42.0 to 99.0^o in 0.5^o step, at χ=45.0^o and ϕ = 90.0^o. The exposure rate was 30.0 [sec./^{o}]. The detector swing angle was 14.93^o. Another sweep was performed using ω scans from -75.0 to 15.0^o in 0.5^o step, at χ=45.0^o and ϕ = 180.0^o. The exposure rate was

30.0 [sec./^{o}]. The detector swing angle was 14.93^{o}. The crystal-to-detector distance was 40.06 mm. Readout was performed in the 0.137 mm pixel mode.

Data Reduction

Of the 16029 reflections that were collected, 6949 were unique (R_{int} = 0.0370); equivalent reflections were merged. Data were collected and processed using CrystalClear (Rigaku). Net intensities and sigmas were derived as follows:

$$F^2 = [\Sigma(P_i - mB_{ave})] \cdot Lp^{-1}$$

where P_i is the value in counts of the i^{th} pixel
m is the number of pixels in the integration area
B_{ave} is the background average
Lp is the Lorentz and polarization factor

$$B_{ave} = \Sigma(B_j)/n$$

where n is the number of pixels in the background area
B_j is the value of the j^{th} pixel in counts

$$\sigma^2(F^2_{hkl}) = [(\Sigma P_i) + m((\Sigma(B_{ave} - B_j)^2)/(n-1))] \cdot Lp \cdot errmul + (erradd \cdot F^2)^2$$

where erradd = 0.00
errmul = 1.00

The linear absorption coefficient, μ, for Mo-Kα radiation is 0.905 cm^{-1}. A numerical absorption correction was applied which resulted in transmission factors ranging from 0.9893 to 0.9956. The data were corrected for Lorentz and polarization effects.

Structure Solution and Refinement

The structure was solved by direct methods[2] and expanded using Fourier techniques[3]. The non-hydrogen atoms were refined anisotropically. Hydrogen atoms were refined using the riding model. The final cycle of full-matrix least-squares refinement[4] on F^2 was based on 6949 observed reflections and 434 variable parameters and converged (largest parameter shift was 0.00 times its

esd) with unweighted and weighted agreement factors of:

$$R1 = \Sigma \; ||Fo| - |Fc|| \; / \; \Sigma \; |Fo| = 0.0669$$

$$wR2 = [\; \Sigma \; (\; w \; (Fo^2 - Fc^2)^2 \;) / \; \Sigma \; w(Fo^2)^2]^{1/2} = 0.1671$$

The standard deviation of an observation of unit weight[5] was 1.07. Unit weights were used. The maximum and minimum peaks on the final difference Fourier map corresponded to 0.37 and -0.28 $e^-/Å^3$, respectively.

Neutral atom scattering factors were taken from Cromer and Waber[6]. Anomalous dispersion effects were included in Fcalc[7]; the values for $\Delta f'$ and $\Delta f''$ were those of Creagh and McAuley[8]. The values for the mass attenuation coefficients are those of Creagh and Hubbell[9]. All calculations were performed using the CrystalStructure[10,11] crystallographic software package except for refinement, which was performed using SHELXL-97[12].

References

(1) CrystalClear: Rigaku Corporation, 1999. CrystalClear Software User's Guide, Molecular Structure Corporation, (c) 2000.J.W.Pflugrath (1999) Acta Cryst. D55, 1718-1725.

(2) SHELX97: Sheldrick, G.M. (1997).

(3) DIRDIF99: Beurskens, P.T., Admiraal, G., Beurskens, G., Bosman, W.P., de Gelder, R., Israel, R. and Smits, J.M.M.(1999). The DIRDIF-99 program system, Technical Report of the Crystallography Laboratory, University of Nijmegen, The Netherlands.

(4) Least Squares function minimized: (SHELXL97)

$\Sigma w(F_o^2-F_c^2)^2$ where w = Least Squares weights.

(5) Standard deviation of an observation of unit weight:

$[\Sigma w(F_o^2-F_c^2)^2/(N_o-N_v)]^{1/2}$

where: N_o = number of observations

N_v = number of variables

(6) Cromer, D. T. & Waber, J. T.; "International Tables for X-ray Crystallography", Vol. IV, The Kynoch Press, Birmingham, England, Table 2.2 A (1974).

(7) Ibers, J. A. & Hamilton, W. C.; Acta Crystallogr., 17, 781 (1964).

(8) Creagh, D. C. & McAuley, W.J .; "International Tables for Crystallography", Vol C, (A.J.C. Wilson, ed.), Kluwer Academic Publishers, Boston, Table 4.2.6.8, pages 219-222 (1992).

(9) Creagh, D. C. & Hubbell, J.H..; "International Tables for Crystallography", Vol C, (A.J.C. Wilson, ed.), Kluwer Academic Publishers, Boston, Table 4.2.4.3, pages 200-206 (1992).

(10) CrystalStructure 3.7.0: Crystal Structure Analysis Package, Rigaku and Rigaku/MSC (2000-2005). 9009 New Trails Dr. The Woodlands TX 77381 USA.

(11) CRYSTALS Issue 10: Watkin, D.J., Prout, C.K. Carruthers, J.R. & Betteridge, P.W. Chemical Crystallography Laboratory, Oxford, UK. (1996)

(12) SHELX97: Sheldrick, G.M. (1997).

EXPERIMENTAL DETAILS

A. Crystal Data

Empirical Formula	$C_{19}H_{23}NO_4$
Formula Weight	329.39
Crystal Color, Habit	colorless, block
Crystal Dimensions	0.15 X 0.12 X 0.10 mm
Crystal System	monoclinic
Lattice Type	Primitive
Detector Position	40.06 mm
Pixel Size	0.137 mm

Lattice Parameters	a = 8.364(3) Å b = 10.005(4) Å c = 20.210(9) Å β = 93.282(8) ^{o} V = 1688.5(12) Å^{3}
Space Group	$P2_1$ (#4)
Z value	4
D_{calc}	1.296 g/cm^{3}
F_{000}	704
μ(MoKα)	0.90 cm^{-1}

B. Intensity Measurements

Detector Goniometer	Rigaku Saturn Rigaku AFC8
Radiation	MoKα (λ = 0.71075 Å) Rigaku SHINE
Detector Aperture	70 mm x 70 mm
Data Images	762 exposures
ω oscillation Range (χ=45.0, ϕ=0.0)	-75.0 - 75.0^{o}
Exposure Rate	30.0 sec./^{o}
Detector Swing Angle	14.93^{o}
ω oscillation Range (χ=45.0, ϕ=90.0)	-42.0 - 99.0^{o}
Exposure Rate	30.0 sec./^{o}
Detector Swing Angle	14.93^{o}

ω oscillation Range (χ=45.0, ϕ=180.0)	-75.0 - 15.0°
Exposure Rate	30.0 sec./°
Detector Swing Angle	14.93°
Detector Position	40.06 mm
Pixel Size	0.137 mm
$2\theta_{max}$	61.8°
No. of Reflections Measured	Total: 16029 Unique: 6949 (R_{int} = 0.0370) I>2σ(I): 6063
Corrections	Lorentz-polarization (trans. factors: 0.9893 - 0.9956)

C. Structure Solution and Refinement

Structure Solution	Direct Methods (SHELX97)
Refinement	Full-matrix least-squares on F^2
Function Minimized	Σ w $(Fo^2 - Fc^2)^2$
Least Squares Weights	w = 1/ [$\sigma^2(Fo^2)$ + $(0.0725 \cdot P)^2$ + 0.8581 · P] where P = $(Max(Fo^2,0) + 2Fc^2)/3$
$2\theta_{max}$ cutoff	53.0°
Anomalous Dispersion	All non-hydrogen atoms
No. Observations (All reflections)	6949
No. Variables	434

Reflection/Parameter Ratio	16.01
Residuals: R1 (I>2.00σ(I))	0.0669
Residuals: R (All reflections)	0.0768
Residuals: wR2 (All reflections)	0.1671
Goodness of Fit Indicator	1.070
Max Shift/Error in Final Cycle	0.000
Maximum peak in Final Diff. Map	0.37 $e^-/Å^3$
Minimum peak in Final Diff. Map	-0.28 $e^-/Å^3$

Appendix 2:

X-ray crystallographic data for compound **6b**

(Chapter 2)

Sample: 6b

X-ray Structure Report

for
Dr. P. E. Georghiou

Prepared by

Louise N. Dawe, PhD

Centre for Chemical Analysis, Research and Training (C-CART)
Department of Chemistry
Memorial University of Newfoundland
St. Johns, NL, A1B 3X7
(709) 737-4556 (X-Ray Laboratory)

June 23, 2009

Introduction

Collection, solution and refinement proceeded normally. Friedel mates were collected in order to confirm absolute structure configuration. H (13 and 18) were initially introduced in difference map positions with thermal parameters fixed at 1.2 times that of their bonding partners, and were refined on (x,y,z). In the final round of least square analysis they were refined on the riding model. All other hydrogen atoms were introduced in calculated positions with isotropic thermal parameters set twenty percent greater than those of their bonding partners. They were refined on the riding model. All other atoms were refined anisotropically.

Experimental

Data Collection

A colorless prism crystal of $C_{25}H_{29}NO_4$ having approximate dimensions of 0.20 x 0.17 x 0.09 mm was mounted on a low-temperature diffraction loop. All measurements were made on a Rigaku Saturn CCD area detector equipped with a SHINE optic and Mo-Kα radiation.

Indexing was performed from 360 images that were exposed for 25

seconds. The crystal-to-detector distance was 40.10 mm.

Cell constants and an orientation matrix for data collection corresponded to a primitive orthorhombic cell with dimensions:

a = 8.389(2) Å
b = 9.881(3) Å
c = 26.420(7) Å
V = 2190.0(11) $Å^3$

For Z = 4 and F.W. = 407.51, the calculated density is 1.236 g/cm^3. The systematic absences of:

h00: h ± 2n
0k0: k ± 2n
00l: l ± 2n

uniquely determine the space group to be:

$P2_12_12_1$ (#19)

The data were collected at a temperature of -145 ± 1°C to a maximum 2θ value of 61.6°. A total of 1080 oscillation images were collected. A sweep of data was done using ω scans from -75.0 to 105.0° in 0.5° step, at χ=45.0° and φ = 180.0°. The exposure rate was 50.0 [sec./°]. The detector swing angle was 15.09°. A second sweep was performed using ω scans from -75.0 to 105.0° in 0.5° step, at χ=45.0° and φ = 0.0°. The exposure rate was 50.0 [sec./°]. The detector swing angle was 15.09°. Another sweep was performed using ω scans from -75.0 to 105.0° in 0.5° step, at χ=0.0° and φ = 0.0°. The exposure rate was 50.0 [sec./°]. The detector swing angle was 15.09°. The crystal-to-detector distance was 40.10 mm. Readout was performed in the 0.137 mm pixel mode.

Data Reduction

Of the 28739 reflections that were collected, 4545 were unique (R_{int} = 0.0394); equivalent reflections were merged. Data were collected and processed using CrystalClear (Rigaku). Net intensities and sigmas were derived as follows:

$$F^2 = [\Sigma(P_i - mB_{ave})] \cdot Lp^{-1}$$

where P_i is the value in counts of the i^{th} pixel
m is the number of pixels in the integration area
B_{ave} is the background average
Lp is the Lorentz and polarization factor

$$B_{ave} = \Sigma(B_j)/n$$

where n is the number of pixels in the background area
B_j is the value of the j^{th} pixel in counts

$$\sigma^2(F^2_{hkl}) = [(\Sigma P_i) + m((\Sigma(B_{ave} - B_j)^2)/(n-1))] \cdot Lp \cdot errmul + (erradd \cdot F^2)^2$$

where erradd = 0.00
errmul = 1.00

The linear absorption coefficient, μ, for Mo-Kα radiation is 0.83 cm^{-1}. A numerical absorption correction was applied which resulted in transmission factors ranging from 0.9883 to 0.9942. The data were corrected for Lorentz and polarization effects.

Structure Solution and Refinement

The structure was solved by direct methods[2] and expanded using Fourier techniques[3]. The non-hydrogen atoms were refined anisotropically. Hydrogen atoms were refined using the riding model. The final cycle of full-matrix least-squares refinement[4] on F^2 was based on 4545 observed reflections and 272 variable parameters and converged (largest parameter shift was 0.00 times its esd) with unweighted and weighted agreement factors of:

$$R1 = \Sigma \, ||Fo| - |Fc|| \, / \, \Sigma \, |Fo| = 0.0486$$

$$wR2 = [\Sigma \, (w \, (Fo^2 - Fc^2)^2) / \Sigma \, w(Fo^2)^2]^{1/2} = 0.1194$$

The standard deviation of an observation of unit weight[5] was 1.09. Unit weights were used. The maximum and minimum peaks on the final difference Fourier map corresponded to 0.14 and -0.21 $e^-/Å^3$, respectively.

Neutral atom scattering factors were taken from Cromer and Waber[6]. Anomalous dispersion effects were included in Fcalc[7]; the values for $\Delta f'$ and $\Delta f''$ were those of Creagh and McAuley[8]. The values for the mass attenuation coefficients are those of Creagh and Hubbell[9]. All calculations were performed using the CrystalStructure[10,11] crystallographic software package except for refinement, which was performed using SHELXL-97[12].

References

(1) CrystalClear: Rigaku Corporation, 1999. CrystalClear Software User's Guide, Molecular Structure Corporation, (c) 2000.J.W.Pflugrath (1999) Acta Cryst. D55, 1718-1725.

(2) SHELX97: Sheldrick, G.M. (1997).

(3) DIRDIF99: Beurskens, P.T., Admiraal, G., Beurskens, G., Bosman, W.P., de Gelder, R., Israel, R. and Smits, J.M.M.(1999). The DIRDIF-99 program system, Technical Report of the Crystallography Laboratory, University of Nijmegen, The Netherlands.

(4) Least Squares function minimized: (SHELXL97)

$\Sigma w(F_o^2-F_c^2)^2$ where w = Least Squares weights.

(5) Standard deviation of an observation of unit weight:

$[\Sigma w(F_o^2-F_c^2)^2/(N_o-N_v)]^{1/2}$

where: N_o = number of observations

N_v = number of variables

(6) Cromer, D. T. & Waber, J. T.; "International Tables for X-ray Crystallography", Vol. IV, The Kynoch Press, Birmingham, England, Table 2.2 A (1974).

(7) Ibers, J. A. & Hamilton, W. C.; Acta Crystallogr., 17, 781 (1964).

(8) Creagh, D. C. & McAuley, W.J .; "International Tables for Crystallography", Vol C, (A.J.C. Wilson, ed.), Kluwer Academic Publishers, Boston, Table 4.2.6.8, pages 219-222 (1992).

(9) Creagh, D. C. & Hubbell, J.H..; "International Tables for Crystallography", Vol C, (A.J.C. Wilson, ed.), Kluwer Academic Publishers, Boston, Table 4.2.4.3, pages 200-206 (1992).

(10) CrystalStructure 3.7.0: Crystal Structure Analysis Package, Rigaku and Rigaku/MSC (2000-2005). 9009 New Trails Dr. The Woodlands TX 77381 USA.

(11) CRYSTALS Issue 10: Watkin, D.J., Prout, C.K. Carruthers, J.R. & Betteridge, P.W. Chemical Crystallography Laboratory, Oxford, UK. (1996)

(12) SHELX97: Sheldrick, G.M. (1997).

EXPERIMENTAL DETAILS

A. Crystal Data

Empirical Formula	$C_{25}H_{29}NO_4$
Formula Weight	407.51
Crystal Color, Habit	colorless, prism
Crystal Dimensions	0.20 X 0.17 X 0.09 mm
Crystal System	orthorhombic
Lattice Type	Primitive
Detector Position	40.10 mm
Pixel Size	0.137 mm
Lattice Parameters	a = 8.389(2) Å b = 9.881(3) Å c = 26.420(7) Å V = 2190.0(11) Å^3
Space Group	$P2_12_12_1$ (#19)
Z value	4
D_{calc}	1.236 g/cm^3
F_{000}	872
μ(MoKα)	0.83 cm^{-1}

B. Intensity Measurements

Detector	Rigaku Saturn
Goniometer	Rigaku AFC8

Radiation	MoKα (λ = 0.71075 Å) Rigaku SHINE
Detector Aperture	70 mm x 70 mm
Data Images	1080 exposures
ω oscillation Range (χ=45.0, ϕ=180.0)	-75.0 - 105.0^{o}
Exposure Rate	50.0 sec./^{o}
Detector Swing Angle	15.09^{o}
ω oscillation Range (χ=45.0, ϕ=0.0)	-75.0 - 105.0^{o}
Exposure Rate	50.0 sec./^{o}
Detector Swing Angle	15.09^{o}
ω oscillation Range (χ=0.0, ϕ=0.0)	-75.0 - 105.0^{o}
Exposure Rate	50.0 sec./^{o}
Detector Swing Angle	15.09^{o}
Detector Position	40.10 mm
Pixel Size	0.137 mm
$2\theta_{max}$	61.6^{o}
No. of Reflections Measured	Total: 28739 Unique: 4545 (R_{int} = 0.0394) I>2σ(I): 4430
Corrections	Lorentz-polarization (trans. factors: 0.9883 - 0.9942)

C. Structure Solution and Refinement

Structure Solution	Direct Methods (SHELX97)
Refinement	Full-matrix least-squares on F^2
Function Minimized	$\Sigma\, w\,(Fo^2 - Fc^2)^2$
Least Squares Weights	$w = 1/[\,\sigma^2(Fo^2) + (0.0570 \cdot P)^2 + 0.5111 \cdot P\,]$ where $P = (Max(Fo^2,0) + 2Fc^2)/3$
$2\theta_{max}$ cutoff	53.0^o
Anomalous Dispersion	All non-hydrogen atoms
No. Observations (All reflections)	4545
No. Variables	272
Reflection/Parameter Ratio	16.71
Residuals: R1 ($I>2.00\sigma(I)$)	0.0486
Residuals: R (All reflections)	0.0500
Residuals: wR2 (All reflections)	0.1194
Goodness of Fit Indicator	1.090
Max Shift/Error in Final Cycle	0.001
Maximum peak in Final Diff. Map	0.14 $e^-/Å^3$
Minimum peak in Final Diff. Map	-0.21 $e^-/Å^3$

Appendix 3:

X-ray crystallographic data for compound **34**

(Chapter 2)

Sample: 34

X-ray Structure Report

for
Dr. P. E. Georghiou

Prepared by

Louise N. Dawe, PhD

Centre for Chemical Analysis, Research and Training (C-CART)
Department of Chemistry
Memorial University of Newfoundland
St. Johns, NL, A1B 3X7
(709) 737-4556 (X-Ray Laboratory)

May 12, 2010

Introduction

A report was previously prepared for this data, however, up journal submission and crystallographic review, further examination of the reported Flack parameter was requested. This report reflects that evaluation.

Collection, solution and refinement proceeded normally. Friedel mates were collected in order to confirm absolute structure configuration, however, the compound was still a weak anomalous scatterer, and the Flack parameter has a large associated estimated standard deviation, making it essentially meaningless. Unfortunately, using "FCF-Validate (Bijvoet)" (the latest version of Platon via WingGX) returned the result "Low Friedel Pair Coverage: No Hooft y Parameter Calculated". Friedel mates were not averaged however, because the enantiomer was assigned by reference to an unchanging chiral centre in the synthetic procedure.

H(17) was introduced in its difference map position with its thermal parameters fixed at 1.2 times that of O(3), and was refined on (x,y,z). All other hydrogen atoms were introduced in calculated positions with isotropic thermal parameters set twenty percent greater than those of their bonding partners. They were refined on the riding model. All non-hydrogen atoms were refined anisotropically.

Experimental

Data Collection

A colorless prism crystal of $C_{20}H_{23}NO_4$ having approximate dimensions of 0.30 x 0.22 x 0.17 mm was mounted on a low temperature diffraction loop. All measurements were made on a Rigaku Saturn CCD area detector equipped with a SHINE optic and Mo-Kα radiation.

Indexing was performed from 360 images that were exposed for 7 seconds. The crystal-to-detector distance was 50.17 mm.

Cell constants and an orientation matrix for data collection corresponded to a primitive orthorhombic cell with dimensions:

a = 7.2621(12) Å
b = 8.0445(13) Å
c = 28.318(5) Å
V = 1654.3(5) Å^3

For Z = 4 and F.W. = 341.41, the calculated density is 1.371 g/cm^3. The systematic absences of:

h00: h ± 2n
0k0: k ± 2n
00l: l ± 2n

uniquely determine the space group to be:

$P2_12_12_1$ (#19)

The data were collected at a temperature of -120 ± 1°C to a maximum 2θ value of 59.4°. A total of 1440 oscillation images were collected. A sweep of data was done using ω scans from -70.0 to 110.0° in 0.5° step, at χ=45.0° and ϕ = 90.0°. The exposure rate was 14.0 [sec./°]. The detector swing angle was 20.06°. A second sweep was performed using ω scans from -70.0 to 110.0° in 0.5° step, at χ=45.0° and ϕ = 0.0°. The exposure rate was 14.0 [sec./°]. The detector swing angle was 20.06°. Another sweep was performed using ω scans from -70.0 to 110.0° in 0.5° step, at χ=0.0° and ϕ = 0.0°. The exposure rate was 14.0 [sec./°]. The detector swing angle was 20.06°. Another sweep was performed using ω scans from -70.0 to 110.0° in 0.5° step, at χ=45.0° and ϕ =

180.0°. The exposure rate was 14.0 [sec./°]. The detector swing angle was 20.06°. The crystal-to-detector distance was 50.17 mm. Readout was performed in the 0.137 mm pixel mode.

Data Reduction

Of the 22912 reflections that were collected, 3418 were unique (R_{int} = 0.0245); equivalent reflections were merged. Data were collected and processed using CrystalClear (Rigaku). Net intensities and sigmas were derived as follows:

$$F^2 = [\Sigma(P_i - mB_{ave})] \cdot Lp^{-1}$$

where P_i is the value in counts of the i^{th} pixel
m is the number of pixels in the integration area
B_{ave} is the background average
Lp is the Lorentz and polarization factor

$$B_{ave} = \Sigma(B_j)/n$$

where n is the number of pixels in the background area
B_j is the value of the j^{th} pixel in counts

$$\sigma^2(F^2_{hkl}) = [(\Sigma P_i) + m((\Sigma(B_{ave} - B_j)^2)/(n-1))] \cdot Lp \cdot errmul + (erradd \cdot F^2)^2$$

where erradd = 0.00
errmul = 1.00

The linear absorption coefficient, μ, for Mo-Kα radiation is 0.95 cm^{-1}. A numerical absorption correction was applied which resulted in transmission factors ranging from 0.9785 to 0.9886. The data were corrected for Lorentz and polarization effects.

Structure Solution and Refinement

The structure was solved by direct methods[2] and expanded using Fourier techniques[3]. The non-hydrogen atoms were refined anisotropically. Hydrogen atoms were refined using the riding model. The final cycle of full-matrix least-squares refinement[4] on F^2 was based on 3418 observed reflections and 231 variable parameters and converged (largest parameter shift was 0.00 times its

esd) with unweighted and weighted agreement factors of:

$$R1 = \Sigma \; ||Fo| - |Fc|| \; / \; \Sigma \; |Fo| = 0.0325$$

$$wR2 = [\; \Sigma \; (\; w \; (Fo^2 - Fc^2)^2 \;) / \; \Sigma \; w(Fo^2)^2]^{1/2} = 0.0844$$

The standard deviation of an observation of unit weight[5] was 1.06. Unit weights were used. The maximum and minimum peaks on the final difference Fourier map corresponded to 0.16 and -0.21 $e^-/Å^3$, respectively.

Neutral atom scattering factors were taken from Cromer and Waber[6]. Anomalous dispersion effects were included in Fcalc[7]; the values for $\Delta f'$ and $\Delta f''$ were those of Creagh and McAuley[8]. The values for the mass attenuation coefficients are those of Creagh and Hubbell[9]. All calculations were performed using the CrystalStructure[10,11] crystallographic software package except for refinement, which was performed using SHELXL-97[12].

References

(1) CrystalClear: Rigaku Corporation, 1999. CrystalClear Software User's Guide, Molecular Structure Corporation, (c) 2000.J.W.Pflugrath (1999) Acta Cryst. D55, 1718-1725.

(2) SHELX97: Sheldrick, G.M. (1997).

(3) DIRDIF99: Beurskens, P.T., Admiraal, G., Beurskens, G., Bosman, W.P., de Gelder, R., Israel, R. and Smits, J.M.M.(1999). The DIRDIF-99 program system, Technical Report of the Crystallography Laboratory, University of Nijmegen, The Netherlands.

(4) Least Squares function minimized: (SHELXL97)

$\Sigma w(F_o^2-F_c^2)^2$ where w = Least Squares weights.

(5) Standard deviation of an observation of unit weight:

$[\Sigma w(F_o^2-F_c^2)^2/(N_o-N_v)]^{1/2}$

where: N_o = number of observations
N_v = number of variables

(6) Cromer, D. T. & Waber, J. T.; "International Tables for X-ray Crystallography", Vol. IV, The Kynoch Press, Birmingham, England, Table 2.2 A (1974).

(7) Ibers, J. A. & Hamilton, W. C.; Acta Crystallogr., 17, 781 (1964).

(8) Creagh, D. C. & McAuley, W.J .; "International Tables for Crystallography", Vol C, (A.J.C. Wilson, ed.), Kluwer Academic Publishers, Boston, Table 4.2.6.8, pages 219-222 (1992).

(9) Creagh, D. C. & Hubbell, J.H..; "International Tables for Crystallography", Vol C, (A.J.C. Wilson, ed.), Kluwer Academic Publishers, Boston, Table 4.2.4.3, pages 200-206 (1992).

(10) CrystalStructure 3.7.0: Crystal Structure Analysis Package, Rigaku and Rigaku/MSC (2000-2005). 9009 New Trails Dr. The Woodlands TX 77381 USA.

(11) CRYSTALS Issue 10: Watkin, D.J., Prout, C.K. Carruthers, J.R. & Betteridge, P.W. Chemical Crystallography Laboratory, Oxford, UK. (1996)

(12) SHELX97: Sheldrick, G.M. (1997).

EXPERIMENTAL DETAILS

A. Crystal Data

Empirical Formula	$C_{20}H_{23}NO_4$
Formula Weight	341.41
Crystal Color, Habit	colorless, prism
Crystal Dimensions	0.30 X 0.22 X 0.17 mm
Crystal System	orthorhombic
Lattice Type	Primitive
Detector Position	50.17 mm
Pixel Size	0.137 mm

Lattice Parameters	a = 7.2621(12) Å b = 8.0445(13) Å c = 28.318(5) Å V = 1654.3(5) Å^3
Space Group	$P2_12_12_1$ (#19)
Z value	4
D_{calc}	1.371 g/cm^3
F_{000}	728
μ(MoKα)	0.95 cm^{-1}

B. Intensity Measurements

Detector	Rigaku Saturn
Goniometer	Rigaku AFC8
Radiation	MoKα (λ = 0.71075 Å) graphite monochromated-Rigaku
SHINE	
Detector Aperture	70 mm x 70 mm
Data Images	1440 exposures
ω oscillation Range (χ=45.0, ϕ=90.0)	-70.0 - 110.0^o
Exposure Rate	14.0 sec./^{o}
Detector Swing Angle	20.06^o
ω oscillation Range (χ=45.0, ϕ=0.0)	-70.0 - 110.0^o
Exposure Rate	14.0 sec./^{o}

Detector Swing Angle	20.06°
ω oscillation Range (χ=0.0, ϕ=0.0)	-70.0 - 110.0°
Exposure Rate	14.0 sec./°
Detector Swing Angle	20.06°
ω oscillation Range (χ=45.0, ϕ=180.0)	-70.0 - 110.0°
Exposure Rate	14.0 sec./°
Detector Swing Angle	20.06°
Detector Position	50.17 mm
Pixel Size	0.137 mm
$2\theta_{max}$	59.4°
No. of Reflections Measured	Total: 22912 Unique: 3418 (R_{int} = 0.0245) I>2σ(I): 3406
Corrections	Lorentz-polarization (trans. factors: 0.9785 - 0.9886)

C. Structure Solution and Refinement

Structure Solution	Direct Methods (SHELX97)
Refinement	Full-matrix least-squares on F^2
Function Minimized	Σ w $(Fo^2 - Fc^2)^2$
Least Squares Weights	$w = 1/ [\sigma^2(Fo^2) + (0.0488 \cdot P)^2 + 0.3484 \cdot P]$ where $P = (Max(Fo^2,0) + 2Fc^2)/3$

$2\theta_{max}$ cutoff	53.0°
Anomalous Dispersion	All non-hydrogen atoms
No. Observations (All reflections)	3418
No. Variables	231
Reflection/Parameter Ratio	14.80
Residuals: R1 (I>2.00σ(I))	0.0325
Residuals: R (All reflections)	0.0326
Residuals: wR2 (All reflections)	0.0844
Goodness of Fit Indicator	1.057
Max Shift/Error in Final Cycle	0.000
Maximum peak in Final Diff. Map	0.16 $e^-/Å^3$
Minimum peak in Final Diff. Map	-0.21 $e^-/Å^3$

Appendix 4:

X-ray crystallographic data for compound **33**

(Chapter 2)

Sample: 33

X-ray Structure Report

for
Dr. P.E. Georghiou

Prepared by

Louise N. Dawe, PhD

Centre for Chemical Analysis, Research and Training (C-CART)
Department of Chemistry
Memorial University of Newfoundland
St. Johns, NL, A1B 3X7
(709) 737-4556 (X-Ray Laboratory)

May 9, 2010

Introduction

A report was previously prepared for this data, however, upon journal submission and crystallographic review, further examination of difference maps was performed in order to located hydrogen atoms that were omitted from the previous model.

Collection, solution and refinement proceeded normally. All hydrogen atoms were introduced in calculated positions with isotropic thermal parameters set twenty percent greater than those of their bonding partners and were refined on the riding model. All non-hydrogen atoms were refined anisotropically.

The formula is:

$[(C_{20}H_{24}N_1O_4)Cl]\ (H_2O)_2$

Experimental

Data Collection

A colorless needle crystal of $C_{20}H_{28}ClNO_6$ having approximate dimensions of 0.49 x 0.03 x 0.03 mm was mounted on a low temperature diffraction loop. All measurements were made on a Rigaku Saturn CCD area detector with a SHINE optic and Mo-Kα radiation.

Indexing was performed from 360 images that were exposed for 35 seconds. The crystal-to-detector distance was 40.00 mm.

Cell constants and an orientation matrix for data collection corresponded to a primitive monoclinic cell with dimensions:

a = 11.197(6) Å
b = 7.218(4) Å β = 99.841(11)^o
c = 12.421(7) Å
V = 989.2(9) Å^3

For Z = 2 and F.W. = 413.90, the calculated density is 1.390 g/cm^3. Based on the systematic absences of:

0k0: k ± 2n

packing considerations, a statistical analysis of intensity distribution, and the successful solution and refinement of the structure, the space group was determined to be:

$P2_1$ (#4)

The data were collected at a temperature of -120 ± 1^{o}C to a maximum 2θ value of 61.7^o. A total of 720 oscillation images were collected. A sweep of data was done using ω scans from -75.0 to 105.0^o in 0.5^o step, at χ=45.0^o and ϕ = 90.0^o. The exposure rate was 70.0 [sec./^{o}]. The detector swing angle was 15.14^o. A second sweep was performed using ω scans from -75.0 to 105.0^o in 0.5^o step, at χ=0.0^o and ϕ = 0.0^o. The exposure rate was 70.0 [sec./^{o}]. The detector swing angle was 15.14^o. The crystal-to-detector distance was 40.00 mm. Readout was performed in the 0.137 mm pixel mode.

Data Reduction

Of the 8699 reflections that were collected, 4013 were unique (R_{int} = 0.0451); equivalent reflections were merged. Data were collected and processed using CrystalClear (Rigaku). Net intensities and sigmas were derived as follows:

$$F^2 = [\Sigma(P_i - mB_{ave})] \cdot Lp^{-1}$$

where P_i is the value in counts of the i^{th} pixel
m is the number of pixels in the integration area
B_{ave} is the background average
Lp is the Lorentz and polarization factor

$$B_{ave} = \Sigma(B_j)/n$$

where n is the number of pixels in the background area
B_j is the value of the j^{th} pixel in counts

$$\sigma^2(F^2_{hkl}) = [(\Sigma P_i) + m((\Sigma(B_{ave} - B_j)^2)/(n-1))] \cdot Lp \cdot errmul + (erradd \cdot F^2)^2$$

where erradd = 0.00
errmul = 1.00

The linear absorption coefficient, μ, for Mo-Kα radiation is 2.30 cm^{-1}. A numerical absorption correction was applied which resulted in transmission factors ranging from 0.9550 to 0.9968. The data were corrected for Lorentz and polarization effects.

Structure Solution and Refinement

The structure was solved by direct methods[2] and expanded using Fourier techniques[3]. The non-hydrogen atoms were refined anisotropically. Hydrogen atoms were refined using the riding model. The final cycle of full-matrix least-squares refinement[4] on F^2 was based on 4013 observed reflections and 254 variable parameters and converged (largest parameter shift was 0.01 times its esd) with unweighted and weighted agreement factors of:

$$R1 = \Sigma \; ||Fo| - |Fc|| \; / \; \Sigma \; |Fo| = 0.0962$$

$$wR2 = [\Sigma (w (Fo^2 - Fc^2)^2)/ \Sigma w(Fo^2)^2]^{1/2} = 0.2646$$

The standard deviation of an observation of unit weight[5] was 1.05. Unit weights were used. The maximum and minimum peaks on the final difference Fourier map corresponded to 1.17 and -0.47 $e^-/Å^3$, respectively.

Neutral atom scattering factors were taken from Cromer and Waber[6]. Anomalous dispersion effects were included in Fcalc[7]; the values for $\Delta f'$ and $\Delta f''$ were those of Creagh and McAuley[8]. The values for the mass attenuation coefficients are those of Creagh and Hubbell[9]. All calculations were performed using the CrystalStructure[10,11] crystallographic software package except for refinement, which was performed using SHELXL-97[12].

References

(1) CrystalClear: Rigaku Corporation, 1999. CrystalClear Software User's Guide, Molecular Structure Corporation, (c) 2000.J.W.Pflugrath (1999) Acta Cryst. D55, 1718-1725.

(2) SHELX97: Sheldrick, G.M. (1997).

(3) DIRDIF99: Beurskens, P.T., Admiraal, G., Beurskens, G., Bosman, W.P., de Gelder, R., Israel, R. and Smits, J.M.M.(1999). The DIRDIF-99 program system, Technical Report of the Crystallography Laboratory, University of Nijmegen, The Netherlands.

(4) Least Squares function minimized: (SHELXL97)

$\Sigma w(F_o^2-F_c^2)^2$ where w = Least Squares weights.

(5) Standard deviation of an observation of unit weight:

$[\Sigma w(F_o^2-F_c^2)^2/(N_o-N_v)]^{1/2}$

where: N_o = number of observations

N_v = number of variables

(6) Cromer, D. T. & Waber, J. T.; "International Tables for X-ray Crystallography", Vol. IV, The Kynoch Press, Birmingham, England, Table 2.2 A (1974).

(7) Ibers, J. A. & Hamilton, W. C.; Acta Crystallogr., 17, 781 (1964).

(8) Creagh, D. C. & McAuley, W.J .; "International Tables for Crystallography", Vol C, (A.J.C. Wilson, ed.), Kluwer Academic Publishers, Boston, Table 4.2.6.8, pages 219-222 (1992).

(9) Creagh, D. C. & Hubbell, J.H..; "International Tables for Crystallography", Vol C, (A.J.C. Wilson, ed.), Kluwer Academic Publishers, Boston, Table 4.2.4.3, pages 200-206 (1992).

(10) CrystalStructure 3.7.0: Crystal Structure Analysis Package, Rigaku and Rigaku/MSC (2000-2005). 9009 New Trails Dr. The Woodlands TX 77381 USA.

(11) CRYSTALS Issue 10: Watkin, D.J., Prout, C.K. Carruthers, J.R. & Betteridge, P.W. Chemical Crystallography Laboratory, Oxford, UK. (1996)

(12) SHELX97: Sheldrick, G.M. (1997).

EXPERIMENTAL DETAILS

A. Crystal Data

Empirical Formula	$C_{20}H_{28}ClNO_6$
Formula Weight	413.90
Crystal Color, Habit	colorless, needle
Crystal Dimensions	0.49 X 0.03 X 0.03 mm
Crystal System	monoclinic
Lattice Type	Primitive
Detector Position	40.00 mm
Pixel Size	0.137 mm
Lattice Parameters	a = 11.197(6) Å b = 7.218(4) Å c = 12.421(7) Å β = 99.841(11) ^{o} V = 989.2(9) $Å^3$

Space Group	$P2_1$ (#4)
Z value	2
D_{calc}	1.390 g/cm^3
F_{000}	440
μ(MoKα)	2.30 cm^{-1}

B. Intensity Measurements

Detector	Rigaku Saturn
Goniometer	Rigaku AFC8
Radiation	MoKα (λ = 0.71075 Å) graphite monochromated-Rigaku
SHINE	
Detector Aperture	70 mm x 70 mm
Data Images	720 exposures
ω oscillation Range (χ=45.0, ϕ=90.0)	-75.0 - 105.0^o
Exposure Rate	70.0 sec./^{o}
Detector Swing Angle	15.14^o
ω oscillation Range (χ=0.0, ϕ=0.0)	-75.0 - 105.0^o
Exposure Rate	70.0 sec./^{o}
Detector Swing Angle	15.14^o
Detector Position	40.00 mm
Pixel Size	0.137 mm

$2\theta_{max}$	61.7^{o}
No. of Reflections Measured	Total: 8699 Unique: 4013 (R_{int} = 0.0451) I>2σ(I): 3413
Corrections	Lorentz-polarization (trans. factors: 0.9550 - 0.9968)

C. Structure Solution and Refinement

Structure Solution	Direct Methods (SHELX97)
Refinement	Full-matrix least-squares on F^2
Function Minimized	Σ w $(Fo^2 - Fc^2)^2$
Least Squares Weights	$w = 1/[\sigma^2(Fo^2) + (0.1219 \cdot P)^2 + 4.3993 \cdot P]$ where $P = (Max(Fo^2,0) + 2Fc^2)/3$
$2\theta_{max}$ cutoff	53.0^{o}
Anomalous Dispersion	All non-hydrogen atoms
No. Observations (All reflections)	4013
No. Variables	254
Reflection/Parameter Ratio	15.80
Residuals: R1 (I>2.00σ(I))	0.0962
Residuals: R (All reflections)	0.1105
Residuals: wR2 (All reflections)	0.2646
Goodness of Fit Indicator	1.051

Max Shift/Error in Final Cycle	0.006
Maximum peak in Final Diff. Map	1.17 $e^-/Å^3$
Minimum peak in Final Diff. Map	-0.47 $e^-/Å^3$

Appendix 5:

X-ray crystallographic data for compound **25**

(Chapter 3)

Sample: 25

X-ray Structure Report

for

Prof. Paris Georghiou

Prepared by

Louise N. Dawe, PhD

Centre for Chemical Analysis, Research and Training (C-CART)
Department of Chemistry
Memorial University of Newfoundland
St. Johns, NL, A1B 3X7
(709) 864-4556 (X-Ray Laboratory)
(709) 864-8904 (Office)

July 20, 2011

Introduction

Collection, solution and refinement proceeded normally. All non-hydrogen atoms were refined anisotropically. All hydrogen atoms were introduced in calculated positions and refined on a riding model except H4A, which was introduced from its Fourier map position and refined positionally, with a fixed U (1.5U O4), and with a DFIX restraint.

While this crystallized in a non-centrosymmetric space group, absolute configuration could not be established by anomalous dispersion effects. The enantiomer has been assigned by reference to an unchanging chiral centre in the synthetic procedure and SHELXL MERG 4 was used during the final stages of refinement. Both Flack x and Hooft y were calculated prior to employing MERG 4, and both gave ambiguous results. Note, however, that an unchanging chiral auxiliary was used in the synthesis, and that the absolute configuration was assigned on that basis.

Experimental

Data Collection

A colorless prism crystal of $C_{27}H_{31}NO_4$ having approximate dimensions of 0.29 x 0.24 x 0.20 mm was mounted on a low temperature diffraction loop. All measurements were made on a Rigaku Saturn70 CCD diffractometer using graphite monochromated Mo-Kα radiation, equipped with a SHINE optic.

The crystal-to-detector distance was 50.05 mm.

Cell constants and an orientation matrix for data collection corresponded to a primitive monoclinic cell with dimensions:

a = 8.835(7) Å
b = 11.502(8) Å β = 102.770(7)°
c = 11.957(9) Å
V = 1185.0(15) Å^3

For Z = 2 and F.W. = 433.55, the calculated density is 1.215 g/cm^3. Based on the reflection conditions of:

0k0: k = 2n

packing considerations, a statistical analysis of intensity distribution, and the successful solution and refinement of the structure, the space group was determined to be:

$P2_1$ (#4)

The data were collected at a temperature of 23 $\pm$ 1°C to a maximum 2θ value of 59.6°. A total of 972 oscillation images were collected. A sweep of data was done using ω scans from -70.0 to 110.0° in 0.5° step, at χ=45.0° and ϕ = 180.0°. The exposure rate was 30.0 [sec./°]. The detector swing angle was 20.07°. A second sweep was performed using ω scans from -70.0 to 80.0° in 0.5° step, at χ=45.0° and ϕ = 90.0°. The exposure rate was 30.0 [sec./°]. The detector swing angle was 20.07°. Another sweep was performed using ω scans from -70.0 to 86.0° in 0.5° step, at χ=0.0° and ϕ = 0.0°. The exposure rate was 30.0 [sec./°]. The detector swing angle was 20.07°. The crystal-to-detector

distance was 50.05 mm. Readout was performed in the 0.137 mm pixel mode.

Data Reduction

Of the 12080 reflections that were collected, 2861 were unique (R_{int} = 0.0405); equivalent reflections were merged. Data were collected and processed using CrystalClear (Rigaku).

The linear absorption coefficient, μ, for Mo-Kα radiation is 0.81 cm^{-1}. A numerical absorption correction was applied which resulted in transmission factors ranging from 0.984 to 0.991. The data were corrected for Lorentz and polarization effects.

Structure Solution and Refinement

The structure was solved by direct methods[2] and expanded using Fourier techniques. The non-hydrogen atoms were refined anisotropically. Hydrogen atoms were refined using the riding model. The final cycle of full-matrix least-squares refinement[3] on F^2 was based on 2861 observed reflections and 296 variable parameters and converged (largest parameter shift was 0.00 times its esd) with unweighted and weighted agreement factors of:

$$R1 = \Sigma \; ||Fo| - |Fc|| \; / \; \Sigma \; |Fo| = 0.0421$$

$$wR2 = [\; \Sigma \; (\; w \; (Fo^2 - Fc^2)^2 \;) / \; \Sigma \; w(Fo^2)^2]^{1/2} = 0.1115$$

The standard deviation of an observation of unit weight[4] was 1.05. Unit weights were used. The maximum and minimum peaks on the final difference Fourier map corresponded to 0.14 and -0.16 $e^-/Å^3$, respectively.

Neutral atom scattering factors were taken from Cromer and Waber[5]. Anomalous dispersion effects were included in Fcalc[6]; the values for $\Delta f'$ and $\Delta f''$ were those of Creagh and McAuley[7]. The values for the mass attenuation coefficients are those of Creagh and Hubbell[8]. All calculations were performed using the CrystalStructure[9] crystallographic software package except for refinement, which was performed using SHELXL-97[2].

References

(1) CrystalClear: Rigaku Corporation, 1999. CrystalClear Software User's Guide, Molecular Structure Corporation, (c) 2000.J.W.Pflugrath (1999) Acta Cryst. D55, 1718-1725.

(2) SHELX97: Sheldrick, G.M. Acta Cryst. 2008, A64, 112-122

(3) Least Squares function minimized: (SHELXL97)

$$\Sigma w(F_o^2-F_c^2)^2 \quad \text{where w = Least Squares weights.}$$

(4) Standard deviation of an observation of unit weight:

$$[\Sigma w(F_o^2-F_c^2)^2/(N_o-N_v)]^{1/2}$$

where: N_o = number of observations
N_v = number of variables

(5) Cromer, D. T. & Waber, J. T.; "International Tables for X-ray Crystallography", Vol. IV, The Kynoch Press, Birmingham, England, Table 2.2 A (1974).

(6) Ibers, J. A. & Hamilton, W. C.; Acta Crystallogr., 17, 781 (1964).

(7) Creagh, D. C. & McAuley, W.J .; "International Tables for Crystallography", Vol C, (A.J.C. Wilson, ed.), Kluwer Academic Publishers, Boston, Table 4.2.6.8, pages 219-222 (1992).

(8) Creagh, D. C. & Hubbell, J.H..; "International Tables for Crystallography", Vol C, (A.J.C. Wilson, ed.), Kluwer Academic Publishers, Boston, Table 4.2.4.3, pages 200-206 (1992).

(9) CrystalStructure 4.0: Crystal Structure Analysis Package, Rigaku and Rigaku Americas (2000-2010). 9009 New Trails Dr. The Woodlands TX 77381 USA.

EXPERIMENTAL DETAILS

A. Crystal Data

Empirical Formula	$C_{27}H_{31}NO_4$
Formula Weight	433.55
Crystal Color, Habit	colorless, prism
Crystal Dimensions	0.29 X 0.24 X 0.20 mm
Crystal System	monoclinic
Lattice Type	Primitive
Lattice Parameters	a = 8.835(7) Å b = 11.502(8) Å c = 11.957(9) Å β = 102.770(7) ^{o} V = 1185.0(15) Å^3
Space Group	$P2_1$ (#4)
Z value	2
D_{calc}	1.215 g/cm^3
F_{000}	464
μ(MoKα)	0.81 cm^{-1}

B. Intensity Measurements

Diffractometer	Rigaku Saturn70 CCD
Radiation	MoKα (λ = 0.71075 Å) graphite monochromated-Rigaku
SHINE	
Voltage, Current	50kV, 30mA

Temperature	23.0°C
Detector Aperture	70 x 70 mm
Data Images	972 exposures
ω oscillation Range (χ=45.0, ϕ=180.0)	-70.0 - 110.0°
Exposure Rate	30.0 sec./°
Detector Swing Angle	20.07°
ω oscillation Range (χ=45.0, ϕ=90.0)	-70.0 - 80.0°
Exposure Rate	30.0 sec./°
Detector Swing Angle	20.07°
ω oscillation Range (χ=0.0, ϕ=0.0)	-70.0 - 86.0°
Exposure Rate	30.0 sec./°
Detector Swing Angle	20.07°
Detector Position	50.05 mm
Pixel Size	0.137 mm
$2\theta_{max}$	59.6°
No. of Reflections Measured	Total: 12080 Unique: 2861 (R_{int} = 0.0405) I>2σ(I): 2618
Corrections	Lorentz-polarization (trans. factors: 0.984 - 0.991)

C. Structure Solution and Refinement

Structure Solution	Direct Methods
Refinement	Full-matrix least-squares on F^2
Function Minimized	Σ w $(Fo^2 - Fc^2)^2$
Least Squares Weights	$w = 1/ [\sigma^2(Fo^2) + (0.0565 \cdot P)^2 + 0.1113 \cdot P]$ where $P = (Max(Fo^2,0) + 2Fc^2)/3$
$2\theta_{max}$ cutoff	55.0^o
Anomalous Dispersion	All non-hydrogen atoms
No. Observations (All reflections)	2861
No. Variables	296
Reflection/Parameter Ratio	9.67
Residuals: R1 ($I>2.00\sigma(I)$)	0.0421
Residuals: R (All reflections)	0.0462
Residuals: wR2 (All reflections)	0.1115
Goodness of Fit Indicator	1.053
Max Shift/Error in Final Cycle	0.000
Maximum peak in Final Diff. Map	0.14 $e^-/Å^3$
Minimum peak in Final Diff. Map	-0.16 $e^-/Å^3$

Appendix 6:

X-ray crystallographic data for compound **67**

(Chapter 3)

Sample: 67

X-ray Structure Report

for
Dr. P.E. Georghiou

Prepared by

Louise N. Dawe, PhD

Centre for Chemical Analysis, Research and Training (C-CART)
X-Ray Diffraction Laboratory
and
Department of Chemistry
Memorial University of Newfoundland
St. Johns, NL, A1B 3X7
(709) 737-4556 (X-Ray Laboratory)

July 22, 2010

Introduction

Collection, solution and refinement proceeded normally. All hydrogen atoms were introduced in calculated positions with isotropic thermal parameters set twenty percent greater than those of their bonding partners and were refined on the riding model. All non-hydrogen atoms were refined anisotropically. This crystal was a weak anomalous scatterer collected with MoKa radiation, therefore, Friedel mates were merged (MERG 4) and absolute configuration was not determined.

Experimental

Data Collection

A colorless platelet crystal of $C_{13}H_{18}BNO_4$ having approximate

dimensions of 0.30 x 0.09 x 0.06 mm was mounted on a low temperature diffraction loop. All measurements were made on a Rigaku Saturn CCD area detector with a SHINE optic and Mo-Kα radiation.

Indexing was performed from 360 images that were exposed for 22 seconds. The crystal-to-detector distance was 40.13 mm.

Cell constants and an orientation matrix for data collection corresponded to a primitive orthorhombic cell with dimensions:

a = 8.3776(11) Å
b = 8.9269(11) Å
c = 17.369(2) Å
V = 1299.0(3) Å^3

For Z = 4 and F.W. = 263.10, the calculated density is 1.345 g/cm^3. The systematic absences of:

h00: h ± 2n
0k0: k ± 2n
00l: l ± 2n

uniquely determine the space group to be:

$P2_12_12_1$ (#19)

The data were collected at a temperature of -120 ± 1°C to a maximum 2θ value of 61.6°. A total of 956 oscillation images were collected. A sweep of data was done using ω scans from -75.0 to 105.0° in 0.5° step, at χ=45.0° and ϕ = 0.0°. The exposure rate was 44.0 [sec./°]. The detector swing angle was 15.08°. A second sweep was performed using ω scans from -75.0 to 105.0° in 0.5° step, at χ=0.0° and ϕ = 0.0°. The exposure rate was 44.0 [sec./°]. The detector swing angle was 15.08°. Another sweep was performed using ω scans from -35.5 to 82.5° in 0.5° step, at χ=45.0° and ϕ = 180.0°. The exposure rate was 44.0 [sec./°]. The detector swing angle was 15.08°. The crystal-to-detector distance was 40.13 mm. Readout was performed in the 0.137 mm pixel mode.

Data Reduction

Of the 16363 reflections that were collected, 1725 were unique (R_{int} = 0.0370); equivalent reflections were merged. Data were collected and processed using CrystalClear (Rigaku). Net intensities and sigmas were derived as follows:

$$F^2 = [\Sigma(P_i - mB_{ave})] \cdot Lp^{-1}$$

where P_i is the value in counts of the i^{th} pixel
m is the number of pixels in the integration area
B_{ave} is the background average
Lp is the Lorentz and polarization factor

$$B_{ave} = \Sigma(B_j)/n$$

where n is the number of pixels in the background area
B_j is the value of the j^{th} pixel in counts

$$\sigma^2(F^2_{hkl}) = [(\Sigma P_i) + m((\Sigma(B_{ave} - B_j)^2)/(n-1))] \cdot Lp \cdot errmul + (erradd \cdot F^2)^2$$

where erradd = 0.00
errmul = 1.00

The linear absorption coefficient, μ, for Mo-Kα radiation is 0.974 cm^{-1}. A numerical absorption correction was applied which resulted in transmission factors ranging from 0.9852 to 0.9968. The data were corrected for Lorentz and polarization effects.

Structure Solution and Refinement

The structure was solved by direct methods[2] and expanded using Fourier techniques[3]. The non-hydrogen atoms were refined anisotropically. Hydrogen atoms were refined using the riding model. The final cycle of full-matrix least-squares refinement[4] on F^2 was based on 1725 observed reflections and 173 variable parameters and converged (largest parameter shift was 0.00 times its esd) with unweighted and weighted agreement factors of:

$$R1 = \Sigma \, ||Fo| - |Fc|| \, / \, \Sigma \, |Fo| = 0.0434$$

$$wR2 = [\Sigma (w (Fo^2 - Fc^2)^2) / \Sigma \, w(Fo^2)^2]^{1/2} = 0.1123$$

The standard deviation of an observation of unit weight[5] was 1.17. Unit weights were used. The maximum and minimum peaks on the final difference Fourier map corresponded to 0.20 and -0.22 $e^-/Å^3$, respectively.

Neutral atom scattering factors were taken from Cromer and Waber[6]. Anomalous dispersion effects were included in Fcalc[7]; the values for $\Delta f'$ and $\Delta f''$ were those of Creagh and McAuley[8]. The values for the mass attenuation coefficients are those of Creagh and Hubbell[9]. All calculations were performed using the CrystalStructure[10,11] crystallographic software package except for refinement, which was performed using SHELXL-97[12].

References

(1) CrystalClear: Rigaku Corporation, 1999. CrystalClear Software User's Guide, Molecular Structure Corporation, (c) 2000.J.W.Pflugrath (1999) Acta Cryst. D55, 1718-1725.

(2) SHELX97: Sheldrick, G.M. (1997).

(3) DIRDIF99: Beurskens, P.T., Admiraal, G., Beurskens, G., Bosman, W.P., de Gelder, R., Israel, R. and Smits, J.M.M.(1999). The DIRDIF-99 program system, Technical Report of the Crystallography Laboratory, University of Nijmegen, The Netherlands.

(4) Least Squares function minimized: (SHELXL97)

$\Sigma w(F_o^2-F_c^2)^2$ where w = Least Squares weights.

(5) Standard deviation of an observation of unit weight:

$[\Sigma w(F_o^2-F_c^2)^2/(N_o-N_v)]^{1/2}$

where: N_o = number of observations

N_v = number of variables

(6) Cromer, D. T. & Waber, J. T.; "International Tables for X-ray Crystallography", Vol. IV, The Kynoch Press, Birmingham, England, Table 2.2 A (1974).

(7) Ibers, J. A. & Hamilton, W. C.; Acta Crystallogr., 17, 781 (1964).

(8) Creagh, D. C. & McAuley, W.J .; "International Tables for Crystallography", Vol C, (A.J.C. Wilson, ed.), Kluwer Academic Publishers, Boston, Table 4.2.6.8,

pages 219-222 (1992).

(9) Creagh, D. C. & Hubbell, J.H..; "International Tables for Crystallography", Vol C, (A.J.C. Wilson, ed.), Kluwer Academic Publishers, Boston, Table 4.2.4.3, pages 200-206 (1992).

(10) CrystalStructure 3.7.0: Crystal Structure Analysis Package, Rigaku and Rigaku/MSC (2000-2005). 9009 New Trails Dr. The Woodlands TX 77381 USA.

(11) CRYSTALS Issue 10: Watkin, D.J., Prout, C.K. Carruthers, J.R. & Betteridge, P.W. Chemical Crystallography Laboratory, Oxford, UK. (1996)

(12) SHELX97: Sheldrick, G.M. (1997).

EXPERIMENTAL DETAILS

A. Crystal Data

Empirical Formula	$C_{13}H_{18}BNO_4$
Formula Weight	263.10
Crystal Color, Habit	colorless, platelet
Crystal Dimensions	0.30 X 0.09 X 0.06 mm
Crystal System	orthorhombic
Lattice Type	Primitive
Detector Position	40.13 mm
Pixel Size	0.137 mm
Lattice Parameters	a = 8.3776(11) Å b = 8.9269(11) Å c = 17.369(2) Å V = 1299.0(3) $Å^3$
Space Group	$P2_12_12_1$ (#19)

Z value	4
D_{calc}	1.345 g/cm^3
F_{000}	560
μ(MoKα)	0.98 cm^{-1}

B. Intensity Measurements

Detector	Rigaku Saturn
Goniometer	Rigaku AFC8
Radiation	MoKα (λ = 0.71075 Å) graphite monochromated-Rigaku
SHINE	
Detector Aperture	70 mm x 70 mm
Data Images	956 exposures
ω oscillation Range (χ=45.0, ϕ=0.0)	-75.0 - 105.0^o
Exposure Rate	44.0 sec./^{o}
Detector Swing Angle	15.08^o
ω oscillation Range (χ=0.0, ϕ=0.0)	-75.0 - 105.0^o
Exposure Rate	44.0 sec./^{o}
Detector Swing Angle	15.08^o
ω oscillation Range (χ=45.0, ϕ=180.0)	-35.5 - 82.5^o
Exposure Rate	44.0 sec./^{o}
Detector Swing Angle	15.08^o

Detector Position	40.13 mm
Pixel Size	0.137 mm
$2\theta_{max}$	61.6°
No. of Reflections Measured	Total: 16363 Unique: 1725 (R_{int} = 0.0370) I>2σ(I): 1707
Corrections	Lorentz-polarization (trans. factors: 0.9852 - 0.9968)

C. Structure Solution and Refinement

Structure Solution	Direct Methods (SHELX97)
Refinement	Full-matrix least-squares on F^2
Function Minimized	Σ w $(Fo^2 - Fc^2)^2$
Least Squares Weights	$w = 1/[\sigma^2(Fo^2) + (0.0529 \cdot P)^2 + 0.4126 \cdot P]$ where $P = (Max(Fo^2,0) + 2Fc^2)/3$
$2\theta_{max}$ cutoff	55.0°
Anomalous Dispersion	All non-hydrogen atoms
No. Observations (All reflections)	1725
No. Variables	173
Reflection/Parameter Ratio	9.97
Residuals: R1 (I>2.00σ(I))	0.0434
Residuals: R (All reflections)	0.0440

Residuals: wR2 (All reflections)	0.1123
Goodness of Fit Indicator	1.172
Max Shift/Error in Final Cycle	0.000
Maximum peak in Final Diff. Map	0.20 $e^{-}/Å^3$
Minimum peak in Final Diff. Map	-0.22 $e^{-}/Å^3$